Department of Psychology
School of Social and Behavioral Sciences
University of Alabama at Birmingham
UAB Station
Birmingham, AL 35294-1170

Phone: (205) 934-2694
FAX: (205) 975-6110
Bitnet: *amthor@cis.uab.edu*

July 3, 1996

re: Final technical report for N00014-91-J-1280 requested by Stephanie A. Dean
reference ONR Au/246:sad
AUOB/Gen/N-1280
12 June 1996

Dr. Thomas M. McKenna
Office of Naval Research Code 1142BI
Office of the Chief of Naval Research
800 N. Quincy St.
Arlington,VA
22217-5000

Dear Dr. McKenna,

I have received a letter asking for a final progress report for N00014-91-J-1280. I have submitted a similar report on two previous occasions, but apparently I did not submit enough copies to enough places, or some copies were lost. Please do not hesitate to request further material if needed. The report below concerns the scientific progress made while ONR support was in effect, and is mainly evidenced by the papers published crediting ONR support, which are attached and should be considered part of the report. No patents or commercial applications resulted directly from the research. The research project in my lab has benefitted greatly from ONR support, and we look forward to possible future collaborations with the Navy.

Sincerely,

Franklin R. Amthor, Ph.D., Associate Professor
Department of Psychology
Neurobiology Research Center
Dept. of Biomedical Engineering
Dept. of Vision Science, School of Optometry

DISCLAIMER NOTICE

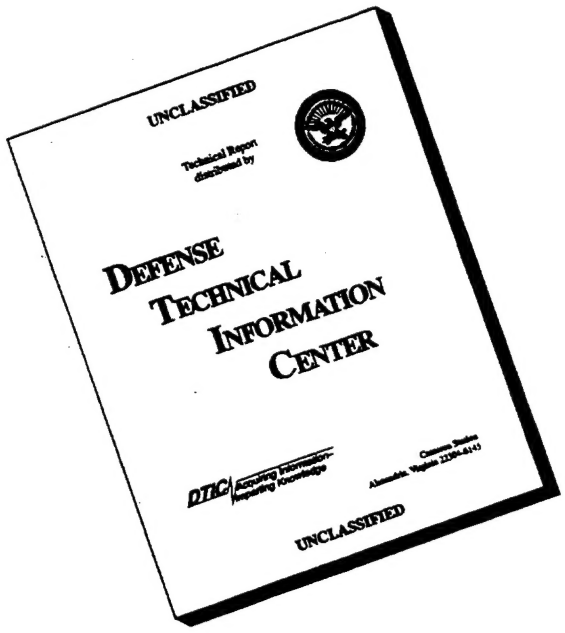

THIS DOCUMENT IS BEST QUALITY AVAILABLE. THE COPY FURNISHED TO DTIC CONTAINED A SIGNIFICANT NUMBER OF PAGES WHICH DO NOT REPRODUCE LEGIBLY.

REPORT DOCUMENTATION PAGE

Form Approved
OMB No. 0704-0188

1. AGENCY USE ONLY (Leave blank)	2. REPORT DATE	3. REPORT TYPE AND DATES COVERED
	Aug 6, 1996	Final 15 Dec 90 - 14 June 94

4. TITLE AND SUBTITLE
Theoretical and Experimental Determination of the Robust Biological Mechanism of Retinal Directional Selectivity

5. FUNDING NUMBERS
G N00014-91-J-1280

6. AUTHOR(S)
Franklin R. Amthor, Ph.D.

7. PERFORMING ORGANIZATION NAME(S) AND ADDRESS(ES)
Dept. of Psychology
Univ. of Alabama at Birmingham
Birmingham, AL 35294-1170

8. PERFORMING ORGANIZATION REPORT NUMBER
N00014-91-J-1280/
SF298

9. SPONSORING/MONITORING AGENCY NAME(S) AND ADDRESS(ES)
Dept. of the Navy
Office of Naval Research
Thomas M. McKenna
800 North Quincy St.
Arlington, VA 22217-5000

10. SPONSORING/MONITORING AGENCY REPORT NUMBER
N00014-91-J-1280/
SF298

11. SUPPLEMENTARY NOTES

12a. DISTRIBUTION/AVAILABILITY STATEMENT
APPROVED FOR PUBLIC RELEASE; DISTRIBUTION IS UNLIMITED.

12b. DISTRIBUTION CODE

13. ABSTRACT (Maximum 200 words)

Physiological experimentation and electrotonic modeling and simulation of On-Off directionally selective ganglion cells of the rabbit retina were interactively conducted to determine (1) the computational algorithms used by these cells to achieve their robust selectivity for direction of motion, (2) the synaptic circuitry which biophysically implements the directional-selective mechanism. The research showed that retinal directional selectivity was based on both a fast facilitative and slower, sustained inhibitory mechanism involving asymmetric contacts from retinal interneurons (amacrine cells). The research showed that this combination of interacting mechanisms could produce robust directionality independent of stimulus contrast sign and amount, speed, and shape. The mechanisms used by these cells perform direction selectivity more precisely and robustly than prior, extant theoretical mechanisms such as Reichardt correlation detectors. As such, artificial mechanisms built to detect direction of motion may fruitfully use the biological mechanisms studied in this research.

14. SUBJECT TERMS
motion detection, retina, directional selectivity, ganglion cells, simulations, biophysics

15. NUMBER OF PAGES

16. PRICE CODE

17. SECURITY CLASSIFICATION OF REPORT	18. SECURITY CLASSIFICATION OF THIS PAGE	19. SECURITY CLASSIFICATION OF ABSTRACT	20. LIMITATION OF ABSTRACT
UL	UL	UL	SAR

NSN 7540-01-280-5500

Standard Form 298 (Rev. 2-89)

FINAL TECHNICAL REPORT FOR ONR N00014-91-J-1280

THEORETICAL AND EXPERIMENTAL DETERMINATION OF THE ROBUST BIOLOGICAL MECHANISM OF DIRECTIONAL SELECTIVITY

Principle Investigator: Franklin R. Amthor[1]

Co-Investigator: Norberto M. Grzywacz[2]

[1]Department of Psychology and
Neurobiology Research Center
University of Alabama at Birmingham
UAB Station
Birmingham, Alabama 35294

[2]The Smith-Kettlewell Eye Research Institute
2232 Webster Street
San Francisco, CA 94115

Address for Correspondence:

Franklin R. Amthor
Department of Psychology
University of Alabama at Birmingham
UAB Station
Birmingham, AL 35294
phone (205) 934-2694
FAX (205) 975-6110
Internet: amthor@cis.uab.edu

1. Scientific progress. We have made technical and scientific progress on understanding how the retina encodes direction of motion. Scientifically, we have determined the nonlinear characteristics of the neural processing mechanisms underlying directional selectivity, and the anatomical substrates for the neural circuitry mediating the directionally selective mechanism in retina. Technically, we have demonstrated a visualized, isolated retinal recording system (for rabbit retina) in which directionally selective (DS) ganglion cells, and the cells that drive them, can be visually selected for simultaneous recording. This has allowed us to make several important and new findings on the anatomical substrate of directional selectivity, the underlying physiological mechanisms, and computational properties:

Anatomical Substrate.

A. DS ganglion cells preferring the same direction of motion form a tiling of the retina in which dendrites of adjacent, same preferred direction cells terminate at "T-type" appositions.

B. Dendrites of DS ganglion cells having different preferred directions fasciculate together over a considerably extent of their courses, possibly forming a novel anatomical substrate for the computation of different directions of motion among DS cell having different preferred directions.

C. There appear to be more contacts between cholinergic (starburst) amacrine cells on the side from which preferred-direction moving objects approach, than the opposite side. This could be an essential part of the anatomical substrate for the cholinergic contribution to directional selectivity.

Physiological Mechanisms.

A. We have shown that the inhibitory mechanism mediating directional selectivity is based on two sustained processes, segregated between the light and dark responding channels in the retina. The finding of sustained nature of the inhibitory DS mechanism invalidates many of the current models for directional selectivity, whose performance tends to be worse than the actual biological mechanism. This has obviously important implications for modelling and VLSI implementation.

B. We have shown that directional selectivity is also based on a facilitatory mechanism that also requires a relatively sustained input, which is then gated by subsequent excitation.

C. We have recently conducted dual extracellular recordings between nearest neighbor pairs of On-Off directionally selective ganglion cells and On-Off directionally selective ganglion cells and starburst amacrine cells. We have found that

1. Although nearest neighbor On-Off DS ganglion cells are neurobiotin dye coupled, their spike discharges are not correlated at the millisecond time scale.
2. Extracellularly recorded spikes from starburst amacrine cells on the preferred direction approaching side of On-Off directionally selective ganglion cells, however, are highly correlated with those in the ganglion cell, suggesting the possibility that either many ganglion cell spikes originate in the starburst amacrine, or alternatively, that the dendrites of the ganglion cell itself spike, and these spikes are communicated back to the starburst soma in a possible positive feedback circuit.

Computational Properties.

A. We have shown that the retinal DS mechanism is extremely robust computationally, being invariant over nearly three orders of magnitude of velocity, and independent of the shape or extent of the flow field.

B. We have also shown that the DS mechanism is contrast invariant, not only to the sign (light or dark) of the contrast, but also its magnitude - these cells respond directionally from 100% to less than 1% contrast.

2. Most exciting accomplishments during the project.

A. The finding of the directionally selective network of close appositions and fasciculations, previously unsuspected, described under the anatomical substrate section above, has far reaching importance for understanding how directional selectivity is computed, and why it is computationally so robust. Even at the retinal level, computation of direction of motion may be influenced by global interactions.

B. The new visualized retina recording technique has been used to record from connected cells to understand the biophysical basis of the DS mechanism. Dual extracellular recordings between nearest neighbor pairs of On-Off directionally selective ganglion cells and On-Off directionally selective ganglion cells and starburst amacrine cells have shown that the spike discharges of nearest neighbor On-Off DS ganglion cells are not correlated at the millisecond time scale, but those of starburst amacrine cells on the preferred direction approaching side of On-Off directionally selective ganglion cells are correlated with those of the ganglion cell, suggesting the possibility that either many ganglion cell spikes originate in the starburst amacrine, or that the dendrites of the ganglion cell itself spike, and these spikes are communicated back to the starburst soma.

3. Publications. The papers we have published citing support by this project are, of course, the best summary of the accomplishments made by this lab during the support. Some reprints (or photocopies, thereof) of our papers supported by ONR were previously submitted, some are also included in this report. Below is a list of papers, abstracts, and book chapters partially creditable to ONR support during the duration of the project (due to space limitations, some abstracts may not have cited ONR in the abstract body):

Refereed papers

Grzywacz NM, Amthor FR and Borg-Graham LJ. (1993) Does synaptic facilitation mediate motion facilitation in the retina. *Computation and Neural Systems, 1992*. F. Eeckman and J. Bower eds. Chapter 24. Kluwer, New York.

Amthor FR and Grzywacz NM. (1993) Inhibition in On-Off directionally selective ganglion cells in the rabbit retina. *J. Neurophysiol.* **69**(6):2174-2187.

Grzywacz NM and Amthor FR. (1993) Facilitation in On-Off directionally selective ganglion cells in the rabbit retina. *J. Neurophysiol.* **69**(6):2188-2199.

Grzywacz NM, Amthor FR and Merwine DK. (1994) Directional hyperacuity in ganglion cells of the rabbit retina. *Visual Neuroscience* **11**: 1019-1025.

Villa MF and Amthor FR. (1995) Automating the quantitative analysis of 2-D neural dendritic trees. *Neuroscience Methods* **56**: 77-88.

Amthor FR and Oyster CW. (1995) Spatial organization of retinal information about movement detection. *Proc. Natl. Acad. Sci. USA*. **92(9)**: 4002-4005.

Merwine DK, Amthor FR and Grzywacz NM. (1995) The interaction between center and surround of rabbit retinal ganglion cells. *J. Neurophysiol.* **73(4)**: 1547-1567.

Amthor FR, Grzywacz NM and Merwine DK. (1996) Extra-receptive field facilitation in On-Off DS ganglion cells of the rabbit retina. *Visual Neuroscience* 13(2): 303-310.

BOOKS and non-peer reviewed PUBLICATIONS

Grzywacz NM, Sernagor E and Amthor FR (1995) Function, mechanism and development of retinal directional selectivity. Accepted for Handbook of Brain Theory and Neural Networks, MA Arbib, ed. Bradford Books, MIT Press, Cambridge.

Amthor FR and Grzywacz NM (1993) Directional Selectivity in Vertebrate Retinal Ganglion Cells. Visual Motion and its Role in the Stabilization of Gaze, FA Miles, ed., Elsevier Press, The Netherlands.

peer-reviewed ABSTRACTS

Amthor FR and Grzywacz NM (1992) Response of rabbit directionally selective ganglion cells to moving gratings and plaids. *Invest. Ophthal. Vis Sci.* 33(4):907.

Grzywacz NM and Amthor FR (1992) Quantitative fits of an amacrine model of directional selectivity to rabbit data. *Neurosci. Abstr.* 18(1):393.

Merwine DK and Amthor FR (1992) Rabbit retinal ganglion cell surround mechanisms: physiology and pharmacology. *Neurosci. Abstr.* 18(1):394.

Amthor FR, Tootle JS and Oyster CW (1993) Dendritic morphologies and sublamination pattern of physiologically identified rabbit retinal ganglion cells. *Invest. Ophthal. Vis Sci.* **34(4)**:985.

Grzywacz NM and Amthor FR (1993) Tests of an asymmetric amacrine cell model for retinal directional selectivity. *Invest. Ophthal. Vis Sci.* **34(4)**:1292.

Merwine DK, Amthor FR and Grzywacz NM (1993) A pharmacological analysis of rabbit retinal ganglion cell surround inhibition. *Invest. Ophthal. Vis Sci.* **34(4)**:1332.

Amthor FR and Oyster CW (1993) Relation between preferred direction and dendritic organization of identified, contacting on-off ds ganglion cells and ach. Amacrine cells in rabbit retina. *Neurosci. Abstr.* 19(2):1258.

Grzywacz NM, Amthor RF and Merwine DK. (1993) Extra receptive field facilitation in rabbit's retinal directional selectivity. *Neurosci. Abstr.* 19(2):1258.

Amthor FR, Oyster CW and Grzywacz NM (1994) Retinal coverage and physiological inputs to directionally selective rabbit retinal ganglion cells. *Invest. Ophthal. Vis Sci.* **35(4)**:2065.

Amthor FR and Grzywacz NM. (1994) Morphological and physiological basis of starburst-ach Amacrine input to directionally selective (DS) ganglion cells in rabbit retina. *Neurosci. Abstr.*

Visual Neuroscience (1994), **11**, 1019–1025. Printed in the USA.

SHORT COMMUNICATION

Directional hyperacuity in ganglion cells of the rabbit retina

NORBERTO M. GRZYWACZ,[1] FRANKLIN R. AMTHOR,[2] AND DAVID K. MERWINE[3]

[1]The Smith-Kettlewell Eye Research Institute, 2232 Webster Street, San Francisco
[2]Department of Psychology and Neurobiology Research Center, University of Alabama at Birmingham, Birmingham
[3]Department of Physiological Optics, School of Optometry, University of Alabama at Birmingham, Birmingham

(RECEIVED September 13, 1993; ACCEPTED February 7, 1994)

Abstract

Biological visual systems can detect positional changes that are finer than these systems' acuity to sine-wave gratings, a property known as hyperacuity. Some systems can even detect changes finer that the photoreceptor spacing. We report here that rabbit's directionally selective ganglion cells not only detect positional changes in the hyperacuity range, but also discriminate the direction of their motion. Our experiments show that directional selectivity occurs for edges of light moving as little as 1.1 μm (26″ of visual angle) across the retina. This distance corresponds to a hyperacuity, since the acuity to sine-wave gratings of rabbit's On–Off DS ganglion cells is about 125 μm (50′). In addition, this distance is smaller than the minimal spacing between rabbit photoreceptors (1.9 μm or 46″), as estimated from cell-density studies (Young & Vaney, 1991). Such a hyperacuity suggests low-noise high-gain signal transmission from photoreceptors to ganglion cells and that directional selectivity can arise in small portions of retinal dendritic processes.

Keywords: Hyperacuity, Directional selectivity, Ganglion cell, Retina, Rabbit

Introduction

The first demonstration of the remarkable sensitivity of visual systems to positional changes was for human psychophysical displacement thresholds (5″—Westheimer & McKee, 1977). They are lower than human grating acuity (and thus the term hyperacuity) and the spacing between foveal cones (27″). Studies of the neural substrate of hyperacuity demonstrated that retinal (Shapley & Victor, 1986; Lee et al., 1993) and cortical neurons (Swindale & Cynader, 1986) can detect displacements in the hyperacuity range. However, these studies did not explain how visual systems not only detect these displacements, but also discriminate their direction. In this paper, we investigate this discrimination, which we call directional hyperacuity.

Barlow and Levick (1965) demonstrated directional selectivity for slits of light moving about 40 μm (17′) across the rabbit's retina. But it has been argued that extended edges, rather than narrow slits of light, are a better stimulus for rabbit's directionally selective (DS) ganglion cells (Amthor & Grzywacz, 1993; Grzywacz & Amthor, 1993). Hence, it became of interest to measure their response to edges of light moving short distances. Demonstration of directional hyperacuity with moving edges would make the rabbit retina a good model for understanding the biophysics of this fine visual discrimination. This is because much is known about the physiology (Oyster, 1968; Wyatt & Daw, 1975; Amthor & Grzywacz, 1993; Grzywacz & Amthor, 1993), anatomy (Masland et al., 1984; Amthor et al., 1989; Famiglietti, 1991), and pharmacology (Caldwell et al., 1978; Ariel & Daw, 1982) of rabbit directional selectivity.

Methods

Eighteen On–Off DS ganglion cells of the rabbit were recorded extracellularly in an everted eyecup preparation (Amthor et al., 1984; Amthor et al., 1989; Amthor & Grzywacz, 1991, 1993). The eyes were from adult Dutch belt-pigmented rabbits weighing at least 1.3 kg. Animals were anesthetized with an initial dose of urethane (2 g/kg), followed by Pentobarbital given to effect. The amount of Pentobarbital brought the animal to a level of anesthesia in which no reflexive movement or change in heart rate resulted from a pinch to the paw. After anesthesia, the right eye was enucleated as the animal was killed with an overdose of Pentobarbital. The eyecup was then prepared as described elsewhere (Amthor et al., 1984; Amthor et al., 1989; Amthor & Grzywacz, 1991, 1993). It was superfused with a transparent medium similar to that in Ames and Nesbett (1981).

We investigated the discrimination of direction of motion by On–Off directionally selective ganglion cells of rabbit by

Reprint requests to: Norberto M. Grzywacz, The Smith-Kettlewell Eye Research Institute, 2232 Webster Street, San Francisco, CA 94115, USA.

using an extended edge undergoing the apparent motion explained in Fig. 1. Extracellular-spike responses were recorded for both preferred- and null-direction motions. We also recorded responses to the edge appearing and disappearing without moving. Poststimulus histograms for the no-motion conditions were subtracted from those obtained from the motions bin by bin in a base-subtraction procedure. This procedure allowed visualizing responses to motion in the absence of spikes elicited by the edge's appearance before motion (Amthor & Grzywacz, 1993; Grzywacz & Amthor, 1993)

In different experiments, several apparent-motion displacement magnitudes were used, ranging from 1.1 μm (26″) to 47 μm (19′). All conditions (combinatorial arrangements of displacement magnitudes, contrast polarity, and preferred and null motions) were presented in random order within an experimental set. The number of such sets in different experiments ranged from 30 to 100 and the random order was different for each set. The delay between the beginning of two consecutive stimuli within a set was 2250 ms.

The apparent-motion stimuli were generated on a Tektronix 608 monitor controlled by computer and a waveform generator (Innisfree, Cambridge, MA) projected to the eyecup from 85 cm through an achromatic plano-convex lens with 17-mm focal length and 12-mm diameter. The contrast of the stimuli was 99.2% (determined with a Spectra Pritchard photometer model 1980A-WB) and the mean illumination (and that of the homogeneous background) was 60 lx. We measured the sharpness of the moving edge on the monitor with the photometer from 1.5 m away and a 0.75′ slit. The edge moved in increments of 50 μm on the monitor, and for each position the luminance was read. It fell from 90% to 10% of maximum in 380 ± 30 μm (standard error). By taking into account the thickness of the slit, the 90%-to-10% edge's spread was 180 ± 50 μm on the monitor. (Under the assumption that the monitor's line-spread function is Gaussian, its spatial standard deviation is around 70 μm.) This spread made the task of responding with directional hyperacuity more difficult, since the shortest motions spanned only 1.1 μm in the retina or equivalently, 55 μm on the monitor. We did not expect the fluid covering the retina to affect this spread or the image's quality. The fluid's height was between 1–2 mm over the recorded cells. The diameter of its surface was about 3 cm, too large to produce much spherical aberration (due to

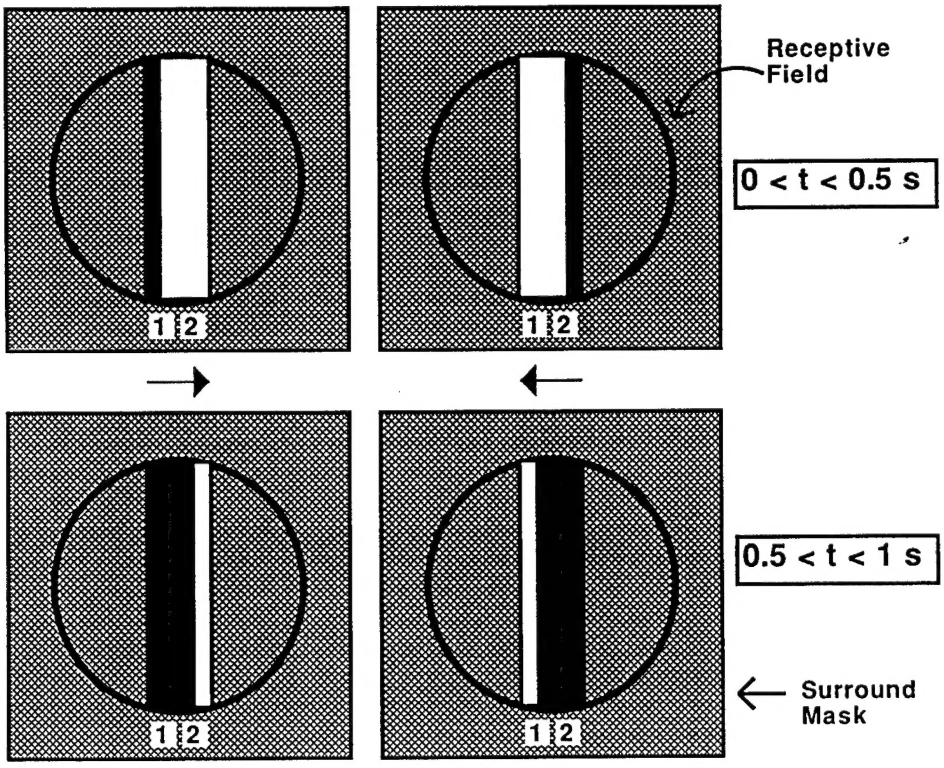

Fig. 1. Schematics of visual display used in experiments. The receptive field (circle) was masked (hatched area) to prevent surround interactions. The visible area always corresponded to 100 × 400 μm^2 in the retina, such that the long axis was perpendicular to the preferred direction. A dark (or light) edge (oriented parallel to the long axis of the visible area) appeared from a homogeneous background in a position of the receptive field, labeled 1, remained there for 500 ms, and then jumped a predetermined distance in the preferred direction to the position labeled 2. The edge remained at "2" for another 500 ms before the stimulus returned to the homogeneous background. Null-direction motion jumps from "2" to "1" were also delivered to the cell. The positions "1" and "2" were symmetrical about the center of the aperture. Furthermore, they were typically symmetrical about the center of the receptive field. The only exceptions occurred in experiments like the one labeled "position = 70 μm" in Fig. 3. For them, the midpoint between positions "1" and "2" was 70 μm away from the center of the receptive field. Because these displacements were back and forth from "1" to "2," they stimulated the exact same area of the retina each time for a given displacement magnitude.

a meniscus) at the center of the fluid's surface. The electrode was also not expected to cause aberrations, because its point of entry in the fluid was typically 3 mm away from the center and the diameter of the electrode's shank was 0.8 mm. To confirm these expectations, we looked at the image through the microscope used to aid electrode placement with a scaled piece of paper placed in lieu of the retina. This microscopic procedure was performed with and without fluid, and with and without the electrode. Presence of fluid or electrode did not cause detectable distortions, rotations, or abnormal magnifications of the image.

The statistical significance of the data obtained with the apparent-motion stimuli was analyzed in two ways: First, we compared the means of the integral of the based subtracted preferred- and null-direction responses with a t-test. Second, we performed an individual trial analysis on these integrals. This analysis compared preferred and null responses trial by trial, and computed the percentage of trials in which the preferred response was larger than the null one. (When the responses were equal, the analysis assigned a "winner"—preferred or null—randomly.) A trial-by-trial analysis, that is, comparing responses separately for trial 1, then for trial 2, and so on, reduced effects that large temporal separation might have on the comparisons. This analysis assumed that a comparison between two cells with opposite preferred directions and with properties identical to the recorded cell underlies the decisions on direction of motion. The analysis was equivalent to a two-alternative forced-choice paradigm (chance performance at 50%). In such a paradigm, a hit rate of P% (for example, 81%) corresponds to a false-alarm rate of $(100 - P)$% (only 19% in the example). In a system whose performance is limited by a Gaussian additive noise, the hit rate is a monotonic function of a single parameter called d' (Elliot, 1964; Green & Swets, 1966). Therefore, psychophysicists use d' to quantify performance (with threshold typically set at $d' = 1$). For comparison with psychophysical performances, we report d's of Gaussian-noise systems with hit rates as in rabbit DS cells.

The hyperacute behavior reported here was compared to minimal photoreceptor spacing and to square- and sine-wave grating acuity data. To obtain these data, the gratings moved in the preferred direction at various temporal frequencies, with the same contrast and mean luminance as described above, and the surround masked. At the optimal temporal frequency (≈4 Hz), we delivered 128 cycles of the stimulus, an amount comparable (actually, slightly larger) to that delivered in the hyperacuity task. Typically, the response became indistinguishable from the background activity at 8 cycles/mm, although occasionally, cells had small responses at this frequency. [The acuity—$\frac{1}{8}$ mm = 125 μm—was consistent with that of the starburst cell, an important excitatory drive to On-Off DS cells (O'Malley & Masland, 1993).] A manuscript describing the DS ganglion-cell acuity data in detail is currently in preparation.

Results

Fig. 2 displays poststimulus histograms for 1.1 μm preferred- and null-direction motions of a bright edge for one cell. Comparison of the histogram's black bins with activity before the edge's appearance (arrow A) illustrates that the responses to preferred-direction motion were higher (average of 1.39 spikes per 0.5 s interval) than the background activity (average of 0.035 spikes per 0.5 s interval), indicating displacement detection. Furthermore, preferred-direction motion elicited more spikes than null-direction motion (average of 0.19 spikes per 0.5 s interval). Analysis of the histogram's time integral over 500 ms after the jump reveals that this difference is significant ($t = 5.02$, 198 degrees of freedom, $P < 0.001$). Individual-trial analysis (see Methods) shows that comparing responses of two such cells with opposite preferred directions would determine the motion's direction correctly 81% of the time ($d' = 1.24$). Hence, these results demonstrate a directional hyperacuity in DS ganglion cells of rabbit retina.

In experiments such as those reported in Fig. 2, responses were recorded as a function of motion displacement ranging from 1.1 μm (26″) to 47 μm (19′). Fig. 3 presents results of two such experiments, one for short-range motions using data from the cell in Fig. 2 (E514c1), and the other for a wide range of displacements from another cell (E516c1). For Fig. 3, we integrated the base-subtracted responses over 500 ms after the displacement.

Fig. 3 provides further illustration that DS ganglion cells respond with directional hyperacuity to motion. The figure reconfirms this finding for the On responses of E514c1 and presents the displacement behavior for E516c1. (There was no directional selectivity in the Off responses of E514c1 for distances smaller or equal than 2.2 μm. This is a first demonstration that, in general, the degree of directional hyperacuity depends on whether the stimulus is of an On or Off type.) Directional selectivity increases with distance, because of a rapid increase of preferred- but not null-direction responses. At short distances, it is apparent that for E516c1, preferred-direction responses were larger than null-direction responses even at 3.8 μm. This appearance is confirmed by statistics for the On ($t = 4.28$, 58 degrees of freedom, $P < 0.001$) and Off ($t = 6.24$, 58 degrees of freedom, $P < 0.001$) motions, and extended to the Off motion at 1.9 μm ($t = 2.21$, 58 degrees of freedom, $P < 0.025$). The motion responses were highly variable from trial to trial (see representative standard-deviation error bars in Fig. 3). However, as for cell E514c1, individual-trial analysis for cell E516c1 shows that comparing responses of two such cells with opposite preferred directions would determine the motion's direction correctly 82% of the time ($d' = 1.29$) for 3.8-μm motions. Consequently, the directional hyperacute performance is not just the product of extensive accumulation of multiple response trials, but is a robust feature of retinal processing.

It is also possible that the degree of directional hyperacuity depends on receptive-field position. [For 150 μm (1 deg) motions, directional selectivity can be elicited in multiple positions of the receptive field (Barlow & Levick, 1965).] To investigate this issue, we repeated the experiments in two or more positions separated by at least 70 μm (28′). Fig. 4, illustrates the co-dependence of directional hyperacuity on receptive-field position, and On or Off stimuli.

At position 0 μm, On, but not Off edges elicit DS responses for 4.4-μm displacements ($t = 2.42$, 198 degrees of freedom, $P < 0.01$, and 62% performance in individual-trial analysis or $d' = 0.43$). In contrast, at position 70 μm, Off edges now elicit strong DS responses ($t = 8.45$, 58 degrees of freedom, $P < 0.001$, and 84% performance in individual-trial analysis or $d' = 1.4$). [Variations in On and Off responses with position have been attributed to variations in the size of the On and Off strata of DS ganglion cells' dendritic trees (Amthor et al., 1984).] Directional selectivity for 4.4-μm displacements is a directional hyper-

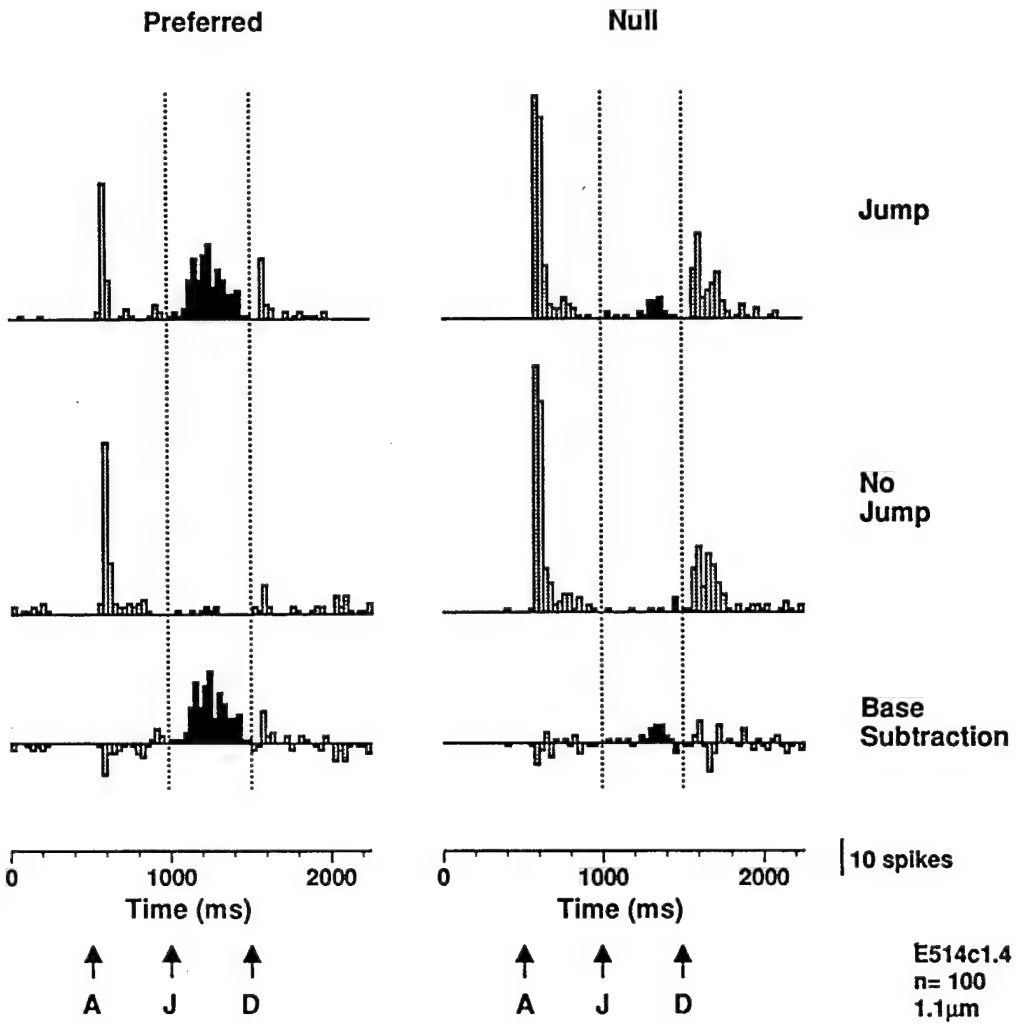

Fig. 2. Poststimulus histograms for a 1.1 μm (26″) motion of a bright edge. Histograms labeled "Jump" are responses of one cell to 100 trials of preferred- and null-direction displacements. Histograms labeled "No Jump" are responses to the edge appearing and disappearing without being displaced. Histograms labeled "Base Subtraction" are the result of subtracting bin by bin the "No Jump" histograms from the "Jump" histograms. This subtraction was shown to correspond to the response to the jump in the absence of spikes elicited by the appearance of the edge before the motion (Amthor & Grzywacz, 1993; Grzywacz & Amthor, 1993). The times of appearance, motion jump, and disappearance of the edges are marked with the arrows labeled A, J, and D, respectively. While the majority of the histogram is textured, we painted the histograms' portion between J and D in black to emphasize the response to the displacement itself. Moreover, the black bins are the data used in later figures. Base-subtracted responses to preferred-direction displacements are larger than those to null-direction displacements. This difference at such a short motion displacement (smaller than photoreceptor spacing) indicates that this cell exhibits directional hyperacuity.

acuity, since the acuity to square- and sine-wave gratings of rabbit's On–Off DS ganglion cells is about 125 μm (50′; Fig. 3; see Methods). (In this regard, the minimal distance for which Barlow and Levick observed DS responses with slits of light also constitutes directional hyperacuity. However, this distance is more than an order of magnitude larger than the minimal values reported here.) We conclude that the mechanism allowing for directional hyperacuity has multiple replicas in the receptive field, but depends on contrast polarity.

We completed the several-hours-long experiments on directional hyperacuity in 18 cells (13 with the protocol of Fig. 1 and five with a protocol using a central position for the motions' beginning). In all cells, the preferred-null bias was identical for displacements smaller than 15 μm (6′) and larger, continuous motions, indicating that all cells had correct directional hyperacuity. (That small displacements had always the same preferred direction as large motions indicates that directional hyperacuity is not due to edge-of-receptive-field effects. They could induce artifactual directionality, but not always in the correct direction.) Four out of the 13 cells (31%) tested with displacements smaller than the minimal photoreceptor spacing (1.9 μm) showed directional selectivity for these displacements. [The minimal photoreceptor spacing was estimated by assuming tight hexagonal packing, and maximal cone and rod densities of 16,000 and 308,000 cells/mm^2 respectively (Young & Vaney, 1991). However, the spacing relevant for directional selectivity might be much higher, since rod bipolar and amacrine cells do not appear to contact On starburst cells (Famiglietti, 1991), which

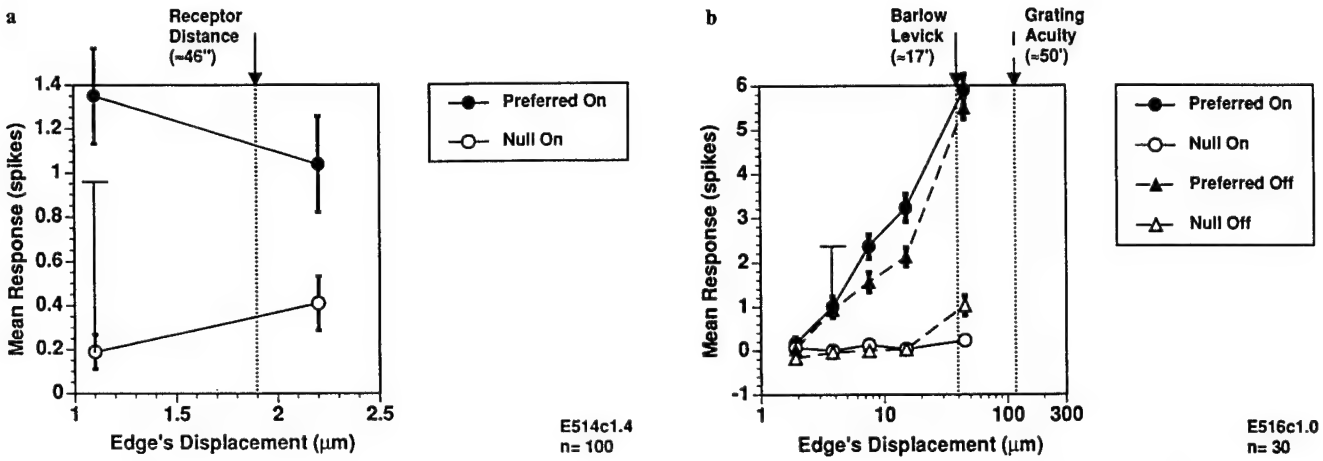

Fig. 3. Preferred and null responses as a function of displacement. The ordinates are the mean number of spikes during 500 ms after the displacement. This number corresponds to the mean integral of the black portion of base-subtracted histograms like those in Fig. 2. The bold error bars are standard errors of the ordinates, while the thin error bars are representative standard deviations. Solid and dashed lines correspond to responses to bright (On) or dark (Off) edges, respectively. For comparison's sake, we labeled with arrows and dotted lines the minimal photoreceptor distance, minimal distance for which Barlow and Levick observed DS responses with slits of light, and sine-wave grating acuity. a: Responses of the cell in Fig. 2 to one hundred short-range motion trials. This cell was particularly sensitive to On edges (responses to Off edges were not DS for these displacements—data not presented). Its directional selectivity threshold was at least 70% better than the photoreceptor spacing. b: Responses of another cell to a wide range of displacements over 30 trials. The preferred, but not null responses, rise fast with displacement for both On and Off stimuli. Already at displacements below photoreceptor spacing (and below Barlow and Levick limit, and grating acuity), one observes directional selectivity. These two cells provide further evidence that On–Off DS ganglion cells of the rabbit retina exhibit directional hyperacuity.

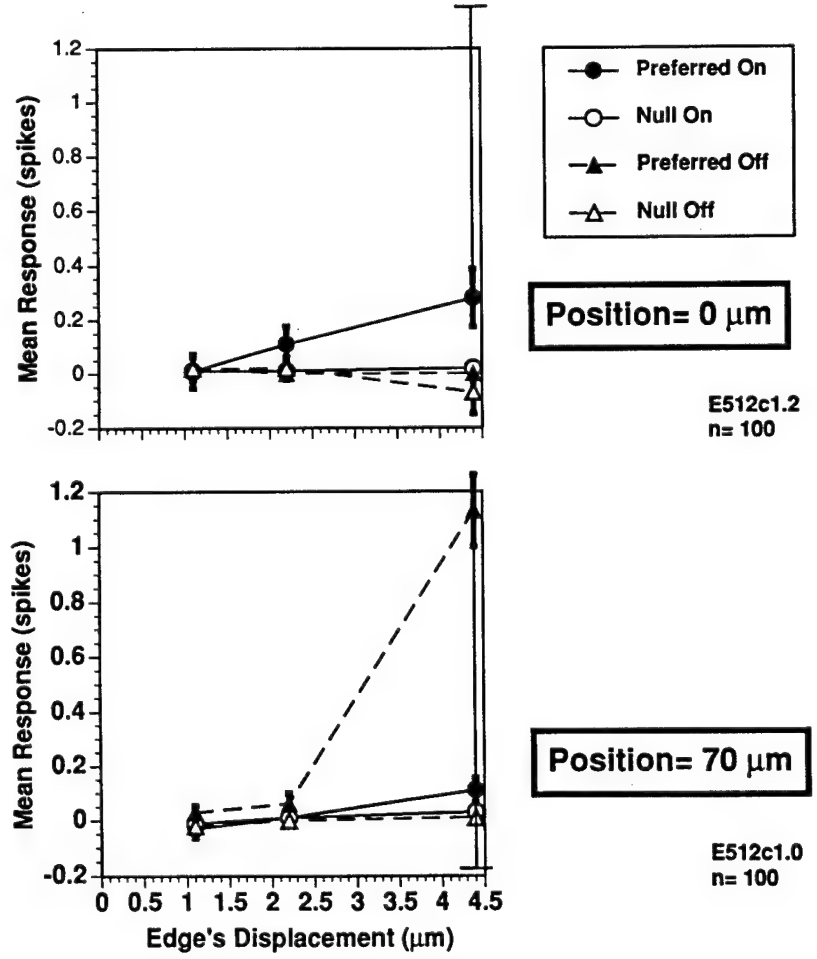

Fig. 4. Co-dependence of directional hyperacuity on receptive-field position, and On or Off stimuli. The meaning of ordinates, error bars, and solid and dashed lines are the same as in Fig. 3. This experiment was identical to those in Fig. 3, but the cell was stimulated over 100 trials with motions whose centers were separated by 70 μm. At the position labeled 0 μm, only On responses showed directional selectivity for 4.4-μm displacements. In contrast, at the position labeled 70 μm, the Off responses were the ones displaying strong directionality for the same displacements. Because these displacements were lower than the acuity to square- and sine-wave gratings (Fig. 3), this directional selectivity corresponds to a directional hyperacuity. Therefore, directional hyperacuity, but not preferred and null directions, depends on receptive-field position and contrast polarity.

might be the site where the computation of directional selectivity for On stimuli takes place. Consequently, the incidence of cells showing directional selectivity for displacements smaller than the photoreceptor spacing might be much higher than 31%.] In three cells, there was directional selectivity at 1.1 μm (Fig. 2). The directional hyperacuity of these highly sensitive cells was only at most a factor of 5.2 worse than human performance.

Discussion

Directionally selective cells must overcome two problems to display directional hyperacuity: (1) they must respond to small displacements, and (2) they must do so in a DS manner. The first problem is raised by the wide receptive-field centers of bipolar cells. Their diameters are about 300 μm (Dacheux & Raviola, 1986) and arise from photoreceptor gap junctions (Smith & Sterling, 1990), and not dendritic processes (Dacheux & Raviola, 1986). If one assumes that the photoreceptors' receptive field has a Gaussian profile of 75 μm standard deviation (two standard deviations on each side of center $\Rightarrow$ 300 μm diameter), and that the monitor's line-spread function is Gaussian with a 70 μm standard deviation (see Methods), then a 1.1 μm displacement would cause at most 0.8% change in photoreceptors' response. (This is consistent with the 0.5% sine-wave grating's contrast necessary to elicit directional selectivity—Grzywacz et al., 1990.) This 0.8% change would correspond to at most 0.8 mV modulation. Thus, such a small photoreceptor voltage should generate reliably about one spike for the best ganglion cells (Fig. 2), implying low noise and high gain (Shapley & Victor, 1986). Spatial filtering of photoreceptors electrical coupling should help to reduce noise. High gain could arise from photoreceptors' resting transmitter release (Fain, 1977; Fain et al., 1977), high-pass filtering of bipolar-cell inputs to inner plexiform layer (Werblin et al., 1988), and recruitment of several DS subunits (Barlow & Levick, 1965) across the edge. We wish to emphasize the recruitment, since in our experiment, the edge spanned 400 μm over the photoreceptor array (Fig. 1). Therefore, even for the smallest displacements used (1.1 μm), the edge (including its spread) would cause a small increase in light stimulation (<0.8%) in up to 18,000 photoreceptors. Furthermore, analysis of null-direction inhibition (Amthor & Grzywacz, 1993) and preferred-direction facilitation (Grzywacz & Amthor, 1993) recently suggested that the best stimuli to elicit directional selectivity from the rabbit's retina are large edges, rather than small objects.

The second problem raised by directional hyperacuity arises because the ganglion- and amacrine-cell dendritic processes apparently involved in directional selectivity are several hundred micrometers long (Amthor et al., 1984, 1989; Masland et al., 1984; Vaney, 1990; Famiglietti, 1991; Yang & Masland, 1992). Hence, as postulated by some models (Torre & Poggio, 1978; Koch et al., 1982; Grzywacz & Amthor, 1989; Vaney, 1990; Borg-Graham & Grzywacz, 1992), directional selectivity probably requires a small portion of these processes. In these models, directional hyperacuity would involve shunting inhibition, for which there is evidence (Amthor & Grzywacz, 1991). Because displacements causing barely significant responses elicit directional selectivity (Figs. 3 and 4), we conclude that it occurs for all displacements eliciting any response. Such directionality might arise from temporally sustained inhibition (Amthor & Grzywacz, 1993), which for slowly moving edges would be asymmetric and always present.

Acknowledgments

We thank Suzanne McKee for reading the manuscript critically. Also, thanks are due to William Belzer and Mark Villa for computer programming, Lorraine DeAngelis for technical assistance, and Doug Taylor for help with the estimate of the edge's sharpness. This work was supported by National Eye Institute grant EY08921 and by an award from the Paul L. and Phyllis C. Wattis Foundation to N.M. Grzywacz, by National Eye Institute grant EY05070 and a Sloan Foundation grant to F.R. Amthor, by Office of Naval Research grant N0014-91-J-1280, and by National Eye Institute core grants to Smith-Kettlewell and University of Alabama at Birmingham.

References

Ames, A.A., III & Nesbett, F.B. (1981). *In vitro* retina as an experimental model of the central nervous system. *Journal of Neurochemistry* **37**, 867–877.

Amthor, F.R. & Grzywacz, N.M. (1991). The nonlinearity of the inhibition underlying retinal directional selectivity. *Visual Neuroscience* **6**, 197–206.

Amthor, F.R. & Grzywacz, N.M. (1993). Inhibition in directionally selective ganglion cells of the rabbit retina. *Journal of Neurophysiology* **69**, 2174–2187.

Amthor, F.R., Oyster, C.W. & Takahashi, E.S. (1984). Morphology of ON-OFF direction selective ganglion cells in the rabbit retina. *Brain Research* **298**, 187–190.

Amthor, F.R., Takahashi, E.S. & Oyster, C.W. (1989). Morphologies of rabbit retinal ganglion cells with complex receptive fields. *Journal of Comparative Neurology* **280**, 97–121.

Ariel, M. & Daw, N.W. (1982). Pharmacological analysis of directionally sensitive rabbit retinal ganglion cells. *Journal of Physiology* **324**, 161–185.

Barlow, H.B. & Levick, W.R. (1965). The mechanism of directionally selective units in the rabbit's retina. *Journal of Physiology* **178**, 477–504.

Borg-Graham, L.J. & Grzywacz, N.M. (1992). A model of the direction selectivity circuit in retina: Transformations by neurons singly and in concert. In *Single Neuron Computation*, ed. McKenna, T., Davis, J. & Zornetzer, S.F., pp. 347–375. Orlando, Florida: Academic Press.

Caldwell, J.H., Daw, N.W. & Wyatt, H.J. (1978). Effects of picrotoxin and strychnine on rabbit retinal ganglion cells: Lateral interactions for cells with more complex receptive fields. *Journal of Physiology* **276**, 277–298.

Dacheux, R.F. & Raviola, E. (1986). The rod pathway in the rabbit retina: A depolarizing bipolar and amacrine cell. *Journal of Neuroscience* **6**, 331–345.

Elliot, P.B. (1964). Tables of *d'*. In *Signal Detection and Recognition by Human Observers*, ed. Swets, J.A., pp. 651–684. New York, New York: John Wiley.

Fain, G.L. (1977). The threshold signal of photoreceptors. In *Vertebrate Photoreception*, ed. Barlow, H.B. & Fatt, P., pp. 305–323. London, England: Academic Press.

Fain, G.L., Granda, A.M. & Maxwell, J.H. (1977). The voltage signal of photoreceptors at visual threshold. *Nature* **265**, 181–183.

Famiglietti, E.V. (1991). Synaptic organization of starburst amacrine cells in rabbit retina: Analysis of serial thin sections by electron microscopy and graphic reconstruction. *Journal of Comparative Neurology* **309**, 40–70.

Green, D.M. & Swets, J.A. (1966). *Signal Detection Theory and Psychophysics*. New York, New York: John Wiley.

Grzywacz, N.M. & Amthor, F.R. (1989). A model for neural directional selectivity that exhibits robust direction of motion computation. In *Advances in Neural Information I. Processing Systems I.*, ed. Touretzky, D.S., pp. 477–484. San Mateo, California: Morgan Kaufman.

Grzywacz, N.M., Amthor, F.R. & Mistler, L.A. (1990). Applicability of quadratic and threshold models to motion discrimination in the rabbit retina. *Biological Cybernetics* **64**, 41–49.

Grzywacz, N.M. & Amthor, F.R. (1993). Facilitation in directionally selective ganglion cells of the rabbit retina. *Journal of Neurophysiology* **69**, 2188–2199.

Koch, C., Poggio, T. & Torre, V. (1982). Retinal ganglion cells: A

functional interpretation of dendritic morphology. *Philosophical Transactions of the Royal Society B* (London) **298**, 227–264.

LEE, B.B., WEHRHAHN, C., WESTHEIMER, G. & KREMERS, J. (1993). Macaque ganglion cell responses to stimuli that elicit hyperacuity in man: Detection of small displacements. *Journal of Neuroscience* **13**, 1001–1009.

MASLAND, R.H., MILLS, J.W. & CASSIDY, C. (1984). The functions of acetylcholine in the rabbit retina. *Proceedings of the Royal Society B* (London) **223**, 121–139.

O'MALLEY, D.M. & MASLAND, R.H. (1993). Responses of the starburst amacrine cells to moving stimuli. *Journal of Neurophysiology* **69**, 730–738.

OYSTER, C.W. (1968). The analysis of image motion by the rabbit retina. *Journal of Physiology* **199**, 613–635.

SHAPLEY, R. & VICTOR, J. (1986). Hyperacuity in cat retinal ganglion cells. *Science* **231**, 999–1002.

SMITH, R.G. & STERLING, P. (1990). Cone receptive field in cat retina computed from microcircuitry. *Visual Neuroscience* **5**, 453–461.

SWINDALE, N.V. & CYNADER, M.S. (1986). Vernier acuity of neurones in cat visual cortex. *Nature* **319**, 591–593.

TORRE, V. & POGGIO, T. (1978). A synaptic mechanism possibly underlying directional selectivity to motion. *Proceedings of the Royal Society B* (London) **202**, 409–416.

VANEY, D.I. (1990). The mosaic of amacrine cells in the mammalian retina. In *Progress in Retinal Research (Vol. 9)*, ed. OSBORNE, N. & CHADER, J., pp. 49–100. Oxford, England: Pergamon Press.

WERBLIN, F., MAGUIRE, G., LUKASIEWICZ, P., ELIASOF, S. & WU, S.M. (1988). Neural interactions mediating the detection of motion in the retina of the tiger salamander. *Visual Neuroscience* **1**, 317–329.

WESTHEIMER, G. & MCKEE, S.P. (1977). Spatial configuration for visual hyperacuity. *Vision Research* **17**, 941–947.

WYATT, H.J. & DAW, N.W. (1975). Directionally sensitive ganglion cells in the rabbit retina: Specificity for stimulus direction, size and speed. *Journal of Neurophysiology* **38**, 613–626.

YANG, G. & MASLAND, R.H. (1992). Direct visualization of the dendritic and receptive fields of directionally selective retinal ganglion cells. *Science* **258**, 1949–1952.

YOUNG, H.M. & VANEY, D.I. (1991). Rod-signal interneurons in the rabbit retina: 1. Rod bipolar cells. *Journal of Comparative Physiology* **310**, 139–153.

Visual Neuroscience (1996), **13**, 303–309. Printed in the USA.

Extra-receptive-field motion facilitation in on–off directionally selective ganglion cells of the rabbit retina

FRANKLIN R. AMTHOR,[1] NORBERTO M. GRZYWACZ,[2] AND DAVID K. MERWINE[3]

[1]Department of Psychology and Neurobiology Research Center, University of Alabama at Birmingham, Birmingham
[2]The Smith-Kettlewell Eye Research Institute, San Francisco
[3]School of Optometry, University of Alabama at Birmingham, Birmingham

(RECEIVED March 29, 1995; ACCEPTED July 28, 1995)

Abstract

The excitatory receptive-field centers of On–Off directionally selective (DS) ganglion cells of the rabbit retina correspond closely to the lateral extent of their dendritic arborizations. Some investigators have hypothesized from this that theories for directional selectivity that entail a lateral spread of excitation from outside the ganglion cell dendritic tree, such as from starburst amacrine cells, are therefore untenable. We show here that significant motion facilitation is conducted from well outside the classical excitatory receptive-field center (and, therefore, dendritic arborization) of On–Off DS ganglion cells for preferred-direction, but not null-direction moving stimuli. These results are consistent with a role in directional selectivity for cells with processes lying beyond the On–Off ganglion cell's excitatory receptive-field center. These results also highlight the fundamental distinction in retinal ganglion cell receptive-field organization between classical excitatory mechanisms and those that facilitate other excitation without producing directly observable excitation by themselves.

Keywords: Retina, Electrophysiology, Ganglion cells, Motion detection, Directional selectivity

Introduction

On–Off directionally selective (DS) ganglion cells of the rabbit retina, like other On–Off center ganglion cells, have a receptive-field (RF) structure that "classically" is considered to consist of an excitatory center region embedded within a "silent", or purely suppressive inhibitory surround. Within the RF center, excitatory responses (increases in firing rate) are elicited at both light onset and offset. Light modulation within the surround is generally thought only to suppress firing evoked by stimulation within the center (Barlow et al., 1964; Barlow & Levick, 1965; Levick, 1967).

The excitatory RF centers of ganglion cells in a number of mammalian species have been shown to be more or less congruent with the extent of their dendritic arborizations; for example, cat alpha and beta cells (Wässle et al., 1981; Peichl & Wässle, 1983), and primate "blue-on," bistratified ganglion cells (Dacey & Lee, 1994). This congruence is particularly precise for On–Off DS ganglion cells of the rabbit retina. In the first reports of their dendritic morphology following intracellular recording, it was shown that differences in the extents of their On- and Off-excitatory RF center regions were reflected in corresponding differences in the inner *vs.* outer sublaminar dendritic arborizations that presumably mediate those responses (Amthor et al., 1984; Amthor et al., 1989).

Recently, it was shown by staining in a visualized, isolated rabbit retina preparation that the excitatory RF center maps and dendritic arborizations of On–Off DS ganglion cells are not only congruent, but about 90% of them are in good register (Yang & Masland, 1992, 1994). These investigators asserted from this finding that because no excitatory responses could be evoked from the region outside the DS ganglion cell's dendritic tree, theories for directional selectivity that postulate a lateral spread of excitation from outside the ganglion cell dendritic tree, such as from starburst (cholinergic) amacrine cells, may be *ipso facto* untenable, because the large dendritic fields of starburst amacrine cells would be expected to conduct excitation laterally from considerable distances outside the ganglion cell dendritic arborization.

In this study, we tested the hypothesis that the role played by laterally extended (amacrine) cells might be primarily to conduct motion facilitation, rather than direct excitation to the On–Off DS ganglion cell. We did this by (1) determining the extent of the excitatory RF center, and therefore dendritic arborization of On–Off DS ganglion cells using small flashing spots; (2) determining whether spots considerably outside the excit-

Reprint requests to: Franklin R. Amthor, Department of Psychology, University of Alabama at Birmingham, UAB Station, Birmingham, AL 35294, USA.

atory RF center could facilitate the responses of spots presented inside the center, using an apparent motion protocol; and (3) determining whether this extra-receptive-field-center facilitation was spatially asymmetric along the preferred-null axis. It should be noted that the demonstration of extra-receptive facilitation (requiring an interaction with intra-receptive-field-center excitation to elicit an effect) does not preclude the possibility that some direct, but subthreshold extra-receptive-field excitation may also be conveyed to the RF center from outside it.

The importance of understanding the roles of facilitation *vs.* excitation, and the involvement of possible extra-receptive-field-center mechanisms in the computation of direction of motion in these ganglion cells is a fundamental one. Differential responsivity to opposite directions of motion across the same path occurs in neurons throughout the visual system of vertebrates. Considerable computational modeling of DS mechanisms has been made in species ranging from flies to humans, in central nervous system loci from retina to cortex (see Grzywacz et al., 1994*a*, for a review). On–Off DS ganglion cells of the rabbit retina are a particularly important case for which to resolve this issue, because they exhibit a robust selectivity for direction of motion (Grzywacz et al., 1988, 1990, 1994*a*,1994*b*), and have been particularly well studied physiologically, pharmacologically, and anatomically. Part of the material presented in this paper appeared previously in abstract form (Grzywacz et al., 1993).

Methods

Conventional, single-unit extracellular recordings were obtained from On–Off DS ganglion cells in an isolated retina-eyecup preparation, as described previously (Amthor & Grzywacz, 1991). Adult Dutch belt-pigmented rabbits weighing at least 1.3 kg were anesthetized with an initial dose of urethane (2 g/kg), followed by Pentobarbital given to effect. The amount of Pentobarbital brought the animal to a level of anesthesia in which no reflexive movement or change in heart rate resulted from a pinch to the paw. After anesthesia, the right eye was enucleated as the animal was killed with an overdose of Pentobarbital. The eyecup was then superfused as in the reference above. All surgery and experimental procedures were conducted in rooms illuminated only by very dim, deep red light. Stimuli were presented on a Tektronix 608 CRT monitor, controlled by a Picasso video frame generator, which was in turn controlled by a DOS microcomputer that also recorded the times of occurrence of recorded action potentials. On stimuli were presented against a dark background and Off stimuli were the return to it. The contrast was 99.2% (determined with a Spectra Pritchard photometer model 1980A-WB) and the bright stimulus illumination was 120 lux.

The experimental protocol consisted of three phases. In the first, we determined the preferred direction of the cell and the approximate shape of the excitatory RF center by using hand-controlled stimuli. In the second phase, we determined the RF profile more quantitatively by stimulating the cells with a linear array of 15 60 × 60 μm contiguous spots along the preferred-null axis. The spots (whose centers were 60 μm apart) spanned 900 μm on a line through the middle of the excitatory RF center, as illustrated schematically in Fig. 1A. The response profile was determined by extracellularly recording the light onset and offset responses to a minimum of 30 repetitions of each of these 15 spots, which were presented in a pseudorandom sequence.

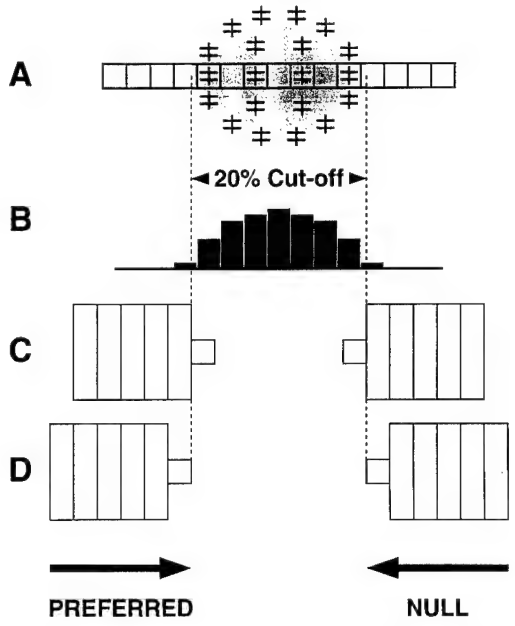

Fig. 1. Schematic illustration of the protocols used in the experiment. A: Illustration of the extent of excitatory RF center defined by excitatory response elicited at the onset (+) and offset (−) of small flashing spots (plus/minus combined symbols; spot size corresponds approximately to symbol size). The excitatory RF center determined by this method, indicated by the shaded area, has been shown to correspond closely to the extent of the cell's dendritic arborization. Superimposed on this excitatory RF center, and extending beyond it, is a linear array of 15 spots used to assess quantitatively the sensitivity profile of the excitatory RF center. B: Schematic response profile obtained after averaging 30 stimulus presentations of each spot position. The 20% cutoff boundary is estimated by linear interpolation. C: Positions of apparent motion stimuli for determining the effect of extra-receptive-field-center slits on responses to spots just inside the 20% cutoff boundary for the excitatory RF center. D: Positions of apparent motion stimuli for determining the effect of extra-receptive-field-center slits on responses to spots just outside the 20% cutoff boundary for the excitatory RF center.

A plot of a "typical" profile obtained at each of the spot positions (averaged combined onset and offset responses) is shown schematically in Fig. 1B. The limits of the excitatory RF center along this line were estimated by linear interpolation as the positions where the responses became less than 20% of the maximum obtained in the middle of the RF. These boundaries are indicated schematically by the vertical dashed lines in Fig. 1B. This 20% contour definition provides a reasonable estimate of the extent of the dendritic field (as demonstrated by Yang & Masland, 1992, using the identical criteria). The steep decline in excitability beyond this 20% point is due to the very strong inhibitory surround of these cells (Barlow et al., 1964; Barlow & Levick, 1965; Levick, 1967).

The third phase of the experiment used the protocol illustrated in Figs. 1C and 1D. We picked four locations for small (60 × 60 μm) spots, two of which were just inside, and two just outside the 20% borders determined above, and six to ten locations for slits 60 μm wide and 400 μm long, placed at 60-μm intervals from just outside the excitatory RF center border to considerably outside the excitatory RF center in the surround.

The scheme for apparent motions towards the spots just inside the excitatory RF center border is shown in Fig. 1C (preferred-direction apparent motion on the left, null-direction apparent motion on the right); that for apparent motion towards spots placed just outside the excitatory RF center border is shown in Fig. 1D. The apparent motion protocol was used to determine if apparent motion stimulation involving any of the slits outside the excitatory RF center could facilitate (or inhibit) the responses to either of the spots just inside or just outside the excitatory RF center.

The apparent motion protocol involved both On and Off modulation of each of the slits 200 ms prior to similar modulation of one of the spots. The onset of the slit occurred 200 ms before the onset of the spot, and likewise, the offset of the slit occurred 200 ms before offset of the spot, so that On–On and Off–Off interaction effects could be segregated from On–Off interactions. (The slits remained on for 1 s, and the delay between the beginning of two consecutive On stimuli was 2250 ms.) This protocol was based on previous findings within the RF center of these cells that facilitatory and inhibitory effects tend to be segregated between On and Off pathways, and that using a 200-ms delay, both facilitatory and inhibitory apparent motion effects could be observed (Amthor & Grzywacz, 1993; Grzywacz & Amthor, 1993).

The strength of facilitation and inhibition was determined by comparing the response of the spots by themselves to the responses obtained when their modulations were preceded by modulations of one of the slits located in the surround. In a few cases, where small excitatory responses were elicited from the slits in the surround (mainly for the slits closest to the excitatory RF center), the method of "base subtraction" described previously (Amthor & Grzywacz, 1991) was used to compensate for the expected small excitatory response due to the slit occurring during, and therefore contributing to, the spot response histogram. For the vast majority of slit presentations base subtraction had little or no effect on the results, because rarely was there any response elicited by slits in the surround, consistent with previous findings cited in the Introduction.

Results

We completed our experimental protocol on a total of 24 cells. All were located within 1 to 2 mm of the visual streak of the rabbit retina, and had RF sizes ranging from 200 to 300 μm. Fig. 2 shows the peristimulus-time (PST) histograms of the responses obtained in the experimental protocol shown in Fig. 1C for an On–Off DS ganglion cell (E525C7), plotted here with the orientation of the preferred direction shown as downward. The results presented for this cell are generally typical for the sample of 24 cells, except where noted. The top and bottom most histograms in Fig. 2 are the extracellularly recorded responses to slits "X" and "Y", respectively, whose centers were 150 μm outside the nearest excitatory RF center border. The modulation of slit X in the surround on the "preferred side" (from which preferred-direction-moving spots approach the RF center) elicited no response whatsoever, as was generally the rule. Mod-

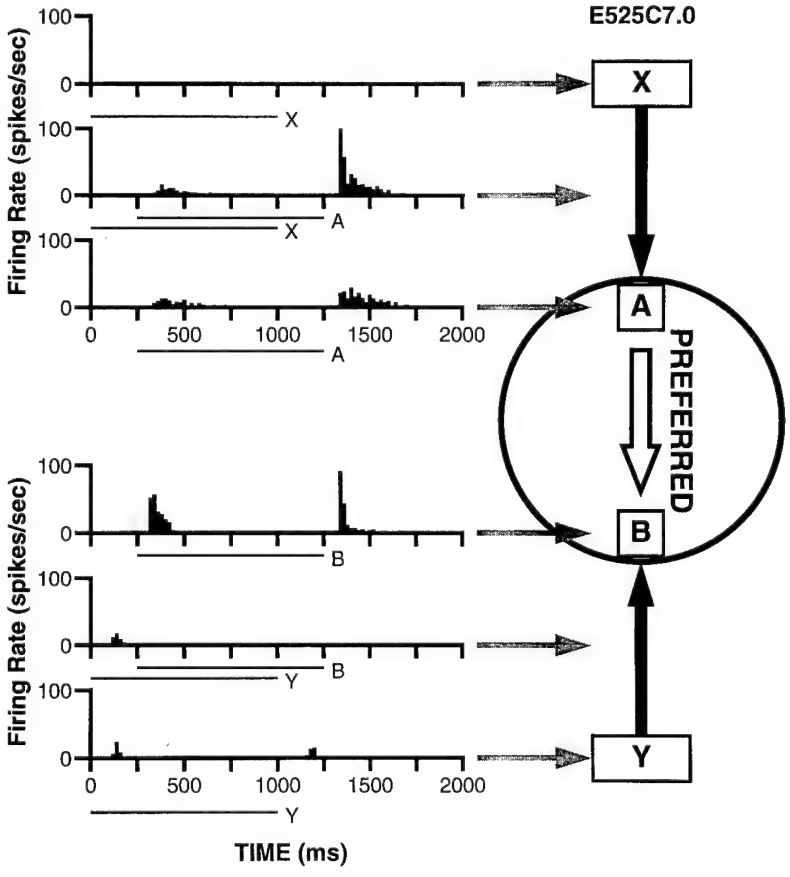

Fig. 2. The PST histograms of the responses obtained in experimental protocol 1C for On–Off DS ganglion cell E525C7. The top most and bottom most histograms are the responses elicited by the slits X and Y whose centers were 150 μm outside the RF center borders. The third and fourth histograms are the responses elicited by the two spots (A and B) just inside the RF center borders. The second and fifth histograms are the responses to the preferred- and null-direction apparent motions (respectively) from the slits towards the spots (indicated by the arrows: X to A is preferred-direction apparent motion, Y to B null-direction apparent motion). Lines underneath the histograms followed by letters A, B, X, or Y give the duration of the stimulus above background. Bin size in this and all other histograms was 20 ms. Histograms are the averages of 50 trials.

ulation of slit Y on the "null side" (from which null-direction-moving spots approach the RF center) elicited a very small response (surround stimulations generally produced little or no responses by themselves).

The third and fourth histograms in Fig. 2 are the responses elicited by spots A and B, which are just inside the top and bottom excitatory RF center borders, respectively. Both spots elicit significant Off responses; the On response of spot A, while significant, is smaller than that of spot B. Small differences in the extent and relative sensitivity of the On- *vs.* Off-center excitatory RF areas are not unusual, and have been previously well documented, as discussed in the Introduction.

The second histogram in Fig. 2 is the preferred-direction apparent-motion response from slit X towards spot A (motion indicated by the heavy, dark, downward-pointing arrow). This histogram shows that the preferred-direction apparent motion increases the spot A offset response significantly (approximately by a factor of 1.8) and the spot A onset response to a somewhat lesser extent. Thus, modulation of a slit located in the surround of a considerable distance from the border of the excitatory RF center, which itself elicits no response whatsoever (top histogram), can facilitate the On and Off responses elicited by a spot within the excitatory RF center. This demonstrates that the facilitatory receptive field extends significantly outside the traditional excitatory RF center.

We used an identical, mirror-image null-direction apparent motion protocol from the surround to the null side of the excitatory RF center border, to determine whether extra-RF-motion facilitation was spatially asymmetric. The fifth histogram shows the response to the null-direction apparent motion (indicated by the dark, heavy, upward-pointing arrow) from the slit Y, outside the RF center, towards the spot B, just inside the RF center. In contrast to the result obtained for the preferred-direction apparent motion (second histogram), the null-direction apparent motion dramatically reduced the spot B onset and offset responses (comparing histogram 5 with histogram 4), despite the fact that a small excitatory response was actually elicited by slit Y in the surround, when presented by itself.

The asymmetry of the motion facilitation effect suggests that the facilitatory RF is direction-of-motion specific, and thus, likely to involve a mechanism distinct from that which mediates the stationary, excitatory RF center that is coincident with the dendritic arborization. However, it should be kept in mind that the protocols reported here can only show that the facilitation observed is *effectively* direction-of-motion specific, and that it could arise either from a truly asymmetric facilitatory mechanism, or a symmetrical mechanism interacting with an asymmetrical inhibitory one.

Fig. 3 shows the average responses (total spikes) elicited by each of the 60 μm × 60 μm spots in the linear array experiment (dashed lines) and for the apparent motions from all of the slits toward the spots just inside the excitatory RF center borders (as shown schematically in Fig. 1C). Fig. 3A (top) shows the results for the Off responses of cell E525C7 (same cell as Fig. 2); Fig. 3B (bottom) shows the results for the On responses of another On–Off DS ganglion cell (E523C2). The responses elicited along the linear array of spots (dashed lines) declines abruptly past the 20% cutoff loci, as reported earlier by Yang and Masland (1992), who showed that the excitatory RF center borders of these cells are similar in size and extent to the underlying On–Off DS ganglion cell dendritic trees. The excitatory RF center diameters for these two cells (which were within 1 mm

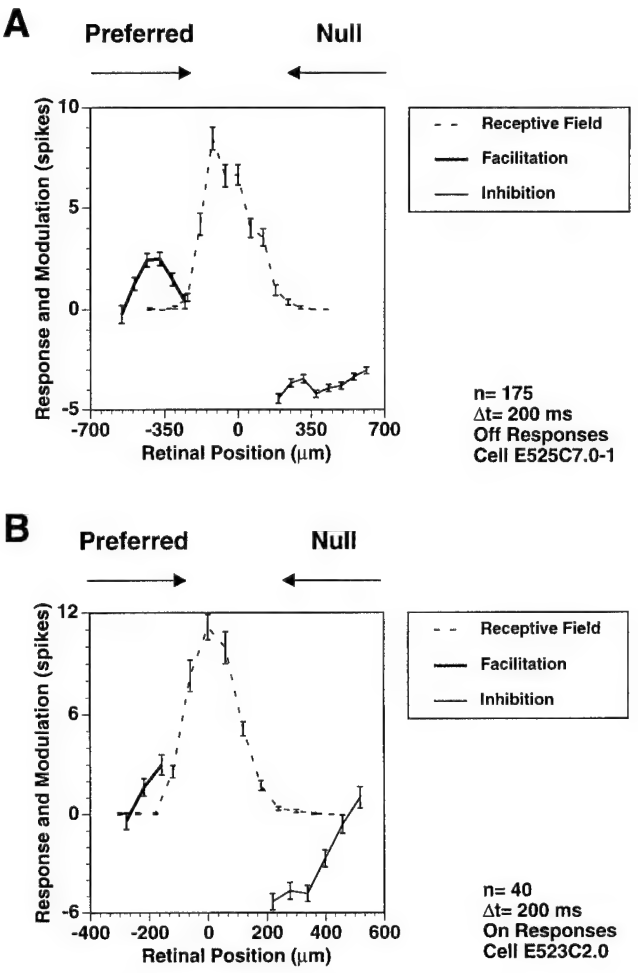

Fig. 3. Extra-receptive-field facilitation and inhibition elicited by apparent motion. The dashed lines show the average responses (number of spikes) for each of the 60 μm × 60 μm spots in the linear array experiment (shown schematically in Figs. 1A and 1B). The solid lines show the changes in the responses to the spots during the apparent motions from each of the slits toward the spots just inside the excitatory RF center borders (as shown schematically in Fig. 1C). The heavy solid lines on the left sides of A and B show the extra number of spikes the apparent-motion facilitatory process elicited as a function of distance (at each slit position). The lighter solid lines on the right sides of A and B show the reduction in the spikes elicited by the spots due to modulation of the slits at various distances on the null side of the excitatory RF center border. The error bars represent standard errors. A: The Off responses of On–Off DS ganglion cell E525C7 (175 trials). B: The On responses of On–Off DS ganglion cell E523C2 (40 trials). In both cells the facilitation effect on the "preferred side" declined to become marginally significant inhibition at the farthest distance shown. At farther distances on the preferred side (not shown), surround stimulation typically produced surround-like inhibition, similar to that observed on the "null side".

of the visual streak) were on the order of 300 μm; those of all 24 On–Off DS ganglion cells recorded within 1 to 2 mm of the visual streak ranged from 200 to 300 μm.

The heavy solid lines on the left side of Figs. 3A and 3B show, as a function of position, the extra number of spikes by which the apparent-motion facilitatory process from each of the slit positions incremented the response to spot A. The results in

Fig. 3A demonstrate that facilitation can be propagated to the RF center from distances as much as 300 μm outside the closest edge of the excitatory RF center. The lighter solid lines on the right side of Figs. 3A and 3B show, as a function of position, the number of spikes by which the inhibitory process (on the opposite side of the RF center) decremented the center excitatory response. The range of inhibition is longer than that of facilitation, and generally exceeded that of the farthest inhibiting slit used in these experiments.

We observed significant extra-RF-center facilitation in fifteen of twenty four cells. For all cells, the facilitation effect elicited by stimuli within the surround declined with distance. At very large distances (beyond that shown in Fig. 3), stimulation within the surround typically became inhibitory, presumably reflecting the normal surround inhibitory mechanism of the cells, which is masked by strong facilitation only at short distances. For the On responses of cell E523C2 (Fig. 3B), facilitation was maximal at the shortest distance tested (30 μm; center of 60 μm wide slit), and was significant out to about 90 μm. For the Off responses of E525C7 (Fig. 3A), the facilitation was not maximal, or even significant, at 30 μm, the shortest distance tested. Instead, the maximum occurred at 150 μm, and facilitation was significant out to 270 μm. The occasional finding of an optimal distance to elicit facilitation is further evidence that it is direction-of-motion specific, and not due to a general summation of the responses to the spot and slit, or to an error in locating the border of the exact excitatory RF center border. In the latter case, the strongest facilitation effect would always be expected to be produced by slits closest to the excitatory RF center, where the greatest excitation would be expected.

The inhibition elicited by the null-direction apparent motion from the surround tended to be strongest for the shortest distances, but its range typically exceeded 300 μm. This result is consistent with previous findings within the RF center of these cells (Amthor & Grzywacz, 1993; Grzywacz & Amthor, 1993) that the spatial range of null-direction inhibition is larger than that of preferred-direction facilitation. It is also consistent with previous results that null-direction inhibition is mediated by a separate mechanism from that of surround inhibition, having distinct timing and spatial range properties; normal surround inhibition is more transient than null-direction inhibition (Amthor & Grzywacz, 1993; Merwine et al., 1995) and thus has a relatively weak effect at the 200-ms delay used in our protocols. As the first stimulus (the slit) in the null-direction apparent motion protocol is placed farther outside the RF center, the specific null-direction inhibitory mechanism declines in strength, and inhibitory effects observed appear to be more dominated by the normal inhibitory surround.

The population statistics for the spatial parameters of preferred-direction facilitation, obtained with the protocol of Fig. 1C, are shown in Fig. 4 for the 24 cells of this study. Fig. 4A shows the percentage of cells having maximal facilitation at particular distances from the excitatory RF center border. As seen for the Off response of cell E525C7 (Fig. 3A), the maximum facilitation distance for many cells was not always the position of the closest slit, suggesting, as discussed above, that the facilitatory effect was truly motion specific.

Fig. 4B shows the percent of cells in which facilitation could be elicited at various distances. In nine of 24 cells, we observed no statistically significant facilitation at any distance outside the RF center (see Discussion). In the other 15 cells, the spatial range of facilitation outside the RF border from which slits could elicit facilitation was highly variable, ranging from less than 60 μm to about 300 μm, with the most typical facilitatory range lying between 60 and 120 μm.

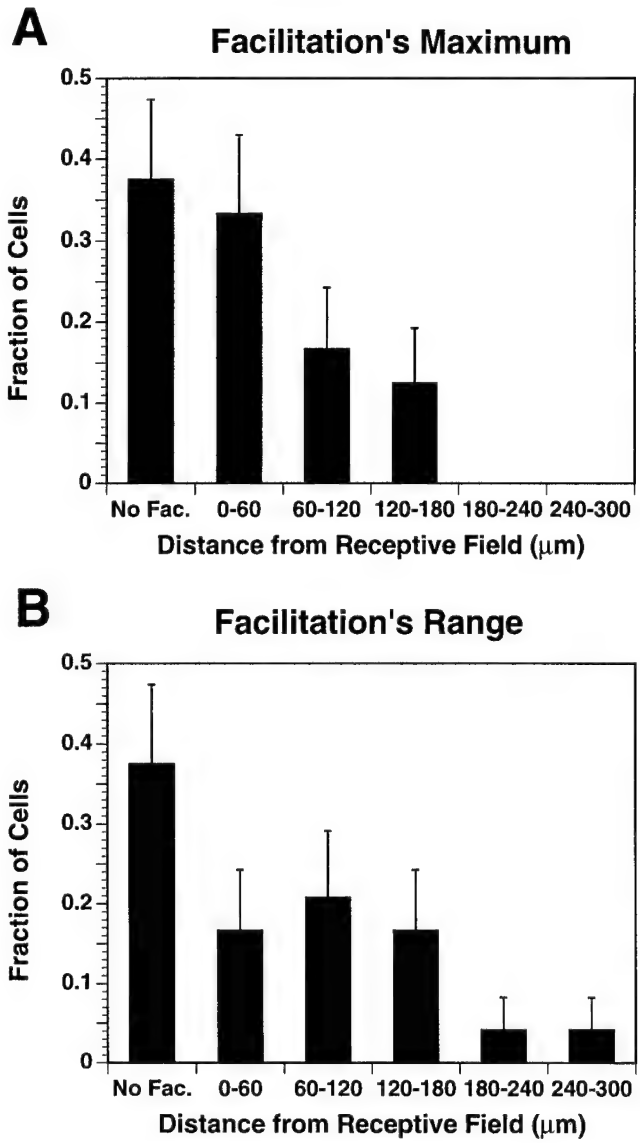

Fig. 4. The population statistics for the spatial parameters of preferred-direction facilitation, obtained with the protocols of Figs. 1C and 1D. A: The percentage of cells having maximal facilitation at particular distances from the excitatory RF center border. B: The percent of cells in which facilitation could be elicited at various distances. The error bars are the standard error bars for each bin assuming that the distributions follow a multinomial distribution, with each bin representing a separate category. In nine of 24 cells, we observed no statistically significant facilitation at any distance outside the RF center (see Discussion). In the other 15 cells, the spatial range of facilitation outside the RF border from which slits could elicit facilitation was highly variable, ranging from less than 60 μm to about 300 μm, with the most typical facilitatory range lying between 60 and 120 μm. The relatively narrow range of facilitation compared to inhibition is consistent with the previous findings of Grzywacz and Amthor in apparent-motion protocols inside the RF center (1993).

The spatial parameters of facilitation were similar for apparent motions ending just inside or just outside the RF (proto-

cols of Figs. 1C and 1D, respectively). However, facilitation was much harder to detect for spots placed just outside the excitatory RF center border, probably because the spot responses there still tended to be below threshold. Overall, there were no significant trends in the spatial parameters of facilitation as a function of the polarity (On or Off) of the stimulus contrast. That is, in some cells, facilitation was stronger for Off than for On stimuli, in others, the reverse was true. We did not explicitly test interactions between slit onset and spot offset (and *vice versa*) in these experiments because previous results using similar protocols within the excitatory RF center showed little significant cross-sign (On and Off) effects (Grzywacz & Amthor, 1993).

Discussion

Our experimental results show that both facilitation and inhibition of responses to spots within the excitatory RF center can be elicited from distances of 200 μm or more outside the excitatory RF center. These response modulations are asymmetric as a function of direction of motion, with facilitation occurring only for preferred-direction motions and inhibition occurring mostly for null-direction motions. This asymmetry, and the finding that facilitation occasionally requires a minimal distance before being optimal, suggest that facilitation depends on motion and is not simply summation of excitation, such as might be expected to occur within the RF center (see Grzywacz & Amthor, 1993 for a broader discussion on this issue). The data here confirm the existence of extra-receptive-field facilitation that was observed previously by Grzywacz and Amthor (1993, Fig. 6); in that study it was also shown that the directional tuning of facilitation is broad (>90 deg).

The failure to observe extra-receptive-field facilitation in 37% of the cells (Fig. 4) does not necessarily mean that some cells lack a facilitatory mechanism. Rather, the inability to detect facilitation may be due to variation in the balance between facilitation and surround inhibition (which clearly can be seen at large distances even in experiments where facilitation is significant at shorter ones, see Fig. 3). This inhibition might often be counteracted by preferred-direction facilitation due to short, but not long-distance motions, since the spatial range of facilitation is relatively narrow. Detection of facilitation may also be sensitive to the positioning of the facilitated spot in a region where the facilitation effect is suprathreshold. It is also possible that continuous motion in the preferred direction from the surround to the excitatory RF center border might provide a more effective facilitatory stimulus than the particular apparent motion protocol used here.

Because the majority of cells showed preferred-direction facilitation from outside the excitatory RF center, the data reported here suggest reassessing the objection raised by Yang and Masland (1992) to models of directional selectivity based on asymmetric excitatory-amacrine inputs to DS cells. There is considerable anatomical and pharmacological evidence (Masland & Ames, 1976; Ariel & Daw, 1982; Famiglietti, 1992) for the involvement, in retinal directional selectivity, of starburst amacrine cells whose processes extend considerably outside the DS ganglion cell excitatory RF center. Two such models, proposed by Vaney (1990) and Borg-Graham and Grzywacz (1992), postulated that starburst amacrine dendrites pointing (from cell body to dendritic ending, or tip) towards the preferred direction of a DS ganglion cell might contact that cell more often than dendrites pointing in the opposite direction. Because the release of acetylcholine is from the region near the dendritic tip of the amacrine cells, starburst dendrites just contacting the edge of the DS ganglion cell's dendritic tree (from where preferred-direction motions first enter the cell's excitatory RF center) would be expected to convey inputs to the DS ganglion cell from outside its own dendritic arborization. The coincidence between the spatial range of extra-receptive-field facilitation (Fig. 4) and the sizes of starburst amacrine cells at the same eccentricity (Tauchi & Masland, 1984) lends further support for these asymmetric amacrine models.

Yang and Masland argued that because the DS ganglion cell dendritic tree and excitatory RF center were relatively in good register, models such as those of Vaney, and Borg-Graham and Grzywacz involving the lateral spread of excitation from outside this area were untenable. Our data suggest, however, a different interpretation of Yang and Masland's results. The role of excitatory amacrine cells might be to modulate, *via* a motion-specific facilitation, the responses of DS cells to give rise to their directional selectivity. In this case, although the profile of the traditional RF might be dominated by direct bipolar inputs to the DS cell within the region of its dendritic arborization, facilitatory inputs, which themselves might not be capable of directly eliciting suprathreshold excitatory responses, could affect the ganglion cell from outside this region.

That significant, direction-of-motion specific facilitation is conducted from well outside the classical excitatory receptive-field center (and, therefore, dendritic arborization) of On–Off DS ganglion cells highlights the fundamental distinction between excitatory and facilitatory mechanisms in retinal ganglion cell receptive-field organization. One long-standing, well-studied precedent for this distinction is the McIlwain (shift) effect (1964), which is an example of a motion-sensitive, extra-receptive-field facilitation capable of elevating the maintained, or excitatory RF center modulation spiking activity of Y, and to a lesser extent, X and some W ganglion cells in cat. Although almost certainly mediated by a different mechanism than reported here, it serves as a classical forerunner for retinal processes whose action is primarily facilitatory, rather than directly excitatory themselves. Unraveling the biophysical basis of this example of a facilitatory mechanism in On–Off DS ganglion cells of the rabbit retina, and determining whether it is indeed based on cholinergic amacrine cells, is clearly an important challenge for future research efforts.

Acknowledgments

We wish to thank William W. Belser III and Mark Villa for programming support and Lorraine DeAngelis for technical assistance. Supported by NEI EY05070, EY08921, and ONR N00014-91-J-1280.

References

Amthor, F.R. & Grzywacz, N.M. (1988). The time course of inhibition and the velocity independence of direction selectivity in the rabbit retina. *Investigative Ophthalmology and Visual Science* **29**, 225.

Amthor, F.R., Oyster, C.W. & Takahashi, E.S. (1984). Morphology of ON-OFF direction-selective ganglion cells in the rabbit retina. *Brain Research* **298**, 187–190.

Amthor, F.R., Takahashi, E.S. & Oyster, C.W. (1989). Morphologies of rabbit retinal ganglion cells with complex receptive fields. *Journal of Comparative Neurology* **280**(1), 97–121.

AMTHOR, F.R. & GRZYWACZ, N.M. (1991). The nonlinearity of the inhibition underlying retinal directional selectivity. *Visual Neuroscience* **6**, 197–206.

AMTHOR, F.R. & GRZYWACZ, N.M. (1993). Inhibition in On–Off directionally selective ganglion cells in the rabbit retina. *Journal of Neurophysiology* **69**(6), 2174–2187.

ARIEL, M. & DAW, N.W. (1982). Effects of cholinergic drugs on receptive field properties of rabbit retinal ganglion cells. *Journal of Physiology* **324**, 135–160.

BARLOW, H.B., HILL, R.M. & LEVICK, W.R. (1964). Retinal ganglion cells responding selectively to direction & speed of image motion in the rabbit. *Journal of Physiology* **173**, 377–407.

BARLOW, H.B. & LEVICK, W.R. (1965). The mechanism of directionally selective units in the rabbit's retina. *Journal of Physiology* **178**, 477–504.

BORG-GRAHAM, L.J. & GRZYWACZ, N.M. (1992). A model of the directional selectivity circuit in retina: transformations by neurons singly and in concert. In *Single Neuron Computation*, ed. MCKENNA, T., DAVIS, J. & ZORNETZER, S.F. pp. 347–375. Orlando, Florida: Academic Press.

DACEY D.M. & LEE, B.B. (1994). The 'blue-on' opponent pathway in primate retina originates from a distinct bistratified ganglion cell type. *Nature* **367**(24), 731–735.

FAMIGLIETTI, E.V. (1992). Dendritic co-stratification of ON and ON–OFF directionally selective ganglion cells with starburst amacrine cells in rabbit retina. *Journal of Comparative Neurology* **324**, 322–335.

GRZYWACZ, N.M., AMTHOR, F.R. & MERWINE, D.K. (1993). Extra receptive field facilitation in rabbit's retinal directional selectivity. *Neuroscience Abstracts* **19**, 1258.

GRZYWACZ, N.M., AMTHOR, F.R. & MISTLER, L.A. (1990). Applicability of quadratic and threshold models to motion discrimination in the rabbit retina. *Biological Cybernetics* **64**, 41–49.

GRZYWACZ, N.M., AMTHOR, F.R. & MERWINE, D.K. (1994*a*). Directional hyperacuity in ganglion cells of the rabbit retina. *Visual Neuroscience* **11**, 1019–1025.

GRZYWACZ, N.M., HARRIS, J.M. & AMTHOR, F.R. (1994*b*). Computational and neural constraints for the measurement of local visual motion. In *Visual Detection of Motion*, ed. SMITH, A.T. & SNOWDEN, R.J., pp. 19–50. San Diego, California: Academic Press.

GRZYWACZ, N.M. & AMTHOR, F.R. (1993). Facilitation in On–Off directionally selective ganglion cells in the rabbit retina. *Journal of Neurophysiology* **69**(6), 2188–2199.

LEVICK, W.R. (1967). Receptive fields and trigger features of ganglion cells in the visual streak of the rabbit's retina. *Journal of Physiology* **188**, 285–307.

MASLAND, R.H. & AMES, A., III. (1976). Responses to acetylcholine of ganglion cells in an isolated mammalian retina. *Journal of Neurophysiology* **39**(6), 1220–1235.

MCILWAIN, J.T. (1964). Receptive fields of optic tract axons and lateral geniculate cells: Peripheral extent and barbiturate sensitivity. *Journal of Neurophysiology* **27**, 1154–1173.

MERWINE, D.K., AMTHOR, F.R. & GRZYWACZ, N.M. (1995). The interaction between center and surround in rabbit retinal ganglion cells. *Journal of Neurophysiology* **73**, 1547–1567.

PEICHL, L. & WÄSSLE, H. (1983). The structural correlate of the receptive field centre of alpha ganglion cells in the cat retina. *Journal of Physiology* **341**, 309–324.

TAUCHI, M. & MASLAND, R.H. (1984). The shape and arrangement of the cholinergic neurons in the rabbit retina. *Proceedings of the Royal Society B* (London) **223**, 101–119.

VANEY, D.I. (1990). The mosaic of amacrine cells in the mammalian retina. In *Progress in Retinal Research, (Vol. 9)*, ed. OSBORNE, N. & CHADER, J., pp. 49–100. Oxford, England: Pergamon Press.

WÄSSLE, H., BOYCOTT, B.B. & ILLING, R.-B. (1981). Morphology and mosaic of on- and off-beta cells in the cat retina and some functional considerations. *Proceedings of the Royal Society B* (London) **212**, 177–195.

YANG, G. & MASLAND, R.H. (1992). Direct visualization of the dendritic and receptive fields of directionally selective retinal ganglion cells. Science **258**, 1949–1952.

YANG, G. & MASLAND, R.H. (1994). Receptive fields and dendritic structure of directionally selective retinal ganglion cells. *Journal of Neuroscience* **14**(9), 5267–5280.

Proc. Natl. Acad. Sci. USA
Vol. 92, pp. 4002–4005, April 1995
Neurobiology

Spatial organization of retinal information about the direction of image motion

FRANKLIN R. AMTHOR*† AND CLYDE W. OYSTER‡

*Department of Psychology and Neurobiology Research Center and ‡Department of Physiological Optics, School of Optometry, University of Alabama at Birmingham, Birmingham, AL 35294-1170

Communicated by John E. Dowling, Harvard University, Cambridge, MA, January 3, 1995

ABSTRACT **The visual stimuli that elicit neural activity differ for different retinal ganglion cells and these cells have been categorized by the visual information that they transmit. If specific visual information is conveyed exclusively or primarily by a particular set of ganglion cells, one might expect the cells to be organized spatially so that their sampling of information from the visual field is complete but not redundant. In other words, the laterally spreading dendrites of the ganglion cells should completely cover the retinal plane without gaps or significant overlap. The first evidence for this sort of arrangement, which has been called a tiling or tessellation, was for the two types of "α" ganglion cells in cat retina. Other reports of tiling by ganglion cells have been made subsequently. We have found evidence of a particularly rigorous tiling for the four types of ganglion cells in rabbit retina that convey information about the direction of retinal image motion (the ON–OFF direction-selective cells). Although individual cells in the four groups are morphologically indistinguishable, they are organized as four overlaid tilings, each tiling consisting of like-type cells that respond preferentially to a particular direction of retinal image motion. These observations lend support to the hypothesis that tiling is a general feature of the organization of information outflow from the retina and clearly implicate mechanisms for recognition of like-type cells and establishment of mutually acceptable territories during retinal development.**

The four types of ON–OFF direction-selective ganglion cells in the rabbit retina are distinguished from one another by the direction of stimulus motion to which they respond maximally; the preferred directions are orthogonal and correspond roughly to up, down, anterior, and posterior in the visual field (1). And as a class, the ON–OFF direction-selective cells have a distinctive dendritic morphology; each cell has dendrites ramifying at two levels within the inner plexiform layer (IPL) and both ramifications form a mesh-like space-filling array of processes (2, 3). The four types of direction-selective cells, however, cannot be distinguished from one another by their morphology (2, 3).

Estimates of direction-selective cell density and the average size of their dendritic fields suggest that the direction-selective cells have a retinal coverage factor equal to four (2, 3). Since there are four functional cell types, the obvious possibility is unity coverage by each of them. Vaney (4) provided experimental support for the hypothesis that direction-selective cells, or some subset thereof, had unity coverage by showing that an injection of biocytin into a single ganglion cell soma could label an array of six or so cells, whose dendrites touched, but did not cross, and whose morphology was consistent with that of ON–OFF direction-selective cells.

The original demonstrations of the α (Y) cell tiling in cat retina (5–7) used a selective stain to label the α cells that were shown to map, one to one, with physiologically identified Y cells from earlier extracellular recordings. Here, we have used a direct method in which we physiologically identified neighboring ON–OFF direction-selective cells, thereby establishing their directional type, and injected the identified cells with horseradish peroxidase under visual control. In the anatomical analysis, it was readily apparent that some neighboring dendritic fields did not overlap while others overlapped extensively. The nonoverlapping cells were of the same physiological type, and the overlapping cells were of a different physiological type. These observations can be explained only by the existence of four spatially independent dendritic mosaics, one for each of the four cell types.

METHODS

Except for mounting and visualizing the retinas, the methods were similar to those we used earlier (8). The rabbits were deeply anesthetized by intravenous injection of urethane (1.5 g/kg), and under dim red illumination, one eye was removed and hemisected (the animals were then given a lethal dose of anesthetic). The vitreous was removed from the posterior segment of the eye and the retina was carefully removed from the eye cup. The retina was hemisected so that it could be flattened onto a porous tissue culture membrane and placed in a perfusion chamber mounted on a microscope stage. A small amount of methylene blue added to the perfusate was incorporated into the ganglion cell somata, allowing them to be seen with a ×20 or ×40 water-immersion objective.

Under visual control, an extracellular electrode was used to record the responses of ganglion cells to visual stimuli focused on the retina, thereby allowing the cells to be classified by their response properties. By recording from a number of cells in the field, we generated a map showing the relative locations of various types of cells. These same cells were then impaled with a micropipet, their identity was confirmed, and cells were injected with horseradish peroxidase to produce a dark reaction product throughout the cells' dendrites when the retina was reacted with diaminobenzidine. After the processed retina was mounted on a slide and covered with a coverslip, the labeled cells were drawn with the aid of a camera lucida using a ×100 objective on the microscope.

RESULTS

Unity coverage for each of the direction-selective cell types can be seen in the morphological relationships between pairs or triplets of neighboring direction-selective cells with the same or different preferred directions. Fig. 1 illustrates the key result. In this case, three neighboring ON–OFF direction-selective cells were injected with horseradish peroxidase; their dendritic branching in the outer part of the IPL is shown in Fig.

The publication costs of this article were defrayed in part by page charge payment. This article must therefore be hereby marked "*advertisement*" in accordance with 18 U.S.C. §1734 solely to indicate this fact.

Abbreviation: IPL, inner plexiform layer.

†To whom reprint requests should be addressed at: Department of Psychology, University of Alabama at Birmingham, Birmingham, AL 35294-1170.

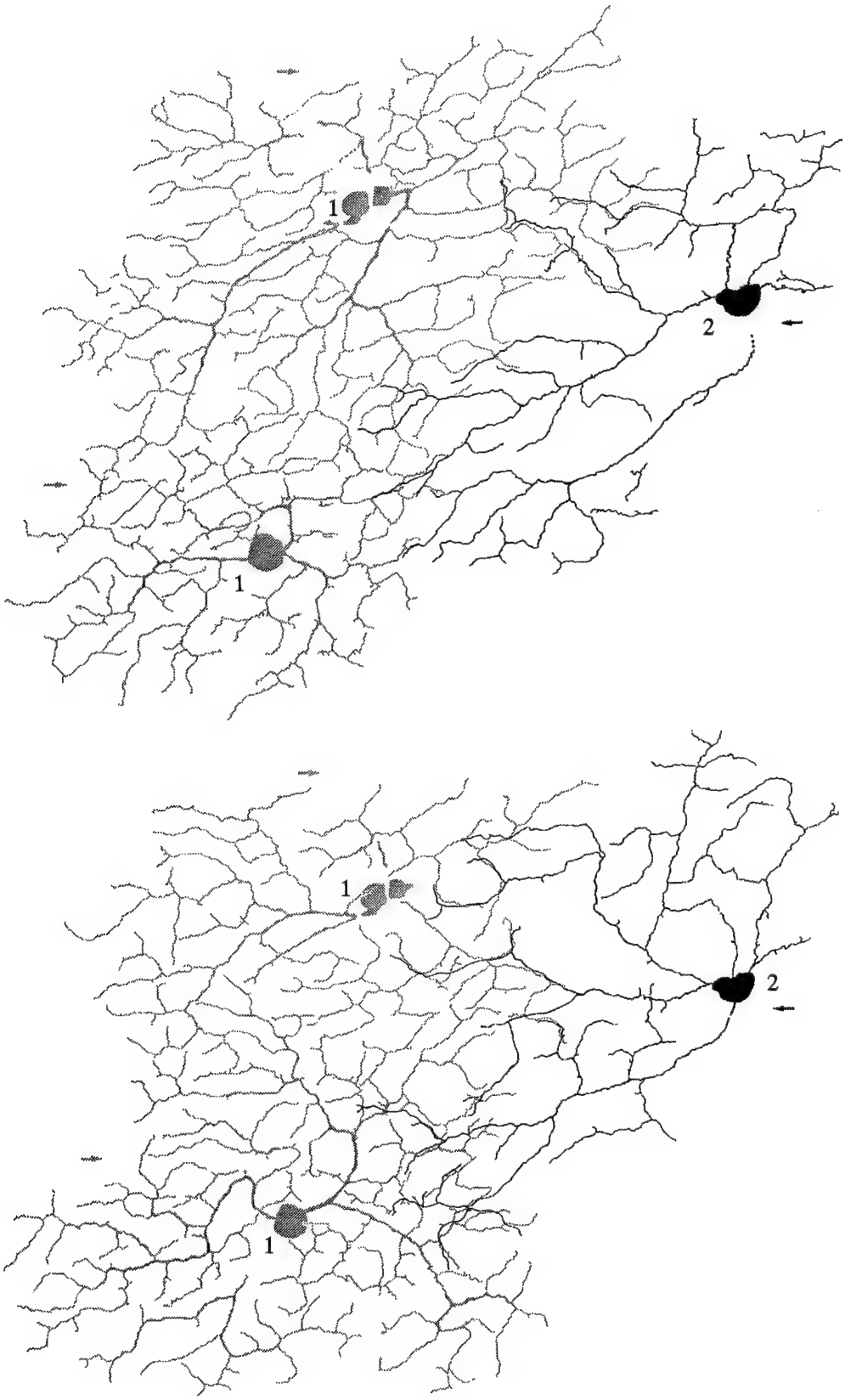

FIG. 1. Like and unlike-type ON–OFF direction-selective ganglion cells. The dendritic arbors of these cells are bistratified in the IPL and the two branching planes are shown separately. (*Upper*) The outer IPL level. (*Lower*) The inner IPL level. The two cells with the same preferred direction are labeled cell 1; the cell with the opposite preferred direction is labeled cell 2. The like-type cells (cells 1) have dendrites that touch but do not cross and the dendritic domains of the two cells do not overlap. Cell 2 does not respect the territories occupied by dendrites of the other two cells; there are numerous dendritic crossings and overlap of the dendritic fields. In places, the dendrites of cell 2 run parallel to or intertwine with those of the other cells (cells 1). This sort of fasciculation is characteristic of the relationship between unlike-type cells. The three cells here demonstrate the pattern we have found consistently; cells of the same type participate in tilings of the branching planes, but cells of unlike type belong to different tilings.

1 *Upper* and the inner IPL branching is in Fig. 1 *Lower*. The two cells labeled 1 had the same preferred direction (rightward in the figure or posterior on the retina), whereas the cell labeled 2 had a preferred direction opposite to the other two cells.

The dendrites of the like-type pair (cells 1) do not overlap in either of the IPL branching planes; there are places where the dendrites touch but there is no significant crossing of dendrites. The two cells have different ramification areas in the two branching planes—the upper cell 1 branches more extensively in the outer IPL, whereas the lower cell 1 branches more extensively in the inner IPL—but each cell establishes separate domains in the respective sublayer on which the other cell does not intrude. Thus, the dendritic ramifications of these two cells form independent tilings in each of the IPL branching planes.

The cell labeled 2 has a preferred direction opposite to the others and its dendrites do not respect the territories of the other two cells; crossing branches are quite apparent and there is considerable overlap of the dendritic fields. (This cell was lightly labeled and we have not drawn all of its dendrites; the overlap was actually more extensive than is shown here.) This result is very straightforward and the conclusion is obvious; cells with different preferred directions do not respect one another's spatial domains. The amount of overlap between unlike pairs varies, and the overlap shown here is neither the most nor the least extensive we have seen; the fact that there is variability in the amount of overlap suggests that the mosaics of unlike-type cells have considerable spatial independence.

Some details of the dendritic interactions between neighboring cells are shown in Fig. 2. The arrowheads in Fig. 2 *A* and *B* show sites of contact or near contact between the dendrites of two cells with the same preferred direction (like-type cells). In some instances, a small gap can be seen between adjacent dendrites, but in others one dendrite appears to abut the other (it is not shown here, but these dendritic terminals often have terminal swellings at the contact sites). These dendritic appositions between cells having the same preferred direction are like those of the biocytin-coupled cells reported by Vaney (4).

Where dendrites of the cell labeled 2 overlap those of cells labeled 1 in Fig. 1, the overlapping dendrites tend to run in parallel or fasiculate. The dendrites often intertwine very tightly, a feature best seen in Fig. 2 *C* and *D* (arrowheads). We do not know if this fasciculation results from an active interaction between cells or some passive constraint on the paths that developing dendrites can follow. It is, in any event, an unexpected observation that is characteristic of all the unlike-type cell pairs we have seen. It is interesting that the fasciculating dendrites of the unlike pairs, where opportunities for junctional coupling could be most numerous, do not appear to be those that are biocytin-coupled (4).

We have labeled all four possible like-type pairs and several like-type triplets with results identical to those illustrated in Figs. 1 and 2 (see Table 1); the dendrites of like-type neighbors always tile, abutting one another without gaps or overlap. Of the various possible unlike pairs, we have labeled orthogonal cases, where the cells had horizontal and vertical preferred directions, and pairs with opposite horizontal preferred directions (Table 1). We are missing only the case where cells had vertical but opposite preferred directions. With this modest caveat, we conclude that unlike pairs always invade one another's territory with crossing and fasciculating dendrites. Unlike-type cells are not members of the same tiling.

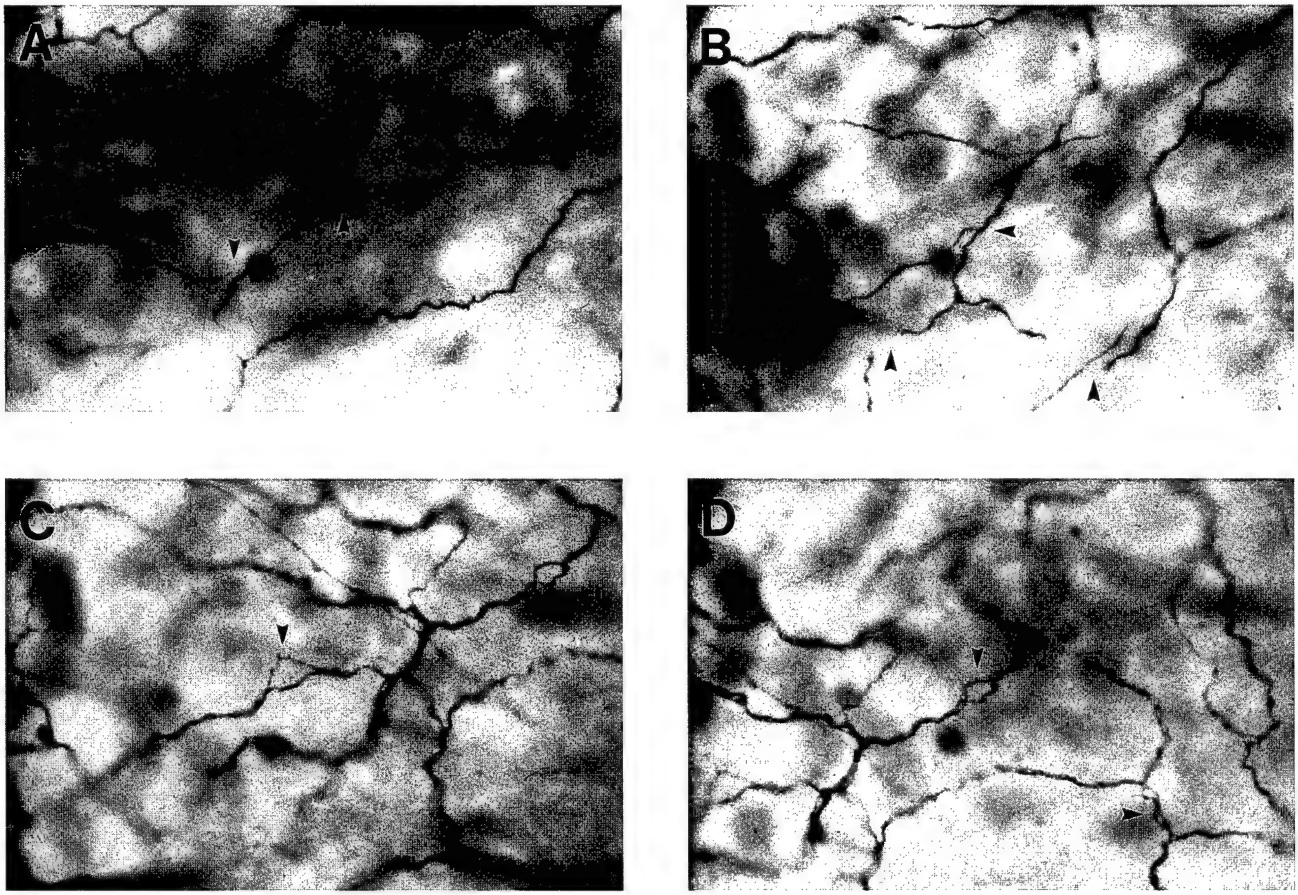

FIG. 2. Dendritic appositions and fasciculations between like and unlike-type cells. These photomicrographs are from a set of labeled cells in which there were three like-type cells and one other cell with a different preferred direction. (*A* and *B*) Dendrites from like-type neighbors come close to or abut one another without crossing (arrows). (*C* and *D*) Displaced but overlapping pictures at slightly different planes of focus that show the dendrities of unlike-type neighbors often run parallel to one another with considerable intertwining of the two cells' dendrites (arrowheads).

Table 1. Sample of like and unlike cell pairs or triplets

	Like type, both				Unlike type		
Preferred direction	←	→	↑	↓	H	V	O
Number in sample	12	3	1	1	10	0	5

Triplets with two like-type and one unlike-type cells have been counted twice, once for the like-type pairing and once for the like–unlike pairing. H, horizontal; V, vertical; O, orthogonal.

DISCUSSION

The class of ON–OFF direction-selective cells is composed of four cell types, each with a different preferred direction. Since like-type cells have nonoverlapping dendritic domains but overlap with unlike-type neighbors, the spatial organization of each cell type can be described as a tiling that provides unity coverage of the retinal plane. In fact, each cell type participates in two tilings with its dendrites, one in the inner IPL and one in the outer IPL. Thus several isomorphic ganglion cell types from a single cell class can form different independent tilings of the retinal plane and, since the size of the excitatory component of the cells' receptive fields matches the size of the dendritic fields (9), independent tilings of visual information space.

ON–OFF direction-selective cells have been encountered at numerous retinal locations from center to periphery (10, 11) and we have observed tiling at a variety of retinal locations in both superior and inferior retina. It is therefore likely that each of the four tilings extends completely across the retina (although, because peripheral direction-selective cells tend to be larger, the spatial grain of the tiling will vary from center to periphery).

When compared to other species and other cell types, these direction-selective cell tilings are more precise than the mosaics of α and β ganglion cells that have been studied in cat retina. Both the α and β cells in cat have dendrites from neighboring cells that overlap; calculated coverage factors are on the order of 1.5 for the α cells and about 3.0 for the β cells (6). The α cells in other species have similar coverage factors (12, 13). In human retina, however, midget ganglion cells injected with neurobiotin have recently been reported to have very stringent tilings with coverage factors no greater than 1 for both cell types, one of which ramifies in the inner IPL and the other in the outer IPL (14).

An obvious question is whether or not tiling by ganglion cell types is a general principle of retinal organization. At present, it is fair to say that all the results in hand are consistent with the notion of tiling by ganglion cell types. Tiling not only tells us how the retina organizes its multiple streams of information outflow but also has implications for the developmental strategies used to organize the retina. The direction-selective cells, for example, must be able to distinguish between their like and unlike-type neighbors during development and to interact appropriately to join in a tiling with their like-type neighbors. Whatever the mechanism for such recognition may be, it may also allow the different types of ganglion cells to recognize and select the particular inputs that are appropriate for the cell type.

We thank L. DeAngelis, M. Villa, W. Belser, Dr. J. Tootle, and Dr. J. Peduzzi for discussions, technical assistance, and computer programming. This work was supported by grants from the National Eye Institute, the U.S. Public Health Service, and the U.S. Office of Naval Research.

1. Oyster, C. W. & Barlow, H. B. (1967) *Science* **155,** 841–842.
2. Amthor, F. R., Takahashi, E. S. & Oyster, C. W. (1989) *J. Comp. Neurol.* **280,** 97–121.
3. Oyster, C. W., Amthor, F. R. & Takahashi, E. S. (1993) *Vision Res.* **33,** 579–608.
4. Vaney, D. I. (1991) *Neurosci. Lett.* **125,** 187–190.
5. Wässle, H., Peichl, L. & Boycott, B. B. (1981) *Nature (London)* **292,** 344–345.
6. Wässle, H., Peichl, L. & Boycott, B. B. (1981) *Proc. R. Soc. London B* **212,** 157–175.
7. Wässle, H., Boycott, B. B. & Illing, R.-B. (1981) *Proc. R. Soc. London B* **212,** 177–195.
8. Amthor, F. R., Takahashi, E. S. & Oyster, C. W. (1989) *J. Comp. Neurol.* **280,** 72–96.
9. Yang, G. & Masland, R. H. (1992) *Science* **258,** 1949–1952.
10. Levick, W. R. (1967) *J. Physiol. (London)* **188,** 285–307.
11. Oyster, C. W. (1968) *J. Physiol. (London)* **199,** 613–635.
12. Peichl, L., Ott, H. & Boycott, B. B. (1987) *Proc. R. Soc. London B* **231,** 169–197.
13. Peichl, L., Buhl, E. H. & Boycott, B. B. (1987) *J. Comp. Neurol.* **263,** 25–41.
14. Dacey, D. M. (1993) *J. Neurosci.* **13,** 5334–5355.

JOURNAL OF NEUROPHYSIOLOGY
Vol. 73, No. 4, April 1995. *Printed in U.S.A.*

Interaction Between Center and Surround in Rabbit Retinal Ganglion Cells

DAVID K. MERWINE, FRANKLIN R. AMTHOR, AND NORBERTO M. GRZYWACZ
Department of Physiological Optics, School of Optometry; Department of Psychology and Neurobiology Research Center, University of Alabama at Birmingham, Birmingham, Alabama 35294; and The Smith-Kettlewell Eye Research Institute, San Francisco, California 94115

SUMMARY AND CONCLUSIONS

1. The interaction between the center and surround mechanisms of a variety of rabbit retinal ganglion cell classes was examined in extracellular single-unit recordings in an isolated eyecup preparation. Ganglion cell classes studied included ON and OFF brisk sustained and transient, ON and OFF sluggish sustained and transient, ON-OFF and ON directionally selective, orientationally selective, and large field units. The surround effects observed were qualitatively similar in all these ganglion cell classes.

2. The average response-versus-contrast functions for stimuli within the ganglion cells' receptive-field centers were relatively linear between threshold and saturation for all ganglion cell classes examined. The major effect of surround stimulation on the center response-versus-contrast function was a reduction in the slope of the linear portion of the curve, rather than a downward, parallel shift of the function. Stimulation of the surround had no systematically significant effect on the contrast threshold for the center spot, and, when it did have a significant effect, it sometimes decreased, rather than increased the magnitude of the threshold.

3. Step changes in surround contrast were most effective when they were made simultaneously with step changes in the center; surround inhibition decreased significantly when it preceded stimulation of the center by >100 ms and was generally ineffective when preceding the center by >500 ms. The decrease in the inhibitory effect of surround stimulation was a monotonic function of delay between 0 and 500 ms.

4. Stimulation of the surround by step changes in the contrast of a sine-wave grating annulus produced qualitatively similar results to those obtained for pure luminance modulations. This suggests that the surround mechanism observed in these experiments was not due to pure luminance adaptation within the surround. The inhibitory effect of sine-wave gratings in the surround decreased monotonically as a function of spatial frequency.

5. Stimulation with a spot and an annulus that were both entirely within the ganglion cell's excitatory receptive-field center typically yielded nonadditive summation at contrasts whose linear sum of responses were below saturation. The effect of an annulus within the receptive-field center on responses elicited by a central spot quantitatively resembled the inhibition elicited from annuli in the inhibitory surround, after the excitatory center response due to the annulus was taken into account. These results suggest that the inhibition elicited from the surrounds of the ganglion cells in these experiments extended into their receptive-field centers.

6. The strength of inhibition elicited from the surround declined with reductions in the background level, both for a given modulation depth, and for the same absolute modulation amplitude. At the lowest backgrounds used, there was no apparent inhibition of center responses by the surround.

7. Particularly for transient ganglion cells, the nature of the interaction between surround and center mechanisms is generally consistent with nonlinear, division-like models for center-surround interaction, such as contrast gain control, but not with linear models in which the surround is subtractively antagonistic to the center.

INTRODUCTION

Twenty or more distinct physiological classes of ganglion cells are known to convey visual information from the retina to higher centers in the rabbit's CNS (Caldwell and Daw 1978a; Levick 1965, 1967; Vaney et al. 1981). So-called "concentric" cell classes in rabbit were originally characterized as having an ON- or OFF-excitatory receptive-field center region surrounded by an annular zone in which stimulation *1*) inhibited center responses and *2*) elicited excitatory responses at the opposite ON or OFF contrast sign to that which elicited responses in the center (Barlow et al. 1964; Levick 1965). More recently, the brisk/sluggish, sustained/transient and *X*/*Y* terminologies used to differentiate classes of retinal ganglion cells in the cat retina have been applied to ganglion cells in rabbit (Caldwell and Daw 1978a; Hamasaki et al. 1979; Vaney et al. 1981). In both of these species, ganglion cell inhibitory surrounds have been termed "antagonistic" (Kuffler 1953) if surround stimulation yielded excitatory responses of the opposite contrast sign to the center.

Only the brisk sustained, brisk transient, and large field unit concentric ganglion cell classes in rabbit have surrounds from which excitatory responses of the opposite contrast sign to the center are normally elicited (in the absence of strong adaptation of the center mechanism). Brisk sustained and brisk transient rabbit retinal ganglion cell classes bear a number of physiological and morphological similarities (Amthor et al. 1989a) to Xβ and Yα ganglion cells (respectively) in cat retina. Most of the other, "nonbrisk," concentric rabbit retinal ganglion cell classes have surrounds that are purely inhibitory. These "nonconcentric" cells include several types of ON- and OFF-center sluggish sustained (SS) and transient cells and color-coded cells (Caldwell and Daw 1978a). The pure inhibitory surrounds of these cells have been called "silent" or "suppressive" in rabbit and other species (Barlow et al. 1964).

Virtually all so-called nonconcentric ganglion cell classes, which respond to complex spatiotemporal features of the light input, have silent or suppressive surrounds. These include, in rabbit, two classes of directionally selective (DS) cells (ON and ON-OFF), orientation-selective cells, local edge detectors, uniformity detectors, and large field units. Although the surrounds of these nonconcentric ganglion cells

are not "antagonistically" excitatory, they typically very strongly suppress responses elicited from within the receptive-field center. The uniformity detector is noteworthy in this respect, in that it appears to be composed of a single, pure inhibitory region in which all stimuli suppress the rather high ongoing level of maintained activity that exists in the absence of any recent changes in light flux (Levick 1967).

It is unclear whether, in terms of the inhibitory effect on the center, the mechanism of silent inhibitory surrounds is fundamentally different from that of antagonistic, opposite-sign excitatory surrounds. It is possible, for example, that brisk ganglion cells have an antagonistic excitatory surround mechanism that coexists with a silent inhibitory surround mechanism similar to that observed in nonconcentric ganglion cells. A combination of inner and outer plexiform layer surround interactions, combined with synaptic rectifications, could conceivably isolate suppressive versus opposite-contrast-sign excitatory surround components in a manner dependent on stimulus conditions.

In studies in many vertebrate retinas, antagonistic excitatory surrounds have been postulated to interact linearly (subtractively) with the center mechanism (Enroth-Cugell and Lennie 1975; Enroth-Cugell and Robson 1966; Shapley and Victor 1978, 1979b, 1980). A linear, subtractive interaction between center and surround is assumed a priori, for example, in all difference of Gaussian (DOG) models (Enroth-Cugell and Robson 1966; Rodieck and Stone 1965), and in push-pull models for center-surround interactions, such as for cat X cells (Kuffler 1953). Such linear, subtractive surround models for ganglion cell receptive fields have been used to explain data ranging from the responses of concentric cells in mudpuppy (Belgum et al. 1987; Thibos and Werblin 1978a,b; Werblin and Copenhagen 1974) to psychophysical results in humans (Campbell and Robson 1968).

However, only a few studies have directly examined the linearity of center-surround interactions in any detail (Enroth-Cugell and Lennie 1975). The occurrence of hyperpolarization associated with conductance increases (from increased synaptic input) associated with surround stimulation, as in mudpuppy, for example (Belgum et al. 1987), does not by itself demonstrate that the primary nature of surround inhibition is linear, because conductance increases associated with surround stimulation may also cause a nonlinear "shunting" type of inhibition (Torre and Poggio 1978). Parametric fits achieved with DOG models using whole field stimuli of limited contrast range also do not directly address the linearity of the center-surround interaction, because, for small changes in contrast, linear approximations to an overall nonlinear surround effect may produce reasonable fits to the data.

However, a decisive distinction between linear versus nonlinear surround effects can be seen when the effect of various surround contrasts on the entire response-versus-contrast curve elicited by center stimuli is examined. A subtractive-linear interaction between center and surround would tend to cause the center response-versus-contrast function to shift downward, by subtracting a constant number of spikes from the response elicited by the center. In mammals, such a linear, downward shift of the entire center response-versus-contrast function has been explicitly shown only in a few cases, such as for a single surround contrast in a single X cell in the cat retina (Enroth-Cugell and Lennie 1975).

There are many possibilities for nonlinear interactions between center and surround. Perhaps the simplest nonlinear inhibitory mechanism is one whose effect is mathematically equivalent to a division-like operation. It has been shown, for example, that the null-direction inhibition in ON-OFF directionally selective ganglion cells of the rabbit retina approximates a division-like nonlinearity (Amthor and Grzywacz 1991, 1993). Indeed, one motivation for the present study was the possibility that if the DS ganglion cell's surround inhibition were linear, it could be distinguished by this from the division-like null-direction inhibition. However, experiments on DS ganglion cell surround inhibition showed that, although it differed from the null-direction inhibition in such properties as time course and spatial extent, it was also division-like in its interaction with the center mechanism (Amthor and Grzywacz 1993). In this study we have quantitatively expanded those results in DS ganglion cells and extended them to most major rabbit retinal ganglion cell classes. We have also examined a number of parametric attributes of rabbit retinal ganglion cell surround inhibition, including spatial extent and pattern dependence, temporal properties, and dependence on background level.

Preliminary reports of some of these results have been reported previously as abstracts (Merwine et al. 1990, 1991; Merwine and Amthor 1990).

METHODS

Surgery, physiological preparation, and stimulation methods were essentially the same as published previously by Amthor et al. (1989a).

Physiological preparation

Adult pigmented (black and white) Dutch belt rabbits of either sex, which generally weighed between 2.0 and 4.0 kg, were used for all experiments. All animals were dark adapted for at least 30 min before surgery, and all surgery was done in dim red light. Anesthesia was achieved through the combined use of urethan (1.5 g/kg) injected intraperitoneally, and pentobarbital sodium, given to effect by injection in the marginal ear vein. After achievement of a deep anesthetic level, such that no corneal reflex or other reflex could be elicited, one eye (usually the right) was enucleated, hemisected, devitreated, and mounted in the recording chamber as a superfused eyecup preparation. The everted eyecup was mounted on an inflatable latex dome in a superfusion chamber within 5 min of interruption of its blood supply in vivo. The eyecup was superfused with a simulated cerebrospinal fluid (Ames and Nesbitt 1981) saturated with 95% O_2-5% CO_2. The animals were killed with an overdose of pentobarbital sodium shortly after enucleation.

Optics and visual stimulation

Visual stimuli were generated by a Picasso (Innisfree) and presented on a Tektronix 608 monitor as described by Amthor and Grzywacz (1993). The highest light levels used were within the mesopic to low photopic range. Stimulus parameters and presentation times were controlled by a PC-DOS 386 computer, which also recorded the times of occurrence of ganglion cell action potentials to the nearest millisecond.

Stimuli were step contrast modulations within a given region from a maintained background, either to a new intensity (steps), or to a fixed contrast modulation depth (gratings). Contrast modulation defined as $(L_{mod} - L_{background})/L_{background}$ for steps, and $(L_{max} - L_{min})/(L_{max} + L_{min})$ for gratings was either increased or

decreased with respect to background (usually for a period of 1,000 ms) and then returned to background. In cases where the constant background was chosen to be less than one-half the maximum intensity output of the 608 monitor, ON contrast modulations of >100% were possible. In some experiments a black annulus was placed over the 608 monitor's screen between the center and surround regions to increase the spatial separation between the stimuli within the receptive-field center and those in the surround. Our gratings were normally oriented with the bars perpendicular to the long axis of the visual streak. Although we occasionally tried other orientation axes and found little difference in surround effects as a function of grating orientation, we made no systematic study of orientation dependence.

The main differences we have observed between the isolated and in vivo preparations are a general decline in "spontaneous" or maintained activity, and a correlated decline in the sustained component of ganglion cell responses over the ≥6 h that recordings are routinely made in the isolated eyecup preparation (Amthor et al. 1989a). In addition, because the image of the Tektronix 608 monitor is optically reduced by a factor of ~50, and restricted to the region immediately around the electrode tip, the majority of the retina tends to become relatively more dark adapted over time compared with the in vivo preparation (the experiment room was very dimly illuminated with red light that is largely shielded from the retina).

Recording procedure and data analysis

RECORDING. For quantitative analysis, spikes were recorded extracellularly with tungsten in glass microelectrodes, digitized with a Schmitt trigger, and their time of occurrence to the nearest millisecond stored on the computer hard disk. Responses were measured as the average number of spikes within the 1st 500 ms after the onset or offset of the stimulus affecting the receptive-field center.

CONCENTRIC CELL CLASSIFICATION. The receptive fields of all recorded ganglion cells were first mapped with small flashing spots, and moving spots and bars, to determine the conventional ganglion cell class (such as brisk sustained, directionally selective, etc). The class designations used in this study for nonconcentric cells (such as directionally and orientationally selective, local edge detectors, uniformity detectors) correspond generally to the criterion and terminology originally used by Levick (1967). The criteria for classification of concentric cells into brisk versus sluggish and sustained versus transient generally follow criterion and terminology of Caldwell and Daw (1978a) and Amthor et al. (1989a), in rabbit, and that of Cleland and Levick (1974) and Cleland et al. (1973) in the cat.

The response properties of the concentric ganglion cells reported in this paper span the range of those reported previously; however, definitive physiological classification of concentric ganglion cells in rabbit remains controversial, particularly in the absence of accompanying conduction velocity and anatomic data (see, for example, Amthor et al. 1989a; Caldwell and Daw 1978a; Vaney et al. 1981). For example, it is clear that the rabbit retina has a ganglion cell class having an α-like morphology (Peichl et al. 1987), which projects to the dorsal lateral geniculate nucleus (DLGN) (Pu and Amthor 1990) and is Y-like physiologically, in being brisk, transient, and having a large receptive-field center (Amthor et al. 1989a). However, these cells are much less nonlinear in spatial summation (Amthor et al. 1989a) than Yα-cells in cat (Shapley and Victor 1979b). There is also a very small receptive/dendritic field, brisk, sustained, linear, somewhat β-like–morphology ganglion cell that constitutes a large percentage of the retinal ganglion cell projection to the rabbit DLGN (Amthor et al. 1989a; Pu and Amthor 1990). But even at very nearly the same eccentricity (within or near the inferior edge of the visual streak), there are relatively large brisk, sustained, linear ganglion cells and rather small brisk, transient, linear ganglion cells (Vaney et al. 1981). Sustained versus transient distinctions can be problematic in the isolated preparation because there is a general decline of maintained activity and the sustained component of responses over the course of the experiment.

Because of these factors, our assignment of some concentric cells to fine class distinctions may not be completely definitive in these experiments. Brisk versus sluggish cells were distinguished primarily on the basis of the magnitude of the initial transient (70–150 ms) of the response, particularly for low contrast modulations. We distinguished sustained versus transient cells largely on the basis of the magnitude of the response from 200 to 500 ms after stimulus onset or offset. It was not the intention of this study to make a definitive contribution to the concentric cell classification controversy in rabbit, and because qualitatively, and in many cases quantitatively similar findings were obtained for all classes investigated, reassignment of some cells to a different class would not generally influence the results on the nature of the center-surround interaction, which are the focus of this study.

CENTER-SURROUND STIMULUS ORGANIZATION. After cell classification, the spatial arrangement of the "center" and "surround" stimuli to be used for this study were carefully related to the complete receptive-field map made with small flashing spots. The inner border of the surround annulus was fixed to be outside the region from which center responses could be elicited, with the use of, in some cases, opaque masks set between the center and surround regions to isolate the two mechanisms. However, in some cases, centerlike responses were later found to be elicited by large annuli just outside the receptive-field center as previously determined with small flashing spots. Adjustment for the contribution of this small center response component was made with the use of the "base-subtraction" procedure described below.

BASE SUBTRACTION. In cases where stimulation of the surround produced an excitatory response, and for experiments in which two spots were modulated within the excitatory receptive-field center, the excitatory response generated by the first stimulus was sometimes removed to highlight and isolate the effect of the first stimulus on the second, independent of the excitatory response due to the first. We term this operation "base subtraction" and have described it in detail elsewhere (Amthor and Grzywacz 1993). Briefly, the base-subtraction operation subtracts the expected response (number of spikes due to the surround or 1st spot, i.e., the "base" obtained when the surround or 1st spot was presented alone) bin by bin from the histogram obtained in the conditions of the combined stimulation. It is important to point out that *1*) base subtraction was used in a minority of cases overall, and for any particular cell type, *2*) the results using base subtraction were quantitatively similar to those cases where it was not needed, and *3*) the result, in the curve fit, would have been to produce a more positive linear term k_s, because the base subtraction does not change the response-versus-contrast curve shape, but only shifts it down the y-axis. Had we not base subtracted, the result would have been lower values for the linear, subtractive k_s term, and some reviewers might have objected to a situation where some weak excitatory response from the surround, masked its subtractive, linear decrement of the center response. The binwidths used for this procedure, and in all post-stimulus time (PST) histogram figures, is 20 ms.

Quantitative analysis

Plots were made of the average spike response-versus-contrast function of the center spot, with various independent modulations of an annulus either within the surround or the center. For most response-versus-contrast curves, linear regression lines fit to data between threshold and saturation showed a clear slope reduction as a function of increasing surround modulation. However, it could have been argued that both the assumption of linear response-

versus-contrast functions, and our selection of the points used, versus those excluded from the fit, were arbitrary, so we sought a more general means of distinguishing linear versus nonlinear components of the surround effects that entailed the minimum number of arbitrary assumptions about the form of the data and could use as much of the response curves that were measured as possible, including points near threshold and saturation.

We first sought an analytic description function for the entire center-alone response-versus-contrast function of the ganglion cell. We chose a Michaelis-Menten function for two reasons: *1*) photoreceptor responses have been well fit by a Michaelis-Menten (Michaelis and Menten 1913) equation (Baylor and Fuortes 1970); without any significant intervening nonlinearity other than a threshold between the photoreceptor and the ganglion cell, the latters' suprathreshold response might be expected to resemble such a function; and *2*) we found that the ganglion cell center response-versus-contrast functions generally could indeed be well fit by Michaelis-Menten equations with the inclusion of a threshold term, similar to the fittings previously shown for ON-OFF directionally selective ganglion cells (Amthor and Grzywacz 1991).

In fitting the Michaelis-Menten equations to the data, we explicitly wished to avoid an exercise in meaningless, multivariable curve fitting involving simultaneous optimization of a number of parameters having no assignable physical identity and therefore no independent experimental verification. We thus reduced the degrees of freedom to be fit in the equation by identifying and assigning variables sequentially to specific, measurable data values whenever possible. The coefficients of the Michaelis-Menten equation were thus evaluated in two steps, so that at no time was the curve-fitting program operating on more than two variables.

First, the ganglion cell center-alone response-versus-contrast function above threshold was modeled (no-surround case) with the following Michaelis-Menten–like equation (*Eq. 1*)

$$R_c = R_{sat} * \frac{g * (c_e - c_{thr})}{1 + g * (c_e - c_{thr})} \qquad (1)$$

where c_e is the excitatory (center spot) contrast (percent), c_{thr} is the contrast threshold, R_{sat} is the response maximum at saturation, and g is the contrast gain. We used the Minerr function of Mathcad 4.0 (Mathsoft; Cambridge, MA) to perform a least-squares (quasi-Newton) optimization of the center-only response-versus-contrast curve to evaluate the parameters c_{thr} and g (the parameter R_{sat} was not independent and was calculated from these parameters as shown in *Eq. 2* below). As discussed in Amthor and Grzywacz (1991), we made sure that the minimum error function of Mathcad converged to the same value for these two terms from a number of starting guesses (usually taken from the range of values from all previous fits). The insensitivity to starting guesses, the arrival at an estimate for c_{thr} that corresponded well with that that could be linearly extrapolated from the suprathreshold data, and the quality of the fit ($r^2 > 0.95$ for most receptive-field center–only curves) were used as indicators of a true best fit (global rather than local minimum least-squared error).

The parameter c_{thr} is the contrast at which the response-versus-contrast function exceeds threshold. In early versions of the fitting, we used an explicit *ganglion cell threshold* term subtracted from the entire response expression above, as in Amthor and Grzywacz (1991). However, after trying ~20 cells both ways, we chose the c_{thr} parameter over the explicit ganglion cell threshold for three reasons. *1*) The ganglion cell threshold estimated this way is the extrapolated y-axis (Response Spikes) intercept of the response-versus-contrast curve. When negative, the interpretation of this intercept as "negative spikes" has no biophysical meaning, because it really corresponds to the situation where the membrane potential is below threshold for the first spike. *2*) In any case, no levels of subthreshold activity of the ganglion cell is accessible via any measurement obtained in our extracellular recording experiments, but the contrast threshold, which is the contrast that is just adequate to produce a suprathreshold response, is. The reasonableness of the Mathcad fit could be much better gauged by how closely its estimate of c_{thr} agreed with the c_{thr} that we could directly estimate from the data. *3*) Better fits were produced with the use of c_{thr} than an absolute ganglion cell threshold, in part because, for large thresholds, the Michaelis-Menten function becomes very close to being parallel to the vertical (response) axis at 0 contrast, and therefore the exact intercept (ganglion cell threshold) varied widely for small amounts of noise in the observable suprathreshold curves.

The g term is analogous to a kind of contrast gain; for small center (c_e) contrasts, where $g * (c_e - c_{thr}) \ll 1$, the response as a function of center contrast c_e is proportional to g, which thus maps contrast (in percent) to response (in spikes). Because of the identifiability of g as a kind of contrast gain, we used this form (algebraically equivalent) of the Michaelis-Menten equation (*Eq. 1*, above), rather than the traditional version (Baylor and Fuortes 1970).

The R_{sat} parameter was calculated from the parameters c_{thr} and g discussed above. Let us define R_{max} as the maximum response obtained with the highest contrast center-only stimulus ($c_{e\,max}$) used. If a clear saturation of the ganglion cell response was obtained, then the parameter R_{sat} would equal R_{max}. However, if $c_{e\,max}$ did not completely saturate the ganglion cell response, the fitting procedure allowed for estimation of a higher value for the true R_{sat}, as follows in *Eq. 2* below.

$$R_{sat} = \frac{R_{max}}{g * c_{e\,max}} * (1 + g * c_{e\,max}) \qquad (2)$$

After c_{thr} and g were evaluated for the center-stimulus–alone functions (and R_{sat} was calculated), we expanded *Eq. 1* to include two terms for the effect of the inhibitory surround, one mediating a purely subtractive, and the other, a purely division-like surround interaction. The expanded equation, which included models for the two types of inhibition, is given below (*Eq. 3*).

In *Eq. 3* the subtractive inhibitory term, k_s, consists simply of a response decrement (or increment) proportional to the inhibitory contrast, c_i. The division-like inhibitory term k_d is contained in an expression that had the effect of reducing the contrast gain term, g, in proportion to the inhibitory contrast, thus $g \rightarrow g/(1 + k_d * c_i)$. Some of the biophysical motivation for the division-like model of inhibition in *Eq. 3* is given in the DISCUSSION. Computationally, the form of this expression was chosen so that k_d would equal zero if the division-like term had no contribution, or assume a finite positive value in proportion to the division-like contribution of the surround inhibition. To satisfy these two conditions, the mapping of inhibitory contrast to the magnitude of division-like inhibition was nonlinear. It is entirely possible that some other formulation of division-like inhibition could have fit the data better; nevertheless, in our results, Mathcad virtually always performed most of the fit with this form of the division-like, rather than subtractive inhibition. Were a potentially better formulation for division-like inhibition used, the results only would have more strongly favored the division-like over the subtractive fit.

Mathcad used *Eq. 3* below to fit all the surround inhibitory data by varying only the two inhibitory terms (k_s and k_d), representing subtractive and division-like inhibition, respectively. As described above, fitting runs were started from a number of guesses for the two inhibitory terms, including, *in every case,* one run starting with the best fit obtainable with only the subtractive inhibition term, while the division-like inhibitory term was initialized to zero. The parameters k_s and k_d were then used to calculate equivalent subtractive and division-like spikes at a c_i of 25%

$$R = R_{sat} * \frac{\frac{g}{1 + k_d * c_i} * (c_e - c_{thr})}{1 + \frac{g}{1 + k_d * c_i} * (c_e - c_{thr})} + k_s * c_i \qquad (3)$$

where c_i is the total inhibitory contrast (percent), k_s is the subtractive inhibitory term, and k_d is the division-like inhibitory term. Visual inspection of a number of plots suggested that better fits could have been made in some cells by assuming that R_{sat} declined somewhat in the presence of surround stimulation. However, it was also possible that the same R_{sat} would have been obtained during surround stimulation had the center contrast modulation depth been extended to higher contrasts than the limit found for center-only stimulation.

We also tried several other formulations for both subtractive and division-like inhibition, in addition to that in *Eq. 3.* These included *1*) an alternative subtractive inhibition in which the surround contrast multiplied by a coefficient was subtracted from the center contrast, *2*) an alternative division-like formulation in which the entire response, rather than *g,* was divided by $1 + k_d * c_i$, and *3*) another alternative division-like formulation in which the entire response was divided by $k_d * c_i$, rather than $1 + k_d * c_i$. These three formulations for the surround inhibition produced generally much inferior fits to those discussed in this paper, and they will not be discussed further here.

To verify the fits obtained with the quasi-Newton procedure in Mathcad, we also performed all the fits again with the use of a different software package, SCIENTIST (ver. 2.01; MicroMath Scientific Software, Salt Lake City, UT), that converged on a minimum least-squared solution by a different algorithm (Powell 1970). As with the Mathcad fits, we used a number of different starting guesses. The SCIENTIST fits also reported 95% limit goodness-of-fit standard deviations for each of the parameters, which are listed in the tables in this paper. The agreement between Mathcad and SCIENTIST best fits for all parameters was generally better than 5%, and virtually always within the standard deviations reported by SCIENTIST. Only cells for which fits using *Eq. 3* having a correlation coefficient squared (r^2) for all the curves (center only and all surround cases) >0.90 are reported here. Fits whose $r^2 < 0.90$ were generally due to noise in the average responses caused by an insufficient number of trials being completed, rather than from systematic failures to fit the data. However, there were a few cases, even where the data were relatively noiseless, in which there was a detectable, systematic error in the best fit of *Eq. 3.* These cases are noted and discussed in RESULTS.

Experimental protocols

The results were obtained with five experimental protocols with the use of pseudorandom stimulus presentation order for center and surround contrast modulations.

PROTOCOL I. CENTER-SURROUND INTERACTION DURING SURROUND LUMINANCE MODULATION. Light onset or offset (from background) in the receptive-field center was accompanied by light onset or offset in the surround. The contrast of the center and surround stimuli were varied independently. Response-versus-contrast functions for the center response were then generated for each discrete surround contrast (in cases where significant spiking from surround stimulation invaded the "window" attributed to the center response, the base-subtraction procedure, described above, was used to remove the effects of excitation elicited from the annulus in the surround).

PROTOCOL II. TEMPORAL PROPERTIES OF CENTER-SURROUND INTERACTION. Step changes in the surround luminance were made as in *Protocol I* above, except that the center modulation was delayed up to 500 ms relative to that of the surround.

PROTOCOL III. MODULATION OF THE SURROUND WITH SINE-WAVE GRATINGS. These experiments were similar to those of *Protocol I,* except that the surround modulation consisted of a step change from background to a stationary equiluminant sine-wave grating. Spatial frequencies presented to the surround were in the range of 1.4–5.8 cycles/mm on the retina. An opaque mask was usually used to block the surround modulation from regions near the outer edge of the receptive-field center where spatial phase effects might be largest. Although spatial phase was not systematically varied or studied in these experiments, the results obtained in preliminary experiments, and those reported here, did not appear to be strongly phase dependent. For example, because the phase angle was locked for all spatial frequencies, variation of the spatial frequency for a given cell, or between receptive-field positions between cells, had the effect of varying spatial phase. Yet, despite this uncontrolled phase variation, all inhibition-versus-spatial-frequency curves decreased monotonically from the lowest spatial frequency used, to the highest, for all cells.

PROTOCOL IV. SURROUND INFLUENCES WITHIN THE CENTER REGION. A mask was used to restrict the annular area modulated by the second channel of the Picasso (normally used for the surround) to the center region, so that both the spot and annulus were confined to the receptive-field center. Otherwise, the same protocol as *Protocol I* was employed.

PROTOCOL V. ADAPTATION LEVEL INFLUENCES ON SURROUND INHIBITION. We investigated the effect of the background luminance level on the surround inhibition. The experimental protocols were the same as in *Protocol I,* except that *Protocol I* type of series was run at a number of background levels, usually starting with the weakest. Because the strength of inhibition declined monotonically with background level, it was generally necessary to increase the depth of modulation, and sometimes even the absolute magnitude of the modulation, at the lower background levels to see any significant effect.

Data were obtained for at least one of the five protocols from >288 ganglion cells of various ganglion cell classes, in 100 animals. All cells were recorded in or near the rabbit's visual streak, where their properties could be directly compared with those of previous studies (Amthor et al. 1989a). Presented here are the analyses of the responses of 35 cells that met 3 criteria. *1*) The responsivity of the cell remained reasonably constant during the data run, so that the standard errors of the mean of the average responses were not excessively large, and the overall fit of *Eq. 3* to the data (r^2) exceeded 0.90. *2*) The range of center contrasts chosen for the data run was such that the ganglion cell response range was spanned adequately. For example, in some data sets, responses to center contrasts jumped from threshold to saturation on the first, or second from lowest contrast used in the quantitative data run, so there were no intermediate response-versus-contrast curve values to fit. At the other extreme, sometimes the full range of center contrasts never approached ganglion cell–response saturation. *3*) At least two inhibitory contrasts used for the surround produced reasonably intermediate response-versus-contrast curves between the center-only curve and no response. For some cells the surround contrasts chosen were not high enough to inhibit significantly the center response, so that even at the highest surround contrast used, the response-versus-contrast curve was very close to the center-alone curve, despite the fact that we knew, from preliminary exploration of the cell's properties, that whole field or sufficiently strong surround stimuli could completely suppress the center response. At the other extreme, in some cases the lowest surround contrast chosen was so effective that it already almost completely suppressed the center response, and so all the higher surround contrast curves just fell on top of the first, almost flat line. In between these errors were cases where we inappropriately chose surround contrasts too close together, so that the ganglion cell response-versus-contrast curves they elicited fell nearly on top of each other.

The response data obtained in all the cells not presented here were quantitatively similar to the ones presented, and there were no systematic differences between the excluded versus included set, beyond what is described above. This is not to say, however,

that there were not some systematic failures of the model's fit. We present in RESULTS three types of cases where the model's fit, using both subtractive and division-like inhibition, exhibited a systematic deviation from the data. We did not observe additional types of systematic deviation in the nonincluded cells that was different from those shown here.

RESULTS

Interactions between center and surround (Protocol I)

BRISK GANGLION CELLS. Figure 1 shows center spot PST histograms for the 18 brisk ganglion cells reported in this study, at the highest contrast ($c_{e\,max}$) used to stimulate the receptive-field centers of each cell. Brisk cells were distinguished from sluggish cells primarily on the basis of a larger response in the initial 70–150 ms after stimulus onset or offset, particularly for stimulus contrasts of ≤25%. The shape of the initial transient component of all brisk cells was similar, consisting of a relatively rapid rise in ~80 ms to a peak firing rate typically ~5 spikes per 20-ms bin. Sustained versus transient distinctions were made on the basis of the response level 200–500 ms after stimulus onset or offset, where the firing of most cells we classified as transient had returned to near baseline. Nine of the brisk cells were classified as transient, nine as sustained. It is clear from Fig. 1 that some cells classified as transient by this criterion had significant firing at 200 ms after stimulus offset, usually in what resembled a damped oscillation at a frequency of ~5–7 Hz, whereas cells classified as sustained exhibited a flatter firing level 200–500 ms after the contrast transition, although some sustained cells exhibited oscillations as well. Thus, although the presence of oscillations in the response does not distinguish transient versus sustained cells, more often in transient cells the response becomes close to zero in one or more bins after the first peak, before becoming nonzero later. Further analyses of these and other

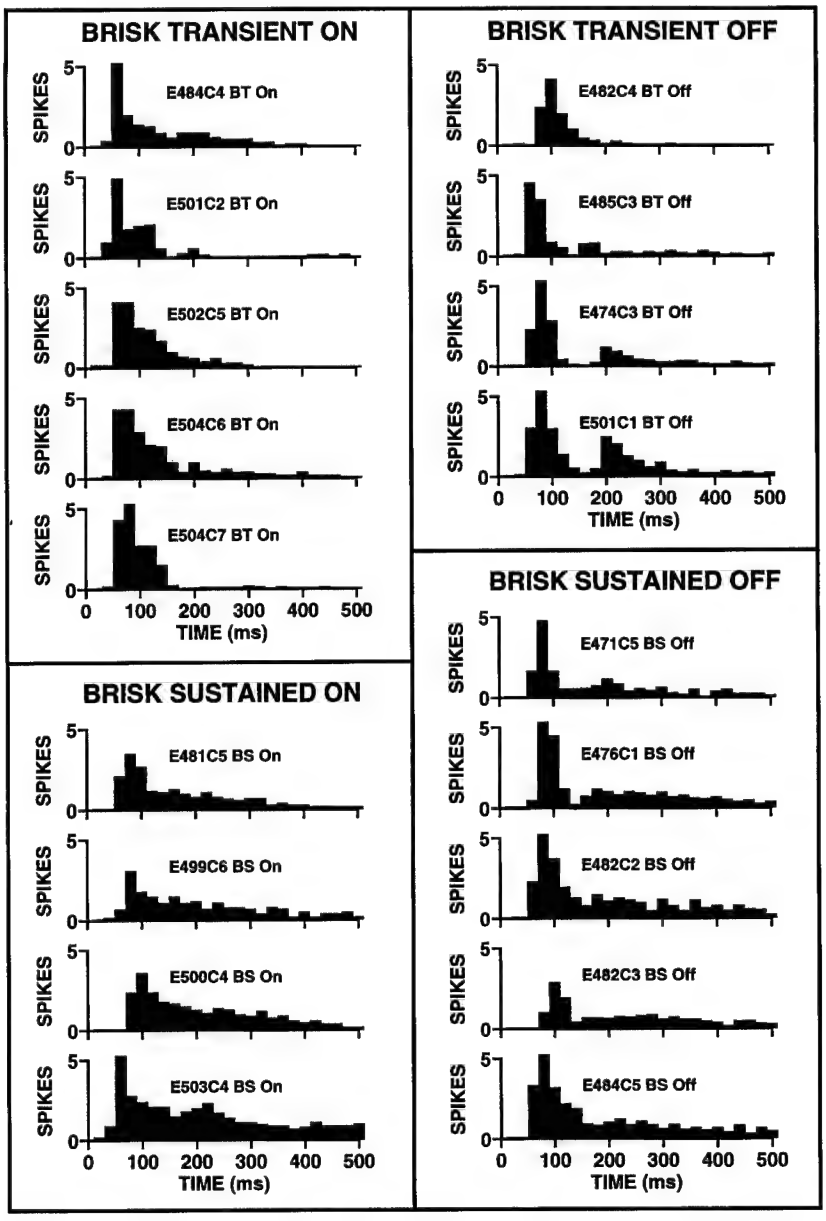

FIG. 1. Mean poststimulus time (PST) histograms for the 18 brisk transient and sustained cells that were analyzed in this study. Responses to the highest center spot contrast used are shown for 500 ms after center stimulation of the appropriate ON or OFF sign. (The binwidth for this and all other PST histograms shown in this paper is 20 ms.)

TABLE 1. *Concentric cell parameter summary*

Cell	Class	RF Area	R_{sat}	g	c_{thr}	k_s	s_{sp}	k_d	d_{sp}	r^2
E484C4	BT ON	0.560	18.2	0.07 ± 0.02	7.4 ± 1.6	−0.04 ± 0.03	−1.0	0.11 ± 0.04	−2.3	0.93
E501C2	BT ON	0.403	14.5	0.05 ± 0.00	7.6 ± 0.5	−0.02 ± 0.03	−0.5	0.10 ± 0.03	−2.8	0.96
E502C5	BT ON	0.813	19.6	0.07 ± 0.01	8.7 ± 0.7	0.02 ± 0.01	0.5	0.11 ± 0.02	−3.7	0.97
E504C6	BT ON	0.566	20.8	0.20 ± 0.10	9.8 ± 0.4	0.00 ± 0.03	0.0	0.18 ± 0.03	−5.9	0.97
E504C7	BT ON	0.417	18.2	0.11 ± 0.02	8.8 ± 0.6	0.02 ± 0.01	0.5	0.18 ± 0.02	−5.1	0.99
E482C4	BT OFF	0.328	10.7	0.69 ± 0.07	4.7 ± 0.5	−0.23 ± 0.10	−5.8	0.62 ± 0.27	−5.6	0.92
E485C3	BT OFF	0.358	13.9	0.26 ± 0.03	4.4 ± 0.2	−0.04 ± 0.01	−1.0	0.53 ± 0.09	−6.9	0.96
E474C3	BT OFF	0.883	22.7	0.04 ± 0.01	8.5 ± 1.1	−0.01 ± 0.01	−0.3	0.03 ± 0.01	−1.6	0.97
*E501C1**	BT OFF	1.408	29.9	0.03 ± 0.00	9.0 ± 1.0	−0.04 ± 0.02	−1.0	0.05 ± 0.01	−3.4	0.93
*E481C5**	BS ON	0.351	20.3	0.15 ± 0.02	3.7 ± 0.3	−0.08 ± 0.03	−2.0	0.18 ± 0.04	−5.9	0.98
*E499C6**	BS ON	0.176	30.5	0.02 ± 0.01	6.4 ± 3.0	0.01 ± 0.01	0.3	0.04 ± 0.01	−2.7	0.95
E500C4	BS ON	0.927	26.1	0.04 ± 0.01	9.5 ± 1.7	0.03 ± 0.02	0.8	0.05 ± 0.01	−1.1	0.97
*E503C4**	BS ON	0.244	43.5	0.03 ± 0.00	5.9 ± 1.1	−0.06 ± 0.02	−1.5	0.05 ± 0.01	−3.2	0.95
E471C5	BS OFF	0.119	18.5	0.10 ± 0.02	2.5 ± 0.6	−0.12 ± 0.04	−3.0	0.64 ± 0.07	−9.6	0.99
*E476C1**	BS OFF	0.351	29.8	0.05 ± 0.01	7.3 ± 0.8	−0.02 ± 0.02	−0.5	0.03 ± 0.01	−1.7	0.97
E482C2	BS OFF	0.492	34.0	0.08 ± 0.01	4.2 ± 0.5	0.00 ± 0.04	0.0	0.13 ± 0.02	−8.1	0.99
E482C3	BS OFF	0.191	21.6	0.04 ± 0.02	6.4 ± 2.2	−0.13 ± 0.05	−3.3	0.34 ± 0.05	−9.3	0.99
E484C5	BS OFF	0.485	30.6	0.08 ± 0.01	4.3 ± 0.6	0.00 ± 0.02	0.0	0.04 ± 0.01	−2.8	0.98
E480C8	ST ON	0.131	11.5	0.08 ± 0.03	20.2 ± 1.1	0.00 ± 0.02	0.0	0.10 ± 0.03	−2.2	0.93
E504C1	ST ON	0.196	10.8	0.07 ± 0.01	9.7 ± 0.7	0.00 ± 0.01	0.0	0.15 ± 0.03	−2.1	0.96
E476C4	ST OFF	0.297	11.3	0.01 ± 0.00	10.0 ± 1.7	−0.01 ± 0.01	−0.3	0.11 ± 0.02	−7.5	0.98
E501C6	ST OFF	1.144	10.2	0.11 ± 0.06	20.7 ± 2.6	0.01 ± 0.00	0.3	0.19 ± 0.03	−2.6	0.98
E484C2	SS ON	0.224	15.1	0.02 ± 0.01	44.5 ± 5.1	−0.01 ± 0.00	−0.3	0.04 ± 0.01	−1.3	0.97
E502C3	SS OFF	0.440	21.0	0.04 ± 0.01	19.7 ± 1.5	−0.05 ± 0.02	−1.3	0.13 ± 0.02	−5.1	0.96
E503C1	SS OFF	0.379	17.1	0.08 ± 0.04	10.1 ± 1.3	−0.04 ± 0.03	−1.0	0.10 ± 0.04	−1.3	0.92
E498C7	SS OFF	0.397	22.2	0.04 ± 0.00	0.2 ± 0.9	−0.01 ± 0.00	−0.3	0.17 ± 0.03	−5.4	0.92

Values in g, c_{thr}, k_s, and k_d are means ± SE. Summary of concentric cell parameters obtained from the fits to the equations for brisk and sluggish concentric ganglion cells. As described in METHODS, R_{sat} is the calculated response saturation level; g is the contrast gain mapping stimulus contrast to total spikes in the response; c_{thr} is the calculated contrast for response threshold; k_s and k_d are the coefficients of the subtractive and division-like inhibition terms, respectively, in *Eq. 3* (METHODS); s_{sp} and d_{sp} are the calculated reduction in spikes due to the subtractive and division-like inhibitory components, respectively, at a surround contrast of 25%, as described in METHODS; r^2 refers to the fit of *Eq. 3* to all the data, including the center-only curves and curves for as many surround contrasts as were used. RF, receptive field; BT, brisk transient; BS, brisk sustained; ST, sluggish transient; SS, sluggish sustained; ON or OFF indicates whether ON- or OFF-center. Asterisks indicate cells in which base subtraction was used.

details of the shape of the PST histograms, and their possible impact on transient versus sustained classifications were not carried out in this study but are the subject of ongoing research (surround effects were similar for all brisk cells; see METHODS).

Brisk sustained (BS) ganglion cell characteristics. Four of the nine BS ganglion cells shown in Fig. 1 were ON-center, and five were OFF-center. The receptive-field centers of the ON-center BS cells were slightly larger (0.42 ± 0.30 mm^2, mean ± SE) than those of the OFF-center BS cells (0.33 ± 0.15 mm^2), as shown in Table 1. Overall, BS cells in the sample had smaller receptive-field centers than brisk transient (BT) cells (BS 0.38 ± 0.23 vs. BT 0.64 ± 0.33 mm^2); three of the nine BS cells had center areas <0.2 mm^2, whereas the smallest BT cell center area exceeded 0.3 mm^2. However, there appears to be considerable overlap in receptive-field center areas between the two groups (BS and BT), as reported by Vaney et al. previously (1981).

ON-Center BS cell center response-versus-contrast functions. Figure 2 shows the response-versus-contrast functions for the four ON-center BS ganglion cells analyzed in this study. Parameters for the Michaelis-Menten (*Eq. 3*) fits (solid lines) are given for these and the other concentric ganglion cells in Table 1. The initial portions of the center-only stimulus functions (empty circles) of these four ON-center BS cells exhibited an initial steep slope from a contrast threshold (c_{thr}) of ~5–10% (6.38 ± 2.07). This slope declined gradually with contrast until response saturation (R_{sat}) at ~30 (30.1 ± 8.5) spikes. The contrast of the center spot at which saturation occurred (in the absence of surround stimulation) varied considerably among the four cells: *E481C5* and *E500C4* (*top left* and *right,* Fig. 2) saturated at <60% center contrast, but the other two cells (*E499C6* and *E503C4, bottom*) were not saturated at center contrasts of 100%. The contrast gain parameter, g, for BS ON-center cells ranged from 0.02 to 0.15 (0.06 ± 0.05). The high g of 0.15 for *cell E481C5* reflected a particularly steep (compared with other BS cells) response-versus-contrast function, which saturated near 50% center contrast.

Effects of surround excitation. Simultaneous modulation of the surround (hatched and filled symbols, Fig. 2) with the center reduced the initial slope of the center response-versus-contrast function in all four BS ON-center cells, and, in most cases, appeared to increase the contrast at which center modulation saturated the response. The data for *cell E481C5* (*top left,* Fig. 1), are typical for all cases where stimulation within the surround, as established with small flashing spots, elicited no (ON) center-type response. In this cell, surround stimulations at up to 25% contrast produced little change of the contrast threshold of the center mechanism. Surround stimulation at higher contrasts in the other three BS cells shown in Fig. 2 resulted, however, in observable changes in the extrapolated contrast thresholds. This occurred primarily because higher contrast stimulation of annuli in the *surround* of these cells also produced small ON excitatory responses characteristic of the *center*. This appeared to occur because

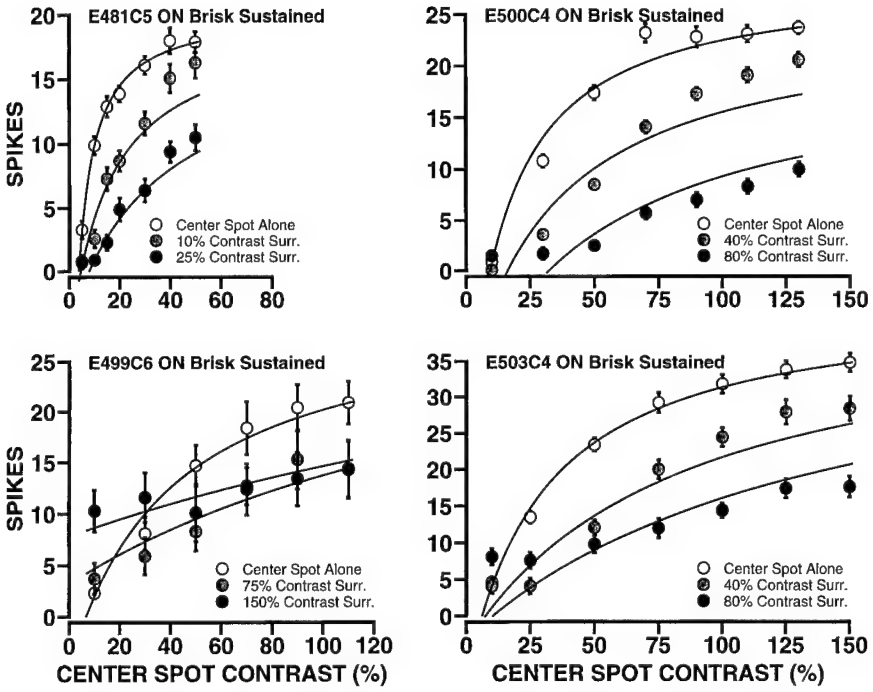

FIG. 2. Response-vs.-contrast functions for 4 ON-center brisk sustained (BS) ganglion cells. In each plot, the x-axis indicates percent contrast change presented to the center, the y-axis shows the mean number of spikes elicited in the 1st 500 ms of the cell's response. Empty circles plot the cell's response to center stimulation only, whereas filled circles plot responses with simultaneous surround stimulation at low (gray-filled) and high (black-filled) contrasts. Solid lines show the fit to the model (*Eq. 3*). Parameter values for the Michaelis-Menten fits are listed in Table 1. The center stimulus was 300 μm^2 (on the retina) for *cell E500C4,* 200 μm^2 for the other 3 cells. Surround stimuli consisted of the whole field of the Tektronix monitor, excluding the area for the center stimulus, and separated from the center stimulus by an opaque mask to isolate the 2 mechanisms (as described in METHODS). The outer radius of the annular mask was 520 μm for *cell E500C4,* 360 μm for the other 3 cells.

the large area annulus was much more effective for eliciting responses at the edge of the center mechanism, where its sensitivity was low, than were small spots.

The excitatory ON-center response component elicited from the annuli used to stimulate the surround of *cell E503C4* (*bottom right* of Fig. 2) can be seen in the PST histograms shown in Fig. 3. In this figure the *left column* shows the responses to center-alone stimulation, whereas the *middle* and *right* columns show the responses with 40 and 80% surround contrast modulations, respectively. At the top of the *middle* and *right columns* are histograms obtained with the surround annuli alone. The histogram for the 40% annulus alone (*top middle,* Fig. 3) shows that the response to the annulus consists primarily of an OFF response of the expected opposite sign to the ON center, but with a small sustained ON response, characteristic of the center mechanism of this cell, also evident. The 80% contrast annulus in the surround (*top right,* Fig. 3) shows a larger ON, center-type response component elicited from the area designated as "surround" from the small spot maps.

Because the onset excitation elicited in this area of the surround annulus falls into the 500-ms data window attributed to the ON response of the center, it shifts the center response-versus-contrast curve up by that amount (an *additive,* linear contribution). We used the base-subtraction procedure described in METHODS to replot the data with the ON-center component of the excitatory response elicited from the surround removed, to isolate the effect of the surround on the center, and so as not to mask whatever linear *subtractive* component might be elicited by inhibition in the surround.

Figure 4 shows two of the four plots shown in Fig. 1 (*E499C6, bottom left* and *E503C4, bottom right*) replotted after base subtraction to remove the ON-center excitatory component elicited by stimulation of the surround. The base-subtracted curves in Fig. 4 overall more closely resemble those obtained when excitation evoked by surround stimulation did not "contaminate" the responses attributed to the center. For example, removal of this ON excitatory surround component moved the projected contrast thresholds during surround stimulation nearer that of the center-only stimulus curve. Center-type responses obtained from locating the inner border of the surround annulus too close to the receptive-field center were removed by base subtraction for 6 of 35 ganglion cells presented in this paper; 4 of these 6 were BS cells (4/9 total BS cells). When the parameter values shown in Tables 1 or 2 were obtained after this response adjustment, they are indicated by asterisks beside the cell name.

OFF-Center BS cells. Figure 5 shows the fitted response-versus-contrast curves for five OFF-center BS concentric ganglion cells. The data for one of these plots (*E476C1*) were base subtracted to remove center polarity (OFF) responses elicited from the surround, in the same manner as described above for several of the ON-center cells in Fig. 4. The effects of surround stimulation on the center responses of OFF BS cells were quantitatively similar to those of ON-center BS cells. Table 1 shows the fitted coefficients of *Eq. 1* for the OFF-center BS cells. The three parameters estimated from the center-alone data were the maximum (asymptote) response (R_{sat}), contrast threshold (c_{thr}), and contrast gain (g). The means for OFF-center BS cells were R_{sat}, 26.9 ± 5.9 spikes; c_{thr}, 4.9 ± 1.7%; and g, 0.07 ± 0.02.

SUBTRACTIVE VERSUS DIVISION-LIKE EFFECTS OF SURROUND STIMULATION ON BS GANGLION CELLS. Surround stimulation caused a reduction in the responses elicited by center stimulation, which, in the fit of the data to *Eq. 3,* was accounted for by the optimum weighted combination of subtractive inhibition, mediated by the k_s term, and division-like inhibition, mediated by k_d. For subtractive inhibition, multiplying k_s by the surround contrast gives the subtractive (linear) reduction in the number of spikes due to the sur-

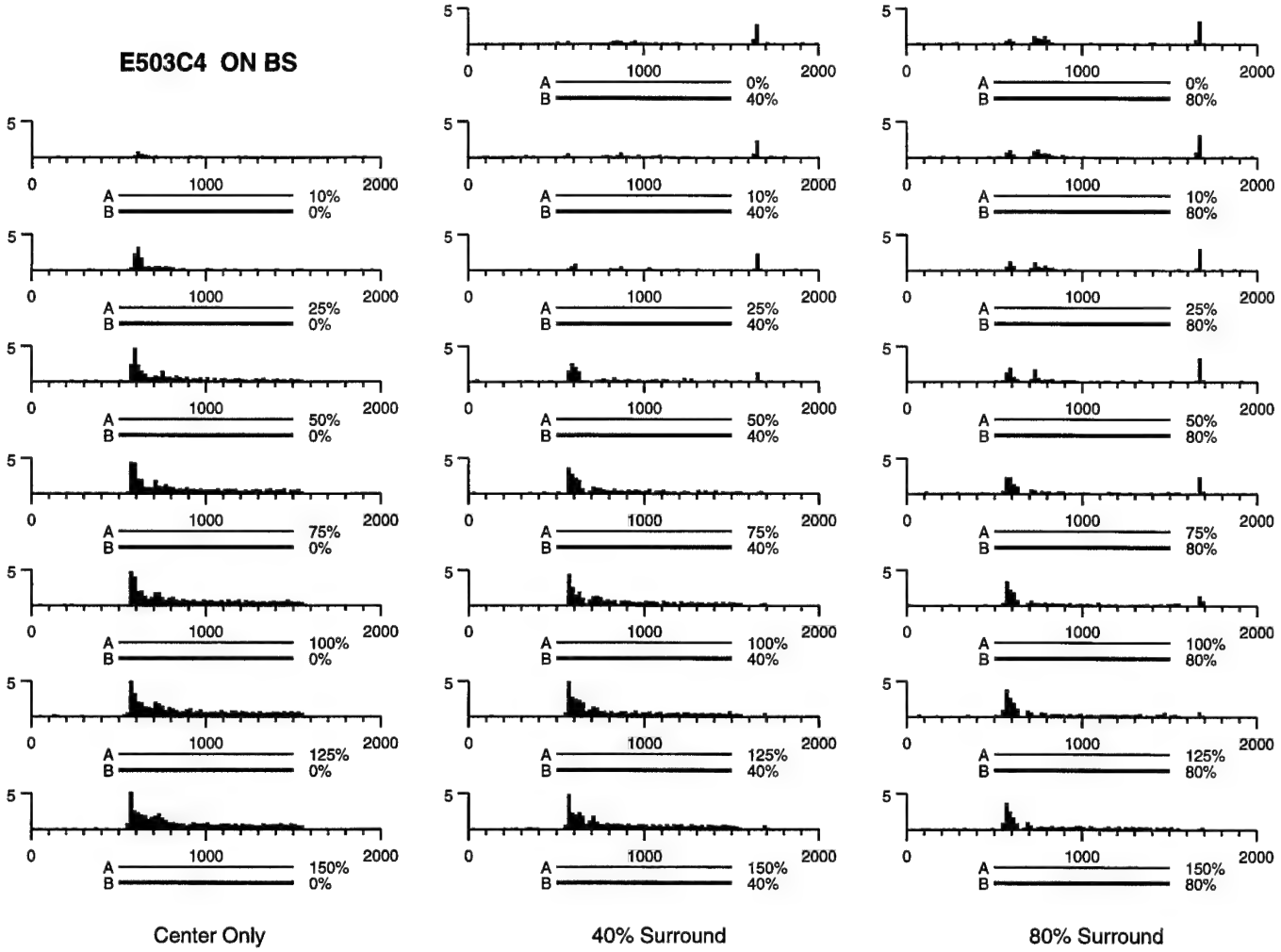

FIG. 3. Mean poststimulus histograms of *cell E503C4. Left column*: responses to center stimulation alone (A), whereas the *middle* and *right columns* show responses with the addition of low and high contrast surround stimulation (B), respectively. Center and surround onset were simultaneous, stimulus areas are given in Fig. 2. It is clear from the histograms at the top of the *middle* and *right columns* that annular stimulation alone produces small ON excitatory responses characteristic of the *center,* presumably because the annulus was more effective than a small spot in eliciting responses at the edge of the center mechanism. These responses were base subtracted to isolate the inhibitory effects of the surround on the center (see METHODS).

round stimulation. The subtractive reduction in spikes at a 25% surround contrast due to the k_s term is listed in Table 1 for all concentric cells as the term s_{sp} (for subtractive spikes), which can be interpreted as the number of spikes the center response is reduced by the subtractive component of surround inhibition at 25% contrast. The reduction in the number of spikes attributed to the division-like component, mediated by the k_d term, depends on both the surround contrast and the response level. This is because the division-like nature of the inhibition contributed by the k_d term causes a larger absolute reduction in spikes at higher than lower response levels, because division of a large number by a fixed divisor produces a larger absolute change than division of a small number. To compare the magnitudes of the two types of inhibition across all the cells, we computed the expected spike reduction due to the division-like inhibition for the same 25% surround contrast, at a center contrast that produced a 90% maximal response for each cell. The division-like inhibitory reduction in spikes is listed under the d_{sp} term (for division-like spikes).

For all BS cells, the decrement in the center response due to the subtractive component of the surround at 25% contrast, s_{sp}, had a mean of only -1.0 ± 0.7 spikes. The k_s term was only weakly significantly negative in four of the nine BS cells (*E481C5, E503C4, E471C5,* and *E482C3*), implying a small negative contribution from surround stimulation, but in the other five BS cells, k_s was not significantly different from zero at the $P = 0.01$ level and occasionally was weakly positive.

The k_d values in Table 1 give the division-like component of inhibition for each cell, which can be regarded as equivalent to a reduction of the contrast gain term g, as described in METHODS. The average reduction in center spikes attributable to the division-like component of the surround, d_{sp}, for all the BS cells, was -5.1 ± 4.5 spikes. Unlike the subtractive contribution from the k_s term, the k_d term was significant at the $P = 0.01$ level (95% goodness of fit) for all BS cells. Thus the effect of the surround inhibition in BS cells was accounted for in the fit to *Eq. 3* almost entirely by a division-like, rather than a subtractive component. The r^2 fits of *Eq. 3* for all the BS cells equaled or exceeded 0.95, as shown in Table 1.

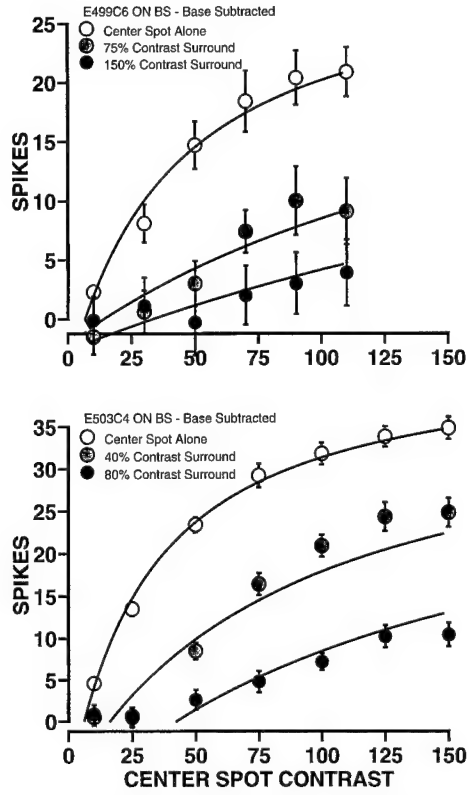

FIG. 4. Response-vs.-contrast functions replotted after the base-subtraction procedure (see METHODS) for 2 ON-center BS cells from Fig. 1. Conventions and stimulus areas are described in Fig. 2. Note that base subtraction shifts the projected contrast thresholds nearer to those obtained with center-only stimulation.

BT CONCENTRIC CELLS. Data were obtained on nine (5 ON, 4 OFF) BT cells whose $r^2 > 0.90$ for the overall fit of *Eq. 3*.

ON-Center BT cell responses to receptive-field center stimulation. Figure 6 shows the response-versus-contrast functions for the five ON-center BT ganglion cells; the numerical values for the fitting parameters are shown in Table 1 as for the BS cells. The response-versus-contrast functions were generally similar to those obtained for the BS cells. However, R_{sat}, the maximum response, averaged 18.3 ± 2.1 spikes for BT cells, which is much lower than the value of ~30 obtained for the BS cells, largely because the 500-ms response window integrated over the much longer time that the BS cells responded. R_{sat} appears in Fig. 6 to vary for BT cells from ~50% to ~100%. The contrast threshold, c_{thr}, of BT ON-center cells averaged 8.5 ± 0.9, slightly higher than the value for the BS cells. The average g term for ON-center BT cells was 0.1 ± 0.05, which was marginally higher than the value obtained for the ON-center BS cells.

OFF-Center BT cell responses to receptive-field center stimulation. Figure 7 shows the fitted response-versus-contrast functions for the four OFF-center BT ganglion cells. Similar functions were obtained for the parameters R_{sat} (19.3 ± 6.7) and c_{thr} (6.7 ± 1.9) as those of the ON-center BT cells. The effects of surround stimulation on OFF BT cells were generally similar to those for ON-center BT cells, except that the contrast gain term, g, was somewhat higher for OFF-center BT cells (0.26 ± 0.24). OFF-Center BT *cell 501C1* had an unusually high R_{sat} of ~30, as well as by far the largest receptive-field center of any cell in this study, >1.4 mm^2. These values are consistent with those obtained for a large field unit discussed later. Unfortunately, this particular cell was not tested for features that would distinguish it as a large field unit from similar OFF-center BT cells.

Surround effects on BT cells. For the nine BT cells, the decrement in the center response due to the subtractive component of the surround at 25% contrast, s_{sp}, had a mean of −0.96 ± 1.91 spikes. The k_s term was weakly significantly negative in five of these cells (*E502C5, E504C7, E482C4, E485C3,* and *E501C1*). For four of these five, this implied a small negative contribution from surround stimulation, but in *E504C7,* the marginally significant linear contribution of the surround was actually positive. For the other four BT cells, k_s was not significantly different from zero at the P = 0.01 level. The average reduction in center spikes attributable to the division-like component of the surround, d_{sp}, for all the BT cells was −4.1 ± 1.81 spikes. Unlike the subtractive contribution from the k_s term, the k_d term was significant at the P = 0.01 level (95% goodness of fit) for all BT cells. Thus the effect of the surround inhibition in BT cells was accounted for in the fit to *Eq. 3* almost entirely by a division-like, rather than a subtractive component. The r^2 fits of *Eq. 3* for all the BT cells equaled or exceeded 0.92, as shown in Table 1.

SLUGGISH GANGLION CELLS. Figure 8 shows the PST histograms of the four SS and four sluggish transient (ST) cells that met the criteria for this study. As described in METHODS, sluggish cells were distinguished from brisk cells primarily on the basis of a smaller response in the initial 70–150 ms after stimulus onset or offset, particularly for stimulus contrasts of ≤25%. Sluggish cells also had a tendency to have longer latencies to peak than brisk cells, although this

TABLE 2. *Complex cell parameter summary*

Cell	Class	R_{sat}	cg_0	c_{thr}	k_{ss}	s_{sp}	k_{sd}	d_{sp}	r^2
E472C5	ON-OFF DS	23.9	0.41 ± 0.38	29.1 ± 1.0	−0.04 ± 0.06	−1.4	0.30 ± 0.13	−7.0	0.91
E473C4	ON-OFF DS	30.5	0.09 ± 0.02	5.2 ± 0.6	−0.04 ± 0.05	−3.2	0.19 ± 0.05	−7.5	0.95
E475C1	ON-OFF DS	15.4	0.27 ± 0.20	9.5 ± 0.8	−0.01 ± 0.02	−0.2	0.30 ± 0.08	−7.0	0.96
E494C6	ON-OFF DS	32.0	0.09 ± 0.01	4.7 ± 0.4	−0.03 ± 0.02	−0.6	0.09 ± 0.01	−5.3	0.98
E500C1	ON-OFF DS	17.7	0.03 ± 0.00	20.0 ± 1.2	−0.01 ± 0.01	−0.4	0.03 ± 0.01	−0.7	0.93
E502C2	ON-OFF DS	13.0	0.06 ± 0.05	10.1 ± 2.8	−0.01 ± 0.03	−1.8	0.13 ± 0.05	−1.6	0.90
E503C3	ON-OFF DS	27.3	0.09 ± 0.02	9.8 ± 0.5	−0.06 ± 0.04	−1.4	0.08 ± 0.03	−4.4	0.92
E493C5	ON DS	29.0	0.01 ± 0.01	51.3 ± 7.2	−0.04 ± 0.02	−0.9	0.04 ± 0.01	−3.3	0.90
*E414C1**	LFU	63.3	0.01 ± 0.01	−1.6 ± 6.6	−0.05 ± 0.02	−1.1	0.07 ± 0.01	−8.3	0.98

Values in cg_0, c_{thr}, k_{ss}, and k_{sd} are means ± SE. Column heads are as in Table 1. DS, directionally selective; LFU, large field unit.

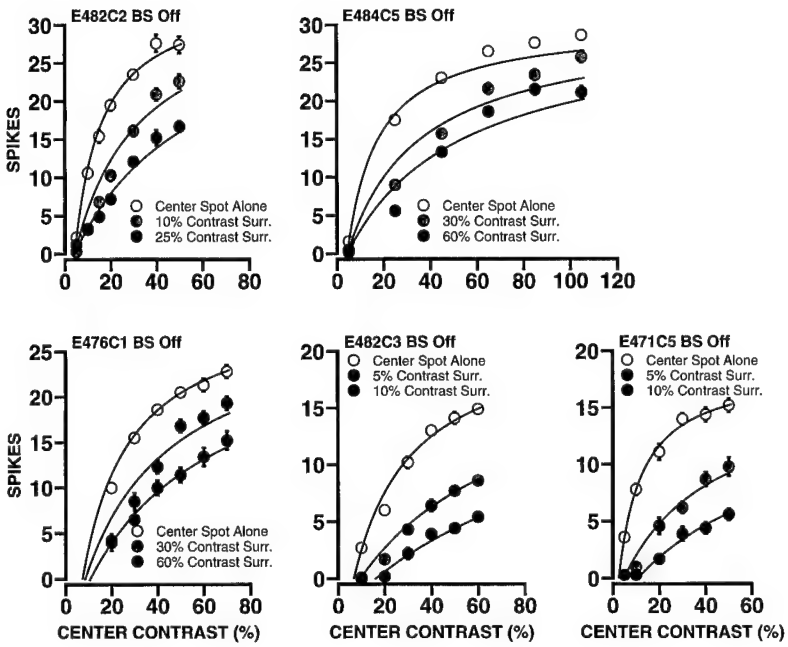

FIG. 5. Response-vs.-contrast functions for 5 OFF-center BS cells. *Cell E476C1* was plotted after base subtraction. Parameter values for the equation fits (solid lines) are given in Table 1. Plotting conventions for this and the remaining response-vs.-contrast plots remain the same as in Fig. 2. The center stimulus area for *E482C3* and *E484C5* was 300 μm^2, mask radius equals 520 μm. *Cell E482C2* used a 200-μm^2 center area, mask radius equals 360 μm. For *E471C5,* the center stimulus was 150 μm^2, mask radius equals 280 μm. The center stimulus for *E476C1* was a circle whose radius was 100 μm. This cell's surround stimulus was an annular ring of area 4,000 μm^2, inner radius equals 300 μm.

property was not quantitatively investigated in this study. Figure 8 also includes a histogram for a Large Field Unit (LFU), placed here not because its responses were particularly sluggish, but because it was originally (and continues to be, by some workers) distinguished from BT and BS cells in the literature (Barlow et al. 1964).

Receptive-field center properties of SS ON- and OFF-center cells. Figure 8 shows that SS cells tended to have lower amplitude, longer latency initial peaks than BS ganglion cells. R_{sat}, for example, was 18.9 ± 3.3 spikes for SS cells, versus nearly 30 spikes for BS cells. The data in Table 1 and Fig. 9 also show that the contrast threshold, c_{thr}, for center stimulation also tended to be larger (18.6 ± 19%) for SS than BS cells, ranging up to nearly 45% for *E484C2,* although there was considerable variation in this parameter. Despite their sometimes large contrast thresholds, however, SS cells had contrast gains (*g;* Table 1) not too dissimilar to those of BS cells, and somewhat lower than those of BT cells.

ST cells. The PST histograms of the four ST cells (2 ON-center; 2 OFF-center) shown in Fig. 8 have many similarities to those of some of the BT cells shown in Fig. 1, differing primarily in having *1*) slightly lower amplitude, *2*) longer time-to-peak, and *3*) nearly total lack of firing after ~150 ms after stimulus onset or offset, compared with BT cells. R_{sat} for ST cells was 11.0 ± 0.6 spikes, compared with 18.7 for BT cells. Like SS cells, ST cells have a generally higher contrast threshold (15.2 ± 6.1%; see Table 1) than brisk cells. This higher contrast threshold is also evident in the response-versus-contrast plots of the four ST cells shown in Fig. 10.

SURROUND EFFECTS ON SLUGGISH CELLS. Figures 9 and 10 show that the effects of surround stimulation on sluggish cells were quantitatively similar to those observed for brisk ganglion cells. However, although r^2 values for the fits for all sluggish cells were ≥0.92, there was evidence in some sluggish cells for a systematic error in the particular nonlinear mapping of surround contrast to inhibition (as discussed in METHODS). For example, the surround inhibition in *cells E503C1* and *E502C3* in Fig. 9 and *E480C8* in Fig. 10 appears to have a higher gain than in the mapping function of *Eq. 3;* best fits are obtained with the two predicted surround contrast curves falling between the actual data curves. This suggests a possible additional nonlinearity in the division-like mapping function, such as might be accounted for by having an exponent for c_i greater than one. This possibility was not, however, explored further in this study, because fits without this additional parameter were still overall quite good for most sluggish cells.

As found for brisk ganglion cells, the effect of surround inhibition on sluggish cells is best accounted for by a division-like mechanism. Table 1 shows that the k_s fits of all four ST cells were virtually zero (0.00, 0.00, −0.01, 0.01), whereas all four k_d values were significantly nonzero. Among the four SS cells, only *E502C3* had a weakly significant k_s term. The k_d term of all four SS cells was significantly nonzero. For SS *cell E502C3,* the weakly significant k_s term accounted for −1.3 spikes at 25% surround contrast (s_{sp}), whereas the k_d term accounted for −5.1 spikes (d_{sp}).

NONCONCENTRIC GANGLION CELLS. *DS ganglion cells*. Figure 11 shows the response-versus-contrast functions for the seven ON-OFF DS ganglion cells analyzed in this study. Because the statistics for the ON and OFF responses were found to be quantitatively similar, the ON and OFF responses were combined for the fits to *Eqs. 1–3* (estimated parameters of the fits are shown for these and other nonconcentric ganglion cells in Table 2). The center spot response-versus-contrast functions of ON-OFF DS ganglion cells qualitatively resemble those of BT concentric cells, with the R_{sat} parameter (for ON and OFF center responses combined) averaging 22.8 ± 7.6. However, even within the very well defined class of ON-OFF DS ganglion cells, there was considerable parameter variation that appeared to depend on stimulus conditions such as adaptation level, spot size, the state of the isolated preparation, and other parameters that were not systematically explored in this study. For example, Table 2 indicates that the contrast thresh-

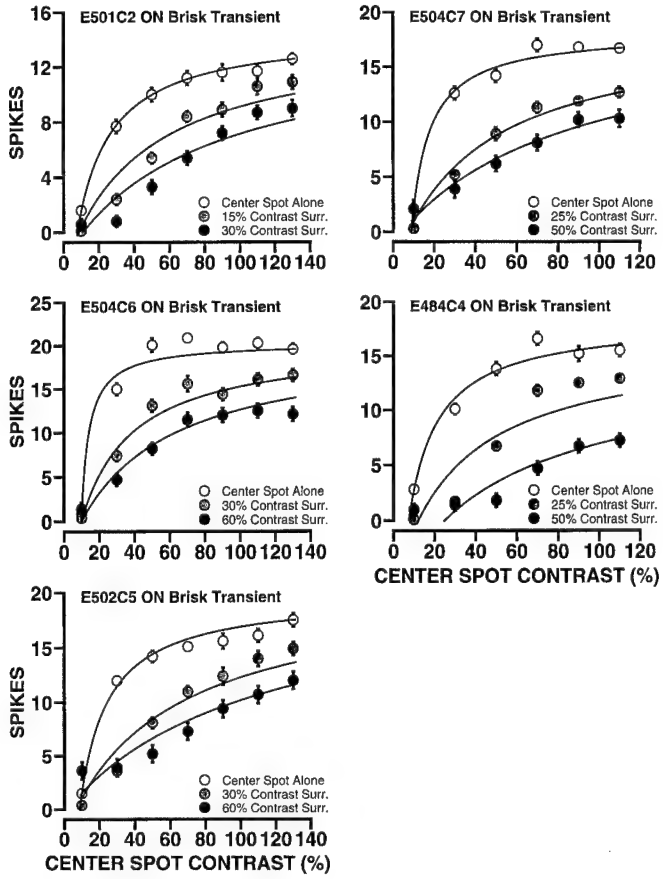

FIG. 6. Response-vs.-contrast functions for 5 ON-center brisk transient (BT) cells. Parameter values for the equation fits are in Table 1. The center mechanism of each cell was stimulated with a 200-μm^2 square. An annular mask whose radius was 360 μm was used.

olds of ON-OFF DS ganglion cells varied from ~5 to ~30% (average 12.6 ± 8.8). Similarly, it can be seen in Fig. 11 that the center contrast at which response saturation occurred varied from less than ~50 to >100%.

The effect of surround stimulation was similar in ON-OFF DS ganglion cells to that observed in brisk and sluggish concentric cells. Surround stimulation can be seen in all seven cells shown in Fig. 11 to reduce the initial slope of the response-versus-contrast function without appreciably changing the threshold. For most of these ON-OFF DS ganglion cells, surround stimulation also tended to increase the center contrast at which response saturation occurred, although this did not appear to be the case for *cell E494C6* (*bottom right,* Fig. 11). For *cell E503C3* (*middle right,* Fig. 11) there was clearly a systematic error in the mapping of surround contrast to magnitude of inhibition. As was the case for some concentric cells, the inhibitory mapping would have been better approximated by introducing an additional nonlinearity, such as an exponent, for the surround contrast, but this was not analytically investigated for either concentric or nonconcentric cells. The effect of surround inhibition on ON-OFF DS ganglion cells, like brisk and sluggish concentric cells, also appeared to be best accounted for by a division-like mechanism. Table 2 shows that none of the k_s fits of the seven DS ganglion cells were significantly nonzero, whereas all seven k_d values were significantly nonzero.

The response-versus-contrast function for an ON DS ganglion cell (*E473C4*) are shown on the *left* in Fig. 12. This cell exhibited an unusually high threshold (51.3%) for center stimulation. Table 2 shows that it also had an unusually low contrast gain coefficient (g = 0.01), possibly related to the extremely slow rise time of its response, which caused much of its response to miss the 500-ms counting window (our sample was clearly too small to indicate whether these unusual parameter values are characteristic of ON DS ganglion cells in general). Surround effects observed for this cell were similar to those of concentric and ON-OFF DS ganglion cells. The k_s parameter for this cell, mediating subtractive inhibition, was not significantly nonzero, whereas the k_d parameter, mediating division-like inhibition, was (Table 2). Qualitatively similar surround effects were observed for a single local edge detector recorded in this study, which was not included in the quantitative analyses presented here because of loss of the recording too early in the data acquisition protocol.

Data were obtained for one ganglion cell (*E414C1*) identified as a LFU in this study. (*E501C1,* which was included with BT cells in Fig. 1, may also have been an LFU, but was not tested to determine this possibility). The PST histogram for the center response of the *LFU E414C1* is shown in Fig. 8 with those of the sluggish concentric cells (although LFUs are definitely not sluggish). Figure 12 shows the LFU response-versus-contrast functions. This cell had the highest R_{sat} (63.3) for any ganglion cell in this study; it also exhibited a very low contrast gain coefficient of 0.01 (Table 2). Its estimated contrast threshold (c_{thr}) was very close to zero (−1.6 ± 6.6; Table 2), however, like that of most brisk cells. The effect of surround stimulation on the center response was similar to that found for other ganglion cell types. The k_s parameter mediating subtractive inhibition was marginally significantly nonzero but only accounted for a

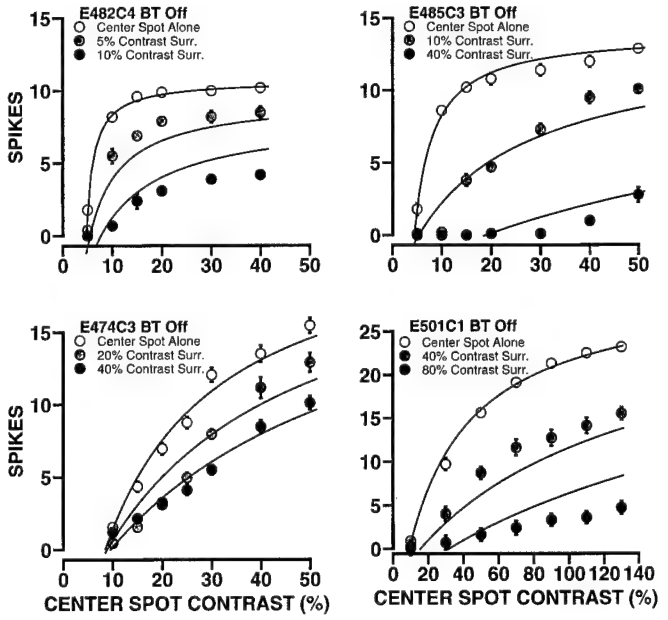

FIG. 7. Response-vs.-contrast functions for 4 OFF-center BT cells. Parameter values for the fitted curves are given in Table 1. *Cell E501C1* is shown after base subtraction. *Cells E474C3, E485C3,* and *E501C1* used the center equal to 300 μm^2, mask radius equal to 520-μm stimulus parameters. The center stimulus for *E482C4* was 200 μm^2, mask radius equals 360 μm.

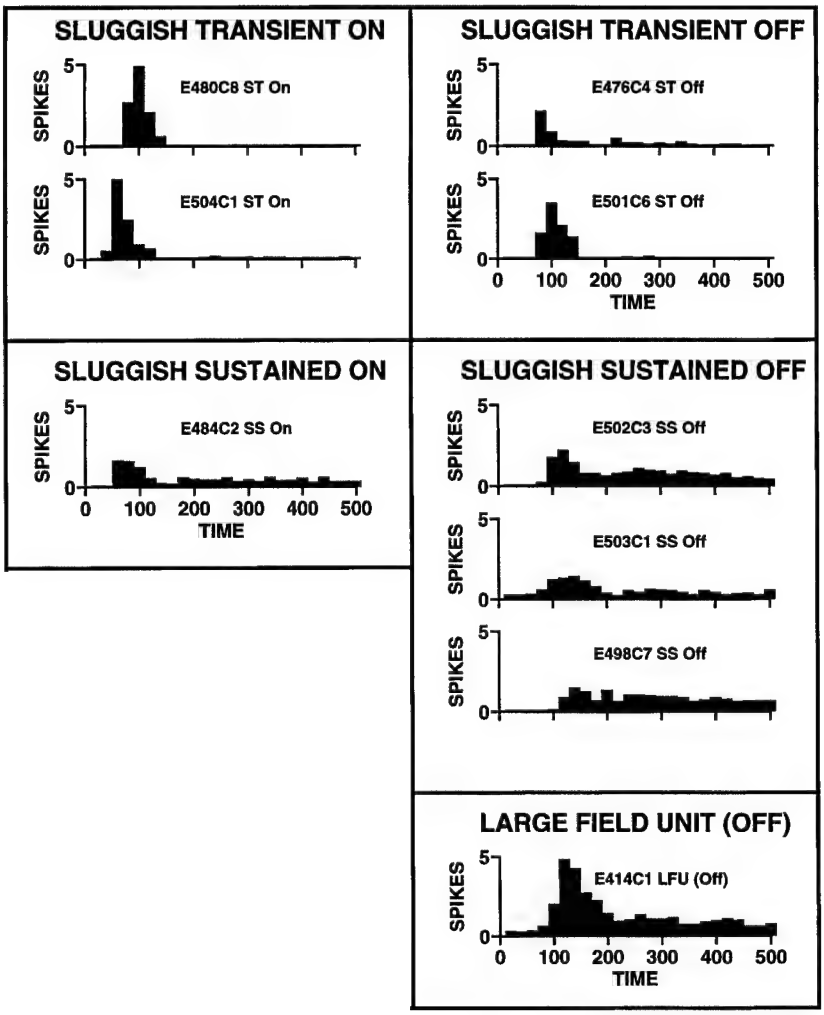

FIG. 8. Mean poststimulus histograms for the sluggish cell types and a large field unit (LFU). Responses are shown (at the highest center spot contrast used) for 500 ms after center stimulation of the appropriate ON or OFF sign. Stimulus conditions are given in Figs. 9, 10, and 12. Note that the sluggish cells have generally lower amplitude, longer latency peak responses than those of the brisk cells shown in Fig. 1. The placement of the large field unit LFU in this figure with sluggish cells is only for convenience; LFUs are most like BT cells, and in fact, sometimes difficult to distinguish from them.

decrement of ~1 spike at 25% surround contrast, whereas the k_d parameter accounted for a decrement of >8 spikes at the same surround contrast.

Time course of surround inhibition (Protocol II)

It has been hypothesized that the time course of inhibition conducted from the surround might be delayed relative to that of the center excitation to explain temporal characteristics of center-surround interactions in vertebrate species ranging from frog (Nye and Naka 1971) to the cat (Barlow et al. 1957; Enroth-Cugell and Lennie 1975). If so, it might be expected that step changes in surround illumination might be more effective in inhibiting center responses if they occurred some time before similar changes in the center, to give the slower surround mechanism time to build up or propagate so that it could affect the very earliest portion of the center response.

We investigated the effectiveness of step changes in surround contrast as a function of delay before similar changes in center contrast for several ganglion cell classes. The effects we observed were similar across all cell classes, as with the general nature of the nonlinear interaction between the center and surround.

Figure 13 shows response-versus-contrast functions of an OFF BS (*left*) and an ON BT concentric cell (*right*) when the delay between surround and center onset was varied between 0 and 500 ms. The effect of delaying contrast changes in the center with respect to contrast changes in the surround is a monotonic decrease in surround inhibitory effectiveness as a function of delay. For both these cells, and in general for all cells examined, delays of as little as 100 ms produced measurable reductions in surround inhibition; longer delays on the order of 500 ms typically resulted in almost complete abolition of the surround effect. These results indicate that the effect of surround inhibition on ganglion cell center responses is relatively transient with a time course similar to that of the ganglion cell's center excitatory response component itself.

The delay protocol (*Protocol II*) was conducted for a number of other brisk and sluggish concentric cells and complex cells with similar results. Delays as short as 40 ms were also tested. In no case did we find that any nonzero delay between surround and center modulation produced statistically significantly larger inhibition than that obtained at 0 ms (no delay). However, our results do not exclude the possibility that, for some cells, stimulation of the surround before the center might have been slightly more efficacious

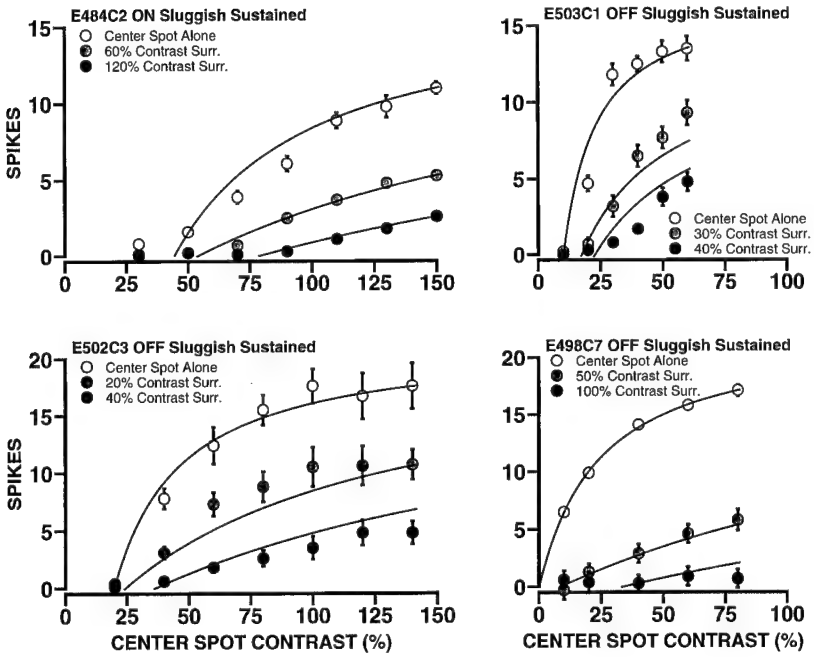

FIG. 9. Response-vs.-contrast functions for 4 sluggish sustained cells. Note that the contrast thresholds for these cells tend to be higher than those of the BS cells. Parameter values for the solid line curve fits are listed in Table 1. All 4 cells were tested with the 200-μm^2 center area, mask radius equals 360-μm stimulus configuration parameters.

than simultaneous stimulation in reducing a response attribute such as the amplitude of the early response peak, which has been used in some studies as the response measure.

Spatial frequency characteristics of the surround inhibition (Protocol III)

The experiments in *Protocol III* attempted to address the question of whether the surround inhibitory effects on the center observed in these experiments were due strictly to a luminance adaptation effect, or whether the surround inhibitory properties evoked in these experiments had the same spatial frequency characteristics as those associated with the surround mechanism, as determined in earlier studies in rabbit and other mammals. To examine this hypothesis, we stimulated the surrounds in this protocol with a step change from background to an equiluminant sine-wave grating, instead of an overall luminance change. We used a number of different spatial frequencies in the surround to determine the spatial frequency characteristics of the mechanism mediating the surround inhibition. Although we did not vary the spatial phase systematically in these experiments, results from preliminary experiments and the monotonicity of the curves as a function of variation in spatial frequency (whose change effectively varied spatial phase) indicated no strong dependence on spatial phase.

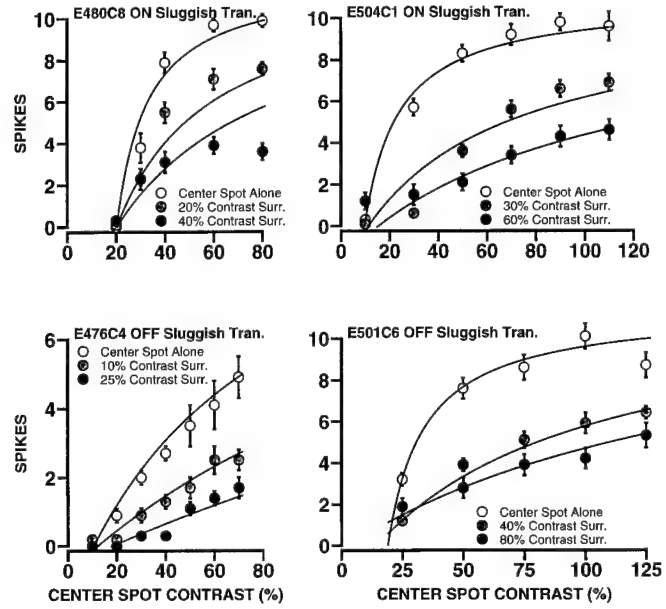

FIG. 10. Response-vs.-contrast functions for 4 sluggish transient cells. Table 1 lists the values used for the curve fits. Again, note the generally higher contrast threshold values. The areas of center stimulation for *cells E504C1, E480C8,* and *E501C6* were 200, 300, and 340 μm^2, respectively. The mask radius for the 1st 2 cells was 360 μm, for the last, 730 μm. The center of *E476C4* was stimulated with a circle whose radius was 100 μm. This cell's surround stimulus was an annular ring of area 4,000 μm^2, inner radius equals 300 μm.

CONCENTRIC CELLS. Figure 14 shows the results of a step change in surround modulation to an equiluminant sine-wave grating for an OFF-center BS ganglion cell (*E444C2*). The curve indicated by filled circles is the response-versus-contrast function of the center mechanism alone, as in the previous protocols. The other curves show the effects on the center's response-versus-contrast function of surround stimulation at two different spatial frequencies, each of which was tested at two different modulation depths. All surround modulations were done at zero relative delay, which was previously shown to be the most effective delay. The effects of equiluminant modulation of a grating in the surround are qualitatively similar to those found for pure luminance modulation. Gratings are quite effective for inhibiting the center responses, with the lower spatial frequency grating being more effective than the higher spatial frequency grating. Increasing the contrast of either spatial frequency grating increases the amount of inhibition. The changes in the shape of the center response-versus-contrast curve induced

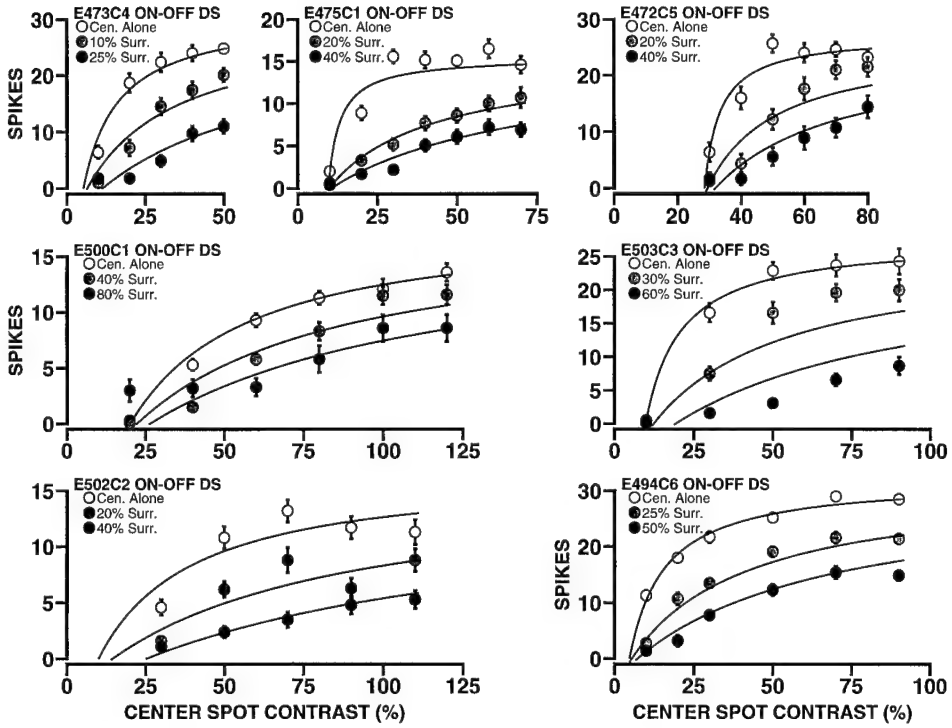

FIG. 11. Response-vs.-contrast functions for 7 ON-OFF directionally selective (DS) ganglion cells. Plotted are the combined ON and OFF responses. The parameter values for the solid line fits to these cells are listed in Table 2. Note that the response functions and the effects of inhibition are qualitatively similar to those of the BT cells. *Cells E473C4, E475C1,* and *E503C3* were stimulated with 150-μm^2 center stimuli, mask radii equals 280 μm. *E472C5* used the same center area, but with a mask radius equal to 360 μm. The remaining cells used 200-μm^2 center areas with mask radius equal to 360 μm.

by gratings in the surround, such as a reduction of the initial slope with little change in the contrast threshold, and division-like versus subtractive mediation of inhibition, were also found to be similar to those found for surround luminance modulation (although the calculated curves and fitting parameters are not shown here).

COMPLEX RECEPTIVE-FIELD GANGLION CELLS. Gratings are effective for inhibiting the surrounds of complex receptive-field ganglion cells, as for concentric cells. Figure 15 shows surround grating modulation results for an ON-OFF DS ganglion cell (*left*), and a horizontal, orientation-selective ganglion cell (*right*). The results for these and other complex receptive-field ganglion cell results were qualitatively similar to those obtained for concentric classes (as for concentric cells using this protocol, we do not show the calculated curves and fitting parameters that distinguish the relevant contribution of subtractive vs. division-like inhibition for these cells).

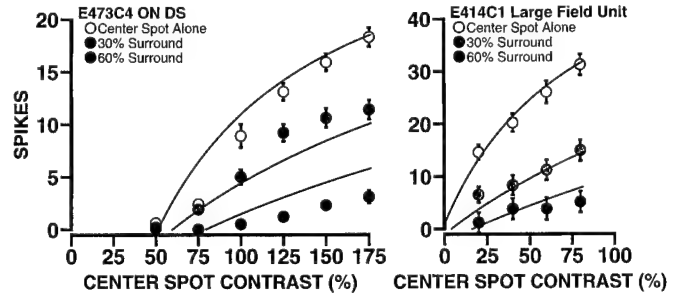

FIG. 12. Response-vs.-contrast functions for an ON DS cell and a LFU. The data points for the LFU were base subtracted. See Table 2 for the fitted-curve parameter values. Although the ON DS cell had a remarkably high threshold and the LFU had the highest R_{sat} found in this study, both cells nonetheless display similar surround effects to those of the concentric and ON-OFF DS cell types. The stimulus configuration for *E493C5* was center area equal to 200 μm^2, mask radius equal to 360 μm. *Cell E414C1* used center area equal to 340 μm^2, mask radius equal to 730 μm.

EFFECTIVE SPATIAL FREQUENCY RANGE. We found the surround inhibition of the center to decline monotonically for most ganglion cells across the range of spatial frequencies we tested, from ~1 to 4.5 cycles/mm on the retina. Figure 16 shows a plot of spike-decrement versus spatial frequency in the surround for two brisk concentric and two complex receptive-field ganglion cells (the 2 complex cells were the same as those in Figs. 15 and 16). The reduction in spikes caused by five different spatial frequencies in the surround is shown at a receptive-field center contrast that elicited a response near saturation for a center-only stimulus for each cell.

Center-center interactions (Protocol IV)

We tested the effect of an annulus contained entirely within the excitatory receptive-field center on the response versus center-spot contrast in a number of cells to determine whether the mechanism we had observed in the surround existed within the excitatory receptive-field center. In these experiments, a small spot and annulus, both within the excitatory receptive-field center, were used in protocols that were otherwise identical to *Protocol I.* The results for an ON-center BS cell and an OFF-center BT cell are plotted in Fig. 17. The excitatory responses due to the annuli were removed in both cases by the base-subtraction procedure, which is described in METHODS. It is apparent that the effects of annular stimulation within the center on a center spot were qualitatively similar to those for annuli in the surround. These results are similar to the two-spot results of a number of other studies (Hickey et al. 1973; Kuffler 1953; Werblin and Copenhagen 1974) that found that responses to combined stimulations yielded outputs less than linear predictions.

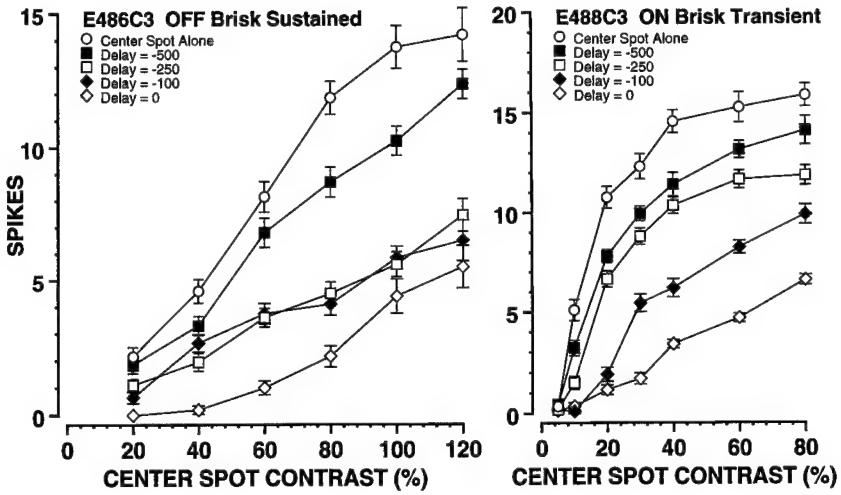

FIG. 13. Effect of surround-center onset delay. Response-vs.-contrast functions are shown for a BS (*left*) and a BT (*right*) cell. Individual curves now show the effect of delay (rather than surround contrast) on the center-alone function. Solid lines are fitted point-to-point because no effort was made to model the temporal dependence of the inhibition parameters (k_d and k_s). Note the rapid, monotonic decrease in surround inhibition with time. *Cell E486C3* was stimulated with a center square equal to 200 μm^2, mask radius equal to 360 μm. Surround stimulation contrast is 25%. *E488C3* used a center square equal to 300 μm^2, mask radius equal to 520 μm; surround stimulation contrast equals 50%.

EFFECT OF CENTER SPOT SIZE ON CENTER RESPONSE-VERSUS-CONTRAST CURVES. The similarity of the inhibitory effect on center spots from annuli contained within the excitatory receptive-field center and in the surround motivated us to examine some of the effects of varying center spot size on center response-versus-contrast functions. In particular, we wondered whether some nonlinearities might be explained if the responses elicited by small center spots saturated some mechanism (such as a bipolar cell) before the ganglion cell. Figure 18 shows the center response-versus-contrast functions for a BS cell obtained at three different spot sizes. The response curve obtained at the smallest spot size, radius 1, is shown with open circles. The slope of this curve is shallower than those elicited by larger spots. The ganglion cell response at the highest contrast used for this spot was ~25 spikes. Although the steep slope at this contrast, and the fact that larger spots elicited larger maximal ganglion cell spots, would argue that this was not the saturating response level for this spot size, unfortunately, because we did not use higher contrasts, we cannot tell this from the data.

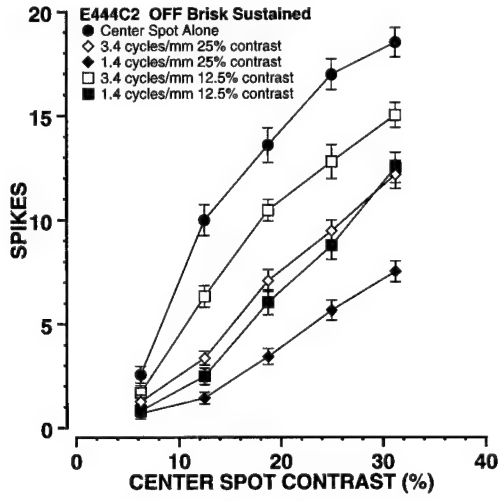

FIG. 14. Effect of spatial frequency on a BS concentric cell. Point-to-point fits are shown for the effects of 2 different spatial frequencies (at 2 contrasts each) on the center-alone response-vs.-contrast function of an OFF-center BS cell. Note the similarity to the surround luminance modulation data, and the decrease in effect at each contrast as spatial frequency is increased. Center stimulation area equals 200 μm^2, mask radius equals 360 μm.

The center response-versus-contrast function for the radius 4 spot is shown in hatched circles in Fig. 18. This spot nearly optimally filled the excitatory receptive-field center and was more typical in size to those used in preceding experiments. The center response-versus-contrast function for this spot exhibited a higher initial slope and contrast gain, and a contrast threshold closer to 0%, than that obtained for the radius 1 spot. The response-versus-contrast function of the radius 10 spot is shown in filled circles in Fig. 18. This spot was larger than the excitatory receptive center and invaded the inhibitory surround, and therefore this experiment was similar to protocols in which center and annular stimuli were delivered at zero relatively delay, except with no gap between the outer border of the center spot and the inner border of the surround annulus. The result obtained was similar to that in *Protocol I* experiments; namely, there appeared to be a marked reduction in the initial slope of the function, with little change in the projected contrast threshold. On the other hand, the response saturation level also appeared to decline somewhat. The cause of this apparent lower saturation level is unclear. A nonlinearity that divided the entire response function, such as discussed in METHODS, would appear to account for this data, but we did not attempt to assess this possibility quantitatively.

Effect of background level on surround inhibition (Protocol V)

In cat it has been established (Enroth-Cugell and Robson 1966; Enroth-Cugell and Shapley 1973) that the strength of the inhibitory surround declines during dark adaptation. To determine whether the surround inhibition we observed was of the same type as observed in those experiments in cat, we checked the effect of reducing the mean background level on the surround inhibition observed in our protocols for a number of rabbit retinal ganglion cells. The typical result is shown for one such cell (*E534C4*) in Fig. 19. For the lowest background used (*rightmost panel* of Fig. 19, in which the 25 units corresponds to ~10% of the maximum luminance available from our Tektronix 608 monitor), the

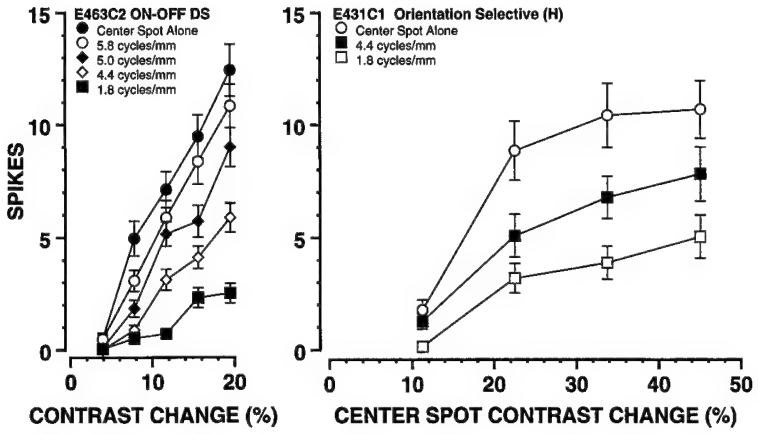

FIG. 15. Effect of spatial frequency on complex cells. Point-to-point fits are shown for the effects of various spatial frequencies on the center-alone response-vs.-contrast functions of an ON-OFF DS cell (*left*) and an orientation-selective cell (*right*). Although the effects of spatial frequency were not specifically modeled, it is clear that the nature of surround inhibition is qualitatively the same as in the surround luminance cases. As with the concentric cell shown in Fig. 14, inhibition decreases as spatial frequency increases. The ON-OFF DS cell (*E463C2*) surround grating contrast was 9.4%, center stimulation area equals 200 μm^2, mask radius equals 280 μm. The orientation-selective cell (*E431C1*) used a surround grating contrast of 22.5%, center area equals 150 μm^2, mask radius equals 360 μm.

surround stimulation is completely ineffective even at 60% modulation, which is the same absolute change in surround luminance as 30% of the 50-unit background, which was significantly inhibitory. Qualitatively similar results were found for a number of other ganglion cells tested during this study, but detailed results will not be presented here.

DISCUSSION

Step changes in the contrasts of spots within ganglion cells' receptive-field centers yielded response-versus-contrast functions that were generally well fit by the Michaelis-Menten equation. Simultaneous luminance modulations within the receptive-field surround produced a functionally similar characteristic inhibition of the center response of virtually all rabbit retinal ganglion cells examined. When observed over the full contrast range between threshold and saturation, the inhibition was best functionally characterized as a reduction of the slope or gain of the center mechanism's response-versus-contrast function, with little change in the contrast threshold.

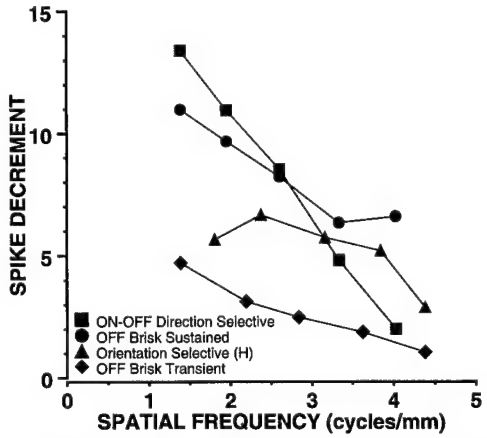

FIG. 16. Plot of the decrease in surround inhibition with increasing spatial frequency of the surround grating stimulus. The absolute spike decrement caused by surround grating stimulation (at the highest c_e tested) is shown plotted against spatial frequency. Note the monotonic decrease with increasing spatial frequency. Parameter values for the OFF-center BT cell are as follows: center area equals 200 μm^2, mask radius equals 360 μm, surround grating contrast equals 27.3%. Parameter values for the ON-OFF DS cell are as follows: center area equals 200 μm^2, mask radius equals 360 μm, surround grating contrast equals 12.5%. Remaining data are from Figs. 14 and 15.

Surround inhibition was most effective when it occurred simultaneously with excitation in the center; in most cells its effect decreased monotonically to insignificance by 500 ms. Similar results obtained with contrast modulation of sine-wave gratings as with luminance modulation of annuli in the surround suggest that the surround effects observed were not due to pure luminance adaptation but had spatial frequency characteristics similar to those observed by workers in other mammalian preparations such as cat. The responses to annuli placed within the excitatory receptive-field center summated nonlinearly with center spots in a manner that was functionally equivalent to the type of inhibition observed in the surround, suggesting that the surround mechanism observed in these experiments extended into the excitatory receptive-field center region. These results are generally consistent with the idea that the ganglion cell surround, in addition to its spatial antagonism, functions as a gain control mechanism, as suggested by Shapley and Victor in cat retina (1978, 1979a, 1981), and by Benardete, Kaplan and Knight in primate retina (Benardete et al. 1992).

Nonlinearity of the surround mechanism in different ganglion cell classes

Surround effects observed for all ganglion cell classes were qualitatively similar and well fit by the division-of-contrast-gain model (*Eq. 3*), although the parameters of the fitted equations varied across classes and to some extent within classes, depending on the exact stimulus parameters. Although there were significant differences in some parameter averages as a function of ganglion cell class, we did not explore the full range of parameter variation as a function of stimulus configuration to determine whether the parameter values found in this study could be used as ganglion cell class identifiers.

There were three general kinds of systematic deviations from the fittings of the division-like inhibitory model to account for surround inhibitory effects. *1*) Some BS cells appeared to have a marginally significant subtractive (linear) component of surround inhibition. In this, they resembled cat Xβ cells, whose inhibitory surrounds have been reported to have a large linear-subtractive component (Enroth-Cugell and Lennie 1975). *2*) The center-response saturation level for some ganglion cells appeared to be reduced under the influence of surround modulation. This effect could be best

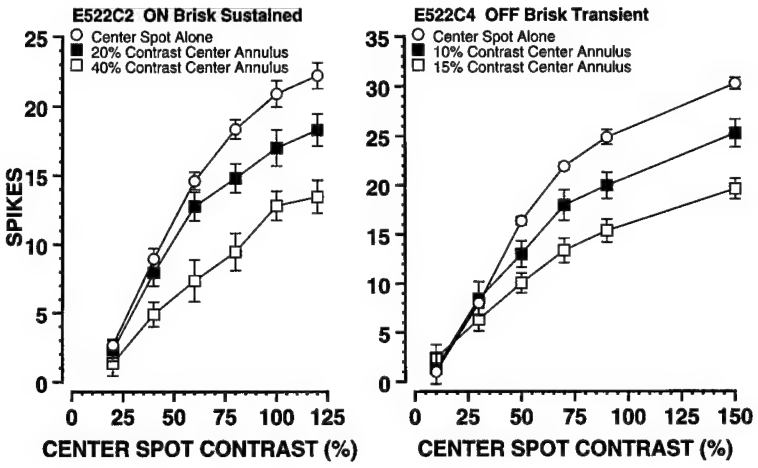

FIG. 17. Nonadditive effect of confining the center-surround protocol (*Protocol I*) entirely within the mapped center region. The response-vs.-contrast function for a center stimulus (○) is shown along with the base-subtracted functions for stimulation of this plus an annular area contained within the center region (□ and ■) for a BS (*left*) and a BT cell (*right*). The center-alone area for both cells was 120 μm^2. The annulus was a hollow square with inner area equal to 120 μm^2, outer area equal to 300 μm^2. Note that, once the excitatory effect of the annulus is removed by base subtraction, the response curves appear qualitatively similar to the surround luminance modulation data.

accounted for by using an inhibitory parameter that scaled (divided) the entire response-versus-contrast function, as described in METHODS. However, replacement of the division-of-contrast-gain term by a term dividing the entire response function produced, over all cells, much poorer fits than those we report here with the use of *Eq. 3*, as described in METHODS. Nevertheless, it is conceivable that the surround mechanism varies somewhat between ganglion cell classes, such as in the balance of outer versus inner plexiform layer input. *3*) For some cells the nonlinear mapping of surround contrast to the contrast gain division term showed a systematic deviation. This deviation could have been resolved by modification of the mapping function with an additional parameter, such as an exponent for the surround contrast term. However, because this deviation occurred only in a minority of cells of several ganglion cell classes, we did not include the additional parameter in the analysis presented here.

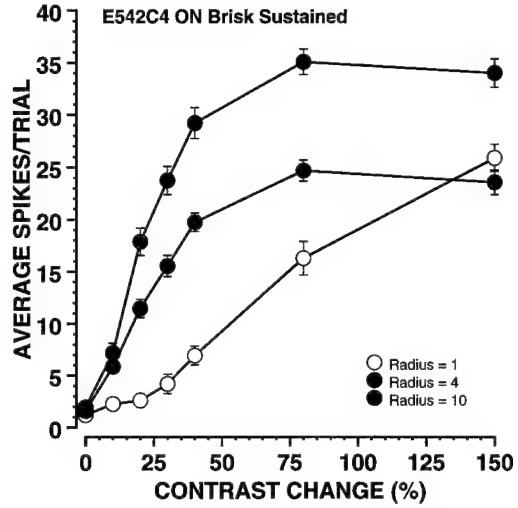

FIG. 18. Response-vs.-contrast functions for an ON-center BS ganglion cell with varying stimulus spot sizes. The *x*-axis shows percent contrast change of the spot, and the *y*-axis shows the mean number of spikes elicited in the 1st 500 ms of the cell's response. Symbols plot the responses to spots of 600, 240, or 60 μm^2 (on the retina). The measured receptive-field center of this cell was 137,700 μm^2. Note that surround inhibition is evident for the largest spot size. Both the slope of the response-vs.-contrast function and the saturation level are reduced. Interestingly, the smallest spot size does not saturate, even for very large contrasts, but climbs toward the same asymptote as the optimally sized spot. We interpret this as an indication that the saturation level of the response-vs.-contrast function is set by the ganglion cell itself, and not its inputs.

Surround effectiveness as a function of delay

Inhibition was always as good or better for simultaneous modulation of surround and center contrasts as when center modulation was delayed with respect to that in the surround. A delay in the time course of inhibition conducted from the surround has previously been hypothesized to explain some temporal characteristics of center-surround interactions and the transient nature of some responses in other species, as discussed in the INTRODUCTION. For example, Nye and Naka (1971) found maximal surround inhibitory effects in frog retinal ganglion cells when surround modulation preceded the center by 50–100 ms. This difference may be a real difference between species, given the generally much slower ganglion cell responses in amphibians than mammals. However, a number of models based on sine-wave grating data in cat retina also frequently postulate a temporal phase offset between center and surround mechanism (see, for example, Enroth-Cugell et al. 1983). Although this phase delay is often interpreted as the rise of surround inhibition being slower than that of center excitation, it could equally result from the fall time of surround inhibition being slower than that of center excitation. The results here suggest that the surround mechanism transiently modifies the gain of the center mechanism, and is therefore most effective when modulated simultaneously with it, but that the fall time of the surround mechanism is slow enough to allow it to have some effectiveness even if its modulation precedes that of the center by up to several hundred milliseconds. These findings are generally consonant with the idea of negative feedback contrast gain control mechanisms, such as proposed for cat retinal ganglion cells by Shapley and Victor (1981).

Surround versus luminance adaptation mechanisms

Modulation of sine-wave gratings in the surround produced qualitatively similar effects to that of pure luminance modulations. These results suggest that the inhibition observed in our experiments was due to the same type of spatial low-pass filter surround mechanism that is postulated in DOG models (Enroth-Cugell and Robson 1966; Rodieck and Stone 1965).

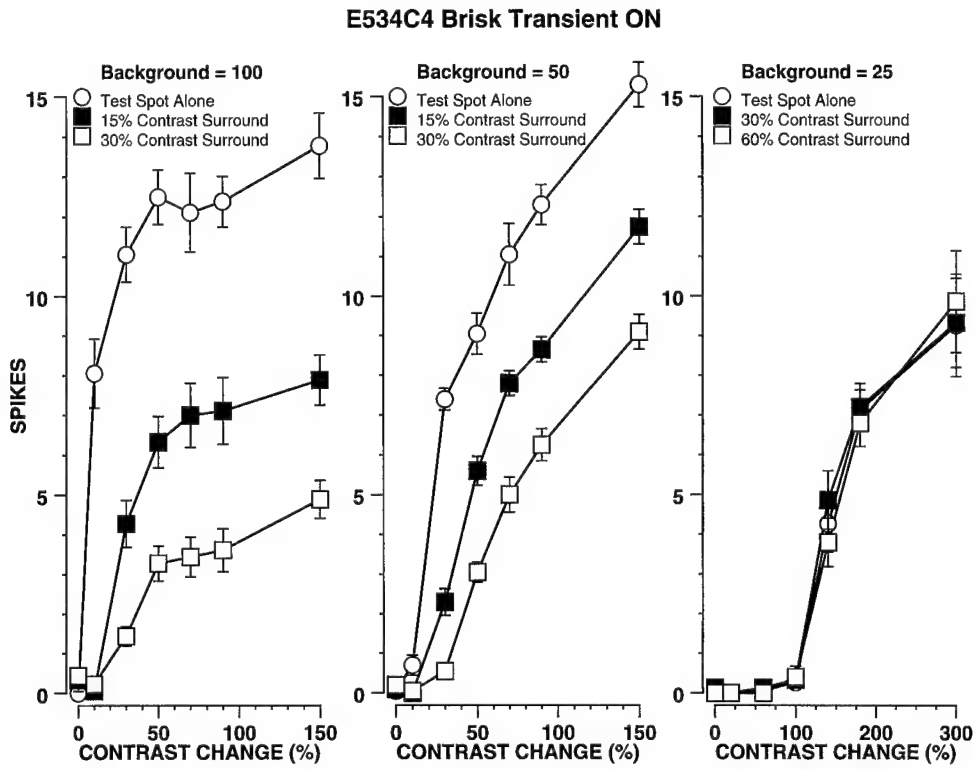

FIG. 19. Effect of lowering the background luminance on the surround inhibition of an ON-center BT cell. Each plot shows the response-vs.-contrast functions as before. It is clear that the surround fails to inhibit center responses at the lowest background level. The cell was masked with an annulus whose inner opening measured 200 μm^2, outer radius 360 μm.

This transient mechanism appears to be distinct from long-term luminance adaptation effects, such as observed by Mangel (1991) in his study relating steady-state luminance changes and injection of current in horizontal cells to center responses of rabbit retinal ganglion cells. The surround effects observed in our experiments are those that occur transiently during modulations around a given (primarily mesopic to low photopic) adaptation level, presumably as would occur during normal active visual behavior.

Intrinsic nonlinearity of the surround mechanism

The assignment, by the curve-fitting algorithm used in this study, of the surround-center interaction to the nonlinear term appears to be at odds with a number of studies (particularly in cat, as described in the INTRODUCTION) that have used a linear DOG model to explain the effects of surround inhibition on center responses. Recently, however, Rowe and Cox (1993) have reported significant nonlinearities in surround effects in ON-OFF ganglion cells and DS cells (but not ON- and OFF-center W cells) in cat retina, with the use of frequency domain analysis. To understand the differences between these and previous results, it is necessary to be clear about the correspondences between the nonlinear model used by the curve-fitting procedure here, and parameters of the DOG models. DOG models typically make two principal assumptions about the center and surround mechanisms: *1*) a spatial assumption, that the strength of both center and surround mechanisms has a Gaussian (usually, but not necessarily, radially symmetrical) distribution about some locus that could be referred to as the absolute receptive-field center and *2*) an interaction assumption that hypothesizes that the ganglion cell response is a function of the linear difference between the integrated responses of the center and surround mechanisms.

Our data do not directly address the hypothesis of a Gaussian spatial distribution for the center and surround mechanisms, except that our center annuli experiments tend to confirm the existence of a strong inhibitory mechanism, like that evoked from the surround, extending within the excitatory receptive-field center. Where the data obtained in this study are not well accounted for by the DOG model is in the interaction between center and surround. The DOG model appears to fail when a larger range of center and surround contrasts are explored than used in previous studies. Formally, it is clear that regions of nonlinear functions that are relatively smooth can often be well approximated by linear functions, for small parameter modulations, such as by the Taylor series expansion. Thus, although our data indicate that the effect of surround stimulation appears to be primarily a reduction in the slope ("contrast gain") of the center mechanism, linear approximations of inhibition as subtractive, such as in the DOG model, may fit the data arbitrarily well for small contrast changes.

To see the "linearizing" effect of reducing contrast modulation, we can rewrite *Eq. 3,* ignoring the contrast threshold (setting it equal to 0), to include only the division-like inhibition term, k_d

$$R = R_{sat} * \frac{\frac{g * c_e}{1 + k_d * c_i}}{1 + \frac{g * c_e}{1 + k_d * c_i}} \qquad (4)$$

For the case of center only stimulation, this equation reduces to

$$R_c = \frac{R_{sat} * g * c_e}{1 + g * c_e} \quad (5)$$

Taking the difference between these two cases, and rearranging terms, yields

$$\Delta R = R_{sat} * g * c_e * \frac{k_d * c_i}{(1 + g * c_e) * (1 + g * c_e + k_d * c_i)} \quad (6)$$

As long as $k_d * c_i \ll 1 + g * c_e$, that is, at sufficiently low contrasts, then the spike reduction due to the surround, ΔR, can be seen to be approximately linearly proportional to surround contrast.

The nonlinear mechanism proposed here attempts to account for the entire functional contrast range of center and surround stimuli effective for the ganglion cell, beyond that which is valid for the DOG model, including response regions near threshold and saturation. The data presented here show that the slope of the response-versus-contrast function decreases smoothly over the range from threshold to saturation. The model we have used attempts to determine the contrast gain of the center response-versus-contrast function without making arbitrary assumptions about where the slope should be measured, by fitting the entire response curve to a Michaelis-Menten–like equation, modified to include a contrast threshold. Good fits of an equation allowing subtractive and division-like inhibition almost exclusively converged with the major effect of the surround being a reduction of the contrast gain of the center, a division-like mechanism, rather than a subtractive, linear effect.

Biophysical motivation for the form of division-like inhibition in Eq. 3

The model of division-like inhibition used in *Eq. 3* has a simple and plausible biophysical interpretation. This equation approximates the behavior of a cell whose excitatory and inhibitory synaptic inputs are proportional to stimulus contrast (if one neglects threshold and the subtractive terms), and whose inhibitory mechanism is of the shunting-inhibition type. To see this point for an idealized, "silent" shunting inhibition, consider a model whose response is proportional to the voltage across the membrane of an equipotential cell composed of three conductances in parallel: a constant leak conductance (g_l), an excitatory synaptic conductance (g_e) with a positive battery in series (E_e), and an inhibitory synaptic conductance (g_i). Assume (without loss of generality) that the resting potential of the cell is zero; that is, the leak conductance has no associated battery ($E_l = 0$). Then, if the inhibitory battery is of a pure shunting-inhibition type, its reversal potential is also zero. If one further neglects this cell's capacitance, then this cell's response is given by *Eq. 7*, where K is the constant of proportionality relating voltage to the spike rate, and $ig_e = g_e/g_l$ and $ig_i = g_i/g_l$

$$R = K * \frac{i_{g_e} * E_e}{i_{g_e} + i_{g_i} + 1} \quad (7)$$

Now, assume that the excitatory and inhibitory conductances are activated by light in proportion to contrast, such that the constants of proportionality are the gain (g) and division constants (k_d) of *Eq. 3*, that is, $i_{ge} = g * c_e$ and $i_{gi} = k_d * c_i$. By making these substitutions, and dividing the numerator and denominator of *Eq. 7* by $(1 + i_{gi})$, one gets *Eq. 3* (without threshold and the subtractive term) if $R_{sat} = K * E_e$. Hence a possible mechanism for the contrast gain control exhibited by the surround of rabbit retinal ganglion cells is the shunting inhibition of excitatory responses, where the magnitude of both shunting and excitatory responses are directly related to the contrast of light.

Of course, it is clear that virtually any synapse that brings about a conductance increase will have a shunting component. For a synapse whose reversal potential is different from the current membrane potential, both linear (subtractive) and nonlinear shunting effects will occur. In such a case, a linear inhibitory contribution would have to be added to the idealized, silent shunting contribution described above.

Extension of the nonlinear surround into the center

Stimulation with a spot and an annulus that were both entirely within the excitatory receptive-field center of ganglion cells yielded nonadditive summation at contrasts whose linear sum of responses should have been below saturation. This result is not predicted by DOG models but is easy to account for with the nonlinear, division-like model. In the linear model the two excitatory and two inhibitory mechanisms should add linearly until saturation. However, in the nonlinear, division-like model, the inhibitory division of contrast gain generated by each of the two spots (or a spot and an annulus) should affect both spots. Thus, even without taking into account the excitatory response due to each spot itself within the excitatory receptive-field center, the surround mechanism of each spot should affect both itself, and the other spot, in a manner that is functionally equivalent to inhibition that is elicited from annuli in the inhibitory surround. We found that the surrounds of rabbit ganglion cells generally continued without interruption into their receptive-field centers, but we did not exhaustively test this finding for all cells reported in this quantitative analysis. Of course, as stated above, our results agree with DOG model postulates that the spatial profile of the surround mechanism extends into the receptive-field center, and they do not contradict the DOG model postulate that it may have a Gaussian profile.

Surround inhibition versus surround excitation

As indicated in the INTRODUCTION, there has been little direct evidence in mammals as to whether the ganglion cell surround, as singularly referred to, acts as a single mechanism, in terms of both inhibitory effects on the center, and excitatory responses at the opposite contrast polarity to the center. Given that extensive lateral connections are made on the excitatory pathway to ganglion cells at both the outer plexiform layer, by horizontal cells, and the inner plexiform layer, by a number of different types of amacrine cells, it would be surprising if there were not more than one kind of surround effect. Our data suggest that a significant part of the mechanism mediating inhibition in ganglion cell surrounds is not the same as the mechanism responsible for excitatory responses in some of those surrounds.

We thank W. W. Belser, III, and M. Villa for programming support and L. DeAngelis for technical assistance.

This work was supported by National Eye Institute Grants EY-05070 and EY-08921 and Office of Naval Research Grant N00014-91-J-1280.

Address for reprint requests: F. R. Amthor, Dept. of Psychology, University of Alabama at Birmingham, Birmingham, AL 35294.

Received 15 July 1994; accepted in final form 16 December 1994.

REFERENCES

AMES, A. A., III, AND NESBETT, F. B. In vitro retina as an experimental model of the central nervous system. *J. Neurochem.* 37: 867–877, 1981.

AMTHOR, F. R. AND GRZYWACZ, N. M. The nonlinearity of the inhibition underlying retinal directional selectivity. *Visual Neurosci.* 6: 197–206, 1991.

AMTHOR, F. R. AND GRZYWACZ, N. M. Inhibition in ON-OFF directionally selective ganglion cells in the rabbit retina. *J. Neurophysiol.* 69: 2174–2187, 1993.

AMTHOR, F. R., OYSTER, C. W., AND TAKAHASHI, E. S. Morphology of ON-OFF direction selective ganglion cells in the rabbit retina. *Brain Res.* 198: 187–190, 1984.

AMTHOR, F. R., TAKAHASHI, E. S., AND OYSTER, C. W. Morphologies of rabbit retinal ganglion cells with concentric receptive fields. *J. Comp. Neurol.* 280: 72–96, 1989a.

AMTHOR, F. R., TAKAHASHI, E. S., AND OYSTER, C. W. Morphologies of rabbit retinal ganglion cells with complex receptive fields. *J. Comp. Neurol.* 280: 97–121, 1989b.

ARIEL, M. AND DAW, N. W. Effects of cholinergic drugs on receptive field properties of rabbit retinal ganglion cells *J. Physiol. Lond.* 324: 135–160, 1982.

BARLOW, H. B., FITZHUGH, R., AND KUFFLER, S. W. Change of organization in the receptive fields of the cat's retina during dark adaptation. *J. Physiol. Lond.* 137: 338–354, 1957.

BARLOW, H. B., HILL, R. M., AND LEVICK, W. R. Retinal ganglion cells responding selectively to direction and speed of image motion in the rabbit. *J. Physiol. Lond.* 173: 377–407, 1964.

BAYLOR, D. A. AND FUORTES, G. F. Electrical responses of single cones in the retina of the turtle. *J. Physiol. Lond.* 207: 77–92, 1970.

BELGUM, J. H., DVORAK, D. R., MCREYNOLDS, J. S., AND MIYACHI, E.-I. Push-pull effect of surround illumination on excitatory and inhibitory inputs to mudpuppy retinal ganglion cells. *J. Physiol. Lond.* 388: 233–243, 1987.

BENARDETE, E. A., KAPLAN, E., AND KNIGHT, B. W. Contrast gain control in the primate retina: P cells are not X-like, some M cells are. *Visual Neurosci.* 8: 483–486, 1992.

CALDWELL, J. H. AND DAW, N. W. New properties of rabbit retinal ganglion cells. *J. Physiol. Lond.* 276: 257–276, 1978a.

CALDWELL, J. H. AND DAW, N. W. Effects of picrotoxin and strychnine on rabbit retinal ganglion cells: changes in centre surround receptive fields. *J. Physiol. Lond.* 276: 299–310, 1978b.

CALDWELL, J. H., DAW, N. W., AND WYATT, H. J. Effects of picrotoxin and strychnine on rabbit retinal ganglion cells: lateral interactions for cells with more complex receptive fields. *J. Physiol. Lond.* 276: 277–298, 1978.

CAMPBELL, F. W. C. AND ROBSON, J. Application of Fourier Analysis to the visibility of gratings. *J. Physiol. Lond.* 197: 551–566, 1968.

CLELAND, B. G. AND LEVICK, W. R. Brisk and sluggish concentrically organized ganglion cells in the cat's retina. *J. Physiol. Lond.* 240: 421–456, 1974.

CLELAND, B. G., LEVICK, W. R., AND SANDERSON, K. J. Properties of sustained and transient ganglion cells in the cat retina. *J. Physiol. Lond.* 228: 649–680, 1973.

DAW, N. W., ARIEL, M., AND CALDWELL, J. H. Function of neurotransmitters in the retina. *Retina* 2: 322–331, 1982.

ENROTH-CUGELL, C. AND LENNIE, P. The control of retinal ganglion cell discharge by receptive field surrounds. *J. Physiol. Lond.* 247: 551–578, 1975.

ENROTH-CUGELL, C., LENNIE, P., AND SHAPLEY, R. M. Surround contribution to light adaption in cat retinal ganglion cells. *J. Physiol. Lond.* 247: 579–588, 1975.

ENROTH-CUGELL, C. AND ROBSON, J. G. The contrast sensitivity of retinal ganglion cells of the cat. *J. Physiol. Lond.* 187: 517–552, 1966.

ENROTH-CUGELL, C., ROBSON, J. G., SCHWEITZER-TONG, D. E., AND WATSON, A. B. Spatio-temporal interactions in cat retinal ganglion cells showing linear spatial summation. *J. Physiol. Lond.* 341: 279–307, 1983.

ENROTH-CUGELL, C. AND SHAPLEY, R. M. Adaptation and dynamics of cat retinal ganglion cells. *J. Physiol. Lond.* 233: 271–309, 1973.

HAMASAKI, D. I., TASAKI, K., AND HITOSHI, S. Properties of X- and Y-cells in the rabbit retina. *Jpn. J. Physiol.* 29: 445–457, 1979.

HICKEY, T. L., WINTERS, R. W., AND POLLACK, J. G. Center-surround interactions in two types of ON-center ganglion cells in the cat. *Vision Res.* 13: 1511–1526, 1973.

KUFFLER, S. W. Discharge patterns and functional organization of mammalian retina. *J. Neurophysiol.* 16: 37–68, 1953.

LEVICK, W. R. Receptive fields of rabbit retinal ganglion cells. *Am. J. Optom.* 42: 337–343, 1965.

LEVICK, W. R. Receptive fields and trigger features of ganglion cells in the visual streak of the rabbit's retina. *J. Physiol. Lond.* 188: 285–307, 1967.

MANGEL, S. C. Analysis of the horizontal cell contribution to the receptive field surround of ganglion cells in the rabbit retina. *J. Physiol. Lond.* 442: 211–234, 1991.

MERWINE, D. K. AND AMTHOR, F. R. Ganglion cell surround inhibition is divisive, not linear, in rabbit retina. *Soc. Neurosci. Abstr.* 16: 466, 1990.

MERWINE, D. K., AMTHOR, F. R., AND GRZYWACZ, N. M. Ganglion cell surround inhibition is divisive, not linear, in rabbit retina (Abstract). *Invest. Ophthalmol. Visual Sci.* 31: 115, 1990.

MERWINE, D. K., AMTHOR, F. R., AND GRZYWACZ, N. M. Characteristics of divisive ganglion cell surround inhibition in the rabbit retina (Abstract). *Invest. Ophthalmol. Visual Sci.* 32: 1132, 1991.

MICHAELIS, L. AND MENTEN, M. I. Die Kinetik der Invertinwirkung. *Biochem. Z.* 49: 333–369, 1913.

NYE, P. W. AND NAKA, K.-I. The dynamics of inhibitory interaction in a frog receptive field: a paradigm of paracontrast. *Vision Res.* 11: 377–392, 1971.

PEICHL, L., BUHL, E. H., AND BOYCOTT, B. B. Alpha ganglion cells in the rabbit retina. *J. Comp. Neurol.* 263: 25–41, 1987.

POWELL, M. J. D. A FORTRAN subroutine for solving system of nonlinear algebraic equations. In: *Numerical Methods for Nonlinear Algebraic Equations,* edited by P. Robinowitz. New York: Gordon & Breach, 1970.

PU, M.-L. AND AMTHOR, F. R. Dendritic morphologies of retinal ganglion cells projecting to the lateral geniculate nucleus in rabbit. *J. Comp. Neurol.* 302: 675–693, 1990.

RODIECK, R. W. AND STONE, J. Analysis of receptive fields of cat retinal ganglion cells. *J. Neurophysiol.* 28: 832–849, 1965.

ROWE, M. H. AND COX, J. F. Spatial receptive-field structure of cat retinal W cells. *Visual Neurosci.* 10: 765–779, 1993.

SHAPLEY, R. AND VICTOR, J. D. The contrast gain control of the cat retina. *Vision Res.* 19: 431–434, 1979a.

SHAPLEY, R. M. AND VICTOR, J. D. The effect of contrast on the transfer properties of cat retinal ganglion cells. *J. Physiol. Lond.* 285: 275–298, 1978.

SHAPLEY, R. M. AND VICTOR J. D. Nonlinear spatial summation and the contrast gain control of cat retinal ganglion cells. *J. Physiol. Lond.* 290: 141–161, 1979b.

SHAPLEY, R. M. AND VICTOR, J. D. The effect of contrast on the non-linear response of the Y cell. *J. Physiol. Lond.* 302: 535–547, 1980.

SHAPLEY, R. M. AND VICTOR, J. D. How the contrast gain control modifies the frequency responses of cat retinal ganglion cells. *J. Physiol. Lond.* 318: 161–179, 1981.

THIBOS, L. N. AND WERBLIN, F. S. The response properties of the steady antagonistic surround in the mudpuppy retina. *J. Physiol. Lond.* 278: 79–99, 1978a.

THIBOS, L. N. AND WERBLIN, F. S. The properties of surround antagonism elicited by spinning windmill patterns in the mudpuppy retina. *J. Physiol. Lond.* 278: 101–116, 1978b.

TORRE, V. AND POGGIO, T. A synaptic mechanism possibly underlying directional selectivity to motion. *Proc. R. Soc. Lond. B Biol. Sci.* 202: 409–416, 1978.

VANEY, D. I., LEVICK, W. R., AND THIBOS, L. N. Rabbit retinal ganglion cells. *Exp. Brain Res.* 44: 27–33, 1981.

WERBLIN, F. S. AND COPENHAGEN, D. R. Control of retinal sensitivity: lateral interactions at the inner plexiform layer. *J. Gen. Physiol.* 63: 88–110, 1974.

WYATT, H. J. AND DAW, N. W. Directionally sensitive ganglion cells in the rabbit retina: specificity for stimulus direction, size and speed. *J. Neurophysiol.* 38: 613–26, 1975.

JOURNAL OF NEUROPHYSIOLOGY
Vol. 69, No. 6, June 1993. *Printed in U.S.A.*

Facilitation in ON-OFF Directionally Selective Ganglion Cells of the Rabbit Retina

NORBERTO M. GRZYWACZ AND FRANKLIN R. AMTHOR
The Smith-Kettlewell Eye Research Institute, San Francisco, California 94115; and Department of Psychology and Neurobiology Research Center, University of Alabama at Birmingham, Birmingham, Alabama 35294

SUMMARY AND CONCLUSIONS

1. We have investigated the facilitation of extracellularly recorded responses of ON-OFF directionally selective (DS) ganglion cells of the rabbit retina to two-slit preferred-direction apparent motion produced by both prolonged light steps, which simulate movement of an edge past two apertures, and light flashes, which simulate movement of a spot or slit.

2. Within the excitatory receptive-field center of DS ganglion cells, apparent motion with prolonged light steps elicits preferred-direction facilitation whose rise time (220 ± 150 ms, average rise to 90% of maximum for 6 cells) is typically longer than the rise time of the excitatory response elicited by each slit. The decay time to baseline of facilitation during prolonged light steps is generally longer than 500 ms and hence greatly exceeds the typical duration of the excitatory response elicited by the slits.

3. Prolonged light steps are generally effective for facilitating any given excitatory receptive-field locus from a roughly ovoid area that typically extends on the order of 100–200 μm in the preferred direction, which is less than one-half the size of the excitatory receptive-field center. Within 100 μm, facilitation can occur for motion diagonal to the preferred-null axis as long as the projection of the motion on the preferred-null axis points in the preferred direction.

4. The time course of preferred-direction facilitation between two slits does not appear to have a strong systematical dependence on the interslit distance over the range in which facilitation is effective.

5. Short light flashes are ineffective for eliciting facilitation and, at sufficiently long interslit delays, elicit inhibition all around the test slit. This inhibition may be due to the antagonistic surround mechanism within the receptive-field center, which is effectively elicited by short-duration stimuli.

6. The effect of preferred-direction facilitation is addition-like, rather than multiplication-like. That is, the facilitatory effect of the first slit appears as the addition of a fixed value to the response-versus-contrast curve of the second slit, rather than a multiplication of the curve by a constant factor. The functional relationship between strength of facilitation and contrast of the first slit is sigmoidal, however, and thus nonlinear.

7. Experiments with long light steps show that the interaction between excitation and preferred-direction facilitation is largely segregated between the ON and OFF pathways. Thus, for preferred-direction apparent motion, light onset of the first slit strongly facilitates the response to the onset, but generally not the offset, of the second slit. Light offset of the first slit similarly tends to facilitate only the response to light offset of the second slit. However, at short distances, where like-sign interactions are significantly facilitatory, opposite sign interactions tend to be inhibitory.

8. We discuss several models for facilitation from the perspective of the above data and propose a new class of models, called "gated-enhancer" models, that can account for the data. The gated-enhancer model postulates that an enhancer (such as a molecule) that is produced by a previous light stimulus enhances the response to subsequent stimuli along trajectories corresponding to preferred-direction movement. This enhancer cannot produce a response by itself, however, because it is only effective when gated by a subsequent, active input.

INTRODUCTION

The role of facilitation for preferred-direction motion in the directional and motion sensitivities of ON-OFF directionally selective (DS) ganglion cells of the rabbit retina has been unclear from previous studies. Barlow and Levick (1965) reported that the total response to preferred-direction apparent motion with two slits is larger than the sum of the responses elicited by each of the slits when presented alone. However, in their experimental conditions, this preferred-direction facilitation seemed only marginally significant compared with null-direction inhibition, and they did not pursue its investigation further or incorporate a facilitatory mechanism in their model for retinal directional selectivity. In apparent motion experiments with flashed stimuli, Wyatt and Daw (1975) found no preferred-direction facilitation.

In contrast to those earlier results, apparent motion experiments of Amthor and Grzywacz (1993) sometimes elicited strong preferred-direction facilitation, particularly when *1*) the presentation of the slits was sustained, *2*) the delay between the slits was sufficiently long, and *3*) the distances between the slits were sufficiently short. In some of these experiments, preferred-direction facilitation produced a greater change in the total number of elicited spikes than null-direction inhibition.

The sensitivity of facilitation to stimulus parameters may explain the relatively small facilitatory effects observed by Barlow and Levick (1965) in their apparent-motion experiments. Their technique of manually moving targets behind a dual-slit aperture mask may not, for example, have reproducibly generated the appropriate interslit delay needed to elicit facilitation. In the experiments of Wyatt and Daw (1975), the use of flashed rather than sustained stimuli may not have been effective for eliciting facilitation, because facilitation apparently requires a sustained stimulus. This paper reports the results of experiments that quantitatively investigated the spatiotemporal conditions under which facilitation contributes to motion sensitivity and directional selectivity in ON-OFF DS ganglion cells of the rabbit retina.

We also tested whether the preferred-direction facilitatory effect of the first slit on the second is additive by exam-

ining the effect of varying the contrast of the first slit on the response-versus-contrast curve of the second. Facilitatory mechanisms, such as a threshold followed by linear suprathreshold behavior, would facilitate the responses elicited by the second slit in an addition-like manner, whereas multiplicative facilitatory mechanisms, such as modulation of the membrane resistance (Borg-Graham and Grzywacz 1991), would scale the response-versus-contrast curve of the second slit in a multiplication-like manner, similar to, but in the opposite direction of, the mechanism demonstrated for inhibition (Amthor and Grzywacz 1991, 1993).

Some of the results in this paper appeared previously in abstract form (Grzywacz and Amthor 1989, 1991).

METHODS

Retina-eyecup preparation

The preparation was the same as in the accompanying paper (Amthor and Grzywacz 1993). We used eyes from both sexes of adult Dutch belt pigmented rabbits weighing ≥1.3 kg. The surgery was performed in dim red light on animals that had been dark adapted for ≥30 min. An initial dose of urethan (2 g/kg) was used to anesthetize the animals deeply. This was followed by thiamylal sodium (Surital, 0.25 g/50 ml wt/vol), or pentobarbital sodium given to effect. After the animal was deeply anesthetized, we enucleated the right eye as the animal was killed with a massive overdose of Surital. The enucleated eye was hemisected, devitreated, everted, and superfused, as described in the accompanying paper (Amthor and Grzywacz 1993) and previously (Amthor et al. 1984, 1989).

Stimulation and recording

The methods of stimulation, recording, and data collection are also the same as those in the accompanying paper (Amthor and Grzywacz 1993). Well-isolated, single unit extracellular recordings were made from ON-OFF DS ganglion cells in the isolated retina-eyecup preparation for up to 10 h. Stimuli generated by a Picasso video controller were presented on a Tektronix 608 monitor. Stimuli were imaged on the retina by a 17-mm-focal-length, 12-mm-diam achromatic lens ~870 mm from the Tektronix 608 screen or LED array. A MS-DOS 80286 computer controlled stimulus parameter settings on the Picasso and sequencing of stimuli and also stored the time of occurrence of all action potentials elicited by various stimuli to the nearest millisecond.

Data collection

All experimental protocols involved the initial steps of obtaining a well-isolated recording; making a receptive-field map with flashing spots to determine the shape of the excitatory receptive-field center and inhibitory surround; verifying, from its response properties to moving stimuli, that the cell recorded from was an ON-OFF DS ganglion cell; and determining the preferred-null axis of the cell. Cumulative poststimulus time (PST) histograms were computed from the time-of-spike-occurrence data. Average spike counts in the first 500 ms after the onset and offset of spots or slits were also accumulated as one response measure.

Base subtraction

For some two-slit apparent-motion experiments, the expected average number of spikes due to the first slit occurring in the 500-ms window of the second slit were subtracted, bin by bin, from the response histogram accumulated for the second slit. Removal of the excitatory response of the first slit highlights the changes in the response to the second slit due to the interaction with the first slit, independent of the first slit's excitatory response. We refer to this procedure as "base subtraction," the base being the excitation expected from the first slit alone.

Data for this paper were obtained in a variety of experimental protocols from 60 ON-OFF DS ganglion cells from 20 animals.

RESULTS

Facilitation (and inhibition) elicited by apparent motion

We recorded the responses of ON-OFF DS ganglion cells to single slits presented by themselves and to apparent motion elicited by sequential stimulation of two slits within the cell's excitatory receptive-field center. PST histograms showing the responses to such stimuli are shown for *cell E384C2.1* in Fig. 1. The responses elicited by the Slits A, B, and C presented by themselves appear in the *top, middle,* and *bottom* histograms, respectively. The *second histogram from the top* is the response to preferred-direction apparent motion from Slit A to Slit B; the *fourth histogram from the top* is the response to null-direction apparent motion from Slit C to Slit B.

The *top PST histogram* in Fig. 1 shows the result of presenting Slit A by itself with stimulus onset at 1,800 ms and offset at 2,800 ms. This stimulation yielded ON and OFF responses that started at ~1,900 and 2,900 ms, respectively. The *middle PST histogram* in Fig. 1 shows the response to the presentation of Slit B by itself with onset at 2,000 ms and offset at 3,000 ms. Stimulation of this slit elicited a relatively weak ON response that started around 2,100 ms and a stronger OFF response that started around 3,100 ms. Presenting these two stimuli with the same relative delay as in the *top* and *middle histograms* yields preferred-direction apparent motion from Slit A to Slit B of a light and then a dark edge, with an interslit delay for each edge of 200 ms. The response to this apparent motion is shown in the *second PST histogram from the top.* This histogram reveals a strong enhancement of both the ON and OFF responses attributable to Slit B by prior stimulation of Slit A.

The interslit delay is sufficiently long in this (*2nd from the top*) histogram to distinguish, by their separation in time, much of the (facilitated) response of Slit B from the response elicited by Slit A. The portions of the preferred-direction apparent-motion histogram (*2nd from top*) in which the excitation due to Slit A by itself would be expected to occur, from 1,900 to 2,100 and from 2,900 to 3,100 ms, appear essentially the same as in the corresponding period in the *top histogram,* where Slit A alone is modulated. Because the response due to Slit B occurs later than most of the excitatory response attributable to Slit A, the enhancement of the Slit B response does not appear to reflect merely the addition of the suprathreshold excitatory response of Slit A to that of Slit B. It cannot be determined from this experiment, however (but will be considered in later sections of the paper), whether the facilitation of the response due to Slit B occurs because of a long-lasting, but subthreshold, "tail" of the excitatory response elicited by Slit A.

In contrast to the facilitatory effect of Slit A on Slit B, the *fourth PST histogram* shows the inhibitory effect of stimula-

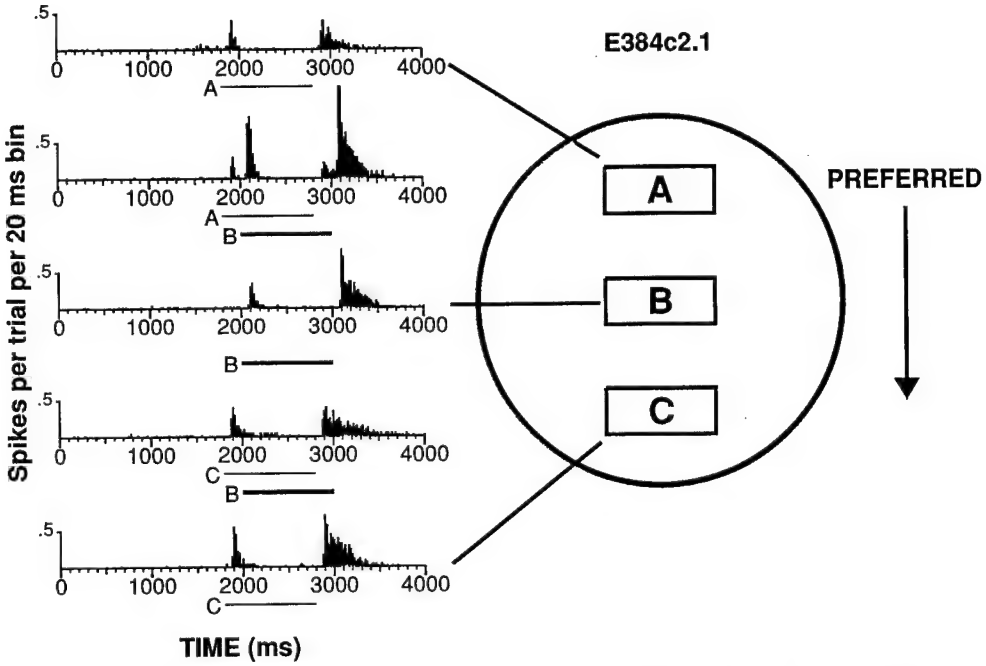

FIG. 1. *Left*: average poststimulus time (PST) histogram responses of an ON-OFF directionally selective ganglion cell (*E384C2.1*) to each of 3 slits within receptive-field center presented in isolation (*top, middle,* and *bottom traces,* respectively), and in apparent-motion sequences simulating preferred-direction motion of A to B (*2nd histogram from top*) and null-direction apparent motion from C to B (*4th histogram from top*). Ordinates are average spike counts per bin, where bin size is 20 ms. Each slit was modulated to a level 30% above background for 1,000 ms and then returned to background. Time each slit is above background is indicated by heavy line below each horizontal time axis. Slit pairs are presented with a 200-ms delay between similar-sign contrast transitions of the 1st and 2nd slits, so that onset on the 1st slit occurred 200 ms before onset of the 2nd, and offset of the 1st slit 200 ms before offset of the 2nd. *Right*: slits A, B, and C within circle to *right* of histograms give the approximate positions of slits eliciting PST histograms to *left* within border of excitatory receptive center, as established by flashing small spots. Excitatory receptive-field diameter of this cell, located at inferior edge of visual streak, was ~500 μm. Data are averages of 100 stimulus presentations. Histograms show that null-direction apparent motion (C → B) elicits inhibition and preferred-direction apparent motion (A → B) elicits facilitation.

tion of Slit C 200 ms before Slit B. Although excitatory responses are elicited to both the onset and offset of Slit C when presented by itself (*bottom PST histogram*), apparent motion in the null direction from Slit C to Slit B with the same relative delay (*the 4th PST histogram*) results in greatly diminished responses to both the onset and offset of Slit B.

Temporal behavior of preferred-direction facilitation

We examined the temporal characteristics of the facilitation of one slit by another by varying the delay between the presentation of the first and second slits in two-slit apparent-motion experiments similar to that illustrated in Fig. 1. Figure 2 shows the histograms that resulted from systematically varying the delay between the presentations of the two slits for *cell E385C1.1.* The *first and second histograms in the left column* of Figure 2 (repeated also on the *right*) show the averaged responses obtained when Slits A and B were presented by themselves, respectively. In this particular experiment, the modulation of Slit B by itself (*2nd histogram from the top*) produced a moderate ON response but an almost negligible OFF response (the balance between the ON and OFF responses varied somewhat from cell to cell and with stimulus conditions).

The *third histogram in the left column* shows that the ON response (and to a lesser extent the OFF response) resulting from simultaneous presentation of Slits A and B is greater than the expected sum of the responses obtained when the slits were presented separately. However, in this and other histograms with short interslit delays (<500 ms), it is difficult to distinguish the effect of stimulating Slit A on the response elicited by Slit B from the contribution of the response elicited by Slit A itself, because the excitatory response due to Slit A overlaps substantially in time with the excitatory response due to Slit B. To examine the effect of stimulation of Slit A on Slit B, independent of the excitatory response due to Slit A, we performed the operation termed base subtraction (see METHODS).

In the *right column* of Fig. 2 are the base-subtracted versions of the *left*-column histograms (except for the *top 2 single-slit presentation histograms,* which are repeated from the *left* column). The *third histogram on the right* in Fig. 2 shows that the ON response elicited by Slit B is significantly enhanced when it is presented simultaneously with Slit A, even with the excitatory response due to Slit A removed from this histogram by the base-subtraction procedure. The base-subtracted OFF response (arrow), however, is still quite weak, although larger than the negligible OFF response produced by Slit B alone.

Base-subtracted histograms obtained at progressively longer interslit delays (*4th and lower histograms on the right*) indicate that the facilitatory effect of Slit A on B becomes even stronger when modulation of Slit A precedes

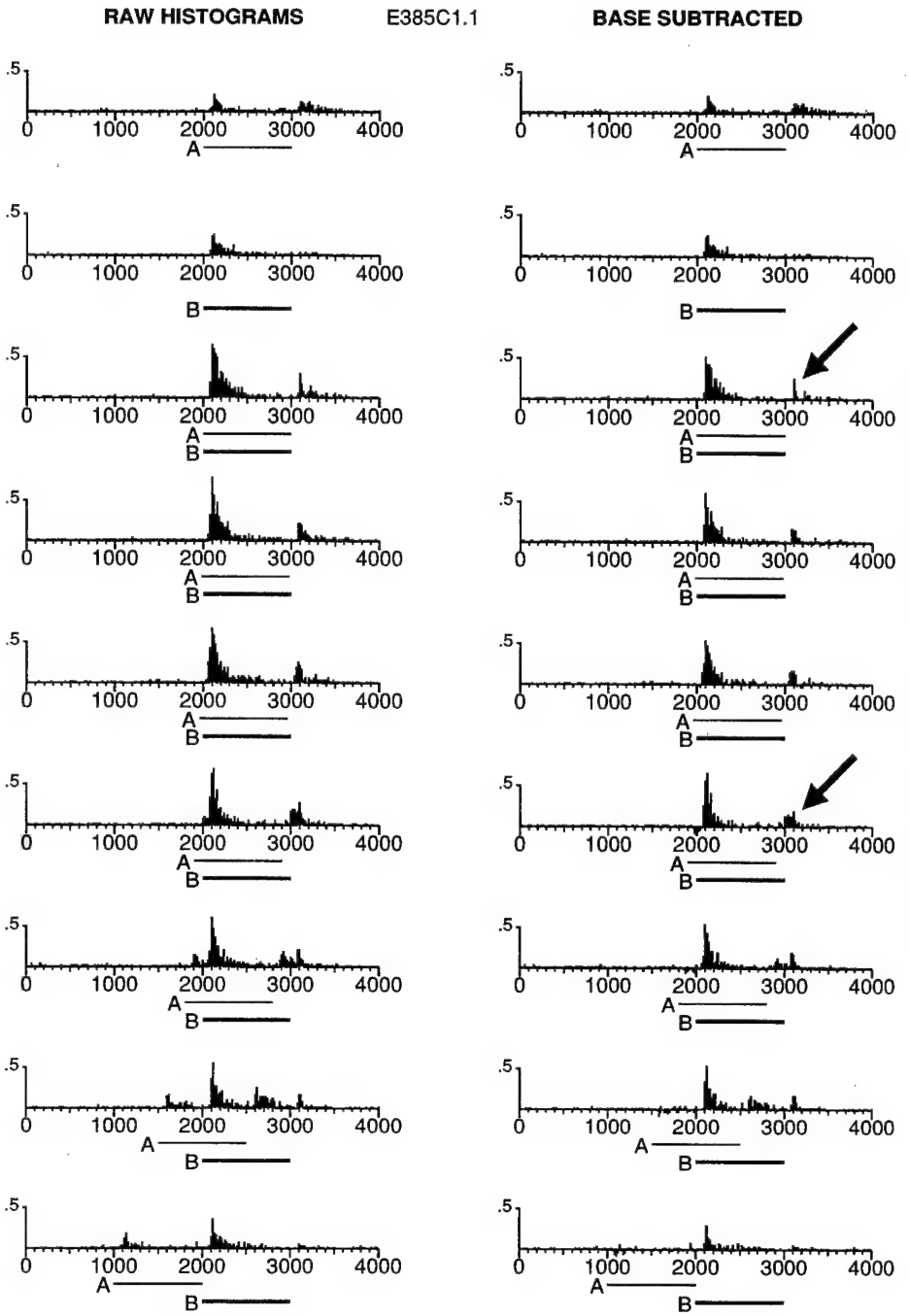

FIG. 2. PST histograms showing effect of varying delay between the 2 slits on resultant facilitated responses. Modulation scheme is same as in Fig. 1, except for variable delay, and modulated contrast is 10% above background and then back to background. The *1st and 2nd histograms in both columns* show response elicited by Slits A and B, respectively, when they were presented alone. *Left*: below the *top 2 single* slit histograms are histograms obtained for 2 slit apparent motion at various interslit delays (*top* to *bottom* order is 0, 20, 50, 100, 200, 500, 1,000 ms). *Right*: 3rd and following histograms from the left are base subtracted, with expected response of the 1st slit [obtained from its average PST histogram when presented alone (as shown in *top histogram in each column*)] subtracted from response obtained when both slits were modulated in sequence. These histograms show effect of contrast modulation of the 1st slit on response elicited by the 2nd slit with excitatory response elicited by the 1st slit removed. Arrows indicate that facilitation is larger at a 100-ms delay than for simultaneous presentation of the 2 slits. Data are averages of 83 stimulus presentations.

modulation of Slit B. This is especially true for the OFF response in this particular experiment. For example, when the interslit delay is 100 ms (*6th histogram from the top*), the base-subtracted OFF response elicited by Slit B (*bottom arrow*) is markedly greater than that obtained at shorter interslit delays. Similar enhancement of the Slit B OFF response also occurs at delays of 200 and 500 ms (*7th and 8th histograms from the top, on the right*). The ON response elicited by Slit B also appears to be facilitated more for delayed than simultaneous presentation of the two slits, although this is somewhat less obvious in this particular experiment. Because the maximum facilitatory effect occurs when the first slit precedes the second by $\geq$100 ms, rather than when it is presented simultaneously, the rise time of the facilitatory mechanism appears to be longer than that of the excitatory response elicited by the first slit. That both ON and OFF responses are facilitated for interslit delays as long as 500 ms (*8th histogram from the top, on the right*) indicates that the mechanism by which the first slit facilitates the response of the second is significantly longer lasting than the suprathreshold excitatory response of the first slit.

The *bottom histogram on the right* in Fig. 2 shows the effect of turning off Slit A simultaneously with the onset of Slit B, with the OFF response of Slit A base-subtracted. Although it can be seen in the *top histogram* of Fig. 2 that an excitatory OFF response results from the offset of Slit A, the *bottom, base-subtracted histogram on the right* shows that

Slit A offset has no substantial effect on the ON response to Slit B when occurring simultaneously with it. This and other results from similar experiments indicate that the response facilitation observed in these experiments was not merely due to the excitation elicited by the second slit summing with some long-lasting, subthreshold tail of the excitatory response elicited by the first slit. Further details concerning the specific interaction between ON and OFF responses in these cells will be presented later in this paper.

The excitatory responses of ON-OFF DS ganglion cells are usually quite transient, returning to baseline well within 500 ms. We therefore used the average number of spikes in the first 500 ms after the onset and offset of a slit as a quantitative measure of the total response elicited by stimulation of that slit. For short interslit delays, the expected excitatory response of the first slit was removed from the response of the second slit accumulated during this time window by the base-subtraction procedure. The difference between the average number of spikes elicited when a slit was presented alone, versus when it was preceded by another slit in an apparent-motion sequence, is indicative of the strength of the facilitatory effect.

The strength of facilitation as a function of the interslit delay, as computed by this response measure, is shown for the ON response of one cell and the ON and OFF responses of another cell in Fig. 3. The base-subtracted response to the second slit, as facilitated by the first, is represented in each plot by the solid line with error bars. The horizontal dashed line in each plot indicates the magnitude of the response obtained when the second slit was presented by itself. The shaded area in each plot represents the normalized PST histogram of the excitatory response due to the first slit. If the facilitatory effect of the first slit were due to a process (such as at the ganglion cell's spike generating mechanism) that closely followed the mechanism that produced the first slit's excitatory response, it should have a similar time course, and the magnitude of facilitation due to the first slit should be correlated with the shaded waveform showing the time course of the excitatory response to the first slit.

Figure 3 shows more quantitatively than the histograms of Fig. 2 that the rise time of the preferred-direction apparent-motion facilitation produced by the first slit is often longer than the rise time of the first slit's excitatory response [for interpolated 90% of peak of facilitation, 220 ± 150 (SD) ms for 5 cells]. The facilitatory effect is much more sustained than the excitatory response due to the first slit; in all three of the plots in Fig. 3, the excitation due to the first slit has essentially returned to baseline by 500 ms, but the facilitatory effect remains significant at that time.

We performed several experiments with interslit delays up to 4 s to determine the maximum time course for which facilitation might be effective. Figure 4 shows the results of one such experiment for the ON and OFF response of *cell E388C1.1*. In this experiment, facilitation was effective for >2,000 ms for the ON stimulus and >1,000 ms for the OFF stimulus. In general, we observed that the facilitatory effect induced by the apparent motion typically lasted considerably longer than the excitatory response of the first slit for both ON and OFF responses, although which response sign was associated with the longest lasting facilitation varied between cells and with particular stimulus conditions.

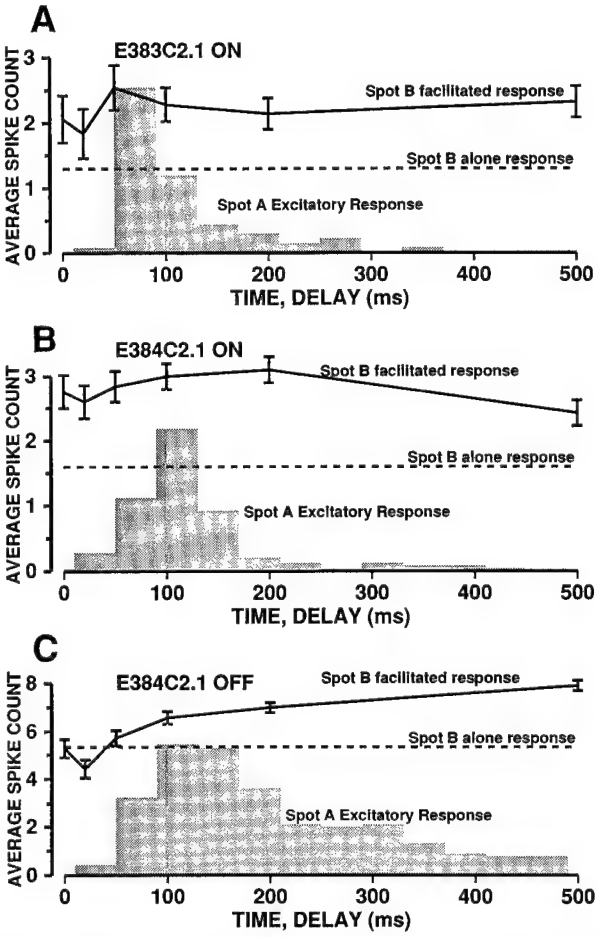

FIG. 3. Facilitation of response of the 2nd (test) slit as a function of the delay after the 1st slit when slits were presented in apparent motion sequences. Modulation was 70% above baseline for *cell E383C2.1* and 30% for *E384C2.1*. *A*: ON response of one cell (*E383C2.1*); *B* and *C*: ON and OFF responses, respectively, of another cell (*E384C2.1*). Dashed horizontal line in each plot is response elicited by test slit when presented by itself. Solid line with error bars shows average number of spikes in the 1st 500 ms after either onset or offset of the 2nd slit when preceded by the 1st slit at indicated delay, with expected response due to the 1st slit removed by the base-subtraction procedure (see METHODS for explanation). Shaded area in each plot represents normalized PST histogram of excitatory response due to the 1st slit. Height of solid facilitated test slit response line above dashed test slit alone response line indicating magnitude of facilitation effect shows that it lasts considerably longer than time course of excitatory response due to the 1st slit, indicated by shaded area.

Compared with the effect of null-direction inhibition, however, the decay of apparent-motion facilitation was faster than that of null-direction inhibition, which could be effective for interslit delays of ≥4 s (Amthor and Grzywacz 1993).

Spatial profile of preferred-direction facilitation

We examined how the strength of facilitation varied not only as a function of interslit delay in apparent motion but also as a function of distance and angle with respect to the preferred-null axis. Figure 5 shows the dependence of the facilitatory strength on the interslit distance along the preferred-null axis for three cells. The interslit delay was 200 ms in all three cases. The solid lines with error bars show the facilitated response elicited by the second slit. Because

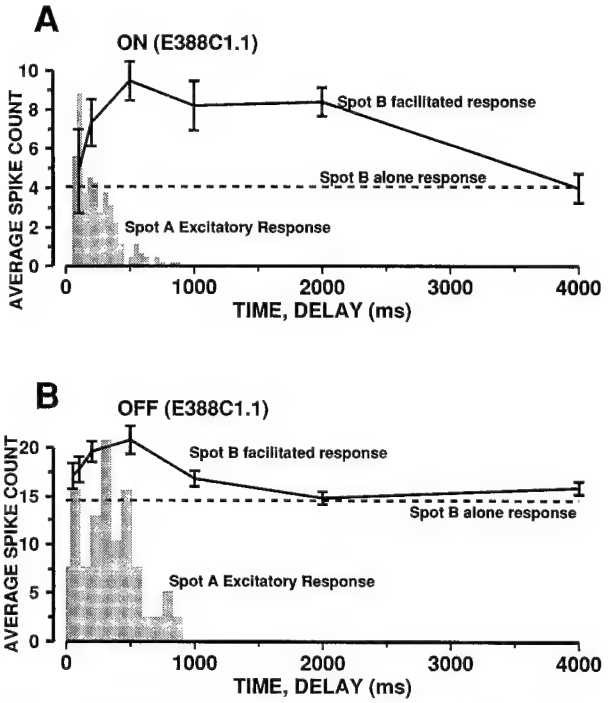

FIG. 4. Facilitation of ON (*A*) and OFF (*B*) responses of a 2nd slit as a function of interslit delays up to 4,000 ms, for *cell E388C1.1*. Plots have same scheme as in Fig. 3. Modulation contrast was to 20% above background. Facilitatory process can be seen to be sustained for ≥2,000 ms for ON response (*top*), and for at least 1,000 ms for OFF response (*bottom*) and clearly lasts much longer than excitatory response of the 1st slit when presented alone, indicated by shaded area.

quantitative aspects of the facilitatory effects were similar for both ON and OFF stimuli, in this and some later figures, where appropriate, we have combined light onset and offset responses obtained in the same cell for the same stimulus. The magnitude of the combined ON and OFF responses elicited by the first slit when presented alone at each distance is indicated by the filled black circle. In the experiments shown in Fig. 5, *A* and *B*, there were five equidistant slits; in the experiment in Fig. 5*C*, there were six. The slit in the bottom panel plotted in a negative preferred direction was on the other side of the test slit from the preferred-direction slits and was used to elicit null-direction apparent-motion as a control. The facilitated response shown at zero distance is the effect on the response of the second slit by prior stimulation at the same receptive-field position.

In the three cells shown in Fig. 5, as was found generally, facilitation exhibited a relatively narrow spatial range. The mean distance and standard deviations for interpolated decay to 10% of peak is 180 ± 50 μm for five cells, which is about one-half of the diameter of the excitatory receptive-field center. (At zero distance there is no net systematic facilitation or inhibition. This apparent linearity of the response lends further support for the base-subtraction procedure.) In comparison, it was found that the inhibition elicited by null-direction apparent motion in similar experiments extended >500 μm (Amthor and Grzywacz 1993).

Figure 5 shows that there is no correlation between the response a slit elicits and the facilitation it can produce. In all three experiments, the closest slit always produced the greatest facilitation, even though in Fig. 5, *A* and *B*, it was not the slit that caused the largest response when presented by itself. Thus, even for interactions of the same (ON/OFF) sign, the facilitation cannot be accounted for by a generalized subthreshold tail of the excitatory response of the first slit but appears to result from a specific mechanism that is restricted in space, as well as being confined to like contrast sign.

We used arrays of slits to measure the two-dimensional

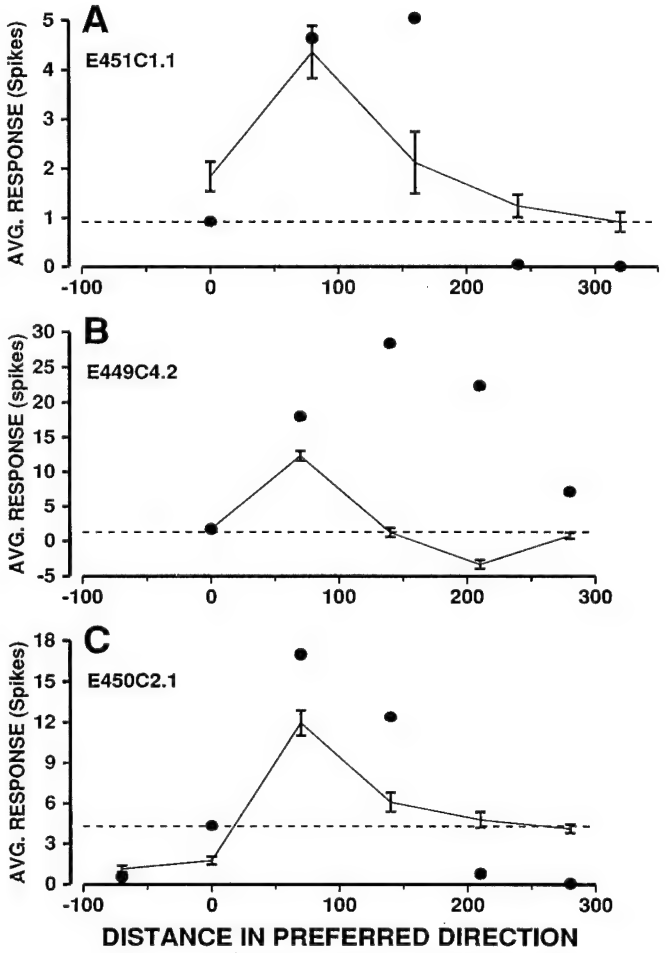

FIG. 5. Dependence of facilitatory strength on interslit distance along preferred-null axis for 3 cells. Average response measure is base-subtracted average total number of spikes within 500 ms of onset and offset of the 2nd slit, as in previous figures. Interslit delay was 200 ms in all 3 cases. Solid lines with error bars show facilitated response elicited by the 2nd slit. Magnitude of response elicited by the 1st slit when presented by itself at each distance is indicated by filled black circle. *A*: *cell E451C1* had an excitatory receptive-field center diameter of ~400 μm on retina. "Test" slit was located near middle of this region, with 4 facilitating slits on preferred-direction side. Two additional slits on null-direction side, whose inhibitory effects on test slit are not plotted, served as controls. *B*: *cell E449C4* had an excitatory receptive-field diameter of ~400 μm on the retina. Test slit was located somewhat off-center toward null-direction-approaching side, so that farthest of the 4 facilitatory slits was just within border of receptive-field center. *C*: *cell E450C2* had a receptive-field diameter of ~350 μm on the retina. Five slits were located on preferred-direction-approaching side from test slit. However, farthest of these slits elicited little excitatory response when presented by itself and thus may have been located in a receptive-field region having considerable surround input. Slit plotted as having a negative direction was used to elicit null-direction motion as a control. Preferred-direction motion elicits facilitation if interslit distance is <200 μm. Strength of facilitation elicited from a given position in receptive-field center is independent of strength of response elicited from that position.

profile of facilitation. The results of these experiments for four cells are shown in Fig. 6. Responses were recorded for each slit by itself and for each possible two-slit apparent motion toward the second, test slit (indicated with a T). The wide boxes show inhibition (black) or facilitation (gray). Facilitation is normalized as follows: the height of the gray boxes equals their width when the facilitated response is twice the response to the test spot presented in isolation. Inhibition is normalized such that total suppression of the response attributable to the test spot results in a black box having equal width and height. The thin vertical white bar to the *right* of each gray or black box shows the magnitude of the excitatory response elicited by the slit itself at each location.

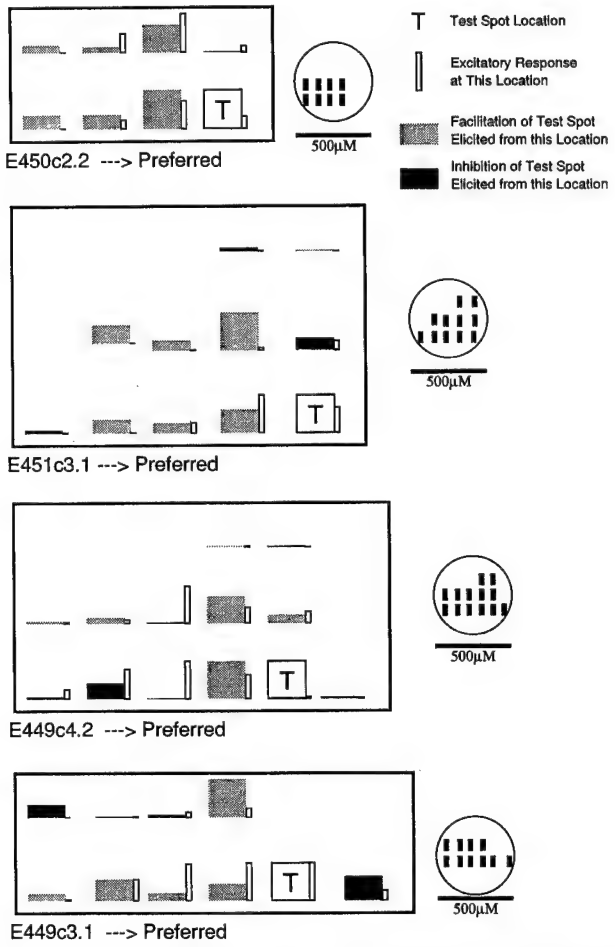

FIG. 6. Two-dimensional profiles of the facilitation (gray) and inhibition (black) field around test slit (T) elicited by prolonged light steps. Height of gray box at each location shows average increase in number of spikes elicited by modulation of test slit after stimulation of the 1st slit at that location. Height of dark box shows amount of reduction in test slit response due to stimulation by the 1st slit. Narrow white bars to *right* of gray or black boxes represent the intrinsic excitatory response elicited at that location. Interslit delays were 200 ms for all cases. Circles to *right* of each box containing slit arrays show approximate location of slit array within excitatory receptive-field center. The 500-μm scale bars below circles apply to these receptive-field center diagrams. Apparent motions whose projection onto the preferred-null axis as in preferred direction, and even some apparent motions orthogonal to preferred-null axis, facilitate response to test slit when location of the 1st slit is close to test slit. Facilitation does not occur, however, if projection of motion onto preferred-null axis points in null direction, even for nearby slits.

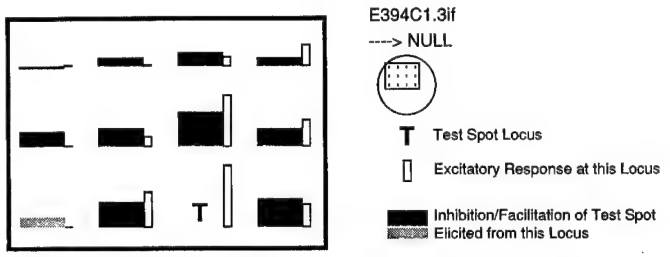

FIG. 7. Two-dimensional profiles of facilitation (gray) and inhibition (black) field around test slit (T) elicited by flashes, rather than prolonged light steps, as in Fig. 6. Representational scheme is same as in Fig. 6. Both the 1st and 2nd slits in this experiment were flashes of duration 100 ms, with a 500-ms delay between offset of the 1st slit and onset of test slit. Receptive-field size of this cell was ~400 μm on the retina. All stimuli in this experiment, including those whose motion projection onto preferred-null axis was in the preferred direction, either inhibited test slit (black-filled rectangles) or had insignificant effects on response of test slit (single small gray-filled rectangle).

The strongest facilitation of the response to the test (T) slit occurs at nearby loci (usually within 100 μm) but not necessarily for motion directly along the preferred-null axis. The asymmetric facilitatory area resembles an ovoid whose major axis is parallel to the preferred-null axis, with the largest end of the ovoid near the test slit (assuming that the profile below the preferred-null axis is similar to the one above it). We never observed facilitation for apparent motion whose projection onto the preferred-null axis was toward the null direction. However, facilitation was occasionally observed for motion perpendicular to the preferred-null axis if the facilitating spot was very close to the test spot (within 100 μm, as in *E449c4.2, 3rd array from the top* in Fig. 6). These results were consistent across 14 experiments that used two-dimensional (2-D) arrays having the majority of slits on the preferred side of the test slit, as well as in apparent-motion experiments on >30 cells using linear arrays.

In similar experiments in which the modulation of the intensity of the first slit was a flash, rather than a step, change in the light intensity, we found no facilitation of the response to the second (test) slit. The data in Fig. 7, which was adapted from Fig. 6 of the accompanying paper (Amthor and Grzywacz 1993), show the responses when the first and second slits were flashed for 100 ms, with the leading edge of the second slit occurring 500 ms after the trailing edge of the first slit. Such flashes elicit almost no significant facilitation, even for preferred-direction motions directly along the preferred-null axis. Rather, at sufficiently long interslit delays, apparent motion by flashing the first slit elicits inhibition of the response to the second slit in all directions. This finding is consistent with the results obtained by Wyatt and Daw (1975) with flashes. Thus sustained stimulation of the first slit appears to be necessary for some mechanism mediating facilitation to build up. The inhibition elicited by flashes for preferred-direction apparent motion in these experiments might be due to the presence of the inhibitory surround mechanism within the excitatory receptive-field center of ON-OFF DS ganglion cells of the rabbit retina (Amthor and Grzywacz 1993).

If a facilitatory mechanism were tuned to a specific velocity, one might expect the delay time for the most effective facilitation to be longer at greater than shorter distances.

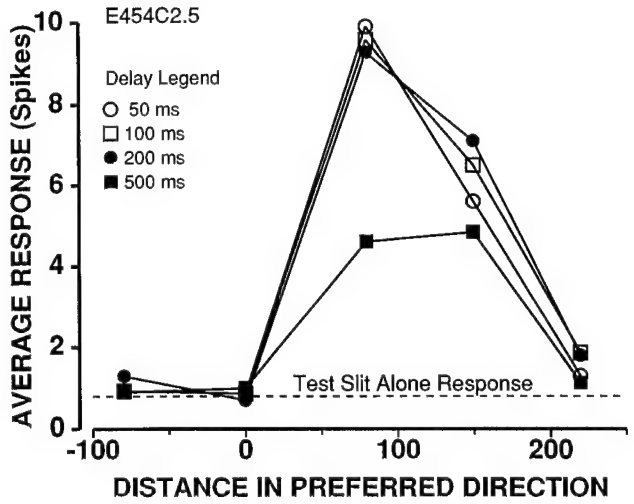

FIG. 8. Effect of covarying both interslit distance and interslit delay on facilitated response elicited by apparent motion. Average response measure was combined base-subtracted average number of spikes elicited in 1st 500 ms after onset and offset of 2nd slit, as in previous figures. Horizontal dashed line gives response to the 2nd, test slit when presented by itself. Excitatory receptive-field center size of this cell was ~500 μm on the retina. For interslit delays of 50, 100, and 200 ms, facilitatory effect varies little between distances of 80 and 220 μm, where facilitatory effect declined to insignificance. A similar result was obtained for interslit delay of 500 ms, except that at 80 μm facilitatory effect was relatively less than that observed at shorter interslit delays.

We examined whether, in two-slit apparent-motion experiments, the time course of the preferred-direction facilitation varied as a function of the interslit distance. The effect on facilitation of covarying interslit distance over a range of 220 μm along the preferred-null axis, and interslit delay over a range of 50–500 ms, are shown for one cell in Fig. 8. ON and OFF data are combined in this plot because their results were quantitatively very similar. Variation in interslit delay between 50 and 200 ms has only a small effect on the strength of facilitatory effect for distances between 80 and 220 μm, where the strength of the facilitatory effect essentially falls to zero. At 80 μm, facilitation rises to near its maximum in 50 ms, is sustained until ~200 ms, and then falls sharply to ~40% of its maximal value by 500 ms. In contrast, at 150 μm, facilitation rises to near its maximum in ~200 ms and then decays more slowly, falling to ~60% of its maximum by 500 ms. The meaning of this relatively larger reduction in facilitation for very long interslit delays at shorter than longer distances is unclear; it may conceivably be due to some inhibitory mechanism that becomes effective at longer delays. Generally, however, no large systematic variation of facilitation with distance was evident from this and other similar experiments.

Mixed ON/OFF interactions

The *bottom histogram* in Fig. 2 indicated that stimulus offset of one slit may not facilitate the response to stimulus onset of another slit. We investigated in more detail the segregation of facilitation between ON and OFF pathways using two-slit apparent-motion stimuli in which the sign of the contrast modulation of the first slit was opposite to that of the second. The results obtained with this stimulus protocol at several interslit distances for five cells are displayed in Fig. 9. The interslit delay in all these cases was 500 ms. Data obtained for apparent motions with similar contrast polarity (ON-ON and OFF-OFF) are shown by the gray boxes. Data obtained for motions with reverse contrast polarity (ON-OFF and OFF-ON) are shown by the white boxes. The strength of facilitation and inhibition are proportional to the heights of the boxes above and below the common dark horizontal line, respectively.

At the shortest interslit distances (data labeled by the termination ".1"), preferred-direction apparent motion elicited by similar polarity modulations of the two slits nearly always elicited significant facilitation, as in earlier figures. Nine out of 10 cases of similar polarity apparent motion at the shortest interslit distances (cases ending in ".1", counting ON-ON and OFF-OFF separately) yielded statistically sig-

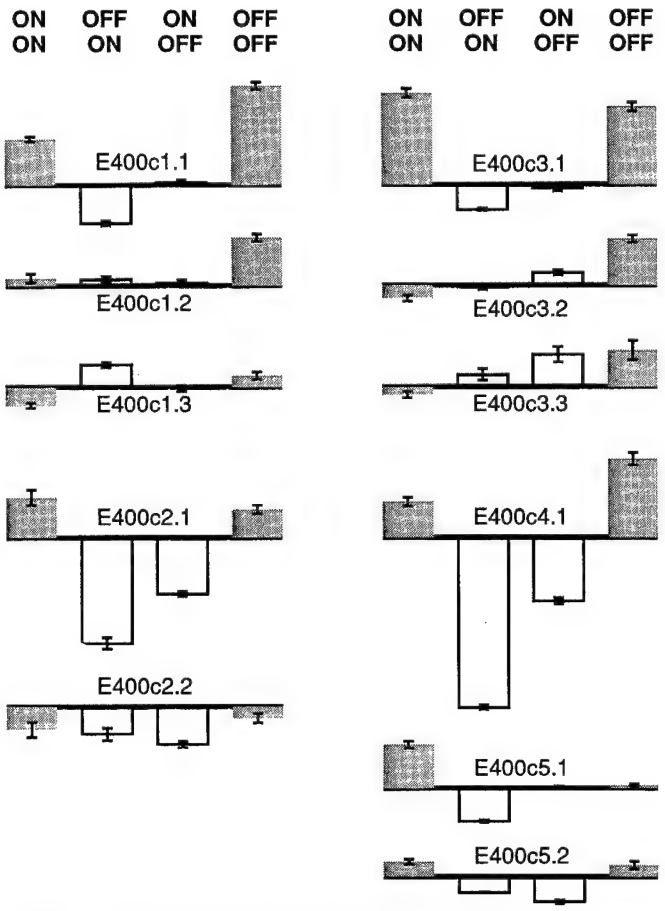

FIG. 9. Apparent motion interactions between like and opposite contrast modulations at various interslit distances within excitatory receptive-field center for several cells. All cells in this figure were located near inferior margin of visual streak and had excitatory receptive-field center sizes in range of 400–600 μm on the retina. Interslit delay is 500 ms in all cases. Like-sign interactions (onset of the 1st slit affecting onset of the 2nd slit, and offset of the 1st slit affecting offset of the 2nd slit) are gray boxes whose height above or below the common horizontal lines indicates the amount of facilitation or inhibition, respectively. Mixed (opposite) sign interactions (ON-OFF or OFF-ON) are shown as empty boxes. Error bars for SEM are on all boxes. Like-sign interactions at shortest interslit distances (gray boxes for cases ending in ".1", with interslit distances generally within 100 μm) are nearly all significantly facilitatory. Mixed sign interactions (empty boxes) tend to be inhibitory for same, short interslit distances. Interactions at longer interslit distances (cases ending in ".2" or ".3") were typically insignificant or inconsistent, being occasionally either slightly facilitatory or slightly inhibitory.

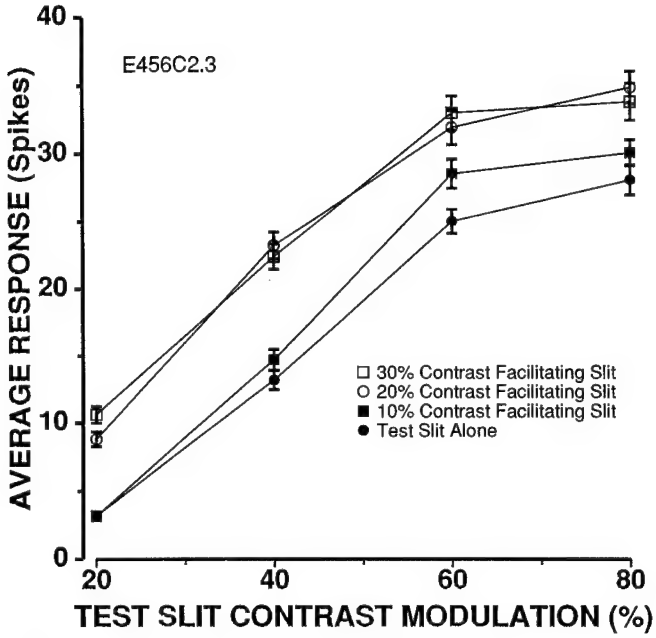

FIG. 10. Response-vs.-contrast curves for apparent motion in which contrasts of the 1st and 2nd slits were varied independently. Interslit delay was 300 ms. *Bottom curve,* with filled circles, shows response-vs.-contrast function of the 2nd slit when it was presented by itself. Curves above that (unfilled circles and filled and unfilled squares) show response-vs.-contrast function obtained with several contrasts (10, 20, and 30%) of the 1st slit. Base subtraction has been used to remove expected excitatory response of the 1st slit. Increasing contrast of the 1st slit appears to additively enhance response elicited by the 2nd, so that curves are shifted upward in parallel.

nificant facilitation at the 1% level. In contrast, preferred-direction apparent motion with opposite polarity modulations at the same distances elicited mostly inhibition of the second slit (7 out of 10 cases of mixed-contrast polarity apparent motion yielded statistically significant inhibition at the 1% level), with the remaining cases showing no significant effect of the first on the second slit. This reversal of interaction sign with reversal of contrast polarity at short distances is surprising, given that no such effect occurs for null-direction apparent motions (Amthor and Grzywacz 1993). At distances >200 μm, both similar and different polarity preferred-direction apparent-motion interactions are either inconsistently facilitatory or inhibitory or show no effect.

Contrast dependence of facilitation

By investigating the contrast dependence of null-direction inhibition, we previously demonstrated (Amthor and Grzywacz 1991, 1993) that the effect of null-direction motion on subsequently elicited excitatory responses is via a mechanism that is nonlinear (division-like), rather than linear (subtraction-like). We used similar experimental techniques to investigate whether facilitation behaved functionally as the reverse of inhibition, namely, as a nonlinear, multiplication-like mechanism. The data in Fig. 10 show, for *cell E456C2.3,* the responses elicited by a second slit as a function of its contrast when presented alone (filled circles, *bottom curve*), and during apparent motion with various contrast modulations of the first slit (open circles and filled and unfilled squares).

It is apparent from Fig. 10 and similar data (16 experiments in 10 cells) that the facilitatory effect of the first slit on the response-versus-contrast function elicited by the second is to shift it up, in parallel to the function obtained in the absence of facilitation. In other words, facilitation tends to add a constant number of spikes to this function. The amount of facilitation elicited by the first slit as a function of its contrast followed a sigmoidal relationship, however. The amount of facilitation increased slowly at low contrasts, then accelerated at intermediate contrasts, and then saturated at higher contrasts. The contrast at which facilitation saturated was still relatively low (around 20%), however, and nonsaturating in terms of the excitatory response such stimuli typically elicited. This sigmoidal dependence of the amount of facilitation on contrast is thus nonlinear. However, although the facilitating effect tends to go from insignificant to saturating over a small range of contrasts of the first, facilitating slit, facilitation, like null-direction inhibition, is not all or none.

Although not all or none, the high gain sigmoidal relationship of the facilitatory mechanism tended to make it difficult in these two spot protocols to select a contrast for the facilitating slit that was effective over a large range of the second slit's response-versus-contrast function, because threshold and saturation nonlinearities tended to make the facilitatory effect appear as a change in slope at the low and high contrast extremes of the curves. In the relatively linear regions of the response-versus-contrast curves of the 15 experiments similar to that shown in Fig. 10 (where both threshold and saturation nonlinearities were avoided), an additive effect of the first on the second slit was consistently found.

The addition-like facilitatory enhancement of the response of the second slit by the first distinguishes the mechanism of facilitation from that mediating null-direction inhibition, which consistently exhibits a division-like, nonlinear effect on the response-versus-contrast function of the second slit. However, this result does not imply that facilitation is mediated by a mechanism that is completely linear, for two reasons. *1*) Facilitation is nonlinear in the sense that the response to the preferred-direction motion is larger than the sum of the responses to the stimuli presented individually. *2*) The data of Fig. 10 show that amount of facilitation is not linearly proportional to the contrast of the facilitatory slit, even at relatively low contrasts, but instead follows a nonlinear, sigmoid relationship.

DISCUSSION

Facilitation significance for directional selectivity

The data in this paper demonstrate that preferred-direction facilitation is a robust and significant contributor to directional selectivity in ON-OFF DS ganglion cells of the rabbit retina. The effect of facilitation frequently more than doubles the total number of spikes elicited by the second slit in an apparent motion protocol (for example, the OFF response in Fig. 2 and several combined ON and OFF responses facilitated by proximal stimuli in Fig. 6). Sometimes, preferred-direction facilitation can enhance responses to movement by many more spikes than null-direction inhibition can remove. This enhancement

can be a factor up to five when the response to the second slit presented by itself is near threshold (for example, Figs. 5 and 8).

Why did earlier studies of directional selectivity using apparent-motion protocols reveal little (Barlow and Levick 1965) or no (Wyatt and Daw 1975) facilitation? In the study of Barlow and Levick, the apparent motion was elicited by manually moving a light edge behind two slits cut out of gray paper. Such manually controlled motion did not allow for precise timing of the slits' presentation, and if the delay between activation of the slits was too long (>500 ms) or too short (<200 ms), optimal facilitation would not have been elicited (see Fig. 3). Nevertheless, the facilitation in their data is not insignificant; for distances of ~100 μm they reported a nearly 50% response increase due to apparent-motion facilitation in some cases. The experiments of Wyatt and Daw probably did not reveal facilitation because their apparent-motion protocol used short-duration flashes (1/60 s). As Fig. 7 illustrates, sustained stimulation by the first slit is necessary for facilitation to build up to effective levels.

Constraints to mechanism of facilitation

Some of our data provide significant constraints for hypotheses about the mechanism that underlies facilitation. For example, our data strongly argue that preferred-direction facilitation is not just disinhibition, that is, the reduction of some chronically active inhibitory mechanism that is reduced during preferred-direction motion and enhanced during null-direction motion. Preferred-direction facilitation and null-direction inhibition differ significantly in several important properties. *1*) Null-direction inhibition is more sustained than preferred-direction facilitation (Figs. 3 and 4). *2*) The spatial range of null-direction inhibition is three times larger than that of facilitation (Fig. 5). *3*) The normalized time course of preferred-direction facilitation is independent of distance (Fig. 8), but the same is not true for null-direction inhibition (Amthor and Grzywacz 1993). *4*) Most importantly, the effect of facilitation is addition-like (as in Fig. 10), whereas the effect of inhibition is division-like (Amthor and Grzywacz 1991, 1993).

In this paper, we also report on experiments that were designed to distinguish whether the mechanism underlying preferred-direction facilitation is due to some general response expansion mechanism not intrinsically related to directional selectivity or to a specifically DS mechanism. By a general response expansion mechanism, we mean a "supralinearity" in the response-versus-driving-force function where its second derivative is positive, such as just above a spike-firing threshold. An example of a general threshold-mechanism model for preferred-direction facilitation suggested by Torre and Poggio (1978) was an excitatory contribution of a null-direction inhibitory synapse whose reversal potential was slightly above resting potential.

Facilitation observed in our experiments is also not likely to be due merely to the general summation of the separate excitations evoked by the two slits [such as at the ganglion-cell firing threshold mechanism, or at a preganglionic synaptic threshold mechanism (Katz and Miledi 1967; Kusano 1970)], because in this case, any excitatory stimulus should facilitate any other excitatory stimulus (up to saturation or some other compressive nonlinearity affecting the sum). In particular, any ON or OFF stimulus that elicits excitation should facilitate the response to any other stimulus, whether of the same or opposite contrast sign. However, the data shown in Fig. 9 indicate that only similar-polarity interactions produce consistent preferred-direction facilitation. The summation hypothesis would also predict that the stronger the excitation elicited by a stimulus at a particular receptive-field locus, the stronger the facilitation that should be produced from that locus, regardless of its distance from the second slit. The data of Fig. 5 clearly show this not to be the case. For any given "test" (second) slit, detectable facilitation is generally restricted to a subset of the excitatory receptive-field within ~200 μm of it (Figs. 5 and 6).

In two-slit apparent-motion experiments, the time course of facilitation elicited by the first slit does not follow the time course of the excitation elicited by it; facilitation has a slower rise time and a much slower decay time than the excitatory response (Figs. 3 and 4). This result also does not support addition of excitation models such as that discussed above. To explain the slow decay time of facilitation by the excitation summation hypothesis, it would be necessary to postulate that the excitation produced by the first slit has a long-lasting subthreshold tail on which the excitation of the second slit is added, thus facilitating the second slit's response. However, no postulated long-lasting subthreshold excitatory waveform at a common summation point such as the ganglion-cell firing mechanism can explain the dependence of facilitation on contrast sign and distance.

The additive nature of the effect of preferred-direction facilitation also distinguishes it from the mechanism that mediates null-direction inhibition and provides constraints for models of the facilitatory mechanism. For example, a facilitatory mechanism in which voltage-dependent channels increase a cell's membrane resistance would increase the excitatory response produced by a given input synaptic current (Borg-Graham and Grzywacz 1991) in a multiplicative (Ohm's law) and therefore nonlinear manner. The multiplicative character of this proposed facilitatory interaction is inconsistent with the data (Fig. 10) that show an addition-like effect of facilitation on the response-versus-contrast curve of the facilitated slit.

A facilitatory mechanism that would appear to be more consistent with the data is the "linear-threshold" mechanism, which would enhance responses in an addition-like manner, such as exhibited by the data in Fig. 10. Such a mechanism could be implemented by voltage-dependent channels or by a synaptic-transmission process in which a threshold of activation is followed by a linear input-output relationship above threshold. However, to account for facilitation of a factor of two or more, the threshold would have to be high, that is, at least of the same order of magnitude as the excitatory inputs. Theoretical analysis of neural DS mechanisms (Grzywacz and Koch 1987), and data obtained from ON-OFF DS ganglion cells using low-contrast sinusoidal gratings (Grzywacz et al. 1990) argue against directional selectivity being mediated by high-threshold mechanisms in these cells.

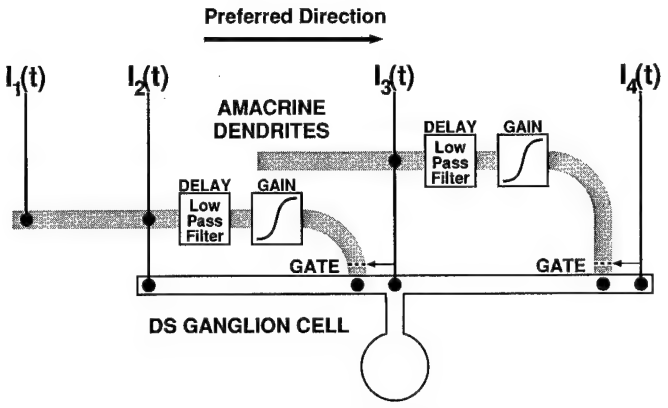

FIG. 11. "Gated-enhancer" model for preferred-direction facilitation. Only retinal circuity postulated for either the ON or OFF pathway is shown. Inputs $I_1(t)$, $I_2(t)$, $I_3(t)$, and $I_4(t)$ represent retinotopic inputs to the inner plexiform layer, presumably via bipolar cell processes. These inputs make excitatory connections (dark-filled circles) to both amacrine cell processes (gray bars) and dendrites of DS ganglion cell (light process) at *bottom*. Contribution of direct excitatory inputs from $I_n(t)$ to ganglion cell are not directionally selective. Inputs to amacrine cell processes build up an enhancer agent whose effect on DS ganglion cell response is gated by large, initial transient component of a subsequent retinotopic input $I_n(t)$ [for example, sustained input at $I_2(t)$ builds up an enhancer agent in the lower amacrine dendrite that would be gated by a subsequent input at $I_3(t)$]. Intrinsic time course of build-up of enhancing agent is slow and requires a sustained input (indicated by DELAY–Low Pass Filter Box). Delay is postulated to be near output of amacrine cell process because of lack of a strong temporal dependence of facilitation on distance observed in experiments. When enhancer gate is opened, its effect adds linearly to various active direct excitatory inputs $I_n(t)$ to ganglion cell dendrite in this model (although addition conceivably occurs at some unspecified presynaptic element). Relationship between driving force (ultimately dependent on contrast) of gated enhancer input from amacrine cell and its contribution to ganglion cell response follows a sigmoidal relationship, indicated by sigmoidal transfer box in diagram. Location of this sigmoidal dependence is arbitrarily placed with machinery of the amacrine cell, possibly, for example, due to build-up of calcium at amacrine-to-ganglion cell synaptic bouton, but could be located at various points in facilitatory pathway. Directional asymmetry of the facilitatory effect occurs because either *1*) amacrine input to ganglion cell is restricted to one end of an oriented amacrine process (as shown), or *2*) amacrine processes of the "wrong" orientation are selectively inhibited. Maximum distance for facilitation is limited by length of postulated amacrine dendrite that mediates facilitation. No minimum distance for facilitation is exhibited in this model. In fact, self facilitation (facilitation of the response at a single locus) is possible if input to amacrine cell process and an input to that amacrine-cell-process gate are spatially proximal and within temporal window. This gated-enhancer model is physiologically plausible and accounts for several features of preferred-direction facilitation (see text for details).

Gated-enhancer model

The models for facilitation discussed above fail to account for the data in this paper. We have, therefore, developed another class of models, which we call "gated-enhancer" models, that may account for the available data on facilitation. Figure 11 shows a schematic example of such a model. The inputs $I_1(t)$, $I_2(t)$, $I_3(t)$, and $I_4(t)$ represent retinotopic inputs to the inner plexiform layer, presumably via bipolar cell processes. These inputs make excitatory connections (dark-filled circles) to both amacrine cell processes (gray bars) and the dendrites of the DS ganglion cell (light process) at the bottom. The direct excitatory inputs (I_n) to the amacrine cells and DS ganglion cell are not directionally selective. The $I_n(t)$ inputs to the amacrine cell processes build up an enhancer agent via a process having a slow time course (indicated by the DELAY–Low Pass Filter Box) and thus require a sustained input. Because of the lack of a strong temporal dependence of facilitation on distance that was observed in the experiments, the slow time course is postulated to be somewhere near the output of the amacrine cell process. The postulated enhancer agent has no effect on the DS ganglion cell response unless gated by the large, initial transient component of a subsequent retinotopic input, such as $I_3(t)$, gating the enhancer agent build-up caused by the earlier $I_2(t)$ input to the lower amacrine process. When the enhancer gate is opened, the effect of the gated enhancer adds linearly to the effects of the various active direct retinotopic excitatory inputs (I_n) to the ganglion cell.

The model in Fig. 11 can account for several significant features of the data. The model predicts that the time course of facilitation is slower than that of excitation (Fig. 3), because facilitation depends on the slow buildup of the enhancer agent. Only long-lasting stimuli (Figs. 3 and 6), but not short flashes (Fig. 7), can produce facilitation because of the slowness of the enhancer agent buildup. The additive interaction between the enhancer and direct excitation in the model accounts for the addition-like property of facilitation (Fig. 11). Because the time course of facilitation is determined by a localized mechanism (the DELAY–Low Pass Filter Box), and not by dendritic-cable propagation, which may typically be on the order of only a few milliseconds (Jack et al. 1975), the time course of facilitation (but not its strength) is essentially independent of distance (Fig. 8). Computer simulations of this model can be found elsewhere (Grzywacz et al. 1993), where we suggest a particular biophysical implementation of this model based on synaptic facilitation (Arechiga et al. 1990; Hochner et al. 1989; Parnas and Parnas 1986).

Role of facilitation in directional selectivity

If the facilitatory mechanism for motion originates in the DS pathway (for example, in some amacrine cells), this does not imply that the facilitatory process must be spatially asymmetric. Recent turtle data show that elimination of inhibition with antagonists to γ-aminobutyric acid (GABA) leads to a more symmetric facilitation that can be elicited with both preferred- and null-direction motions (Smith et al. 1991; Smith, Grzywacz, and Borg-Graham, unpublished data). These data would suggest that the role of facilitation may not be to produce directional selectivity, but rather to enhance the ganglion cells' sensitivity to moving stimuli, as has been postulated explicitly in cat (Schmidt et al. 1987). In ON-OFF DS ganglion cells of the rabbit retina, facilitation, which appears to occur only for motion in the preferred direction, tends to also sharpen directionality by increasing the difference between the preferred and null responses. Our data indicate that this enhancement of responses to motion is particularly important for motion of light (or dark) edges, as opposed to motion of small objects, because long-duration light modulations simulate movement of an edge and are effective facilitators, whereas short-duration flashes, which correspond to a small object that moves behind two apertures, do not elicit strong facilitation.

In this regard it is interesting that long-delay null-direction inhibition requires a sustained stimulus (Amthor and Grzywacz 1993) as well. The symmetric inhibition reported to occur with flashes in this paper might be due to the surround-inhibition mechanism, which appears to be present in the receptive-field center, and act with a relatively short duration (Merwine et al. 1991). Hence, the necessity for sustained stimuli for both preferred-direction facilitation and null-direction inhibition suggests that both facilitatory and inhibitory components of directional selectivity in ON-OFF directionally selective ganglion cells of the rabbit retina may be optimally elicited by moving edges rather than small objects. However, these cells can still be directionally selective for small moving targets, because continuous motion across a spatially extended mechanism can provide a relatively sustained input to that mechanism.

N. M. Grzywacz thanks Drs. Ellen Hildreth and Tomaso Poggio for support during his time at Massachusetts Institute of Technology. He also thanks Drs. Tomaso Poggio, Lyle Borg-Graham, and Evelyne Sernagor, and R. Smith, for several discussions during the course of this project.

This work was supported by the Office of Naval Research (N00014-91-J-1280), by grants to F. R. Amthor from the National Eye Institute (EY-05070) and the Sloan Foundation (86-10-7), by a core grant from the National Eye Institute to the Vision Science Research Center of the University of Alabama at Birmingham (EY-03039), by grants to N. M. Grzywacz from the National Eye Institute (EY-08921) and the National Science Foundation (BNS-8809528), by an award to N. M. Grzywacz from the Paul L. and Phyllis C. Wattis Foundation, and by a core grant from the National Eye Institute to Smith-Kettlewell (EY-06883).

Address for reprint requests: F. R. Amthor, Dept. of Psychology, University of Alabama at Birmingham, WAB Station; Birmingham, AL 35294.

Received 2 March 1992; accepted in final form 24 January 1993.

REFERENCES

AMTHOR, F. R. AND GRZYWACZ, N. M. The nonlinearity of the inhibition underlying retinal directional selectivity. *Visual Neurosci.* 6: 197–206, 1991.

AMTHOR, F. R. AND GRZYWACZ, N. M. Inhibition in ON-OFF directionally selective ganglion cells in the rabbit retina. *J. Neurophysiol.* 69: 2174–2187, 1993.

AMTHOR, F. R., OYSTER, C. W., AND TAKAHASHI, E. S. Morphology of ON-OFF direction-selective ganglion cells in the rabbit retina. *Brain Res.* 298: 187–190, 1984.

AMTHOR, F. R., TAKAHASHI, E. S., AND OYSTER, C. W. Morphologies of rabbit retinal ganglion cells with complex receptive fields. *J. Comp. Neurol.* 280: 97–121, 1989.

ARECHIGA, H., CANNONE, A., PARNAS, H., AND PARNAS, I. Blockage of synaptic release by brief hyperpolarizing pulses in the neuromuscular junction of the crayfish. *J. Physiol. Lond.* 430: 119–133, 1990.

BARLOW, H. B. AND LEVICK, W. R. The mechanism of directionally selective units in the rabbit's retina. *J. Physiol. Lond.* 178: 477–504, 1965.

BORG-GRAHAM, L. J. AND GRZYWACZ, N. M. A model of the directional selectivity circuit in retina: transformations by neurons singly and in concert. In *Single Neuron Computation,* edited by T. McKenna, J. Davis, and S. F. Zornetzer. Orlando, FL: Academic, 1992, p. 347–375.

GRZYWACZ, N. M. AND AMTHOR, F. R. Facilitation in ON-OFF directionally selective ganglion cells of the rabbit retina. *Soc. Neurosci. Abstr.* 15: 969, 1989.

GRZYWACZ, N. M. AND AMTHOR, F. R. Independent ON and OFF computations of retinal directional selectivity in rabbit. *Soc. Neurosci. Abstr.* 17: 344, 1991.

GRZYWACZ, N. M., AMTHOR, F. R., AND BORG-GRAHAM, L. J. Does synaptic facilitation mediate motion facilitation in the retina. In *Computation and Neural Systems, 1992,* edited by F. Eeckman and J. Bower. New York: Kluwer, 1993, chapt. 24, In press.

GRZYWACZ, N. M., AMTHOR, F. R., AND MISTLER, L. A. Applicability of quadratic and threshold models to motion discrimination in the rabbit retina. *Biol. Cybern.* 64: 41–49, 1990.

GRZYWACZ, N. M. AND KOCH, C. Functional properties of models for directional selectivity in the retina. *Synapse* 1: 417–434, 1987.

HOCHNER, B., PARNAS, H., AND PARNAS, I. Membrane depolarization evokes neurotransmitter release in the absence of calcium entry. *Nature Lond.* 342: 433–435, 1989.

JACK, J. J. B., NOBLE, D., AND TSIEN, R. W. *Electric Current Flow in Excitable Cells.* Oxford, UK: Clarendon, 1975.

KATZ, B. AND MILEDI, R. A study of synaptic transmission in the absence of nerve impulses. *J. Physiol. Lond.* 192: 406–436, 1967.

KUSANO, K. Influence of ionic environment on the relationship between pre- and postsynaptic potentials. *J. Neurobiol.* 1: 435–457, 1970.

MERWINE, D. K. AND AMTHOR, F. R. Ganglion cell surround inhibition is divisive, not linear, in rabbit retina. *Soc. Neurosci. Abstr.* 16: 466, 1990.

MERWINE, D. K., AMTHOR, F. R., AND GRZYWACZ, N. M. Characteristics of divisive ganglion cell surround inhibition in the rabbit retina (Abstract). *Invest. Ophthalmol. Visual Sci.* 32: 1132, 1991.

PARNAS, I. AND PARNAS, H. Calcium is essential but insufficient for neurotransmitter release: the calcium-voltage hypothesis. *J. Physiol. Paris* 81: 289–305, 1986.

SCHMIDT, M., HUMPHREY, M., AND WÄSSLE, H. Action and localization of acetylcholine in the cat retina. *J. Neurophysiol.* 58: 997–1015, 1987.

SMITH, R. D., GRZYWACZ, N. M., AND BORG-GRAHAM, L. J. GABA and facilitation in turtle retinal direction selectivity. *Soc. Neurosci Abstr.* 17: 1376, 1991.

SMITH R. D., GRZYWACZ, N. M., AND BORG-GRAHAM L. J. (1992) Effects of GABA-A Antagonists on Preferred Motion Direction of Turtle Ganglion Cells. Submitted for publication.

TORRE, V. AND POGGIO, T. A synaptic mechanism possibly underlying directional selectivity to motion. *Proc. R. Soc. Lond. B Biol. Sci.* 202: 409–416, 1978.

WYATT, H. J. AND DAW, N. W. Directionally sensitive ganglion cells in the rabbit retina: specificity of stimulus direction, size, and speed. *J. Neurophysiol.* 38: 613–626, 1975.

JOURNAL OF NEUROPHYSIOLOGY
Vol. 69, No. 6, June 1993. *Printed in U.S.A.*

Inhibition in ON-OFF Directionally Selective Ganglion Cells of the Rabbit Retina

FRANKLIN R. AMTHOR AND NORBERTO M. GRZYWACZ
Department of Psychology and Neurobiology Research Center, University of Alabama at Birmingham, Birmingham, Alabama 35294; and The Smith-Kettlewell Eye Research Institute, San Francisco, California 94115

SUMMARY AND CONCLUSIONS

1. We have investigated the inhibitory mechanisms modulating the extracellularly recorded responses of ON-OFF directionally selective (DS) ganglion cells of the rabbit retina. Our investigations used both moving spots and apparent motion. The latter was produced by both prolonged light steps, which simulate movement of an edge, and light flashes, which simulate movement of a spot or slit.

2. Within the excitatory receptive-field center of DS ganglion cells, apparent motion with prolonged light steps elicits null-direction inhibition whose strength rises to 90% of maximum in 160 ± 110 ms (7 cells) and then decays slowly, remaining above baseline longer than 2,000 ms for short interslit distances.

3. Prolonged light steps are generally effective for inhibiting any given excitatory receptive-field locus from an ovate-shaped area that extends asymmetrically in the direction that would be previously traversed by null-direction moving objects. This inhibitory area is typically larger than one-half the size of the receptive-field center. The strength of the inhibition is greater at short than long distances within this area.

4. The rise and fall times of the null-direction inhibition elicited by apparent motion using prolonged light steps are somewhat faster at large than short interslit distances.

5. Short light flashes (at sufficiently long interslit delays) elicit inhibition not only from the same asymmetric, ovate-shaped inhibitory field as long steps of light, but also from loci completely surrounding the second slit. This implies that the asymmetric, null-direction–specific inhibition is due to a temporally sustained mechanism. The symmetric inhibition elicited by short flashes may be due to the presence of the antagonistic surround mechanism within the receptive-field center. The apparent absence of this surround inhibition for preferred-direction apparent motion during prolonged light steps may be due to masking by facilitation that is strongly evoked by long steps, but not flashes of light (see accompanying paper).

6. The relatively slow rise time and sustained time course of the inhibition elicited by null-direction apparent motion within the excitatory receptive field center appears to distinguish it from the inhibition elicited by stimulation within the receptive field surround, which has a much faster rise time and more transient time course. However, the sustained, null-direction inhibitory mechanism that can be elicited by prolonged light steps within the excitatory receptive field center extends into the surround on the side of the receptive-field center previously traversed during null-direction motion.

7. The contrast dependency of both the null-direction and the surround inhibition is division-like, rather than subtraction-like. That is, the effect of both types of inhibition is to divide the response-versus-contrast curves by a constant factor rather than to subtract a fixed value.

8. Use of prolonged light steps shows that the interaction between excitation and null-direction inhibition is largely segregated between the ON and the OFF pathways. Thus, for null-direction apparent motion, light onset of the first slit strongly inhibits response to the onset, but generally not the offset, of the second slit. Light offset of the first slit similarly tends to inhibit the response to light offset, but not onset, of the second slit. Thus selectivity for direction of motion appears to be computed independently for light and dark regions of moving objects.

INTRODUCTION

ON-OFF directionally selective (DS) ganglion cells of the rabbit retina respond much better to movement in a preferred direction than to movement in the opposite, null direction (Barlow and Hill 1963; Barlow et al. 1964; Barlow and Levick 1965). Barlow and Levick (1965) observed that this selectivity for direction of motion was associated with asymmetric inhibition elicited by null-direction motion; receptive-field loci where vigorous responses were elicited by stationary flashed spots were silent when traversed by the same spots during null-direction, but not preferred-direction, motion. Pharmacological experiments (Ariel and Daw 1982; Caldwell et al. 1978) demonstrated that antagonists to γ-aminobutyric acid (GABA), an inhibitory transmitter in the retina, can significantly reduce or eliminate directional selectivity in ON-OFF DS ganglion cells. Thus inhibition for null-direction motion appears to have a key role in the DS mechanism, although facilitation for preferred-direction motion seems to be a significant mediator of directional selectivity in these cells as well (see accompanying paper: Grzywacz and Amthor 1993).

Barlow and Levick (1965) showed that movement over only a small portion of the receptive-field center was sufficient to elicit DS responses. In apparent motion experiments in which sequential stimulation of two slits simulated movement, they found that the directional response asymmetry was greater at small than large inter-slit distances within the receptive-field center. From these results, they postulated that directional selectivity was mediated by independent, directionally selective subunits duplicated a dozen or more times across the excitatory receptive-field center. However, their experiments did not directly address the issue of whether inhibition was organized in a finite number of distinct inhibitory subunits, because the stronger directional asymmetry for small motions could have been due to an inhibitory process that was continuous across the receptive-field center, but stronger at short than long distances. Identification of the dendritic morphologies of ON-OFF DS ganglion cells (Amthor et al. 1984, 1989b)

revealed no obvious correlation between their preferred direction of motion and any global or local morphological attributes such as the overall shape and orientation of the cell's dendritic trees or the orientation of individual dendrites or dendritic regions.

The spatiotemporal characteristics of the null-direction inhibition in ON-OFF DS ganglion cells were further investigated by Wyatt and Daw (1975) using moving spots inhibiting stationary flashing ones, and in two spot apparent motion experiments. They suggested from their results that the inhibition observed during null-direction motion arises from an asymmetric organization of the classical inhibitory surround within the excitatory receptive-field center. In their model, each point within the excitatory receptive-field center of the DS ganglion cell was inhibited by an asymmetric region shaped like a cardioid. The involuted aspect of the cardioid at the inhibited locus was postulated to account for inhibitory field shapes calculated from histograms obtained when a flashing spot was inhibited by another spot moving in the null direction along various trajectories parallel to the preferred-null axis, and to explain the somewhat poorer preferred-direction-motion response to bars elongated perpendicular to the preferred-null axis than to small spots, with the latter presumably avoiding the inhibitory lobes of the cardioid extending toward preferred-direction-moving stimuli.

The Wyatt and Daw experiments did not, however, directly test the hypothesis that the inhibition elicited by null-direction-moving objects was identical to that of the classical inhibitory surround of the ON-OFF DS ganglion cells. In addition, data supporting the hypothesis that the shape of the inhibitory region mediating directional selectivity is a cardioid were not conclusive for at least three reasons. *1*) In the moving spot experiments, lack of precise knowledge about the delay between stimulation and the responses elicited by the two spots, and therefore about the time course of their interaction, raises uncertainties about the exact position of the moving spot when its inhibition was effective for the flashing one, and thus, about the exact shape of the inhibitory field determined by this method. *2*) Any misalignment between the trajectory of the moving spot and the true preferred-null axis would have induced a systematic error in the estimation of the shape of the true inhibitory field near the inhibited spot, where the notch of the cardioid was postulated, particularly when the inhibitory field on only one side of the preferred null axis was experimentally determined and then "reflected" across the axis to estimate the entire inhibitory field. *3*) Cardioid shapes were not found for the inhibitory field in all of their experiments.

The time course of the null-direction inhibition underlying directional selectivity was also studied by Wyatt and Daw (1975) in apparent motion experiments in which two spots were briefly flashed in sequence. They found that the null-direction inhibition elicited by a flash rises to a maximum in ~100 ms and decays within ~500–1,000 ms. However, the use of flashed rather than sustained stimuli in those experiments does not provide a basis for concluding that the null-direction inhibitory mechanism itself is transient, as has been hypothesized elsewhere for retinal directionally selective mechanisms (Dowling 1987; Werblin et al. 1988). In principle, the intrinsic time course of inhibition might be sustained during a sustained stimulus, such as after the light/dark edge of an extended object crosses a given locus within the receptive-field center.

The use of transient stimuli in the Wyatt and Daw experiments also did not permit assessment of how ON and OFF channels interact in the DS mechanism. The anatomic finding that the dendritic tree of ON-OFF DS ganglion cells is extensively bistratified in both ON and OFF sublamina of the inner plexiform layer (IPL) (Amthor et al. 1984, 1989b) appears to allow, at least in principle, a separate computation of directional selectivity for light and dark areas of a stimulus, rather than requiring some specific interaction between ON and OFF regions as the basis of directional selectivity.

The manner in which excitation and null-direction and surround inhibition interact has also remained somewhat unclear from previous studies. It has been shown theoretically (Grzywacz and Koch 1987; Poggio and Reichardt 1973) that asymmetric responses to opposite directions of movement must be based on a retinal process that is nonlinear. Use of low-contrast drifting sinusoidal gratings as stimuli demonstrated experimentally that the nonlinear mechanism in rabbit ON-OFF DS ganglion cells cannot be based on a high threshold mechanism (Grzywacz et al. 1990). Shunting inhibition has been suggested as a possible basis of nonlinear, localized interactions between excitation and inhibition underlying directional selectivity (Grzywacz and Amthor 1989; Koch et al. 1982; Torre and Poggio 1978). This hypothesis was supported by the experimental finding that the contrast dependency of the null-direction inhibition is division-like in these cells (Amthor and Grzywacz 1991), consistent with synapses whose major effect is shunting inhibition, which is nonlinear, rather than hyperpolarizing inhibition, which interacts more linearly with excitation.

The division-like character of the DS inhibition might appear to distinguish it from the surround inhibition, which has been postulated to interact linearly with excitation from the receptive-field center in mammalian retinal ganglion cells such as in the cat (Enroth-Cugell and Robson 1966; Rodieck and Stone 1965). However, recent preliminary data have revealed that the surround inhibition of most rabbit retinal ganglion cells, including DS ganglion cells, interacts with excitation in a division-like manner also (Merwine et al. 1990).

In this paper, we report the results of experiments that examine the temporal properties, spatial organization, and inhibitory-excitatory interactions in ON-OFF DS ganglion cells in the rabbit retina. By using prolonged steps rather than flashes of light, the experiments address the questions of whether the time course of the null-direction inhibition is sustained and how ON and OFF pathways interact. Apparent motion protocols demonstrate that the time course of the null-direction inhibition elicited by spots or slits within the excitatory receptive-field center is more sustained than that elicited by annuli in the classical inhibitory surround. Null-direction and surround inhibition may, therefore, be mediated by separate mechanisms. However, both the null-direction inhibition and surround inhibition are functionally division-like, and therefore nonlinear, in their effect on excitation.

The experiments reported in this paper do not resolve the questions of where in the retina (pre- or postsynaptic to the ganglion cell) the null-direction inhibition interacts with excitation or how the spatial resolution of the DS mechanism can be much smaller than the size of the excitatory receptive-field center. Properties of facilitation elicited by preferred-direction motion, which were studied in experiments similar to those used in this paper to examine null-direction inhibition, are presented in the accompanying paper (Grzywacz and Amthor 1993). Some of the results in the present paper appeared previously in abstract form (Amthor and Grzywacz 1988, 1990; Grzywacz and Amthor 1991).

METHODS

Preparation

The surgery and isolated rabbit eyecup preparation were essentially the same as that of Amthor et al. (1989a), except that the more complete superfusate solution of Ames and Nesbett (1981) was used. This preparation yielded stable, single cell recordings for 8–12 h, which was much longer than typical single cell recordings in the in vivo preparation and thus a significant advantage for some of the long recordings required to demonstrate statistically significant effects at relatively small contrast modulations.

Eyes from both sexes of adult Dutch belt pigmented rabbits weighing ≥1.3 kg were used. All surgery was done in dim red light on animals which had been dark adapted for ≥30 min. Animals were deeply anesthetized with an initial dose of urethan (2 g/kg), followed by thiamylal sodium (Surital; 0.25 g/50 ml wt/vol), or pentobarbital sodium, given to effect. After deep anesthesia was achieved, the right eye was enucleated and the animal was killed with a massive overdose of Surital. The eye was then briefly immersed and rinsed in ice-cold superfusate medium. The eye was hemisected slightly anterior to the ora serrata, and the front half of the eye, including the cornea and lens, was removed. The remaining eyecup was held posterior pole upward by the connective tissue near the exit of the optic nerve, and the vitreous body was gently pulled out with toothed forceps until it adhered to a paper towel below. The posterior eyecup was then slowly lifted upward until the entire vitreous fell out onto the towel.

The remaining eyecup was placed (always within 3 min of enucleation) in room-temperature superfusate equilibrated with 95% O_2-5% CO_2, with the pH in the range of 7.35–7.45. Four radial cuts were made 2–3 mm inward from the margin of the retina to facilitate the subsequent eversion of the eyecup over an inflatable latex dome in a Teflon superfusion chamber. The hydraulically inflated latex dome permitted a precise accommodation of variation in eyecup size so that a smooth but unstretched retinal surface was achieved, which was found to be essential for proper access by the flowing superfusate. The superfusate was stirred and bubbled with 95% O_2-5% CO_2 continuously at room temperature during the entire experiment. Just before reaching the retina the superfusate was heated by passing through a bath held at 35.5–36.5°C. The superfusate flow rate was 3–5 ml/min.

Stimulation

In most experiments, two-slit apparent motions were made both in the null and in the preferred directions. Presentations of two slits in various sequences were computer controlled by an 80286 DOS microcomputer that generated stimuli either via controlling a two-dimensional waveform generator (Picasso; Innisfree, Cambridge, MA) driving a monitor (model 608; Tektronix, Beaverton, OR), or by current modulation of an array of yellow light emitting diodes in the shape of slits (Radio-Shack, Tandy, Fort Worth, TX) that had linear intensity versus current functions [as calibrated by a Pritchard photometer (Photoresearch, Kollmorgen, Burbank, CA)] over the intensity range used. The diameter of the excitatory receptive-field centers of most DS ganglion cells studied in these experiments, which were in or just inferior to the visual streak, occupied approximately one-fifth the horizontal dimension of the Tektronix 608 screen.

Stimuli were imaged on the retina by a 17-mm-focal-length, 12-mm-diam achromatic lens ~870 mm from the Tektronix 608 screen or LED array. An adjustable diaphragm in front of the lens allowed the depth of focus to be increased by reducing the aperture. The lens was mounted on a micromanipulator so that the ganglion cell receptive field could be centered within the Tektronix 608 screen. The focus of the lens was checked initially by directly focusing a red incandescent light filament on the retina and later in the experiment by adjusting the distance of the lens from the retina to produce the best ganglion cell response to a high-frequency drifting grating on the Tektronix 608 monitor.

Receptive-field maps and directional responses to moving stimuli were assessed for all cells by using spots and bars swept across the Tektronix 608 monitor screen by a joystick, in a manner analogous to that traditionally used for handheld stimuli. Stimulus intensities during quantitative data collection were square wave modulated above a maintained background level, usually for 1 or 2 s, and then back to background, with the first slit onset and offset preceding the onset and offset of the second slit by an appropriate delay. In most experiments, the delay used was 500 ms, because at this temporal separation, null-direction inhibition was still quite strong, but relatively few of the transient spike responses due to the first slit fell in the data-gathering window of the second slit. Square-wave modulation of slit contrast above and then back to a maintained background level in this manner produces a display that is similar to a low spatial-frequency square-wave grating moving behind two narrow apertures. Stimulus intensities were in the low mesopic range, and contrast modulations <60% were usually used to avoid nonlinearities not related to the DS mechanism. Most stimuli were presented over multiple trials to assess statistical significance of response characteristics.

Three significant advantages accrued from using steps rather than short flashes of light for these apparent motion experiments. *1*) ON and OFF transitions were separated in time, and their distinct interactions involving inhibition could be studied. *2*) The time course of the null-direction inhibition could be observed during a sustained ON or OFF input. *3*) The sustained inhibition allowed delays longer than 500 ms between slit transitions to be used, so that the null-direction apparent-motion inhibition of the second slit could be observed after the transient excitatory response elicited by the first slit had virtually ended.

Recordings and data collection

Recordings were made with glass-insulated tungsten microelectrodes (Levick 1972) connected to an amplifier (model P15; Grass Instruments, Quincy, MA). Well-isolated spikes (monitored on an oscilloscope) were digitized with a Schmitt trigger and their times of occurrence were recorded to the nearest ms by the same DOS 80286 microcomputer used for generating stimuli. Average spike counts in the first 500 ms after the onset and offset of the second slit were accumulated as the response measure. Cumulative poststimulus time (PST) histograms were also computed from the time-of-spike-occurrence data.

BASE SUBTRACTION. For some cells the expected average number of spikes due to the first slit occurring in the 500-ms window of the second slit were subtracted from its responses, bin by bin. Removal of the excitatory response of the first slit highlights the changes in the response to the second slit due to the interaction with the first slit. This allows a comparison to be made between the response elicited by the second slit when presented alone and

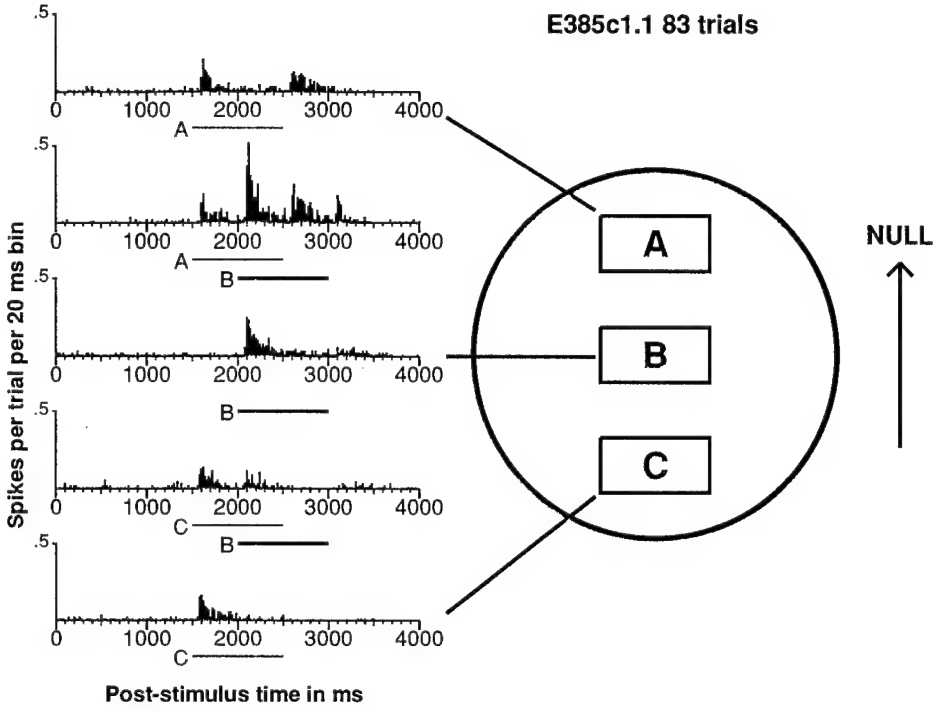

FIG. 1. Poststimulus time histogram responses of an ON-OFF directionally selective ganglion cell to each of 3 slits within receptive-field center presented in isolation and in apparent-motion sequences simulating preferred-direction motion (A then B) and null-direction motion (C then B). Ordinates are average spike counts per bin, where bin size is 20 ms. Each slit is modulated in a 1-s step above background, and then returns to background. Time each slit is above background is indicated by heavy line *below* the horizontal axis. Slit pairs are presented with a 500-ms delay between similar contrast transitions of 1st and 2nd slits, so that onset of the 1st slit occurs 500 ms before onset of the 2nd, and offset of the 1st slit occurs 500 ms before offset of the 2nd. Large circle to *right* of histograms gives approximate border of excitatory receptive center as established by flashing small spots. Ganglion cell was located at inferior edge of visual streak, and its receptive-field center diameter was ~500 μm on the retina. Slits A, B, and C within this circle indicate approximate positions of slits eliciting poststimulus time (PST) histograms to the *left*. Histograms show that null-direction motion (C → B) elicits inhibition and preferred-direction motion (A → B) elicits facilitation.

its response as affected by prior presentation of the first slit, with the excitatory response produced by the first slit itself removed. We refer to this procedure as "base subtraction," the base being the excitation expected from the first slit alone.

Data for this paper were obtained in a variety of different experimental protocols from 64 ON-OFF DS ganglion cells.

RESULTS

Inhibition (and facilitation) elicited by apparent motion

The responses of ON-OFF DS ganglion cells to two-slit apparent motion within their excitatory receptive-field centers is sequence dependent in a manner corresponding to their selectivity for direction of motion for true movement. Histograms showing the null-direction inhibition elicited by two-slit apparent motions are shown for one cell in Fig. 1. The *top, middle,* and *bottom* histograms in this figure are the responses to three slits (A, B, and C, respectively) presented individually. The *second histogram from the top* is the response to a preferred-direction apparent motion sequence from A to B; the *fourth histogram* is the response to a null-direction apparent motion from C to B.

For this cell, presentation of Slit B by itself (*middle histogram*) with an onset at 2,000 ms and offset at 3,000 ms resulted in a vigorous ON response beginning around 2,100 ms and a weaker OFF response beginning around 3,100 ms. Presentation of Slit C by itself (*bottom histogram;* onset at 1,500 ms, offset at 2,500 ms) elicited a strong ON response beginning around 1,600 ms, but very little OFF response. Apparent null-direction motion stimulation with Slit C onset and offset 500 ms before the onset and offset, respectively, of Slit B (*4th histogram from the top*) resulted in a strong suppression of the ON response due to Slit B and nearly a total elimination of its OFF response. The excitatory ON response produced by Slit C itself (beginning around 1,600 ms) was unaffected because it appeared before any change in intensity at Slit B.

That the effect of Slit C on B is due to inhibition, not to response saturation in the ganglion cell, is evident from the *second histogram from the top,* in which Slit A is stimulated before Slit B in a preferred-direction apparent motion. In this case, facilitated increases of both the ON and OFF responses elicited by Slit B occur. These findings confirm generally the results of Barlow and Levick (1965), who showed similar asymmetries in their apparent motion experiments. However, the use of sustained stimuli with a 500-ms relative delay in this experiment allows identification of the excitatory responses due to each of the two slit's ON or OFF contrast transitions, that is, A-ON, B-ON, A-OFF, and B-OFF.

Some differences between ON and OFF response mechanisms are observable in this experiment in terms of the magnitude of excitation elicited and the strength of slit-slit interaction. However, although there was some variation from cell to cell, and with particular stimulus conditions used, ON and OFF mechanisms behaved quantitatively similarly across the population of ON-OFF DS ganglion cells studied in these experiments. Thus, in this and other figures shown, some differences in the behavior of the ON and OFF mechanisms could have been due to true differences in the balance between the ON and OFF pathways for that particular cell but may also have occurred because of specific stimulus conditions, such as asymmetrical stimulation of ON and OFF mechanisms in the experimental protocol. For example, in most experiments reported in this paper, the ON stimuli go above and then back to background, but the OFF stimuli do not go below background but rather return to the previous background.

Temporal behavior of null-direction inhibition

We examined the temporal characteristics of the interaction between the excitation and the null-direction inhibition by varying the delay between the ON and OFF transi-

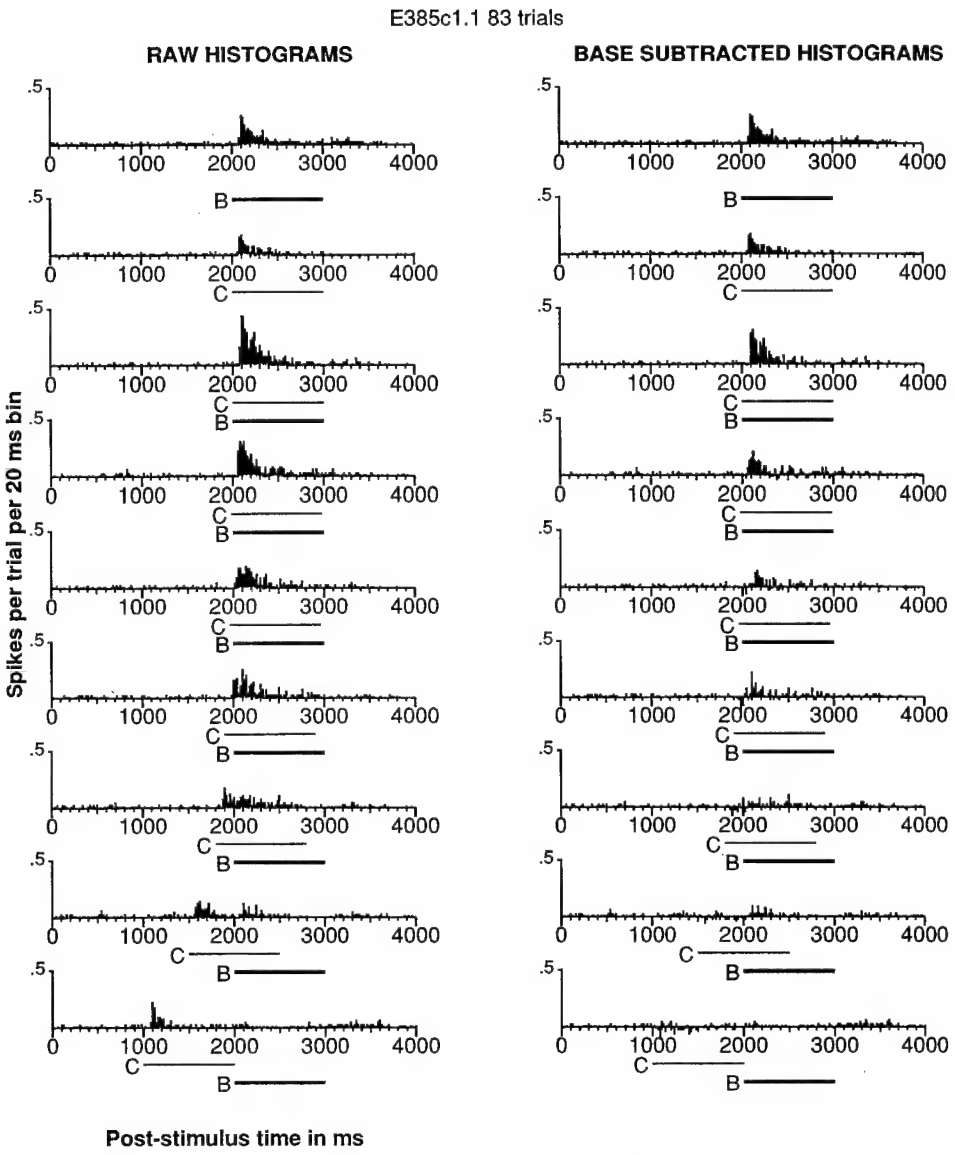

FIG. 2. PST histograms for same cell as in Fig. 1, showing effect of varying delay between 2 slits on resulting responses. *Top 2 histograms on left and right*: responses obtained when Slit A and Slit B, respectively, were presented by themselves. *Below* the top 2 histograms, histograms in *left column* are PST histograms obtained at various delays between Slits C and B. In *right column*, same data are plotted as on *left*, but with expected response of 1st slit (C), obtained from average of its PST histogram when presented alone, subtracted bin by bin from histogram when the 2 slits were presented in sequence (base subtraction). This base subtraction (described in METHODS) shows effect of the 1st slit on response to the 2nd slit with expected excitation due to the 1st slit removed.

tions of the first and second slit in two slit apparent motion experiments. Figure 2 shows the effect of varying the delay between modulation of Slits C and B on the response of Slit B, for the same cell as in Fig. 1. The *top two histograms* in both the *left and right columns* are the average PST histogram responses for Slits B and C presented singly, as in Fig. 1. The *third histogram on each column* shows the response to simultaneous presentation of Slits C and B. Below these in the left column are histograms showing the responses when Slit B is presented at various delays after Slit C.

For delays shorter than 500 ms, it is difficult to tell the effect of Slit C on B, because the excitatory response due to Slit C overlaps the time when the excitatory response due to Slit B occurs. To examine the effect of Slit B on C more precisely, we performed the operation referred to as "base subtraction" in METHODS. The result appears in the histograms *below the top two in the right column* of Fig. 2.

The base-subtracted histograms in the *right column* of Fig. 2 provide evidence that, in this experiment, saturation of the ganglion cell–firing mechanism cannot explain the weak response to the second slit after null-direction apparent motion from the first slit. When Slits B and C are presented simultaneously (*3rd histogram from the top, on the right*), the base-subtracted histogram (which removes the excitation due to Slit C) shows that the residual response, presumably due to Slit B, is not significantly less than that obtained when Slit B is presented alone. Thus, the excitatory responses of Slits B and C do not saturate when presented simultaneously at the contrast modulations used in this experiment, even though the temporal overlap between the two excitatory response histograms is greatest when they are presented simultaneously.

Base-subtracted histograms in which Slit B is presented at various delays relative to Slit C (*bottom* base PST histograms in the *right column* of Fig. 2) show that the inhibitory effect of Slit C on B has a discernible rise time. As described in the paragraph above, the response attributable to Slit B is little changed when presented simultaneously with Slit C. However, it is greatly reduced at longer delays between the two slits; at 500-ms delay (*2nd-to-last PST histogram*), the excitatory response due to Slit C is virtually over by the time the stimulus for Slit C occurs, yet the response due to Slit B is strongly inhibited.

We measured the effect of the delay between the first and

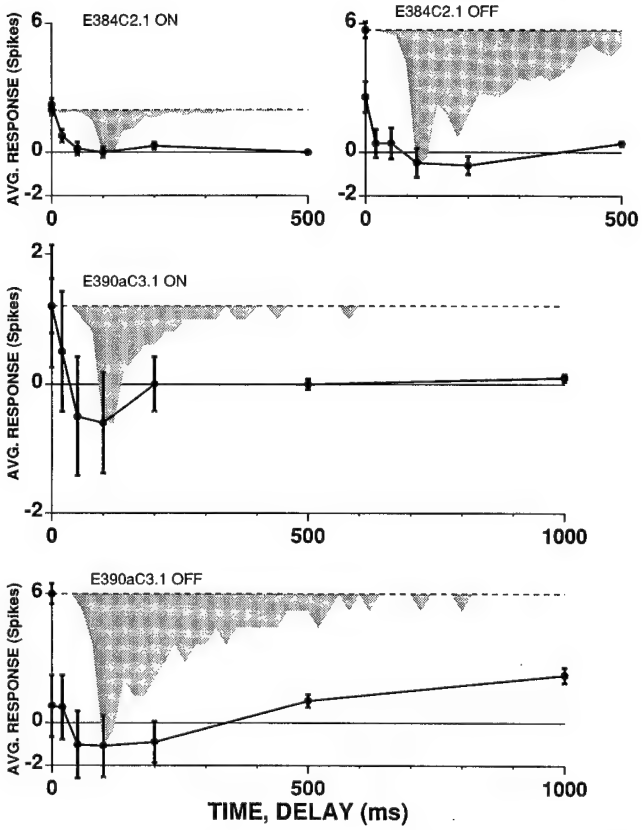

FIG. 3. Inhibition of total response of the 2nd slit as a function of delay between onset or offset of the 1st slit. Response measure for the 2nd slit is average number of spikes in the 1st 500 ms after either slit onset or offset, with excitatory response due to the 1st slit base subtracted. Dashed horizontal line in each plot is response of the 2nd slit by itself; solid line with error bars is response of the 2nd slit when preceded by the 1st slit at various delays, indicated on horizontal axis in milliseconds. Negative of histogram of response of the 1st slit as a function of time is shown in shaded area, for comparison of time course of its excitatory response with its inhibitory effect. ON and OFF responses for 2 cells are shown separately. Inhibitory effect of the 1st slit on the 2nd is sustained, unlike excitatory response elicited by the 1st slit, which is transient.

second slits on the total response elicited by the second slit. We defined the total response magnitude elicited by the onset or offset of the second slit as the average number of spikes during the first 500 ms after the onset or offset step change in the light level of that slit, because the excitatory responses to step changes in contrast were usually quite transient, rarely lasting >500 ms after the step change. The inhibitory effect of the first slit on the second is the difference between the response elicited when the second slit was presented alone and its response when preceded by the first slit at some delay. We used the base subtraction procedure described in METHODS, and shown in Fig. 2, to remove the excitatory response of the first slit from the measure of the response attributable to the second slit, when the interslit delay was short enough (<500 ms) that some of the excitatory response due to the first slit fell in the 500-ms data-gathering window of the second slit.

Figure 3 shows the time course of the inhibitory effect due to the onset of the first slit on the ON response of the second, and that due to the offset of the first slit on the OFF response of the second, separately for two cells. The magnitude of the response to the second slit, presented by itself, is represented by the horizontal dashed line in each plot. The rise time of the null-direction inhibition was generally found to be >150 ms [for 90% of peak, 160 ± 110 (SD) ms for 7 cells]. The inhibitory effect was then sustained for both ON and OFF responses, never returning to baseline before 2,000 ms for short interslit distances. ON-ON and OFF-OFF interactions generally behaved similarly in this and other experiments. This sustained inhibition due to the step change in the contrast of the first slit is markedly different in time course from the much more transient excitatory response elicited by the step change. The time course of the first slit's excitatory response is shown normalized, but negative, as the shaded area below the response to Slit B alone (- - -). If the null-direction inhibition elicited by the first slit were due to a process whose time course closely followed the excitation elicited by the first slit (such as a response saturation), then the inhibitory effect would be expected to follow the shaded waveform. However, the null-direction apparent-motion inhibition elicited at a given locus is more sustained than the suprathreshold excitation elicited from that same locus.

Because the effect of the sustained inhibition did not decline completely by 2 s (the longest interslit delay used in many of these experiments), we did several additional experiments to determine whether inhibition was sustained for times as long as 4 s. This apparent motion would correspond to a very slowly moving edge requiring 4 s to pass two apertures corresponding to the positions of the two slits. Such stimulation is not totally unrealistic physiologically, because, in experiments discussed in more detail elsewhere (Amthor and Grzywacz 1988), we have found that ON-OFF DS ganglion cells respond in a directionally selective manner to movement as slow as a few tenths of a degree per second, corresponding to a transit time of >5 s across the excitatory receptive-field center of one of these ON-OFF DS ganglion cells.

We plotted these long delay results in a separate figure (Fig. 4) for two reasons: *1*) the retina may have adapted significantly to the slit ON stimulus, rather than remaining adapted to the base contrast level; and *2*) combining, in a

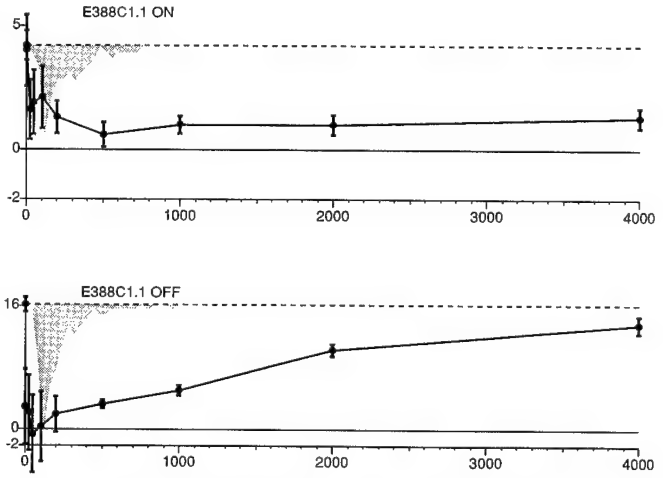

FIG. 4. Long-duration inhibition of total response of the 2nd slit as a function of delay between onset or offset of the 1st slit. Scheme of figure is same as that of Fig. 3. Inhibitory process can be seen to be sustained for ≥4 s for ON response (*top*), and for ≥2–3 s for OFF response (*bottom*).

single figure, the long interslit time data with the short data would have completely obscured details of the short interslit data, because of the scale. Figure 4 shows the time course of the null-direction inhibition for ON-ON and OFF-OFF interactions where interslit delays up to 4 s were used. In this experiment, the ON response of the second slit was still significantly inhibited by the sustained ON step of the first slit at 4 s. The inhibition of the OFF response of the second slit was marginally statistically significant at 4 s, but its interpolated value at 3 s appears to reflect significant inhibition. This latter finding is remarkable, given that this represents significant offset null-direction inhibition ≥3 s after return to background of the first slit.

Spatial profile of null-direction inhibition

We performed three types of experiments to assess the spatial properties of the null-direction inhibition. We measured *1*) the strength of inhibition as a function of interslit distance along the preferred-null axis at a fixed delay of 500 ms, *2*) the strength of inhibition at 11 loci over a two-dimensional area around the test slit at a fixed interslit delay of 500 ms, and *3*) the time course of inhibition as a function of interslit distance along the preferred-null axis.

The first series of experiments measured the dependence of the strength of inhibition as a function of the interslit distance along the preferred-null axis. As in Fig. 1, the responses to slits presented singly and then in apparent-motion sequences toward the test slit were determined at a delay of 500 ms. In most experiments, facilitatory responses of at least one additional slit on the preferred-direction side of the test slit were obtained as a control for saturation. The results of this experiment are illustrated for three cells in Fig. 5. In Fig. 5*A* there were four slits, with the farthest a distance of 600 μm from the test slit. In Fig. 5, *B* and *C*, six equidistant slits spanned a total distance of 250 μm from the test slit to the farthest inhibitory one. In all three experiments, the farthest slits were more than one-half the diameter of the receptive-field center from the test slit.

Figure 5 shows that the null-direction inhibition is effective for interslit distances larger than one-half the size of the receptive-field center. The strength of the inhibition is strongest for short interslit distances and decreases gradually at increasing interslit distances. At zero interslit distance, however, we found no net systematic inhibition or facilitation (see accompanying paper). (This apparent linearity lends further support to the use of the base subtraction procedure.) At interslit distances about one-half the size of the receptive-field center, the inhibitory strength is 71 ± 23% (n = 7) of the maximal inhibitory strength observed at short distances. The most distant slit in Fig. 5*A*, which is 600 μm from the test slit (and thus outside the excitatory receptive-field center), also elicits weak, but statistically significant, null-direction inhibition for the ON-ON interaction.

The two-dimensional spatial profile of the null-direction inhibition was measured with an array of 12 slits in a 4 × 3 rectangular grid having the four-slit side parallel to the preferred-null axis, as shown in Fig. 6. Responses were recorded for each of the 12 slits presented in isolation, and for each of the 11 possible two-slit apparent motions toward

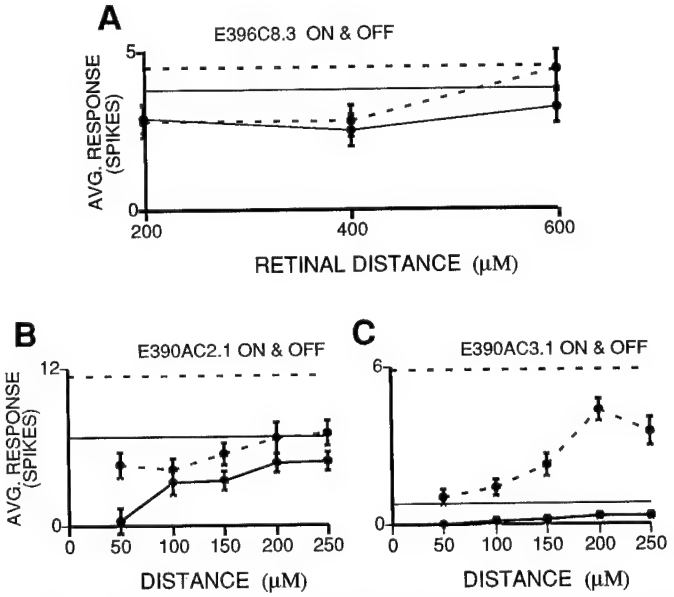

FIG. 5. Null-direction inhibition as a function of distance between the 2 slits along preferred-null axis within receptive-field center, for 3 cells. ON responses are shown as heavy solid lines with error bars; OFF responses as heavy dashed lines with error bars. Expected ON response for test slit presented by itself is shown as a horizontal solid line; that for OFF response is a horizontal dashed line. Thus amount of inhibition at a given interslit distance is difference between horizontal line for that response sign and heavier line with error bars. Null-direction inhibition is elicited for interslit distances as large as one-half receptive-field center diameter of each cell (*E396C8*, 600 μm; *E390AC3* and *E390AC2*, 500 μm).

the slit taken as the test slit. The results of this type of experiment are shown in Fig. 6 for four cells. The interslit delay for all four cells was 500 ms, as in several preceding figures, but for cell E394c1.3if (*bottom right*) the slits were 100-ms flashes, rather than steps, separated in time by 500 ms. The height of the wide box at each location shows the normalized strength of inhibition (dark box) or facilitation (gray box). The normalization scheme for inhibition is that the height of the dark box equals its width when total inhibitory suppression of the test slit (T) response occurs. Facilitation is normalized in the gray boxes so that when their height equals their width the facilitated response is twice the intrinsic response to the test slit itself. The magnitude of the excitatory response produced by the slit at each locus is proportional to the height of the thin vertical white bar on the right of the wider box.

Null-direction inhibition can be observed in all four cells and preferred-direction facilitation in the top two. The strongest inhibition of the test slit (T) tends to occur at nearby loci. Assuming the mapped upper half profiles could be reflected down to obtain the full spatial profile of inhibition, the null-direction inhibitory area observed in these and virtually all other experiments was an ovate shape whose long axis was parallel to the preferred-null axis, with the broader end of the ovate close to the test slit. Generally, significant inhibition was elicited only for null-direction apparent motion (motion whose projection on the preferred-null axis was in the null direction). Strong null-direction apparent-motion inhibition was elicited from slit positions as close as 10 μm from the test slit and even overlapping the test slit. Rarely was inhibition observed for apparent mo-

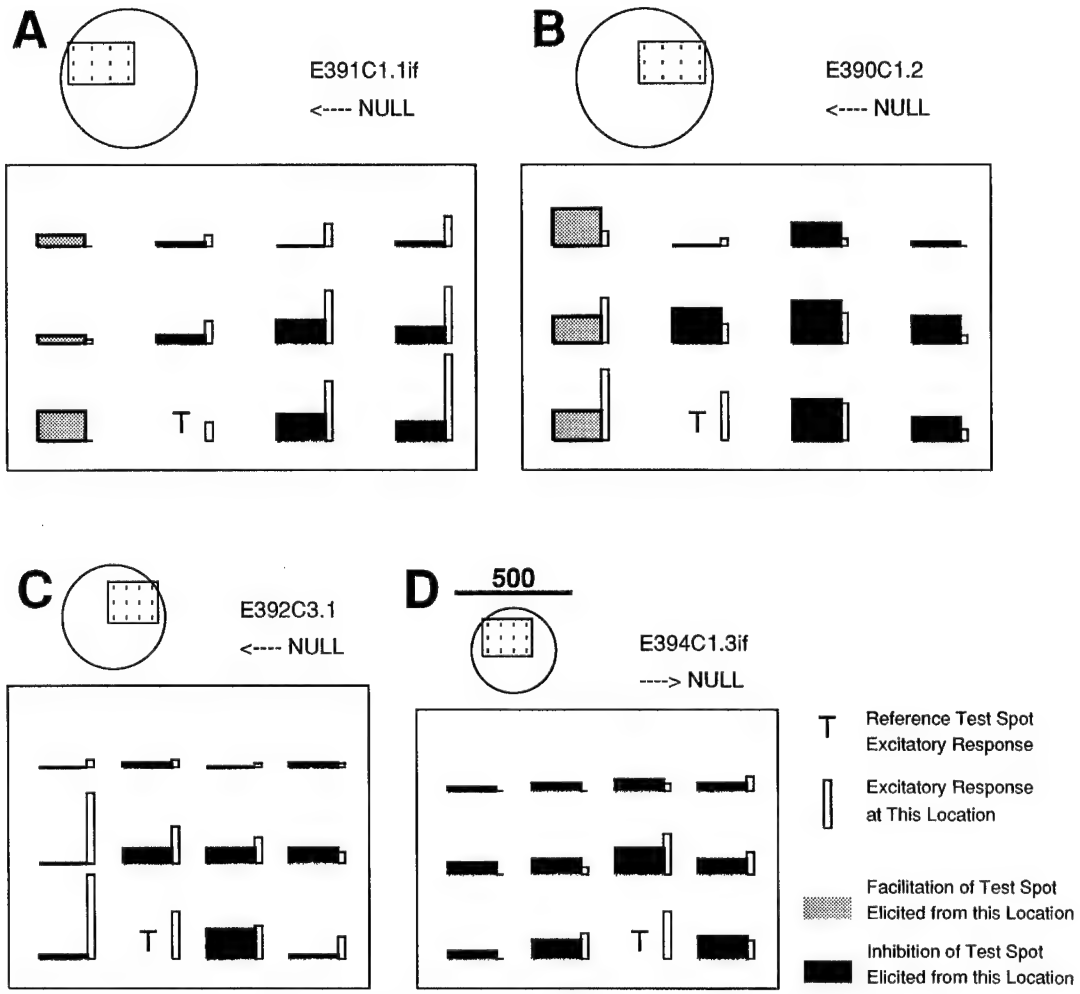

FIG. 6. Two-dimensional profiles of inhibition (black) and facilitation (gray) field around test slit (T). Narrow white bars to *right* of wide boxes represent intrinsic excitatory response at each location. Height of dark box shows amount of reduction in test slit response due to stimulation by the 1st slit 500 ms beforehand. Height of gray box shows the average (facilitated) increase in number of spikes elicited by the 2nd (test) slit after stimulation of the 1st slit in indicated location. Time courses of stimulations are as in earlier figures, except for *D* (*E394c1.3*), in which short flashes (100 ms), rather than longer steps, were used, separated by 500 ms. Circular areas give approximate extent of excitatory receptive-field center of each cell as established by flashing spots (scale indicated by the 500-μm bar near the top of *D*) and approximate location of array of slit stimuli within excitatory receptive-field area. Prolonged light steps revealed an asymmetric, ovate, inhibitory area. Short light flashes, however, elicited inhibition from a larger area completely surrounding test slit.

tion using light steps whose projection onto the preferred-null axis pointed in the preferred direction. This distance and directional dependency for step changes, in contrast, was consistently observed in 12 two-dimensional array experiments in which the majority of slits were on the null side of the test slit, as well as in experiments using linear arrays in >30 additional cells.

However, when flashes (500 ms apart) rather than steps of light were used (*cell E394c1.3if, bottom right,* Fig. 6), the strong asymmetry in the spatial profile of the observed inhibition disappeared. Inhibition was then elicited from slit locations on the preferred-direction side of the test slit as well as from the null-direction side. A similar result was observed by Wyatt and Daw (1975), who could elicit directional selectivity for apparent motion only with flashes separated temporally by <200 ms. This suggests that the mechanism underlying the asymmetry involved in directional selectivity is temporally sustained. On the other hand, this result also suggests that there is a component of inhibition observable within the excitatory receptive-field center that is spatially symmetric and transient. Because this symmetric component of inhibition is weak after 500 ms (see also Wyatt and Daw 1975), it might reflect the presence of a symmetric, classical surround inhibition within the receptive-field center (Merwine et al. 1990). Some parameters of the surround inhibitory mechanism are contrasted with those of the null-direction inhibition in a later section of this paper entitled *Null-direction versus classical-surround inhibition.*

The dependence of the time course of the null-direction inhibition on interslit distance was probed in a third series of experiments. In these experiments, we used a range of interslit delays from 0 to 1,000 ms for each of either three or five slits spaced along the preferred-null axis. Figure 7 shows the results of two such experiments. The ON and OFF responses have been combined in these plots because their results are quantitatively similar.

Figure 7 shows (as in previous figures) that, at a delay of

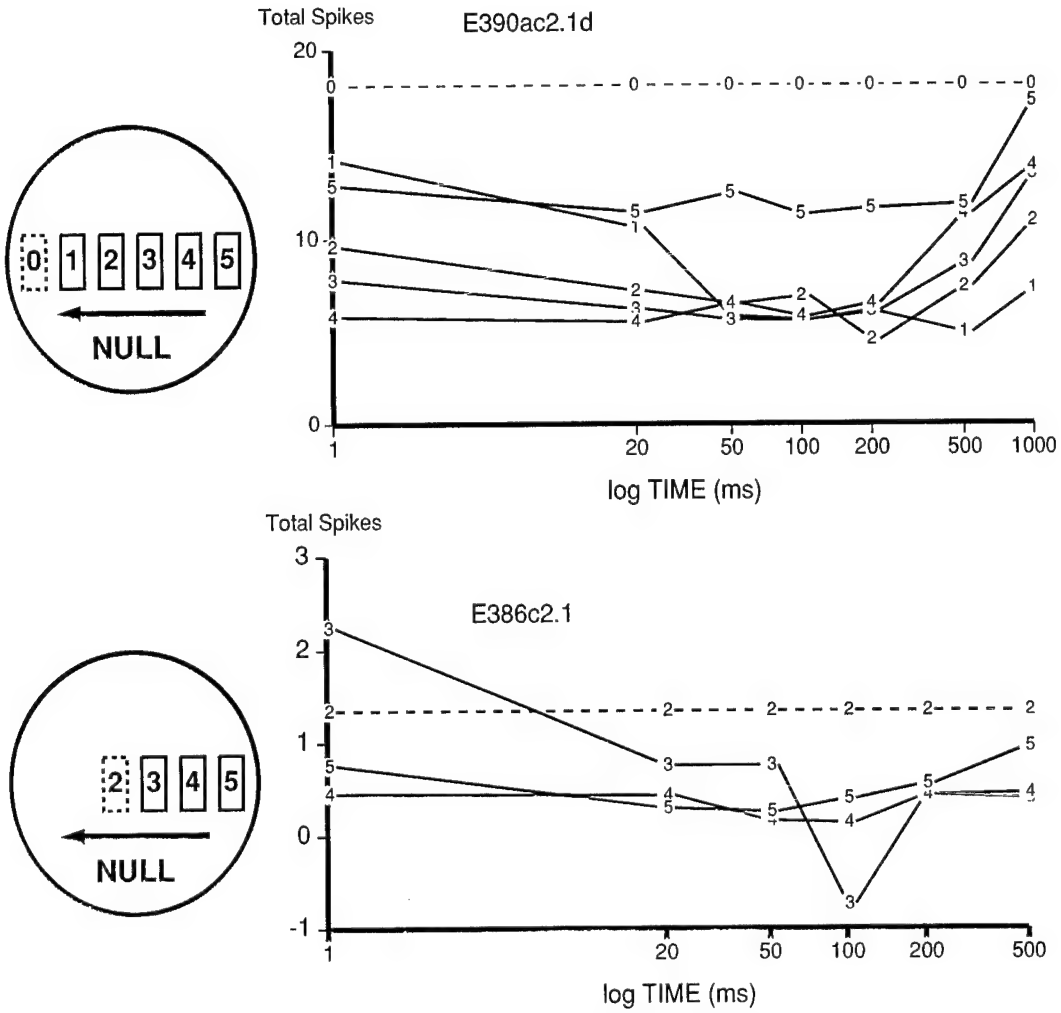

FIG. 7. Spatiotemporal profiles of inhibition along preferred-null axis. On *left* of each plot is a diagram of approximate location of slits within the receptive field. Slit with a dashed outline is test slit. Plot to *right* shows magnitude of response to test slit (dashed line with "0" symbol, *top cell,* and "2" symbol, *bottom cell*), and response of test slit when inhibited by slits at each of various positions shown as solid border boxes, as a function of delay (number symbols). A log scale has been used for time axis to show more clearly the rise time of inhibitory effect. Approximate diameters of receptive-field center of *E390AC2* and *E386C2* were 500 μm on retina. As interslit distance increases, rise and fall times of the inhibition appear to become faster.

500 ms, the peak inhibitory strength is greater for shorter than for larger interslit distances. However, the rise time to peak appears to be faster at larger distances, sometimes nearly reaching its maximal value by 1 ms. The slow rise time of the null-direction inhibition at short interslit distances was a robust finding; in five experiments using protocols similar to that plotted in Fig. 7, for slits ~40 μm from the test slit, virtually no detectable inhibition was elicited at a 1 ms interslit delay (0 ± 19% of the maximal inhibition obtained at larger delays). However, at an interslit distance of ~120 μm in the same cells, the strength of inhibition at 1 ms interslit delay was 57 ± 38% of the maximum elicited by that slit at longer delays (statistically significantly greater than 0 on a 2-sided t test; $P < 0.05$; $n = 5$).

Inhibition also appeared to be more sustained at shorter than longer interslit distances. At an interslit distance of ~40 μm, inhibition was still 77 ± 16% of maximum at a delay of 1 s ($n = 4$ cells). However, inhibition from slits ~120 μm away was not statistically different from zero at 1 s.

Mixed ON/OFF sign interactions

The use of steps, rather than flashes, of light permitted the influence of the onset of the first slit on the ON response of the second slit (ON-ON interactions) to be observed separately from effects on the onset of the second due to offset of the first slit, and similar isolation of OFF-OFF interactions. These experiments demonstrated that the null-direction inhibition mediating directional selectivity did not require an interaction between effects mediated by both stimulus onset and offset. Thus null-direction inhibition elicited from portions of the stimulus lighter than background is effective against subsequent excitation elicited from portions of the stimulus lighter than background; a distinct, but quantitatively similar interaction occurs for portions of the stimulus that are darker than background.

That the null-direction inhibition does not require interactions between light and dark portions of visual stimuli does not imply that no such interactions occur. The histograms of Fig. 1 give some evidence, however, that mixed

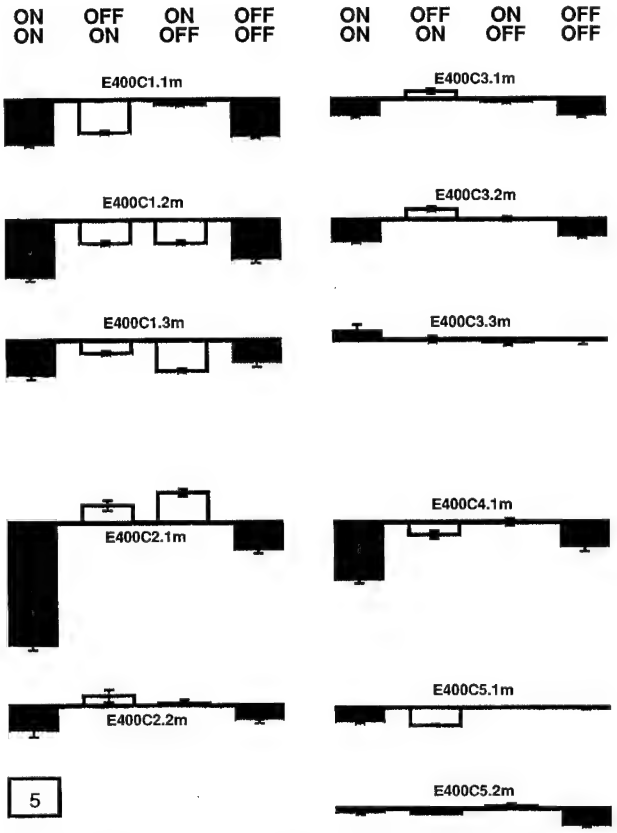

FIG. 8. Apparent motion interactions between like and opposite contrast modulations at various interslit distances within excitatory receptive-field center for several cells. All cells were located within or very near the inferior margin of the visual streak and had excitatory receptive-field diameters in range of 400–600 μm. "Test" slits were located near receptive-field centers. "Conditioning" slits were located symmetrically on preferred and null side of test slit at increasing distances from test slit, ranging from being adjacent (runs with ".1" suffix), to locations near border of excitatory receptive-field center (runs with ".3m" or ".2m" suffixes). Interslit delay was 500 ms in all cases. Like sign interactions (onset of the 1st slit affecting onset of the 2nd slit, and offset of the 1st slit affecting offset of the 2nd slit) are dark boxes whose height above or below the common heavy horizontal line indicate amount of facilitation or inhibition, respectively. Mixed-sign interactions (ON-OFF or OFF-ON) are shown as empty boxes. Error bars for SEM are on all boxes. For all cells at all positions, like-sign interactions are significantly negative, except for largest interslit distance for *E400c3* (*E400c3.3m*), OFF-OFF interaction for *E400c5.1m*, and ON-ON interaction for *E400c5.2m*. Cross-sign interactions (light boxes) are typically insignificant or inconsistently slightly inhibitory or facilitatory. Light box in *bottom left corner* gives scale for an average response change of 5 spikes due to modulation of the 1st slit.

sign interactions are weak in that there is little effect of the onset of Slit B on the offset of Slit A. We did experiments to explore the interactions between like and opposite sign contrast changes more systematically using two-slit stimuli in which the modulation of the contrast of the first slit was of the same and reverse polarity to that of the second. Figure 8 shows the results for five cells of all possible similar and cross sign contrast modulations of two slits, namely, ON-ON, OFF-ON, ON-OFF, and OFF-OFF, at several interslit distances. The delay between the first and second contrast transitions was 500 ms in all cases. Like-sign (ON-ON and OFF-OFF) interactions are shown as dark; opposite-sign interactions (ON-OFF and OFF-ON) as light. The magnitude of the effect of the onset or offset of the first slit on the response to the onset or offset of the second slit is represented by the height of a box above (facilitation) or below (inhibition) the dark horizontal bar.

We found that the effects of mixed sign interactions for sequences appropriate for null-direction apparent motion are usually insignificant. In the few cases where mixed-sign interactions were significant, the interaction was inconsistent, being in some cases slightly inhibitory (*E400c1.2*), and in other cases slightly facilitatory (*E400c2.1*). The sample mean for the interactions in ON-then-OFF sequences were not statistically significant ($10 \pm 28\%$ of the OFF-OFF interaction strength; $n = 5$). The OFF-then-ON sequences behaved similarly ($18 \pm 48\%$ of the ON-ON interaction strength). Thus the interaction between excitation and null-direction inhibition appears to be almost completely segregated between ON and OFF pathways.

Null-direction versus classical-surround inhibition

To test whether null-direction and classical-surround inhibition shared the same mechanism, we examined several quantitative aspects of the inhibition evoked from the classical inhibitory surround and compared those results with those obtained from inhibition elicited from excitatory RF center loci in apparent motion protocols. An experiment similar to that used to determine the time course of the null-direction inhibition was used to determine the time course of the classical-surround inhibition. In this experiment, instead of having two slits whose intensity was modulated at various interslit delays, the onset and offset of an annulus within the receptive-field surround preceded the onset and offset of a large spot within the receptive-field center. As in preceding sections, we then measured the effect of the surround stimulation on the response elicited by the spot in the receptive-field center.

Figure 9 shows the relative response of the center slit as a function of the delay after surround stimulation for three cells. Comparison of Fig. 9 with Fig. 3 shows that the inhibition elicited from the classical inhibitory surround with an annulus is much more transient than that elicited from within the receptive-field center by two-slit null-direction apparent motion. The maximal inhibition evoked by the surround in these experiments always occurred at the zero-delay condition. At 500-ms delay, the strength of surround inhibition tended to be very small or insignificant. This time course contrasts directly with that of the null-direction inhibition, whose rise time for short interslit distances was >150 ms and then sustained for ≥ 2 s. Thus, on the basis of temporal characteristics, the mechanism underlying the null-direction inhibition, at least at short interslit distances, appears to be significantly different from that underlying the classical surround inhibition. As we discuss later, however, there is evidence that surround inhibition is also present in the excitatory receptive-field center (Merwine et al. 1990) and could, under some stimulus conditions, contribute to inhibition of other center loci.

Contrast dependence of inhibition

It has been shown previously (Amthor and Grzywacz 1991) that the contrast dependence of null-direction inhibition acts as a nonlinear, division-like mechanism, rather

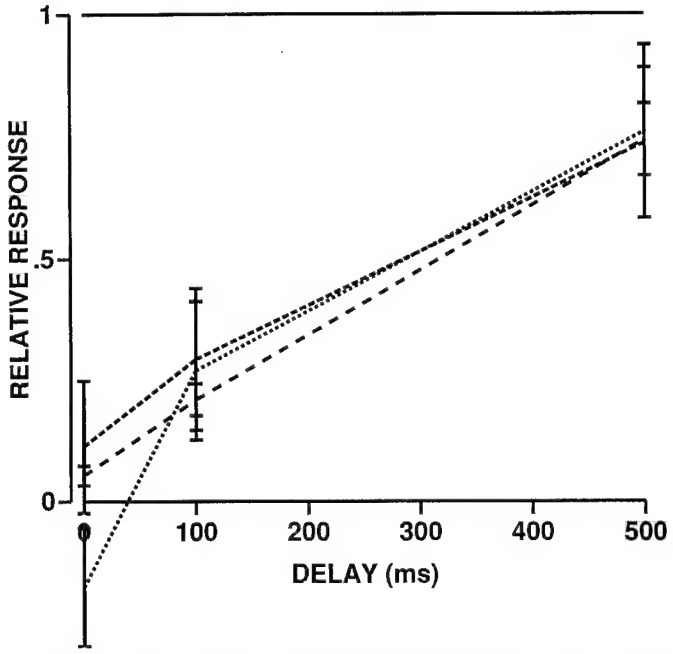

FIG. 9. Relative response to a spot in receptive-field center as a function of delay after stimulation of an annulus in classical inhibitory surround. Results for 3 cells are shown. Stimulation of surround simultaneously with center (delay = 0) produces a larger inhibitory effect than at any delay. By 500 ms, there is little impact of surround stimulation on center response. These results contrast with those for null-direction inhibition within excitatory receptive-field center, which typically exhibits a rise time to maximum >150 ms and remains effective for longer than 500 ms.

than as a linear, subtraction-like one. That the null-direction inhibition is division-like is evident from results of experiments that demonstrate the manner in which stimulation of a first, inhibitory slit affects the response-versus-contrast function of a second slit.

Figure 10*A* shows the response-versus-contrast function for a single slit presented within the receptive-field center by itself (curve 0%), and when it was preceded by another, inhibitory slit having different contrasts (curves 10, 20, 30, and 40%). The interslit delay was 500 ms in all cases. Two features of these data have been quantitatively demonstrated previously (Amthor and Grzywacz 1991). *1*) The effect of the null-direction inhibition increases gradually in strength as a function of contrast. Thus null-direction inhibition is a graded phenomenon, with a large working range between threshold and saturation rather than the absolute veto-type mechanism previously postulated for null-direction inhibition (Barlow and Levick 1965). *2*) The effect of the null-direction inhibition is division-like, rather than subtraction-like. Fits of similar data using a model including both division-like (shunting-inhibition) and subtraction-like (hyperpolarization) components (Amthor and Grzywacz 1991) demonstrated that the contribution of the postulated linear, subtraction-like component was either insignificant or actually slightly positive, rather than negative. The major null-direction apparent-motion inhibitory effect is thus equivalent to a division of the response-versus-contrast curve by a constant factor (reduction in gain), rather than a linear shift of the entire response-versus-contrast curve downward.

Like the difference in time course, the nonlinear, division-like nature of the null-direction inhibition would distinguish it from the inhibitory surround, if the latter has, as long supposed, a linear interaction with excitation, such as in difference-of-Gaussian models (Enroth-Cugell and Robson 1966; Rodieck and Stone 1965). We conducted experiments similar to that shown in Fig. 10*A* to examine the contrast dependence (and therefore the linearity) of the effect of inhibition elicited from the classical receptive-field surround, except that, as in Fig. 9, stimulation of an annulus in the receptive-field surround preceded stimulation of a large spot in the receptive-field center.

The results of this annulus-spot experiment for one cell are shown in Fig. 10*B*. It is apparent from the figure that the effect of the surround inhibition is not all or none, but increases with increasing contrast of the surround annulus. Moreover, the effect of the classical surround inhibition on the response-versus-contrast function of the center slit is manifest as a change in the slope in the response-versus-contrast function, rather than a downward shift, and thus is division-like, rather than subtractive. Thus surround inhibition in ON-OFF DS ganglion cells of the rabbit retina appears to be distinct from null-direction inhibition in both its rise and fall times, but is functionally similar in being a continuous function of contrast, rather than all or none, and in having a nonlinear (division-like) effect on excitation.

DISCUSSION

Time course

The time course of the inhibitory effect observed in Figs. 3, 4, and 7 shows the time course of the interaction between the inhibitory process caused by the first slit and the excitatory process caused by the second slit. This is not the same as the time course of the inhibitory process itself. However, from the time course of the interaction, one can infer two features of the relationship between the time courses of the excitatory and inhibitory processes. First, some effect of inhibition is evident even when there is zero delay between the two slits; therefore, for zero relative delay, at least some (presumably the early) portion of the inhibitory process is effective during some (presumably the late) portion of the time course of the excitatory process. Second, at short interslit distances, the inhibition of the response to the second slit by the first slit does not reach its maximum until the first slit precedes the second slit by $\sim$150 ms. Thus, for the sustained inhibitory process from the first slit to exert its maximal influence on the entire time course of the excitatory process, the activation of the inhibitory process must precede the excitatory activation by $\geq$150 ms.

Interpretation of the data with respect to the rise time of inhibition must also take into account the nonlinear, division-like nature of the interaction between the excitation and null-direction inhibition. A division-like inhibition has a much greater effect on portions of the excitatory response time course when firing is highest than on portions when the excitatory response is very small (Amthor and Grzywacz 1991). Therefore inhibition during portions of the transient excitatory response when the firing rate is low may not reveal itself by significantly altering cell firing rate.

The rise time of the null-direction inhibition appears to exhibit, in some experiments, a weak distance dependency.

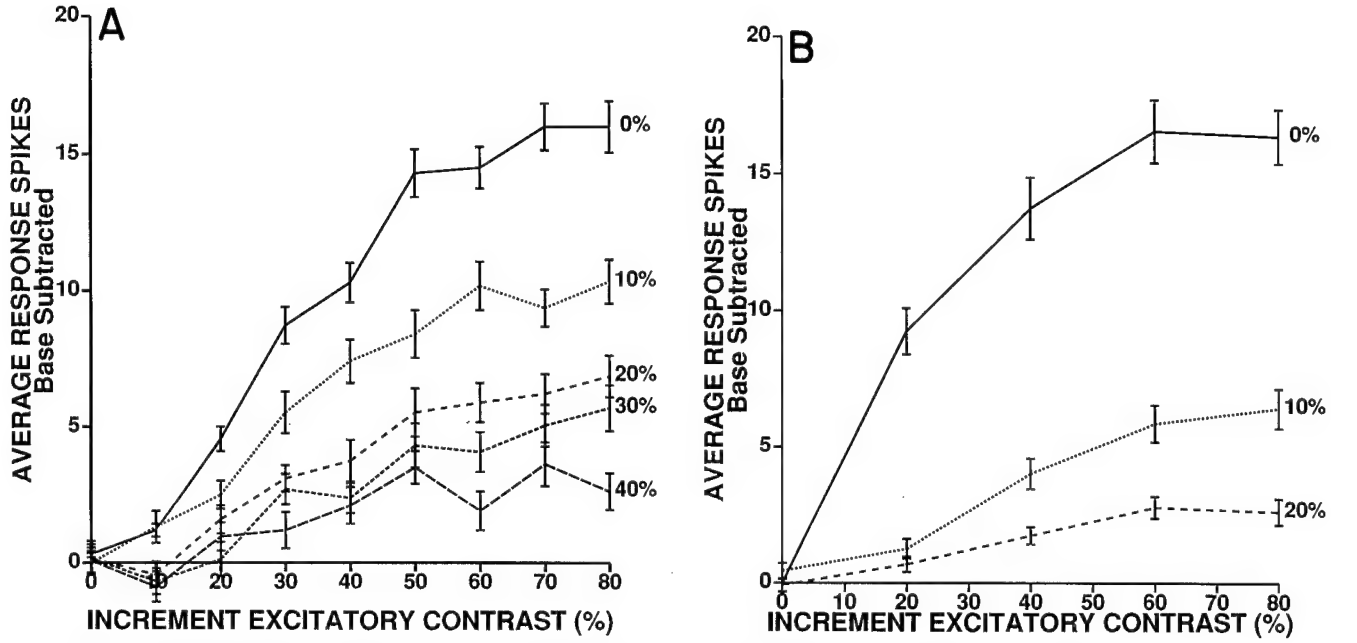

FIG. 10. *A*: average response vs. contrast function of the 2nd slit when presented by itself (curve marked 0%), and when preceded by a 1st slit modulated at contrasts of 10, 20, 30, and 40%. Average spike count is average of all spikes occurring 500 ms after onset and after offset of the 2nd slit, with expected response of the 1st slit removed by base subtraction procedure (see METHODS). Increasing contrasts for the 1st slit produce a gradual decrease in the response-vs.-contrast curve of the 2nd slit that can be approximated, for each curve, by a division by a factor >1 (gain reduction) of curve obtained for the 2nd slit alone. *B*: average response vs. contrast function for a spot within excitatory receptive-field center by itself (0% contrast plot), and when preceded by stimulation of annuli within the inhibitory surround, modulated at contrasts of either 10 or 20% simultaneously with the center spot modulation. Inhibition elicited from classical inhibitory surround has a division-like effect on curves, similar in form to that of null-direction inhibition seen in *A*.

At short interslit distances the inhibition has a rise time to 90% of peak of 160 ± 110 ms, but at sufficiently large interslit distances the null-direction inhibition nearly reaches its maximal effectiveness at zero delay between the two slits (as opposed to surround inhibition, which is always more effective at zero vs. longer delays). This distance dependency could reflect a true inverse distance-dependent delay factor in the biophysical process underlying null-direction inhibition. Alternatively, it could result from the contribution of facilitation at short interslit distances and/or surround inhibition at long interslit distances that confound the "real" time course of the null-direction inhibition. We cannot distinguish between these possibilities with the present data. However, in either case, the form of this distance dependency is inappropriate for delay models in which the inhibition is speed tuned. In such models, inhibition should be more delayed at longer, rather than shorter, distances.

One unequivocal finding about the null-direction inhibition is that its time course is sustained and thus not likely to be based on purely transient amacrine cells, contrary to what has been suggested elsewhere (Dowling 1987; Werblin et al. 1988). The time course of the effect of the null-direction inhibition lasts about as long as the excitatory responses of the brisk sustained ganglion cells in the same isolated rabbit eyecup preparation (Amthor et al. 1989a); the slow decline of the effectiveness of inhibition may, therefore, result from a general decline or adaptation in synaptic drive in some part of the intraretinal pathway shared by both excitation and inhibition.

The fast rise time of inhibition at long interslit distances could reflect a contribution from the normal inhibitory surround. Slits located at the farthest distances from the test slit are typically close to the border between the receptive-field center and the inhibitory surround, where the effect of the latter might be expected to be relatively greater than that of the null-direction inhibition, which declines with distance from the test slit. The inhibition elicited by annuli in the receptive-field surround outside the excitatory receptive-field center was shown to have a very fast rise time, being most effective when activated simultaneously with the center spot. Experiments using flashes instead of steps support the notion that surround inhibition extends into the receptive-field center and contributes some inhibition during null-direction motion (Fig. 6). Further evidence for the presence of the suppressive surround within the excitatory receptive-field center of ON-OFF DS ganglion cells was provided by Merwine et al. (1990). The relatively transient effect of the surround inhibition on these ganglion cells is somewhat surprising, however, if, as has been suggested, surround inhibition arises in the outer plexiform layer (Dowling 1987), because the surround effects on the responses of rabbit bipolar cells are relatively sustained (Dacheux and Miller 1981).

Significant differences found in these experiments in several characteristics of the null-direction versus surround inhibition (such as rise and fall times) suggest that they are mediated by two distinct mechanisms. The finding that null-direction inhibition is somewhat more like surround inhibition in its time course at large interslit distances could conceivably be explained as either a decline in the strength of the former and rise in strength of the latter mechanism or

a change along a continuum of a single mechanism. The two-mechanism explanation contrasts with the suggestion by Wyatt and Daw (1975) that directional selectivity might arise from a spatially asymmetric organization of the classical inhibitory surround. However, in these experiments, we did not observe an overall spatial asymmetry in the transient type of inhibition elicited from the region outside the receptive-field center. We also never observed a complete transition as a function of distance between sustained and transient inhibition. Inhibition is still quite sustained in the surround close to the receptive-field center on the side from which null-direction moving objects approach the receptive-field center, in contrast to other regions of the classical inhibitory surround, which elicit transient inhibition. If a spatially symmetric component of surround inhibition is assumed generally for ganglion cells to arise in the outer, rather than in the inner, plexiform layer, then the present data appear to be more consistent with the idea of null-direction, motion-specific inhibition in ON-OFF DS ganglion cells originating within the inner plexiform layer (Michael 1968).

Spatial properties

Null-direction inhibition has also been shown unequivocally in these experiments to be effective for interslit distances larger than one-half the size of the receptive-field center. This finding contradicts the hypothesis (Barlow and Levick 1965) that the receptive-field center is composed of small (<75 μm), discrete, inhibitory DS subunits. However, it cannot be determined from the present data whether short-distance null-direction inhibition is mediated by a subunit-like mechanism, whereas inhibition over longer distances is at least partly mediated by a different mechanism, such as the classical inhibitory surround existing within the excitatory receptive-field center. No abrupt, distance-dependent variation in any of the parameters associated with inhibition within the excitatory receptive field center in these experiments supported the hypothesis that null-direction specific inhibition was restricted to distances <75 μm.

The shapes of the inhibitory areas obtained in these experiments differ somewhat from those of Wyatt and Daw (1975), who postulated a cardioid inhibitory area effective for each excitatory receptive-field center locus, with the lobes of the cardioid extending somewhat toward preferred-direction moving stimuli. The notch in the cardioid was postulated to explain the result that small spots moving in the preferred direction experience less inhibition than bars extended perpendicular to the preferred-null axis, whose ends would intersect the lobes of the cardioid outside the notch. The data in this study suggest that the null-direction inhibitory area around each receptive-field locus has an ovate shape without any specific notch in the inhibitory field at that locus. This ovate shape was obtained by assuming that the upper half profiles found in Fig. 6 can be reflected down about the cells preferred-null axis. The discrepancy between the notch in the inhibitory field observed in the study of Wyatt and Daw versus the ovate shape found here cannot be ascribed to coarseness of the grid used in the present experiments, because the grids were fine enough to allow observation of spatial details down to 20 μm, whereas the lobes of the cardioids observed by Wyatt and Daw were typically larger than 100 μm. However, the finding of a notch at the test slit could depend on the choice of the preferred-null axis about which the upper half field was reflected, or on differences in experimental techniques, as discussed briefly in the INTRODUCTION.

Contrast dependence

A new and significant finding in this study is that interactions between excitation and null-direction inhibition appear to be almost completely segregated between the ON and the OFF pathways. The weak ON-OFF and OFF-ON interactions irregularly observed might well be completely negligible at contrasts that were lower, and more physiologically plausible, than the ones used in the mixed-sign interaction experiments in this study. The segregation of ON and OFF interactions is significant in allowing a clean separation of the computation of direction of motion for brighter and darker parts of a moving image. However, it is also quite intriguing that ON-OFF and OFF-ON interactions exist in some cases. ON-OFF DS ganglion cells have bistratified dendritic trees in widely separated sublamina of the IPL. Some, but not all, intracellularly stained ON-OFF DS ganglion cells exhibit regions of dendritic stratification in one sublamina of the IPL that arise from high-order, rather than low-order, dendrites in the other sublaminar ramification (Amthor et al. 1984, 1989b). It is conceivable that inputs in these sublaminar regions might be influenced by on-the-path excitatory or inhibitory inputs of the opposite ON or OFF sign in the other sublamina.

Both directionally selective and surround inhibition can be accounted for by a division-like operation. One simple biophysical division-like mechanism is shunting inhibition, which works by lowering the postsynaptic membrane resistance and thus reducing the efficacy of excitatory currents (according to the division formulation of Ohm's law). Shunting inhibition has been postulated as a possible mechanism for mediating null-direction inhibition in retinal directional selectivity by several investigators (Grzywacz and Amthor 1989; Torre and Poggio 1978). An alternative inhibitory mechanism that could exhibit division-like behavior is subtraction-like action (hyperpolarization) followed by an exponential-like nonlinearity. (The exponential of a subtraction is equal to the division of two exponentials.) Such a nonlinearity is not a bad approximation for the input-output relationships in many synapses. Amthor and Grzywacz (1991) discuss how a general expansive nonlinearity after the inhibition may transform an intrinsically subtraction-like inhibitory mechanism into inhibitory behavior that appears division-like.

N. M. Grzywacz thanks Drs. Ellen Hildreth and Tomaso Poggio for support during his time at Massachusetts Institute of Technology. He also thanks Drs. Tomaso Poggio, Lyle Borg-Graham, and Evelyne Sernagor, and R. Smith, for several discussions during the course of this project.

This work was supported by the Office of Naval Research (N00014-91-J-1280) by grants to F. R. Amthor from the National Eye Institute (EY-05070) and the Sloan Foundation (86-10-7), by a core grant from the National Eye Institute to the Vision Science Research Center of the University of Alabama at Birmingham (EY-03039), by grants to N. M. Grzywacz from the National Eye Institute (EY-08921) and the National

Science Foundation (BNS-8809528), by an award to N. M. Grzywacz from the Paul L. and Phyllis C. Wattis Foundation, and by a core grant from the National Eye Institute to Smith-Kettlewell (EY-06883).

Address for reprint requests: F. R. Amthor, Dept. of Psychology, University of Alabama at Birmingham, UAB Station, Birmingham, AL 35294.

Received 2 March 1992; accepted in final form 24 January 1993.

REFERENCES

AMES, A. A. III AND NESBETT, F. B. In vitro retina as an experimental model of the central nervous system. *J. Neurochem.* 37: 867–877, 1981.

AMTHOR, F. R. AND GRZYWACZ, N. M. The time course of inhibition and the velocity independence of direction selectivity in the rabbit retina (Abstract). *Invest. Ophthalmol. Visual Sci. Suppl.* 29: 225, 1988.

AMTHOR, F. R. AND GRZYWACZ, N. M. ON-OFF directionally selective ganglion cells are inhibited by two distinct mechanisms in rabbit retina. *Invest. Ophthalmol. Visual Sci. Suppl.* 31: 115, 1990.

AMTHOR, F. R. AND GRZYWACZ, N. M. The nonlinearity of the inhibition underlying retinal directional selectivity. *Visual Neurosci.* 6: 197–206, 1991.

AMTHOR, F. R., OYSTER, C. W., AND TAKAHASHI, E. S. Morphology of ON-OFF direction selective ganglion cells in the rabbit retina. *Brain Res.* 198: 187–190, 1984.

AMTHOR, R. R., TAKAHASHI, E. S., AND OYSTER, C. W. Morphologies of rabbit retinal ganglion cells with concentric receptive-fields. *J. Comp. Neurol.* 280: 72–96, 1989a.

AMTHOR, F. R., TAKAHASHI, E. S., AND OYSTER, C. W. Morphologies of rabbit retinal ganglion cells with complex receptive-fields. *J. Comp. Neurol.* 280: 97–121, 1989b.

ARIEL, M. AND DAW, N. W. Pharmacological analysis of directionally sensitive rabbit retinal ganglion cells. *J. Physiol. Lond.* 324: 161–185, 1982.

BARLOW, H. B. AND HILL, R. M. Selective sensitivity to direction of movement in ganglion cells of the rabbit retina. *Science Wash. DC* 139: 412–414, 1963.

BARLOW, H. B., HILL, R. M., AND LEVICK, W. R. Retinal ganglion cells responding selectively to direction and speed of image motion in the rabbit. *J. Physiol. Lond.* 173: 377–407, 1964.

BARLOW, H. B. AND LEVICK, W. R. The mechanism of directionally selective units in the rabbit's retina. *J. Physiol. Lond.* 178: 477–504, 1965.

CALDWELL, J. H., DAW, N. W., AND WYATT, H. J. Effects of picrotoxin and strychnine on rabbit retinal ganglion cells: lateral interactions for cells with more complex receptive fields. *J. Physiol. Lond.* 276: 277–298, 1978.

DACHEUX, R. F. AND MILLER, R. F. An intracellular electrophysiological study of the ontogeny of functional synapses in the rabbit retina. I. Receptors, horizontal and bipolar cells. *J. Comp. Neurol.* 198: 307–326, 1981.

DOWLING, J. E. *The Retina: An Approachable Part of the Brain.* Cambridge, MA: Belknap, 1987.

ENROTH-CUGELL, C. AND ROBSON, J. G. The contrast sensitivity of retinal ganglion cells of the cat. *J. Physiol. Lond.* 187: 517–552, 1966.

GRZYWACZ, N. M., AND AMTHOR, F. R. A computationally robust anatomical model for retinal directional selectivity. In: *Advances in Neural Information Processing Systems,* edited by David S. Touretzky. San Mateo, CA: Kaufman, 1989, vol. I, p. 477–484.

GRZYWACZ, N. M. AND AMTHOR, F. R. Independent ON and OFF computations of retinal directional selectivity in rabbit. *Soc. Neurosci. Abstr.* 17: 344, 1991.

GRZYWACZ, N. M. AND AMTHOR, F. R. Facilitation in ON-OFF directionally selective ganglion cells of the rabbit retina. *J. Neurophysiol.* 69: 2188–2199, 1993.

GRZYWACZ, N. M., AMTHOR, F. R., AND MISTLER, L. A. Applicability of quadratic and threshold models to motion discrimination in the rabbit retina. *Biol. Cybern.* 64: 41–49, 1990.

GRZYWACZ, N. M. AND KOCH, C. Functional properties of models for direction selectivity in the retina. *Synapse* 1: 417–434, 1987.

KOCH, C., POGGIO, T., AND TORRE, V. Retinal ganglion cells: a functional interpretation of dendritic morphology. *Philos. Trans. R. Soc. Lond. B Biol. Sci.* 298: 227–264, 1982.

LEVICK, W. R. Another tungsten microelectrode. *Med. Biol. Eng.* 10: 510–515, 1972.

MERWINE, D. K., AMTHOR, F. R., AND GRZYWACZ, N. M. Ganglion cell surround inhibition is divisive, not linear, in rabbit retina. *Invest. Ophthalmol. Visual Sci.* 31: 115, 1990.

MICHAEL, C. R. Receptive fields of single optic nerve fibers in a mammal with an all cone retina. II. Directionally selective units. *J. Neurophysiol.* 31: 257–267, 1968.

POGGIO, T. AND REICHARDT, W. E. Considerations on models of movement detection. *Kybernetik* 13: 223–227, 1973.

RODIECK, R. W. AND STONE, J. Analysis of receptive fields of cat retinal ganglion cells. *J. Neurophysiol.* 28: 832–849, 1965.

TORRE, V. AND POGGIO, T. A. A synaptic mechanism possibly underlying directional selectivity to motion. *Proc. R. Soc. Lond. B Biol. Sci.* 202: 409–416, 1978.

WERBLIN, F., MAGUIRE, G., LUKASIEWICZ, P., ELIASOF, S., AND WU, S. M. Neural interactions mediating the detection of motion in the retina of the tiger salamander. *Visual Neurosci.* 1: 317–329, 1988.

WYATT, H. J. AND DAW, N. W. Directionally sensitive ganglion cells in the rabbit retina: specificity of stimulus direction, size, and speed. *J. Neurophysiol.* 38: 613–626, 1975.

Does Synaptic Facilitation Mediate Motion Facilitation in the Retina?

Norberto M. Grzywacz[1], Franklin R. Amthor[2], and Lyle J. Borg-Graham[3]

[1]Smith-Kettlewell Institute, 2232 Webster Street, San Francisco, CA 94115
[2]Dept. Psychol. and NRC, Univ. Alabama, Birmingham, AL 35294
[3]Massachusetts Institute of Technology, E25-201, Cambridge, MA 02139

Abstract

Responses of retinal directionally selective ganglion cells to preferred-direction motions are larger than expected by the sum of responses to stationary stimuli. Experiments on directional selectivity argue against mechanisms of this motion facilitation based on dis-inhibition, threshold, voltage-dependent conductance decrease, and depolarizing shunting inhibition. We postulate that motion facilitation is mediated by the synaptic facilitation of an amacrine contact to ganglion cells. Simulations with a new retinal neuron simulator and compartmental model of a stained amacrine cell show that this model is feasible. In particular, it accounts for responses to apparent motions with and without antagonists to $GABA_A$ receptors.

Motion Facilitation

Directionally selective (DS) cells respond strongly to motions in a particular (preferred) direction and weakly to motions in the opposite (null) direction[1,2]. This directionality arises from facilitation of preferred-direction motion signals and inhibition of null-direction signals[1,2]. A way to demonstrate facilitation is to compare the extracellular response to a two-slit preferred-direction apparent motion with the responses elicited by the slits presented alone. The response to the motion is larger than the sum of the responses to the individual slits.

Not Applicable Models

Our recent electrophysiological data[2] indicate that four models that have been proposed for preferred-direction facilitation (Figure 1) do not account for it. The first model (A) suggests that facilitation shares the same mechanism with null-direction inhibition, but activates this mechanism with opposite polarity. A second model (B) postulates that co-activation of two or more inputs during motion raise the responses far above some threshold (or supralinearity). A third model (C) proposes that depolarization early in the motion increases the membrane resistance via a voltage-dependent channel thus increasing the voltage due to synaptic currents elicited late in the motion[3]. Finally, a fourth model (D) postulates that the inhibitory mechanism causes facilitation, since it might work through a slighly depolarizing shunting-inhibition synapse[4].

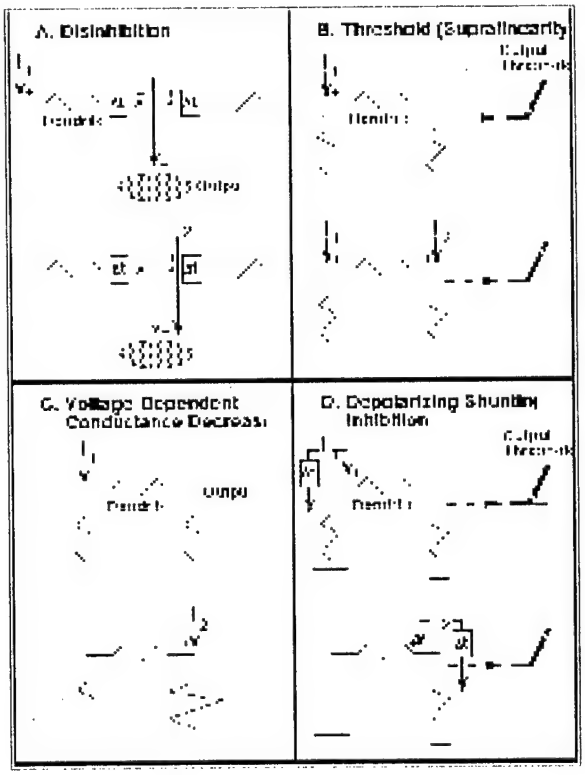

Figure 1: Not applicable models of preferred-direction facilitation.

A Model Based on Synaptic Facilitation

Our model postulates that preferred-direction facilitation occurs when inputs are activated sequentially simulating a propagating wave of synaptic excitatory currents.

This wave moves towards the distal tip of an amacrine-cell dendrite where its excitatory output synapse is located[5]. (For this paper, we performed compartmental-model calculations with a starburst amacrine cell recovered by Tauchi and Masland[6] using Lucifer Yellow. The simulator was Surf-Hippo, a new neuron simulator, which is particularly well suited for retinal studies[3].) The model assumes that the early portions of the motion stimuli produce through depolarization an agent (possibly calcium) that can facilitate the next synaptic release of the output synapse[7]. This release is gated by the depolarization elicited during the late portions of the motion[8]. (Other mechanisms are possible for both the enhancing agent and gating, leading Grzywacz and Amthor[2] to suggest the class of gated-enhancer models for motion facilitation.) Another element incorporated in the model is shunting inhibition of the presynaptic terminal, which can account for null-direction inhibition.

Figure 2: Temporal behavior of a gated-enhancer model based on synaptic facilitation.

The curves in Figure 2 are the results of simulations and calculations with the model. The stimulus was an apparent motion with the first slit delivered at 0 msec and the second at 500 msec (solid lines), or a slit presented alone in the position of the second slit of the motion at 500 msec (dashed line). The top-left panel

shows the presynaptic potential, which does not display facilitation. The top-right panel shows the buildup of calcium in the presynaptic terminal; it is this accumulation after the first slit that causes facilitation in the model. The gating of transmitter release (bottom-left panel) follows the presynaptic potential closely. This gating causes release, which is greatly facilitated (bottom-right panel) by motion.

Results: Time Course of Facilitation

The time course of facilitation was studied by varying the delay between the slits in the apparent motion (Figure 3). The measure of facilitation used was the integral of the response 500 msec after the second slit with the response of the first slit after the delay between the slits subtracted. The inter-slit distance was 100 mm. Facilitation rises in about 500 msec and falls in about 2 sec in the rabbit-retina electrophysiology and model (solid line). This time course is much slower than the time course of the response to the single slit (dashed curve). In the model, the slow rise and fall times of facilitation are due to the slow accumulation and removal of the enhancer agent (possibly calcium), whereas the fast time course of the single-slit response is due to the gating mechanism (possibly depolarization).

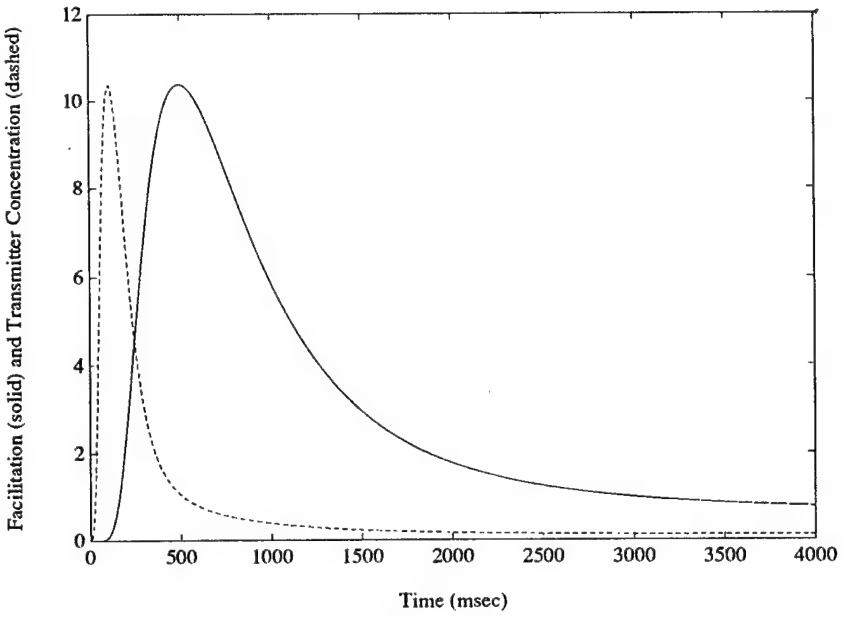

Figure 3: Time Course of facilitation and transmitter release

Results: Effects of $GABA_A$ Antagonists

To study facilitation in the absence of inhibition, we removed the inhibition with $GABA_A$ antagonists (in particular, picrotoxin) and recorded the responses to preferred- and null-direction apparent motions in the turtle retina[9]. Both the physiology and model (Figure 4) showed that when inhibition is absent, facilitation can appear in null-direction responses. This facilitation can be larger than that of the original preferred direction. In the model, null-direction facilitation can be stronger than preferred-direction facilitation, since the first slit of the null-direction motion is closer to the releasing terminal of the amacrine cell than the first slit of the preferred-direction motion. Hence, because of the cable properties of the dendrite, the depolarization and thus calcium accumulation due to the first slit of the null-direction motion can be larger than that of the preferred direction.

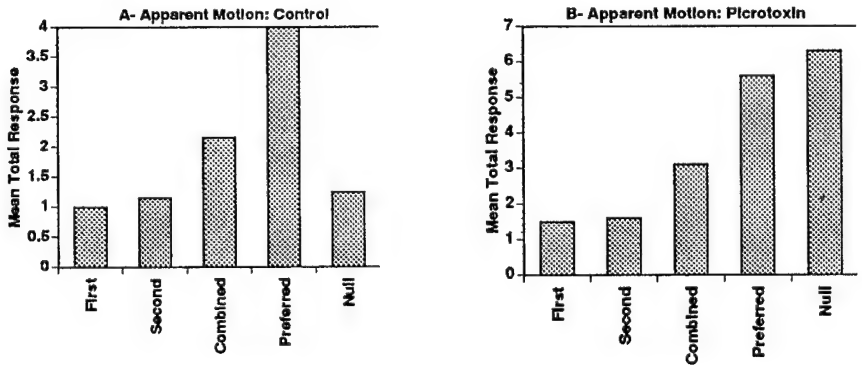

Figure 4: Effects of $GABA_A$ antagonists on motion facilitation and inhibition

Results: Other Simulations

Other simulations demonstrated that the model also accounts for the spatial and contrast properties of motion facilitation.

Acknowledgements

This research was supported by a grant to F.R.A. and N.M.G. from the Office of Naval Research (N00014-91-J-1280), by grants to N.M.G. from the National Eye Institute (EY08921-01A1), from the National Science Foundation (BNS- 8809528), and a NIH core grant to Smith-Kettlewell (EY06883), by grants to F.R.A. from the National Eye Institute (EY05070) and from the Sloan Foundation. L.B.G. was supported by a postdoctoral fellowship from the MIT's McDonnel-Pew Center for Cognitive Science.

References

1 Barlow, H. B. and Levick, W. R. J. Physiol. Lond. 178: 477-504, 1965.
2 Grzywacz, N. M. and Amthor, F. R. Facilitation in directionally selective ganglion cells of the rabbit retina. J. Neurophysiol. In Press. 1992.
3 Borg-Graham, L. J. and Grzywacz, N. M. In: Single Neuron Computation, edited by T. McKenna, J. Davis, and S. F. Zornetzer. Orlando, Florida, USA: Academic Press, 1992, p. 347-375.
4 Torre, V. and Poggio, T. Proc. R. Soc. Lond. B, 202: 409-416, 1978.
5 Famiglietti, E. V. J. Comp. Neurol. 309: 40-70, 1991.
6 Tauchi, M. and Masland, R. H. Proc. R. Soc. Lond. B. 223: 101-119, 1984.
7 Katz, B. and Miledi, R. J. Physiol. Lond. 195: 481-492, 1968.
8 Hochner, B., Parnas, H., and Parnas, I. Nature, Lond. 342: 433-435, 1989.
9 Smith, R. D., Grzywacz, N. M., and Borg-Graham, L. J. Effects of $GABA_A$ antagonists on preferred motion direction of turtle ganglion cells. Submitted for publication, 1992.
^F^F

Grzywacz, N.M., J.M. Harris, and F.R. Amthor (1994) Computational and Neural Constraints for the Measurement of Local Visual Motion, in *Visual Detection of Motion,* A.T. Smith and R.J. Snowden (Eds.), 19-50. Academic Press, Orlando, Florida, USA.

Grzywacz, N.M., F.R. Amthor, and D.K. Merwine (1993) Directional Hyperacuity in Ganglion Cells of the Rabbit Retina. *Visual Neuroscience.* In Press.

Grzywacz, N.M., E. Sernagor, and F.R. Amthor (1994) Retinal Directional Selectivity: Function, Mechanism, and Development, in *The Handbook of Brain Theory and Neural Networks,* M.A. Arbib (Ed.). MIT Press, Cambridge, Massachusetts, USA. In Press.

Visual Motion and its Role in the Stabilization of Gaze
Eds. F.A. Miles and J. Wallman

CHAPTER 4

Directional selectivity in vertebrate retinal ganglion cells

Franklin R. Amthor[1] and Norberto M. Grzywacz[2,3]

[1]*Department of Psychology and Neurobiology Research Center, University of Alabama at Birmingham, Birmingham, AL 35294;*
[2]*Center for Biological Information Processing, Massachusetts Institute of Technology;*
[3]*The Smith-Kettlewell Eye Research Institute, 2232 Webster Street, San Francisco, CA 94115, U.S.A.*

1. Introduction

Directionally selective neurons respond much better to motion in a "preferred" direction than to motion in the opposite, or "null", direction. Cells with this response selectivity are ubiquitous throughout the visual systems of vertebrates, subserving a variety of visual tasks ranging from discrimination of objects from background to control of eye position. Perhaps reflecting this diversity in functional requirements, directional selectivity is computed independently, with somewhat different properties, at multiple visual system loci.

For example, directional selectivity in the primary visual neocortex of mammals such as cats and primates appears to arise de novo there from intracortical circuits that receive largely nondirectionally selective inputs from the lateral geniculate nucleus. On the other hand, aspects of the detection of image motion for gaze stabilization appear to be mediated by directionally selective retinal ganglion cells that project to pretectal and accessory optic system nuclei in an organization that is relatively conserved across many classes of vertebrates. Direction-of-motion discrimination in retinal ganglion cells appears to be considerably more robust and invariant with respect to stimulus parameters than that found in primary visual cortex.

2. Directional selectivity: Problems and hypotheses

In this section, we will identify the main problems facing researchers of directional selectivity and what hypotheses have been proposed to solve these problems. The concepts raised here provide motivation for the experiments described in later sections.

To start the discussion, Fig. 1 shows a schematic diagram illustrating several features of the receptive field organization of a typical On-Off directionally selective ganglion cell in rabbit retinas. The circle encloses the excitatory receptive field center wherein flashes of stationary spots elicit increases in firing at both light increase and decrease, indicated by the plus/minus symbols. Outside this excitatory receptive field center, flashes have an inhibitory effect on spontaneous firing, or on firing produced by another spot flashed within the receptive field center.

Around the receptive field map in Fig. 1 are schematic illustrations of the typical extracellularly recorded firing elicited by movement of a small spot through the receptive field in the directions indicated by the large arrows. Although no asymmetry whatsoever is evident within the excitatory receptive field from the responses to the flashed spots, movement in different directions elicits quite different responses. The pre-

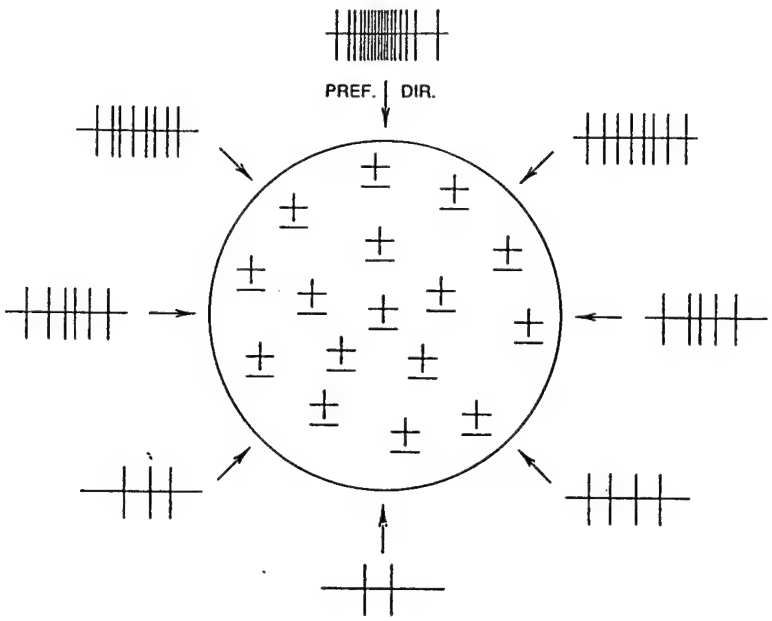

Fig. 1. Schematic organization of the receptive field of an On-Off directionally selective ganglion cell of the rabbit retinas. The region enclosed by the circle is the excitatory receptive field center, wherein flashes of small spots evoke excitatory responses at both light onset (pluses) and light offset (minuses) everywhere. Surrounding this depiction of the receptive field center are schematic extracellularly recorded responses to movement in the directions indicated by the arrows. Movement in the preferred direction, in this case down, evokes a large response during traversal of the spot across the excitatory receptive field center. However, movement across the same path, but in the opposite direction (up arrow) evokes little or no response. Movement directions intermediate between the preferred and null directions produce intermediate responses.

ferred direction, downward in this case, yields a large response. Movement upward, in the null direction, elicits almost no response, although the trajectory of the spot stimulates exactly the same receptive field loci that produced a large response for motion in the preferred direction. Trajectories orthogonal to the preferred-null axis elicit responses that are roughly intermediate in strength between those elicited in the preferred and in the null directions, indicating that the directional tuning is not particularly sharp, although the response differences for preferred versus null-direction motions in these cells are robust with respect to changes in stimulus parameters such as contrast and speed. It is also of considerable importance that small motions downward almost anywhere in the receptive field center elicit more response than small motions upward. This means that the receptive field contains several directionally selective subunits (Barlow and Levick, 1965). In other words, the mechanism of directional selectivity seems to be replicated several times.

2.1. Spatial asymmetry

Figure 1 illustrates the involvement of a spatial asymmetry in the computation of directional selectivity. Because a downward motion elicits a different response than an upward motion, there must be some difference (asymmetry) between the positions above and below the center of the receptive field. Otherwise, the response to the upward and downward motions would have been exactly identical. Moreover, this up-down asymmetry probably holds for almost all positions of the receptive field. This requirement is necessary

to account for the directionally selective subunits.

The first investigators to identify the need for an asymmetry were Reichardt and co-workers (Hassenstein and Reichardt, 1956; Poggio and Reichardt, 1976), who hypothesized a facilitatory (excitatory) asymmetry for insect directional selectivity (Fig. 2A). Their hypothesis applied to Fig. 1 says that any given position in the receptive field center receives facilitatory connections from above, but not from below. Thus, this position's responses are facilitated by downward, but not upward, motion. Such a facilitatory model might also account for certain aspects of human perception of motion (van Santen and Sperling, 1984). In the case of rabbit retinas, Barlow and Levick (1965) tested this model and concluded that another mechanism, null-direction inhibition, was more important for the rabbit's directional selectivity.

Barlow and Levick (1965) hypothesized, based on their rabbit data, that an inhibitory asymmetry mediates its directional selectivity (Fig. 2B). When applied to Fig. 1, their hypothesis postulates that any given position in the receptive field center is inhibited from below, but not from above. Hence, upward, but not downward, motions inhibit this position's responses. Later, several investigators advanced more detailed models of retinal directional selectivity based on asymmetric inhibition (Wyatt and Daw, 1975; Torre and Poggio, 1978; Ariel and Daw, 1982).

Another interpretation for Barlow and Levick's data based on symmetric inhibition and asymmetric facilitation was proposed by Vaney and colleagues (Vaney et al., 1989; Vaney, 1990; see

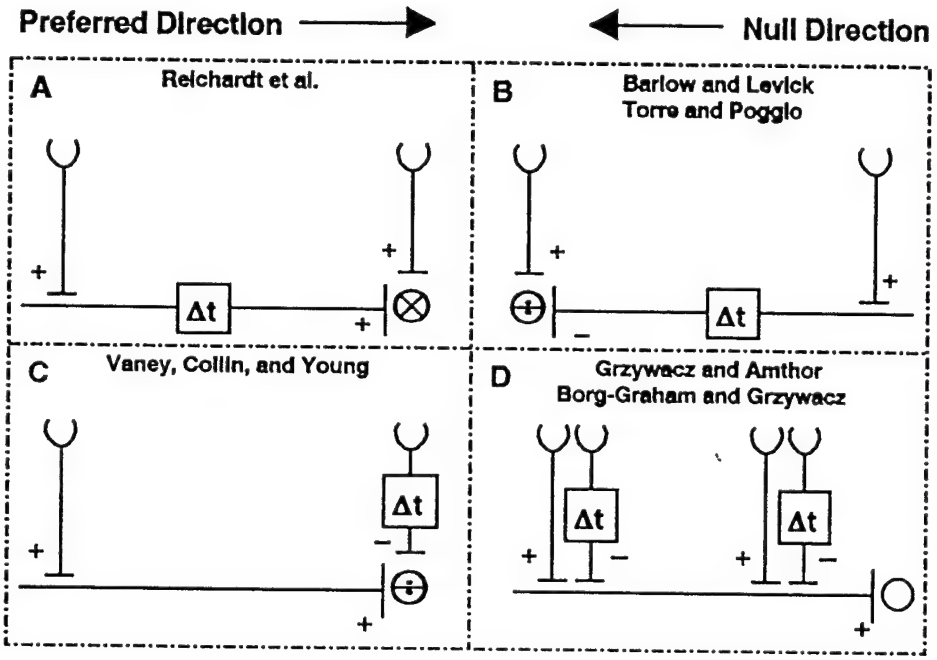

Fig. 2. Models for directional selectivity. **A**, The model proposed by Reichardt and colleagues to account for directional selectivity is based on an asymmetric facilitatory (excitatory) process. This process interacts multiplicatively with a symmetric excitatory process. The asymmetric process is slow (denoted by Δt) relatively to the symmetric process and both processes have receptive fields. **B**, In the version of the Barlow and Levick model advanced by Torre and Poggio, a slow, division-like (shunting) inhibitory asymmetry mediates directional selectivity. **C**, Vaney et al. proposed a model based on the interaction between a facilitatory asymmetry and a slow, symmetric, division-like inhibitory process. **D**, Another model proposes directional selectivity to arise from the interaction between symmetric inhibitory and excitatory processes feeding into an asymmetric excitatory process (see Fig. 3).

Fig. 2C). According to this interpretation, directional selectivity occurs in Fig. 1, since any given receptive-field position receives facilitatory connection from above, but not from below. However, inhibitory connections also exist from above and below. While facilitation overcomes the inhibition from above, the inhibitory connections from below improve directional selectivity by reducing the null-direction signal. Other hypotheses for retinal directional selectivity also exploit both asymmetric facilitation and symmetric inhibition (Grzywacz and Amthor, 1988a; Grzywacz and Borg-Graham, 1991, Borg-Graham and Grzywacz, 1991a). However, these models are different from Vaney's, since in them, excitatory and inhibitory inputs are symmetric while the output is asymmetric (Fig. 2D and see Section 2.2).

In contrast, some hypotheses for cortical directional selectivity postulate that the spatial asymmetry is an asymmetry of time courses in which the impulse responses in different portions of the receptive field are different. For example, certain On portions might respond to light onset with excitation followed by inhibition, while other Off portions would respond with inhibition followed by excitation. Because different motions would start these impulse responses in different orders, the amplitude of these responses' sum would depend on the motion direction. The motion-energy model (Adelson and Bergen, 1985; Heeger, 1987; Grzywacz and Yuille, 1990) is one example of models based on impulse-response asymmetry. Similar models have been advanced by several other investigators (Reid et al., 1987; Emerson and Citron, 1988; McLean and Palmer, 1989).

2.2. *Spatio-temporal properties*

To understand how the models in Fig. 2 work, one must remember that real neural processes have associated spatial and temporal properties. Neural responses will vary with speed of motion depending on how long signals take to travel along the lines of Fig. 2 and on how long these lines are. Hence, in thinking about the models of Fig. 2, one must remember that the lines should not be taken as coming from a single position in space. Rather, there is a receptive field associated with each line. Also, one must attach a time course to each line. The delay symbols (Δt) do not mean that there is a fixed delay for propagation along these lines but that the propagation along these lines is slower than along the other lines. Many of the experiments below were designed to measure the time courses and receptive fields associated with the lines.

The issue of temporal properties has been particularly emphasized by modelers. The models proposed by Reichardt and colleagues (Fig. 2A) emphasized the sluggishness of the asymmetric facilitation (excitation). This sluggishness would ensure that facilitation elicited from the left would arrive at the interaction site almost simultaneously with the excitation elicited from the right. (Optimal simultaneity would occur only for the correct speed.) For similar reasons (but with reversed polarity), the Barlow and Levick (Fig. 2B) and the Vaney models (Fig. 2C) postulated the slowness of inhibition. The models of Fig. 2D (Grzywacz and Amthor, 1988a; Grzywacz and Borg-Graham, 1991; Borg-Graham and Grzywacz, 1991a) also emphasize the slowness of inhibition, but this time, for creating a dynamic asymmetry (Fig. 3). These models postulate that the excitatory and inhibitory inputs onto the asymmetric process are themselves symmetric and homogeneously distributed. In null-direction motion, which is away from the output of the asymmetric process, the wave of inhibition remains closer to this output than the wave of excitation, and thus is very effective. (This special effectiveness is due to the on-the-path condition discussed in Section 2.4). In contrast, in a preferred-direction motion (toward the output), the wave of inhibition remains relatively far from the output, and thus is ineffective.

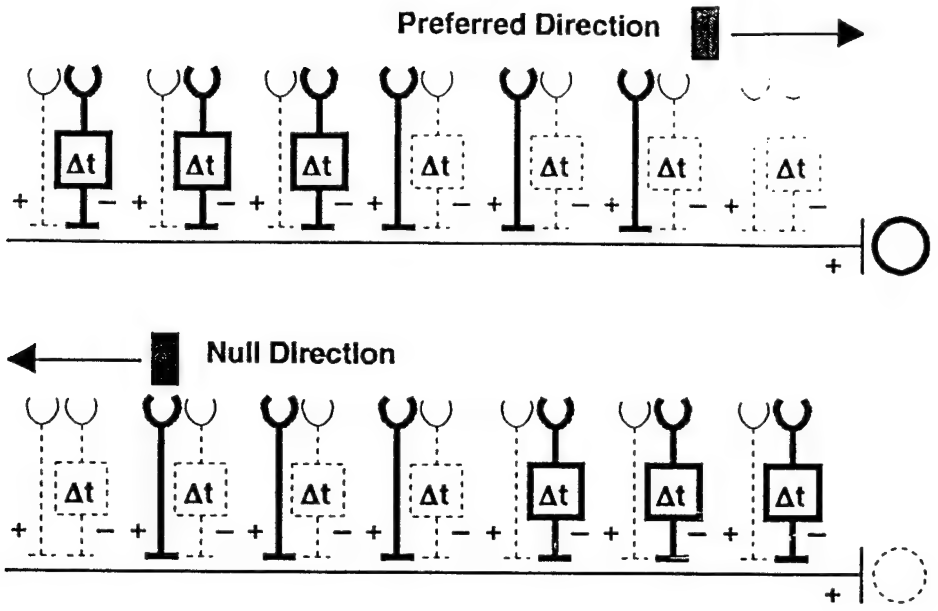

Fig. 3. Dynamic asymmetry. It explains the dynamic properties of the model of Fig. 2D. Because in this model the excitatory inputs are relatively fast, they are presently active (bold lines) near the current position of the stimulus (recent past). In contrast, the inhibitory inputs are slow, and thus are inactive (thin, dashed lines) near the current position of the stimulus. Rather, they are only active in positions that the stimulus occupied a "long" time ago. Hence, this causes a wave of excitation followed by a wave of inhibition during motion. In preferred-direction motion, the wave of excitation is closer to the output than the wave of inhibition and thus is effective. However, for null-direction motion, the wave of inhibition is closer to the output, suppressing the response (see discussion on on-the-path-condition in Section 2.4). Therefore, a dynamic asymmetry is generated by the motion-induced switch of the positions of inhibition and excitation.

2.3. Nonlinearity

Another problem related to directional selectivity is that it is not sufficient for the underlying interactions to be linear (for example, subtraction), but rather, they must be nonlinear. This problem was first described by Poggio and Reichardt (1973) in roughly the following way: A linear system can produce outputs with different time courses in response to motion in different directions. However, a linear functional (for example, time integral) applied to these time courses would yield the same results. Poggio and Reichardt discussed functionals, since they are mappings from functions (for example, time courses) to numbers (for example, number of spikes or maximal spike rate). These investigators pointed out that directional selectivity expresses itself in terms of difference of numbers, not functions. Therefore, a linear system could not produce directional selectivity.

It follows that truly directionally selective neurons differ fundamentally from cells that might be called directionally biased by the essential nonlinearity inherent in the directionally selective response mechanism. Because of this nonlinearity, the difference between the preferred versus null-direction movement responses of directionally selective cells is significantly greater than what would be predicted from linearly summing, in the appropriate temporal sequence, the responses elicited by a sequence of flashes at all the loci along the movement path. For example, elliptically shaped excitatory regions often exhibit a directional bias for trajectories along the major axis of the ellipse (in either direction) versus those perpendicular to it. The larger responses for movement along the ellipse major axis occur because a larger excitatory region is traversed for that trajectory than for orthogonal ones. This direction-

of-motion bias is really a function of the receptive field shape, however. Flash responses for elongated bars are greater for those oriented along, versus perpendicular, to the major axis of such an elliptical receptive field. The apparent selectivity for motion direction in this case is thus the result of a more basic preference for a particular orientation that is obvious from the static receptive field structure.

A somewhat more misunderstood example of a directionally biased, rather than selective receptive field organization is one in which there are adjacent pure excitatory and pure inhibitory areas, which affect cell firing linearly (above and below background firing), but with the effect of the inhibitory area delayed relative to that of the excitatory area. When both areas are traversed in excitatory then inhibitory area sequence, excitation (increased firing) is followed by delayed inhibition (decreased firing). However, in the opposite direction (inhibitory then excitatory area), the delay in the inhibitory pathway causes it to temporally overlap with, and therefore subtract from, the effect of the subsequently elicited excitation, resulting in little or no change from the background firing level. Although the peak firing achieved by the former (excitatory then inhibitory) trajectory is greater than the opposite one, the total "net" response, averaged over time, must be the same for movement in both directions if the interaction between the responses is linear, because exactly the same receptive field regions are traversed in both directions, just in a different order.

The discussion above underscores the importance of nonlinear interactions in the mediation of directional selectivity. A simple type of nonlinearity, common to many neurobiological processes, is threshold. For example, if the background firing rate in the example presented in the last paragraph were zero, then this could "hide" the synaptic inhibition below the firing threshold for the (preferred) motion direction, in which the inhibitory region is traversed after the excitatory one, so that only the excitatory component of the response above threshold is communicated to the next neuron. Motion in the opposite direction, in which delayed inhibition overlapped with, and was subtracted from the subsequently evoked excitation, would yield a lower maximal excitation, perhaps entirely below the threshold, and would thus be the null direction. (For a more extended discussion of threshold models of directional selectivity see Grzywacz and Koch, 1987.)

For the models in Fig. 2, many types of nonlinearities were considered. The first nonlinear mechanism proposed for directional selectivity was multiplication (Hassenstein and Reichardt, 1956 and see Fig. 2A). Later on, Poggio and Reichardt (1973) generalized multiplication to quadratic nonlinearities, that is, nonlinearities that involve not only instantaneous multiplications, but also multiplications of two responses occurring at different time instants. Some cortical modelers tended to use one instance of quadratic nonlinearities that involved squaring operations (Adelson and Bergen, 1985; Heeger, 1987; Grzywacz and Yuille, 1989). An alternative nonlinearity that has been extensively studied in the context of retinal directional selectivity is shunting inhibition (Thorson, 1966; Torre and Poggio, 1978; Grzywacz and Koch, 1987). This mechanism has been proposed for all the inhibition-based mechanisms in Fig. 2. This type of inhibition is a synaptic inhibition which does not involve a hyperpolarizing battery, because the synapse has its reversal potential near the cell's resting potential. This synapse causes inhibition by increasing the membrane conductance and thus by shunting out from the cell incoming excitatory currents. Shunting inhibition is nonlinear, since its effect is like Ohm's law: It tends to divide the excitatory currents by the membrane conductance. Therefore, the functional behavior of this form of inhibition tends to be division-like. Interestingly, Torre and Poggio (1978) suggested that a quadratic nonlinearity could approximate shunting inhibition if the inhibitory conductance were small. However, Grzywacz and Koch (1987) showed that this approximation would

probably not be valid under physiological conditions.

2.4. Locus of computation

An important problem that remains to be definitively resolved experimentally is where in the retina directional selectivity is computed. Early experiments with moving spots (Werblin, 1970; Marchiafava, 1979) found that cells prior to the ganglion cells in mud puppies and turtles were not directionally selective. More recent experiments with gratings (Criswell, 1987; DeVoe et al., 1989) revealed directionality in all turtle cells prior to the ganglion cells, including photoreceptors. The reported proportion of bipolar and amacrine cell directional selectivity in these experiments was very high (40%). However, these directional responses depended critically on the gratings being bounded by a very specific window size (different cells having different window sizes). Such a strict size dependence strongly suggests an accidental window-induced asymmetry due to inhomogeneities of the receptive field. This might produce directionally biased responses of the sort described in Section 2.3. In support of this notion, preliminary experiments (Borg-Graham and Grzywacz, personal communication) show the appearance and disappearance of "artifactual" directional selectivity when one changes the centering of circularly bounded gratings. Hence, bounded gratings are likely to be tapping on nonrobust directionally biased responses.

Because evidence for robust directional selectivity only existed for ganglion cells, Torre and Poggio (1978) suggested that asymmetric inhibitory processes act directly on them (see Fig. 2B). Torre and Poggio argued that if a shunting synapse mediates these inhibitory processes, then dendrites of a single directionally selective ganglion cell could implement the directionally selective subunits (Barlow and Levick, 1965). (The analysis of this argument uses the on-the-path property (Rall, 1964; Koch et al., 1982) of shunting inhibition. This property states that the best place in a dendrite for a shunting synapse to be is between the excitatory synapse and the cell's output.) Another inhibition-based ganglion-cell model was that of Grzywacz and Amthor (1988a) (see Fig. 2D).

Alternatively, directional selectivity would also be only observed in ganglion cells, if it were generated in the dendrites of an amacrine cell with a symmetric morphology and inputs. These dendrites would transmit the directionality to the ganglion cell. The preganglionic version of the Vaney and colleagues' model is one example (Vaney et al., 1989; Vaney, 1990; Fig. 2C). These investigators also proposed that the underlying amacrine cell is the cholinergic one (see Section 4.2.2). Another model based on amacrine-cell dendrites is that of Grzywacz and Borg-Graham (1991) (Borg-Graham and Grzywacz, 1991a; Fig. 2D). They performed simulations with this model and showed that the amacrine-cell soma might not show directional selectivity, while its dendrites may. In this model, the directionally selective subunits are attributable to different amacrine cells rather than different dendrites of the same cell.

3. Vertebrate directionally selective ganglion cells

3.1. Mammals

3.1.1. Monkeys and cats

Directionally selective ganglion cells have been recorded in virtually every vertebrate retina in which investigators have looked for them, but their physiological properties, anatomical characteristics and relative proportions have varied widely across species. The response properties of directionally selective ganglion cells differ both within, and between species, in sensitivity to movement of light versus dark objects, facilitation for preferred-direction motion versus inhibition for null-direction motion, preference for slow or fast speeds, and sensitivity to object shape. Morphological differences in directionally selec-

tive retinal ganglion cells exist in the pattern and ramification levels of their dendritic arborization, and in the destination of their axons in the central nervous system.

The proportion of ganglion cells that exhibit directional selectivity varies widely among vertebrate classes, even among mammals. In primates, for example, what few electrophysiological studies have routinely tested for directional selectivity have typically reported only a small percentage of directionally selective ganglion cells identified as "rarely-encountered" (Schiller and Malpeli, 1977) or "atypical" (DeMonasterio, 1978). Little is known about the mechanisms of directional selectivity in these cells.

In cats, the "classical" division of ganglion cells into X, Y, and W physiological classes (Enroth-Cugell and Robson, 1966; Stone and Hoffman, 1972; Rodieck, 1973) lumped ganglion cells that were directionally selective into the quite heterogeneous, so-called W cell group. Although the cells lumped under the W name comprise numerous, very distinct types that probably account for about half of the total ganglion cell population in cats (Cleland and Levick, 1974; Fukuda and Stone, 1974; Rowe and Stone, 1976), directionally selective ganglion cells still represent only a small fraction of this group, and estimates of their percentage of the total ganglion cell population range as low as 2% (Stone and Fabian, 1966).

3.1.2. Rabbits and squirrels

The percentage of directionally selective ganglion cells recorded in other well studied mammalian retinas is much higher, however. From 20 to 25% of the retinal ganglion cells recorded in both the rabbit (Oyster, 1968) and squirrel (Michael, 1968) have been reported to be directionally selective. In the rabbit, two distinct types of directionally selective ganglion cells have been extensively studied. The On-Off directionally selective ganglion cells (Barlow and Hill, 1963) respond to objects either brighter or darker than the background, and follow relatively rapid movement (6–10 deg/s; Oyster, 1968). The On directionally selective ganglion cells (Barlow et al., 1964) respond only to objects brighter than the background, and are sensitive to slower movement (30 "/s; Oyster, 1968). Both On-Off and On directionally selective ganglion cells respond transiently to nonmoving changes in light level within their excitatory receptive field of the same contrast polarity (On/Off or On, respectively) as the moving edge to which these cells respond.

3.2. Nonmammals

3.2.1. Amphibians, birds, and reptiles

Among nonmammals, retinal directional selectivity has been observed in amphibians, birds and reptiles. The pioneering studies of Barlow (1953) and Lettvin et al. (1959) first classified ganglion cells on the basis of "trigger features", such as directional selectivity, in the frog retina. In some avian species directionally selective ganglion cells have been reported to constitute as much as 30% of the total ganglion cell population (Maturana and Frenk, 1963; Miles, 1972). Among reptiles, directionally selective ganglion cells in the lizard (Dejours, 1965), mud puppy (Werblin, 1970) and especially the turtle (Lipetz and Hill, 1970; Marchiafava, 1979; Bowling, 1980) have been documented. Interestingly, among the major vertebrate classes, directionally selective ganglion cells have rarely been reported in fish (Rodieck, 1973).

3.2.2. Turtles

Directionally selective ganglion cells are particularly abundant in turtles, with estimates of their percentage of the total ganglion cell population ranging from 25% (Jensen and DeVoe, 1983) to 40% (Fulbrook, 1982). Turtle directionally selective ganglion cells include On-Off, On and Off types (Jensen and DeVoe, 1983; Criswell, 1987). The responses of these can be either transient or sustained, in contrast to directionally selective ganglion cells in rabbits, which all respond transiently.

3.3. Differences and similarities between species

Anatomical data are also consistent with major species differences in the proportions of retinal ganglion cells that have complex response properties such as directional selectivity. For example, the relative abundance of amacrine versus bipolar cell input to retinal ganglion cells varies markedly between vertebrate species as different as frog and primate (Dowling, 1968). Because of this, complex visual feature discriminations such as directional selectivity are thought to be based on amacrine cell functions, because there appear (anatomically and physiologically) to be only a small number of distinct types of bipolar cells, and these appear to be fairly linear in their spatiotemporal characteristics. Although the synaptic basis of directional selectivity has not been definitively established in any retina, correlation between physiology and anatomy in the squirrel (West and Dowling, 1972; West, 1976; Dowling, 1987) suggest that, at least in that species, On-Off directionally selective ganglion cells receive most, if not all of their inputs from amacrine cells.

But do such differences imply that directionally selective ganglion cells are vestigial and relatively unimportant in animals phylogenetically close to primates? This seems unlikely given the remarkably conserved vertebrate plan involving the accessory optic and pretectal nuclei (McKenna and Wallman, 1985; Fite, 1985). These nuclei, which receive heavy retinal directionally selective input (Oyster et al., 1980; Ariel, 1991), contribute the optokinetic reflex in all vertebrates studied so far (Collewijn, 1975; Gioanni et al., 1983; Rosenberg and Ariel, 1990), including monkeys (Schiff et al., 1988; Hoffmann, 1989; Schiff et al., 1990). Moreover, even smooth-pursuit related discharges have been recorded in nuclei associated with the accessory optic system in primates (Mustari and Fuchs, 1989), though the main control for smooth-pursuit is cortical (Newsome et al., 1985; Lynch, 1987; Segraves et al., 1987).

4. Mechanisms mediating retinal directional selectivity

4.1. Inhibition

Several distinct types of directionally selective ganglion cells occur in the species in which retinal directional selectivity has been most extensively studied, namely, the rabbit, among mammals, and the turtle, among nonmammalian vertebrates. Although these directionally selective ganglion cells differ in properties such as response to light or dark edges and preferred speed, almost all of them exhibit a nonlinear inhibition that reduces the responses for null-direction movements below that which would be expected from the responses to stationary flashes at the same receptive field loci.

4.1.1. Early experiments on null-direction inhibition

In their classical investigation of the On-Off directionally selective ganglion cells of the rabbit retina, Barlow and Levick (1965) showed the importance of inhibition within the excitatory receptive center for directional selectivity. In their two-slit apparent-motion experiments they demonstrated that turning on and off two spatially separated slits at some appropriate delay, in a manner similar to that which yields apparent motion illusions in humans, elicited direction-associated, asymmetric responses from the On-Off directionally selective ganglion cells. When the two-slit apparent motion corresponded to the null direction, the number of spikes elicited by the second slit was much smaller than that elicited by the second slit when it was presented alone. This reduction occurred even though the response to the first slit itself was excitatory. The inhibitory effect of the first slit on the second was not due to saturation, could be observed virtually everywhere within the excitatory receptive field center, and was effective for interslit distances that were much less than the width of the excitatory center of the receptive field. Barlow and Levick con-

cluded from these and similar data that direction-of-motion response asymmetry was computed by numerous, small "subunits", approximately 0.5 deg wide, replicated across the excitatory receptive field center. The mechanism for the motion asymmetry was postulated to be a delayed inhibitory effect propagated asymmetrically only in the null direction. This inhibitory mechanism, although arising from regions that were excitatory when stimulated in isolation, had the effect of vetoing excitatory responses subsequently elicited from adjacent regions traversed during null-direction motion.

Wyatt and Daw (1975) quantified some aspects of the apparent-motion experiments of Barlow and Levick by using very brief flashes for the two slits. Because of the almost instantaneous nature of such flashes, they could measure the impulse-response duration of inhibition, which was between 0.5 and 1 s. However, the inhibition evoked by such flashes was spatially asymmetric in its effect only for delays between flashes of the two slits of about 100 ms. For longer delays, presumably corresponding to slower motion, inhibition appeared to be propagated toward the preferred direction as well.

Wyatt and Daw also demonstrated that null-direction inhibition was evoked from a continuously moving spot. In these experiments, they made the inhibition evident by raising the activity of the neuron by continuously stimulating a small portion of the excitatory receptive field center with a moving grating, masked from the rest of the receptive field by an aperture of approximately 0.5 deg. They then moved a spot across the receptive field center in various null-direction trajectories. If the trajectory was toward the aperture, then the spot inhibited the response before reaching the aperture, but not after. For other trajectories, the dot crossed positions for which the angle between the motion's direction and the lines linking them to the aperture's center was not zero. Inhibition occurred for all angles between 0 and 180 deg. Wyatt and Daw interpreted these data as indicating that the inhibitory area affecting any locus within the excitatory receptive center had a cardioid shape. However, cardioid shaped inhibitory fields were not found in all experiments, and relating inhibitory effects to a specific position of a continuously moving spot was not without difficulties in interpretation.

Because the null-direction inhibitory effect could be evoked from stationary flashed spots as well as moving ones, and thus did not require movement per se, Wyatt and Daw hypothesized that the null-direction inhibition arose from an asymmetry in the normal inhibitory surround. In this hypothesis, the inhibitory surround for each excitatory receptive field locus was missing on the preferred-direction side in the region outside the cardioid.

Although the directionally selective mechanism has been more extensively investigated in rabbits than perhaps any other retina, experiments in other animals have also demonstrated the role of null-direction inhibition in retinal directional selectivity. In squirrels, apparent motions revealed null-direction inhibition extending for about 15' (Michael, 1968). Null-direction inhibition in directionally selective ganglion cells was also found in pigeon retinas (Maturana and Frenk, 1963). In turtles, Smith et al., (1991, and manuscript submitted) demonstrated null-direction inhibition with an apparent-motion protocol.

4.1.2. The inhibitory neurotransmitter: GABA

Daw and co-workers also conducted pharmacological studies on rabbit retinas (Caldwell et al. 1978; Ariel and Daw, 1982) that indicated that the inhibitory neurotransmitter GABA (via $GABA_A$ receptors) mediates null-direction inhibition in rabbit directionally selective ganglion cells. In the presence of picrotoxin, a GABA antagonist, the null-direction responses of the directionally selective ganglion cells increased to levels similar to the levels elicited by preferred-direction motion. Similar experiments using antagonists to glycine such as strychnine showed that glycine had little specific effect on directional selectivity in either

the On-Off or On directionally selective ganglion cells of the rabbit retina.

GABAergic, but not glycinergic, inhibition was also demonstrated to have a crucial role in turtle retinal directional selectivity (Ariel and Adolph, 1985). As in rabbits, picrotoxin reduced directional selectivity. This inhibitory effect appeared to be at least partly due to $GABA_A$ receptors on the directionally selective ganglion cells themselves, since GABA suppressed firing elicited by exogenous application of excitatory transmitters when ganglion cells were isolated from their presynaptic inputs by perfusion with a low Ca^{2+} perfusate. Because GABA has a direct effect on the directionally selective ganglion cell, Ariel and Adolph hypothesized that the GABAergic mediation of directional selectivity might occur in the dendrites of the ganglion cell itself.

More recently, Smith et al. (1991, and manuscript submitted) extended the analysis of the effect of picrotoxin on turtle retinal directional selectivity. They studied this effect (and of bicuculline) as a function of contrast and speed of a continuously moving slit, and for apparent motions. Their data showed that picrotoxin and bicuculline do not eliminate directional selectivity in every single cell. In 28% of the directionally selective ganglion cells, the preferred and null directions were actually reversed under picrotoxin. In 28% of the cells, directional selectivity was maintained despite saturating concentrations of picrotoxin (or bicuculline). From these results, Smith et al. suggested that GABA does not mediate directional selectivity by being at the output of a synapse whose receptive field is asymmetric (as the Barlow and Levick model would suggest). Otherwise, GABA antagonists should eliminate directional selectivity and most certainly, should not reverse it. Rather, Smith et al. suggested that GABA acts on a spatially asymmetric process, whose output is quite possibly excitatory. They proposed that elimination of GABAergic effects by picrotoxin or bicuculline leaves the output of the asymmetric process at the mercy of other mechanisms like saturation. These mechanisms might cause reversal and maintenance of directional selectivity. Grzywacz and Borg-Graham (1991) and Borg-Graham and Grzywacz (1991a) performed computer simulations to show reversal and maintenance in a model based on Smith et al.'s hypothesis. (See Section 2 for a description of the Grzywacz and Borg-Graham model.)

4.1.3. Recent quantitative experiments on rabbit's null-direction inhibition

Quantitative aspects of the mechanisms mediating inhibition in On-Off directionally selective rabbit retinal ganglion cells were investigated by Amthor and Grzywacz to test several biophysical models formulated to be consistent with, and/or depend on, recent anatomical findings and known retinal circuitry. (See Section 2 for a list of these models.) Four types of data were required to test these models: 1) the rise and fall time courses of inhibition, and its delay, if any, relative to excitation; 2) the spatial extent of inhibition, including its strength and time course as a function of distance; 3) the nature of the interaction between inhibition and excitation (linear or, if not, type of nonlinearity), and 4) the relationship between null-direction inhibition and the normal ganglion cell inhibitory surround mechanism.

An issue left unresolved by Wyatt and Daw's two-spot flash experiments was whether the inhibitory process is transient. Because their stimulus was a brief flash, the inhibition was bound to decline after a while. To determine whether inhibition is transient, Amthor and Grzywacz (1988, and manuscript submitted) recorded the extracellular responses of On-Off directionally selective rabbit retinal ganglion cells to two-slit apparent motions using steps, rather than flashes of light. These sequential intensity step changes in the two slits correspond to a "real" stimulus in which the passage of a moving light or dark edge across the receptive field is screened except through apertures corresponding to the two slits. The apparent motion elicited by this stimulus within the cells' excitatory receptive field center produced null-direction inhibition, as with the

flash experiments. The strength of the inhibitory effect was found to require about 150 ms to rise to a maximum, for either a light or dark edge. From this maximum, the inhibitory effect was found to decay very slowly, never returning to base-line before 2 s for short interslit distances. Some experiments showed null-direction inhibition lasting as long as 4 s, in marked contrast to the time course of inhibition elicited by short light flashes, which rose somewhat more quickly, but decayed in 500 to 1000 ms. Therefore, null-direction inhibition is sustained with light stimulus.

Amthor and Grzywacz (1988, and manuscript submitted) also re-examined the speed sensitivity of the directionally selective mechanism in light of the long lasting inhibition observed for steps of light. By measuring the ratio between the preferred and null direction responses, they discovered that, although there is a speed optimum in the preferred direction (Oyster, 1968; Wyatt and Daw, 1975), On-Off directionally selective rabbit retinal ganglion cells were directionally selective to essentially all speeds to which they responded, covering almost three orders of magnitude of stimulus speed. A possible explanation for this relative speed independence of directional selectivity comes from the sustained null-direction inhibition. Because of it, inhibition remains around if the stimulus persists or moves slowly. Thus, for sufficiently low speeds, the response would be suppressed for null-, but not preferred-direction motion regardless of the speed.

In investigations of the spatial extent of inhibition, Grzywacz and Amthor (1988b) found that, although the null-direction inhibition was strongest for short interslit distances on the order of those postulated for Barlow and Levick's subunits, it was still quite effective for interslit distances larger than half the size of the excitatory receptive field center. (These distances can be larger than 450 μm, that is, larger than 3 deg.) This large effective distance for the null-direction inhibition is at variance with the hypothesis that the directionally selective mechanism is composed of small, discrete inhibitory subunits.

In similar apparent-motion experiments, the shape of the region inhibiting a given locus within the excitatory receptive field center was found to be ovoid (as opposed to Wyatt and Daw's cardioid) with the inhibitory strength falling off gradually with distance both along and perpendicular to the preferred-null axis. Preferred-direction inhibition was never found when step changes of light intensity were used (corresponding to moving edges), but preferred-direction inhibition was observed for flashes, a result similar to that of Wyatt and Daw (1975).

There was no striking functional relationship between the time course of inhibition and distance from the inhibited locus. There did not, for example, appear to be a trade-off between inhibitory rise time and distance such that the absolute delay was constant. This is contrary to models hypothesized for some cortical directionally selective cells (see Section 2.1). There was a tendency in On-Off directionally selective ganglion cells for both the rise and fall times of the null-direction inhibition elicited by apparent motion to be somewhat shorter at the largest interslit distances that yielded effective inhibition, than at smaller distances.

The temporal separation of the On and Off stimulus edges in the two-slit step intensity-change experiments also allowed the investigation of the interaction between On and Off excitation and On and Off null-direction inhibition. Determination of this relationship is essential for understanding the directionally selective mechanism, because some directionally selective models, such as hypothesized for cells in the visual cortex, postulate a specific interaction between On and Off regions for direction-of-motion discrimination. Amthor and Grzywacz (1988, and manuscript submitted) found that inhibitory interactions with excitation are largely segregated between the On and the Off pathways. Thus, in null-direction apparent motions, light onset of the first slit always strongly inhibits excitatory responses to light onset, but not the offset, of the second slit, even for the same absolute time delay.

Light offset of the first slit similarly always inhibits responses to light offset, but not onset, of the second slit. Occasional interactions between On and Off transitions were inconsistent, weak, and not systematically related to the cell's normal preferred direction. Thus, in On-Off directionally selective ganglion cells of the rabbit retina, directional selectivity appears to be computed independently for light and dark regions of moving objects or textures.

Amthor and Grzywacz (1991) also investigated whether the inhibitory interaction with excitation was linear by determining the contrast dependency of the interaction. If the interaction between null-direction inhibition and excitation were linear, such as a subtraction (which would have to be followed later by some nonlinearity essential for the directional selectivity), increasing the contrast of the first (inhibiting) slit in a two-slit experiment should cause a downward shift (subtraction) in the response versus contrast function of the second slit. On the other hand, nonlinear interactions could cause changes in the shape of the response versus contrast function. For example, Torre and Poggio (1978) postulated a shunting inhibition mechanism, which as explained in Section 2.3, tends to be division-like. Hence, this inhibition would tend to divide the response versus contrast function by a constant factor. The data showed that the contrast dependency of the null-direction inhibition is division-like, rather than subtraction-like. This behavior is consistent with inhibitory synapses whose main effect is shunting, rather than hyperpolarizing.

Furthermore, Grzywacz et al. (1990) investigated whether a quadratic nonlinearity, which is essential for correlation models, could approximate shunting inhibition. Torre and Poggio suggested such an approximation (1978, and see Section 2.3). To test this approximation, Grzywacz and Amthor used previously developed Fourier-analysis techniques (Grzywacz and Koch, 1987). The results showed that the nonlinearity underlying directional selectivity in rabbit retinal ganglion cells could not be approximated by a quadratic nonlinearity. The results further showed that half-wave rectifications (another nonlinearity) also contribute to the responses, possibly by segregating the On and Off pathways. (This rectification passes one polarity, say positive, of the input and prevents the passage of the other polarity.)

Amthor and Grzywacz (1990) and Merwine et al. (1990) conducted experiments to determine whether the null-direction inhibition was distinct from the normal ganglion cell surround inhibition. The first experimental paradigm used was based on the finding that the null-direction inhibition was division-like, whereas surround inhibition in retinal ganglion cells was believed to be subtraction-like. However, experiments showed that the surround inhibition of directionally selective, and virtually all other ganglion cell types in rabbit retinas, was actually division-like as well, rather than subtraction-like (Merwine et al., 1990).

These experiments revealed, however, that the sustained time course of the null-direction inhibition distinguished it as a distinct mechanism from that of the surround inhibition, which has a much faster rise time and more transient time course. The sustained null-direction inhibitory mechanism is effective throughout the excitatory receptive field center, and extends into the normal inhibitory surround on the side of the receptive field center first traversed during null-direction motion. This area of sustained null-direction inhibition lying within the classical inhibitory surround was found to be effective for inhibiting points approximately to the middle of the excitatory receptive field center.

4.1.4. Intracellular studies

An important question about the mechanism of null-direction inhibition is its site of action: Does the null-direction inhibition act on the ganglion cell itself or at some presynaptic site? A ganglion-cell mechanism might be evidenced by inhibitory conductances and perhaps hyperpolarizations during null-direction motions in intracellular recordings. Miller (1979) and Werblin (1970) reported

such hyperpolarizations in On-Off directionally selective ganglion cells of rabbits and mud puppies, respectively. However, other recordings in these and other species have not exhibited such hyperpolarizations. Amthor et al. (1989a) observed small depolarizations during null-direction motion in On-Off directionally selective ganglion cells of the rabbit. Figure 4 shows one example of such a recording of the intracellularly recorded responses to three consecutive preferred then null sweeps of a small light spot through the receptive field center. During the first half of each of the three traces, motion in the preferred direction produces an EPSP with spikes, followed by an after repolarization. In the last half of each of the three traces, a similar EPSP is also observed, but without the spikes. Similar depolarizations for null-direction motion have been observed in experiments with turtles (Marchiafava, 1979) and frogs (Watanabe and Murakami, 1984). These experiments also suggested a possible explanation for the different results for null-direction motion. They found that if a small depolarizing current is injected during the null-direction motion, then a negative voltage swing appears. This indicates that the inhibitory synapses have their reversal potential close to the cell's resting potential, and may exert their primary effect by shunting inhibition, rather than hyperpolarization. Because the reversal potential of this inhibitory synapse is close to the normal resting potential, null-direction hyperpolarizations observed in some recordings (Miller, 1979; Werblin, 1970) could easily have been caused by a slight elevation of the resting potential due to cell injury associated with electrode impalement.

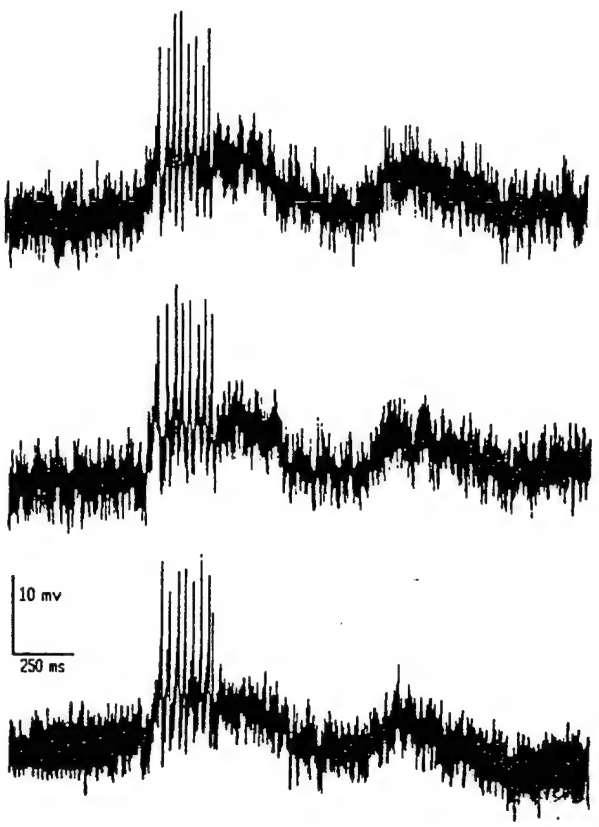

Fig. 4. An intracellular recording of three consecutive preferred then null sweeps of a small light spot through the receptive field center of an On-Off directionally selective ganglion cell of the rabbit retina. During the first half of each of the three traces, motion in the preferred direction produces an EPSP with spikes, followed by an after repolarization. In the last half of each of the three traces, movement in the null direction across the same receptive field region produces an EPSP, but without the spikes elicited in the preferred direction. (Figure adapted from Amthor et al., 1989a, with permission from Wiley Press. Original photograph was digitally scanned and processed to enhance contrast.)

Despite the evidence for inhibitory action directly onto directionally selective ganglion cells, there is data from turtles that indicate that this inhibition is irrelevant for directional selectivity. In whole-cell patch-clamp recordings from these cells with no ATP or Mg^{2+} in the electrode, direct inhibition of the ganglion cell is blocked. (An explanation for the elimination of inhibition comes from experiments – Stelzer et al., 1988; Chen et al., 1990 – in the hippocampus. According to these experiments, the coupling between $GABA_A$ receptors and their chloride channels requires ATP and Mg^{2+}. The large contact surface between the patch electrode and the cell's membrane would allow for diffusional exchange between the electrode's solution and the cytosol.) Under these conditions, ganglion cells maintain

directionality despite lack of inhibition (Borg-Graham and Grzywacz, 1991b). Therefore, directionally selectivity is probably computed in a preganglionic cell in turtles. Because somatic recordings from turtle preganglionic cells did not reveal directional selectivity (Marchiafava, 1979), Grzywacz and Borg-Graham (1991; Borg-Graham and Grzywacz, 1991a) suggested that this computation is performed in amacrine-cell dendrites. This computation would not express itself in amacrine somatic recordings (see Section 2.4). The role of the direct inhibition onto the directionally selective ganglion cells in turtles probably mediates other functions than directional selectivity, such as gain control.

4.2. Facilitation

4.2.1. Early experiments on preferred-direction facilitation

The responses of directionally selective ganglion cells not only exhibit null-direction inhibition, but also, preferred-direction facilitation. In two-spot apparent motions in the preferred direction, more excitation is elicited from the second slit than when it is presented alone (Barlow and Levick, 1965). Preferred-direction facilitation has also been noted in other species, such as the squirrel (Michael, 1968) and the turtle (Smith et al., manuscript submitted).

4.2.2. Does acetylcholine partly mediate preferred-direction facilitation?

Experiments by Daw and co-workers have also shown that directionally selective ganglion cells of the rabbit retina receive cholinergic input, and that pharmacological manipulations of this input affect directional selectivity (Ariel and Daw, 1982). Acetylcholine has been localized in a number of retinas to a particular amacrine cell type having an identifiable morphology called "coronate" (Vaney, 1984), or more commonly, "starburst" (Famiglietti, 1983a,b). By using autoradiographic methods, Masland and co-workers showed that only a small set of amacrine cells in rabbits take up radioactive choline (Masland and Mills, 1979; Hayden et al., 1980). These cells converted choline into ACh (Hayden et al., 1980; Masland et al., 1984a) and released it in response to light (Masland and Livingstone, 1976; Massey and Neal, 1979; Massey and Redburn, 1982). This cholinergic amacrine cell has thus been strongly implicated by a number of workers in the computation of directional selectivity in rabbits (Masland et al., 1984b; Vaney et al., 1989; Vaney, 1990).

A number of similarities have been noted between the dendritic morphologies and dendritic locations within the inner plexiform layer of the cholinergic amacrine cells and the On-Off directionally selective ganglion cells (Vaney, 1984; Tauchi and Masland, 1984). Distal portions of the dendrites of the cholinergic amacrine cell dendrites were found to co-stratify and make direct contact with dendrites of ganglion cells (Famiglietti, 1983a,b; Brandon, 1987) having the morphology of On-Off directionally selective ganglion cells (Amthor et al., 1984, 1989a). Unfortunately, electron microscopic investigations have revealed little about the synaptic organization of the directionally selective mechanism because the general distribution of synaptic inputs along the dendrites of the putative On-Off directionally selective ganglion cells has been reported to be roughly uniform (Famiglietti, 1983a,b).

Pharmacological experiments on rabbits (Ariel and Daw, 1982) and turtles (Ariel and Adolph, 1985) have shown that cholinergic (nicotinic) antagonists reduce directional selectivity. From these experiments, it was hypothesized that directional selectivity arises from a GABAergic inhibitory process inhibiting the release of Ach from a cholinergic amacrine cell during null-direction movement (Ariel and Daw, 1982). However, two pieces of data cast doubt on this interpretation: First, nicotinic antagonists could not completely eliminate directional selectivity (Ariel and Daw, 1982). Second, recent data by Linn and Massey (1990) show that the GABAergic null-direction inhibition does not appear to act directly on the

cholinergic amacrine cells in the rabbit retina. They showed that muscimol, a potent GABA agonist, blocks light evoked release of Ach, but does not block release produced by nonsaturating doses of kainate, a glutamate agonist. This suggests that the GABA receptors are not on the cholinergic amacrine cells, but perhaps on bipolar cell terminals that synapse on cholinergic amacrine cells. Moreover, this indicates that the GABA found in cholinergic amacrine cells (Vaney and Young, 1988; Kosaka et al., 1988; Brecha et al., 1988) is not used for autoinhibition or for inhibiting other cholinergic amacrine cells (Vaney et al., 1989; Vaney, 1990).

Because these data suggest that directional selectivity is not directly mediated by acetylcholine, one wonders whether it might mediate functions that are accessory to directional selectivity, such as for example, general motion facilitation. Results in cats (Schmidt et al., 1987) suggest that the function of cholinergic amacrine cells is to generate motion facilitation regardless of motion direction. The notion above also receives support from rabbit data. For it, cholinergic cells not only contact directionally selective cells, but also other cells that are motion sensitive (Masland et al., 1984b). Furthermore, in turtles, facilitation by itself is not consistently directionally asymmetric (see Section 4.2.4 and Smith et al., manuscript submitted).

4.2.3. Recent quantitative experiments on rabbit's preferred-direction facilitation

Grzywacz and Amthor recently investigated the role of facilitation in On-Off directionally selective ganglion cells of the rabbit retina (Grzywacz and Amthor, 1989; and manuscript submitted). Although facilitation was noted in the early investigations of Barlow and Levick (1965) its role in directional selectivity has remained unclear. The observed facilitation could conceivably be based on at least three distinct mechanisms: 1) a general, nonspecific enhancement of the response to a second spot resulting from a lingering, subthreshold excitatory effect from the first spot; 2) a true enhancement for motion that is, however, not directionally selective; and 3) a directionally selective motion enhancement effect.

Grzywacz and Amthor found that when two-slit apparent motions were presented in a manner similar to that used to study null-direction inhibition, a preferred-direction facilitation was always elicited. They also obtained three pieces of evidence (based on apparent-motion protocols) that the facilitatory effect is not entirely due to nonspecific mechanisms such as ganglion-cell spiking threshold. First, facilitation was largely segregated between the On and Off pathways. Second, the strongest facilitation was not always elicited by positions of the receptive field eliciting the strongest responses. Third, a nonzero interslit delay was necessary to elicit the maximal facilitation. A general mechanism of enhancement would predict that the maximal facilitation should occur with zero interslit delay, because this delay leads to the maximal overlap of excitatory postsynaptic potentials in the ganglion cell.

Grzywacz and Amthor found that the facilitatory strength rises to 90% of its maximum when the interslit delay is about 100 ms. The duration of facilitation during a step increase or decrease in intensity of the first slit is more sustained than the ganglion cell response elicited by the first slit, but less sustained than the inhibition elicited by a similar apparent motion in the null direction. The facilitatory effect decays slowly after reaching its maximum, eventually turning into inhibition when the interslit delay reaches about 700 ms. That the duration of the facilitation due to the first slit is larger than the ganglion cell response due to it also suggests that the facilitation is not merely a consequence of general excitation produced by the first slit.

When facilitatory and inhibitory effects were disentangled with appropriate control of stimulus parameters such as the use of steps, rather than flashes of light, Grzywacz and Amthor showed that the maximal strength of inhibition was only slightly larger (by a factor of about 1.30) than the maximal strength of facilitation across a large

range of contrasts (10% to 70%). Since facilitation and inhibition have comparable maxima under some conditions, one cannot neglect the contributions of facilitation to the properties of retinal directional selectivity. Grzywacz and Amthor also showed that facilitation was effective for interslit distances approximately half the receptive field center apart in the preferred direction. Its spread perpendicular to the preferred-null axis appeared to be somewhat less than that of inhibition, however.

4.2.4. Facilitation in the absence of inhibition

To disentangle the facilitatory and inhibitory effects further, Smith et al. (manuscript submitted) studied facilitation in the presence of picrotoxin or bicuculline (GABAergic antagonists) in turtles. For this purpose, they used an apparent-motion protocol. They found that although there is no null-direction facilitation under physiological conditions, this motion elicits strong facilitation when GABAergic effects are eliminated. The strength of this null-direction facilitation was similar to the preferred-direction strength, sometimes being slightly stronger and sometimes being slightly weaker. Hence, Smith et al. concluded that the facilitation mechanism does not have an asymmetry allowing it to contribute to directional selectivity by itself. However, facilitation might strengthen directional selectivity in the presence of inhibition.

4.3. Morphology of directionally selective ganglion cells

The morphologies of directionally selective ganglion cells are best known in rabbit (Amthor et al., 1984, 1989b) and turtle retinas (Jensen and DeVoe, 1983). In both species distinct physiological types of directionally selective ganglion cells have been shown, by intracellular recording and staining, to be associated with specific dendritic morphologies. In rabbit retina, there are On-Off and On directionally selective ganglion cells. The dendritic morphologies of both types of directionally selective ganglion cell have been shown to be distinguishable from each other as well as from those of other ganglion cell types (Amthor et al., 1984, 1989a,b).

The dendritic arborization of On-Off directionally selective ganglion cells are bistratified. Figure 5 shows a three dimensional reconstruction of an On-Off directionally selective ganglion cell from the rabbit retina. The separate dendritic ramifications in both outer and inner sublamina of the inner plexiform layer are consistent with the cells receiving direct excitatory input at both On and Off stimulus phases, based on the hypothesized major functional division of the inner plexiform layer into On-excitatory (inner) and Off-excitatory (outer) sublamina. Indeed, slight differences in the spatial extent of the On and Off regions commonly observed in static receptive field maps of these cells appear to be reflected in details of the extent of dendritic coverage in the two inner plexiform layer sublamina (Amthor et al., 1989a).

The dendritic ramifications in each inner plexiform layer sublaminar region of the On-Off directionally selective ganglion cells are similarly dense and complex, with many small, high order dendrites. The large number of dendrites at comparatively large electrotonic distances from the soma appear to be consistent with some theoretical models for directional selectivity requiring local, nonlinear interactions between excitation and inhibition within the dendritic tree of the directionally selective ganglion cell (Koch et al., 1982). The similarity and extent of the dendritic arborization in both inner plexiform layer sublamina also are at least consistent with the hypothesis that directional selectivity for light and dark edges are computed separately, and merely share the same soma for output, rather than the directionally selective mechanism being based on some interaction between On and Off pathways. Although On-Off directionally selective ganglion cells are identifiable on the basis of their dendritic morphologies as that ganglion cell type, no obvious global dendritic asymmetry or other mor-

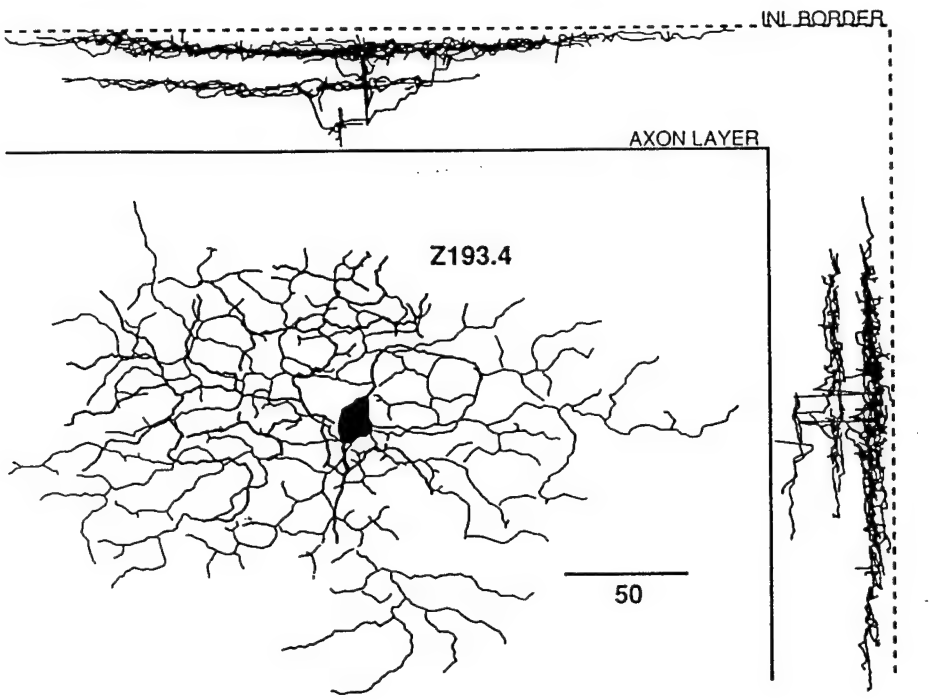

Fig. 5. Three dimensional reconstruction of an On-Off directionally selective ganglion cell of the rabbit retina. Lower center view is a tangential (*X-Y*) plane reconstruction, with dendrites in the inner part of the inner plexiform layer shown thicker to distinguish them from those in the outer portion of the inner plexiform layer. The 50 µm scale bar at the lower right corresponds only to the *X* and *Y* dimensions, the Z dimension is stretched relative to the *X-Y* dimensions to show details in the "section" views. An approximate scale can be derived from the solid and dotted lines, which correspond to the axon layer and the inner plexiform layer/inner nuclear layer border, respectively. At top center is a reconstructed vertical section corresponding to an *X-Z* view; at the right a reconstructed vertical section corresponding to a *Y-Z* view. In these sections, it is apparent that the dendritic arborizations are in two quite separate substrata of the inner plexiform layer. The actual stratifications are much narrower than they appear here because distortion in the tissue mounting and in the reconstruction appear as artifactual dispersion of the dendrites from the extremely narrow sublamina they actually occupy.

phological feature appears to be related to the preferred direction (Amthor et al., 1989a).

The dendritic arborization of the On directionally selective ganglion cell in the rabbit retina is unistratified in the proximal inner plexiform layer, consistent with the On sign of its response to stationary flashes. The dendritic arborization of this cell lacks the stereotyped "loop-like" structures seen in the On-Off directionally selective ganglion cells (Amthor et al., 1984), but there are still many small caliber dendrites and spine-like processes. Whether the complex and distinct morphologies of the directionally selective ganglion cells reflect an underlying significant dendritic computation important for their behavior, or merely reflect their connectivity and sampling of inputs from the inner plexiform layer, remains unresolved at present.

Acknowledgements

F.R.A. wishes to thank Elizabeth McCormick for technical assistance in data gathering and analysis. N.M.G. thanks Lyle Borg-Graham and Randy Smith for their extensive work and discussions on turtle retinal directional selectivity. This research was supported by a grant from the Office of Naval Research (N00014-91-J-1280), by grants to F.R.A. from the National Eye Institute (EY05070) and from the Sloan Foundation, by grants to N.M.G. from the National Eye Institute (EY08921-01A1), from the National Science

Foundation (BNS-8809528) and from the Sloan Foundation, by a grant to Tomaso Poggio, Ellen Hildreth, and Peter Schiller from the Office of Naval Research, Cognitive and Neural Systems Division, and by a grant to Tomaso Poggio, Ellen Hildreth, and Edward Adelson from the National Science Foundation (IRI-8719394).

References

Adelson, E.H. and Bergen, J.R. (1985) Spatiotemporal energy models for the perception of motion. J. Opt. Soc. Am. A. 2, 284–299.

Amthor, F.R. and Grzywacz, N.M. (1988) The time course of inhibition and the velocity independence of direction selectivity in the rabbit retina. Invest. Ophthalmol. Visual Sci. Suppl. 29, 225.

Amthor, F.R. and Grzywacz, N.M. (1990) On-Off directionally selective ganglion cells are inhibited by two distinct mechanisms in the rabbit retina. Invest. Ophthalmol. Visual Sci. 31 (5), 115.

Amthor, F.R. and Grzywacz, N.M. (1991) The nonlinearity of the inhibition underlying retinal directional selectivity. Vis. Neurosci. 6, 197–206.

Amthor, F.R. and Grzywacz, N.M. Inhibition in On-Off directionally selective ganglion cells in the rabbit retina. Manuscript submitted.

Amthor, F.R., Oyster, C.W. and Takahashi, E.S. (1984) Morphology of On-Off direction selective ganglion cells in the rabbit retina. Brain Res. 298, 187–190.

Amthor, F.R., Takahashi, E.S. and Oyster, C.W. (1989a) Morphologies of rabbit retinal ganglion cells with complex receptive fields. J. Comp. Neurol. 280 (1), 97–121.

Amthor, F.R., Takahashi, E.S. and Oyster, C.W. (1989b) Morphologies of rabbit retinal ganglion cells with concentric receptive fields. J. Comp. Neurol. 280 (1), 72–96.

Ariel, M. (1991) Analysis of vertebrate eye movements following intravitreal drug injections. 4. Drug-Induced eye movements are unyoked in the turtle. J. Neurophysiol. 65 (4), 1003–1009.

Ariel, M. and Adolph, A.R. (1985) Neurotransmitter inputs to directionally sensitive turtle retinal ganglion cells. J. Neurophysiol. 54 (5), 1123–1143.

Ariel, M. and Daw, N.W. (1982) Pharmacological analysis of directionally sensitive rabbit retinal ganglion cells. J. Physiol. 324, 161–185.

Barlow, H.B. (1953) Summation and inhibition in the frog's retina. J. Physiol. 119, 69–88.

Barlow, H.B. and Hill, R.M. (1963) Selective sensitivity to direction of movement in ganglion cells of the rabbit retina. Science 139, 412–414.

Barlow, H.B., Hill, R.M. and Levick, W.R. (1964) Retinal ganglion cells responding selectively to direction and speed of image motion in the rabbit. J. Physiol. (Lond) 173, 377–407.

Barlow, H.B. and Levick, W.R. (1965) The mechanism of directionally selective units in the rabbit's retina. J. Physiol. 178, 477–504.

Borg-Graham, L.J. and Grzywacz, N.M. (1991a) A model of the direction selectivity circuit in retina: Transformations by neurons singly and in concert. In: T. McKenna, J. Davis and S.F. Zornetzer (Eds.), Single Neuron Computation, Academic Press, Orlando, Florida, USA. In Press.

Borg-Graham, L.J. and Grzywacz, N.M. (1991b) Whole cell patch recordings and analysis of the input onto turtle directionally selective (DS) ganglion cells. Invest. Ophthalmol. Visual Sci. Suppl. 32, 1090.

Bowling, D.B. (1980) Light responses of ganglion cells in the retina of the turtle. J. Physiol. Lond. 229, 173–196.

Brandon, C. (1987) Cholinergic neurons in the rabbit retina: dendritic branching and ultrastructural connectivity. Brain Res. 426, 119–130.

Brecha, N., Johnson, D., Peichl, L., Wassle, H. (1988) Cholinergic amacrine cells of the rabbit retina contain glutamate decarboxylase and gamma-aminobutyrate immunoreactivity. Proc. Natl. Acad. Sci. USA 85, 6187–6191.

Caldwell, J.H., Daw, N.W. and Wyatt, H.J. (1978) Effects of picrotoxin and strychnine on rabbit retinal ganglion cells: lateral interactions for cells with more complex receptive fields. J. Physiol. 276, 277–298.

Chen, Q.X., Stelzer, A., Kay, A.R. and Wong, R.K. (1990) $GABA_A$ receptor function is regulated by phosphorylation in acutely dissociated guinea-pig hippocampal neurones. J. Physiol. 420, 207–221.

Cleland, B.G. and Levick, W.R. (1974) Properties of rarely encountered types of ganglion cells in the cat's retina and an overall classification. J. Physiol. 240, 457–492.

Collewijn, H. (1975) Direction-selective units in the rabbit's nucleus of the optic tract. Brain Res. 100 (3), 489–508.

Criswell, M.H. (1987) Cellular mechanisms of movement detection and directionality in the turtle retina. Ph.D. dissertation, Indiana University, program in Physiological Optics.

Dejours, S.F. (1965) Receptive fields of optic tract fibers in lizards *Sceloporus* ssp. Doctoral dissertation. Harvard Univ. Press, Cambridge, Mass (Cited by Michael, C.R.; 1968).

DeMonasterio, F.M. (1978) Properties of ganglion cells with atypical receptive-field organization in retina of macaques. J. Neurophysiol. 41 (6), 1435–1449.

DeVoe, R.D., Carras, P.L., Criswell, M.H. and Guy, R.B. (1989) Not by ganglion cells alone: directional selectivity is widespread in identified cells of the turtle retina. In: R. Weiler and N.N. Osborne (Eds.), Neurobiology of the Inner Retina, NATO ASI Series, Vol. H31, Springer Verlag, Berlin, pp. 235–246.

Dowling, J.E. (1968) Synaptic organization of the frog retina: an electron microscopic analysis comparing the retinas of frogs and primates. Proc. R. Soc. B. 170, 205–228.

Dowling, J.E. (1987) The Retina: An Approachable Part of the Brain. Harvard University Press, Cambridge, Mass.

Emerson, R.C. and Citron, M.C. (1988) How linear and non-linear mechanisms contribute to directional selectivity in simple cells of cat striate cortex. Invest. Ophthalmol. Visual Sci. 29, 23.

Enroth-Cugell, C. and Robson, J.G. (1966) The contrast sensitivity of retinal ganglion cells of the cat. J. Physiol. (Lond.) 187, 517–552.

Famiglietti, E.V. Jr. (1983a) "Starburst" amacrine cells and cholinergic neurons: mirror-symmetric On and Off amacrine cells of the rabbit retina. Brain Res. 261, 138–144.

Famiglietti, E.V. (1983b) On and Off pathways through amacrine cells in mammalian retina: the synaptic connections of "starburst" amacrine cells. Vision Res. 23 (11), 1265–1279.

Fite, K.V. (1985) Pretectal and accessory-optic visual nuclei of fish, amphibia and reptiles: theme and variations. Brain Behav. Evol. 26 (2), 71–90.

Fukuda Y. and Stone J. (1974) Retinal distribution and central projections of Y-, X- and W-cells in the cat's retina. J. Neurophysiol. 37, 749–772.

Fullbrook, J.E. (1982) Motion sensitivity of optic nerve axons in turtle Pseudemys scripta elegans (Ph.D. thesis). Univ. of Delaware, Newark, DE.

Gioanni, H., Rey, J., Villalobos, J., Richard, D. and Dalbera A. (1983) Optokinetic nystagmus in the pigeon (*Columba livia*) II. Role of the pretectal nucleus of the accessory optic system (AOS). Exp. Brain. Res. 50, 37–47.

Grzywacz, N.M. and Amthor, F.R. (1988a) A model for neural directional selectivity that exhibits robust direction of motion computation. In: D.S. Touretzky (Ed.), IEEE Conference on Neural Information Processing Systems – Natural and Synthetic. Proceedings published as Advances in Neural Information. I. Processing Systems I. Morgan Kaufman, San Mateo, CA, pp. 477–484.

Grzywacz, N.M. and Amthor, F.R. (1988b) What are the directionally selective subunits of rabbit retinal ganglion cells? Neurosci. Abst. 14 (1), 603.

Grzywacz, N.M. and Amthor, F.R. (1989) Facilitation in On-Off directionally selective ganglion cells of the rabbit retina. Neurosci. Abst. 15 (1), 969.

Grzywacz, N.M. and Amthor, F.R. Excitation, facilitation and motion enhancement in On-Off directionally selective ganglion cells in the rabbit retina. Manuscript submitted.

Grzywacz, N.M., Amthor, F.R. and Mistler, L.A. (1990) Applicability of quadratic and threshold models to motion discrimination in the rabbit retina. Biol. Cybern. 64, 41–49.

Grzywacz, N.M. and Borg-Graham, L. (1991) Model of retinal directional selectivity based on amacrine input/output asymmetry. Invest. Ophthalmol. Visual Sci. Suppl. 32, 1131.

Grzywacz, N.M. and Koch, C. (1987) Functional properties of models for direction selectivity in the retina. Synapse, 1, 417–434.

Grzywacz, N.M. and Yuille, A.L. (1990) A model for the estimate of local image velocity by cells in the visual cortex. Proc. R. Soc. Lond. B. 239, 129–161.

Hassenstein, B. and Reichardt, W.E. (1956) Systemtheoretische analyse der zeit-, reihenfolgen- und vorzeichenauswertung bei der bewegungsperzeption des russelkäfers *Chlorophanus*. Z. Naturforsch. 11b, 513–524.

Hayden, S.A., Mills, J.W. and Masland, R.H. (1980) Acetylcholine synthesis by displaced amacrine cells. Science 210, 435–437.

Heeger, D. (1987) A model for the extraction of image flow. J. Opt. Soc. Am. A. 4, 1455–1471.

Hoffmann, K.P. (1989) Control of the optokinetic reflex by the nucleus of the optic tract in primates. Prog. Brain Res. 80, 173–182.

Jensen, R.J. and DeVoe, R.D. (1983) Comparisons of directionally selective with other ganglion cells of the turtle retina: intracellular recording and staining. J. Comp. Neurol. 217, 271–287.

Koch, C., Poggio, T. and Torre, V. (1982) Retinal ganglion cells: a functional interpretation of dendritic morphology. Phil. Trans. R. Soc. Lond. B 298, 227–264.

Kosaka, T., Tauchi, M. and Dahl, J.L. (1988) Cholinergic neurons containing GABA-like and/or glutamic acid decarboxylase-like immunoreactivities in various brain regions of the rat. Exp. Brain Res. 70, 605–617.

Lettvin, J.Y., Maturana, H.R., McCulloch, W.S. and Pitts, W.H. (1959) What the frog's eye tells the frog's brain. Proc. I.R.E. 47, 1940–1951.

Linn, D.M. and Massey, S.C. (1990) GABA inhibits Ach release from the rabbit retina: a direct effect or bipolar cell feedback? Neurosci. Abst. 16, 713.

Lipetz, L.E. and Hill, R.M. (1970) Discrimination characteristics of the turtle's retinal ganglion cells. Experimentia 26, 373–374.

Lynch, J.C. (1987) Frontal eye field lesions in monkeys disrupt visual pursuit. Exp. Brain Res. 68, 437–441.

Marchiafava, P.L. (1979) The responses of retinal ganglion cells to stationary and moving visual stimuli. Vision Res. 19, 1203–1211.

Masland, R.H. and Livingstone C.J. (1976) Effect of stimulation with light on synthesis and release of acetylcholine by an isolated mammalian retina. J. Neurophysiol. 39, 1220–1235.

Masland, R.H. and Mills, J.W. (1979) Autoradiographic localization of acetylcholine in the rabbit retina. J. Cell Biol. 83, 159–178.

Masland, R.H., Mills, J.W. and Cassidy, C. (1984b) The functions of acetylcholine in the rabbit retina. Proc. R. Soc. Lond. B 223, 121–139.

Masland, R.H., Mills, J.W. and Hayden, S.A. (1984a) Acetylcholine-synthesizing amacrine cells: identification and selective staining by using radioautography and fluorescent markers. Proc. R. Soc. Lond. B 223, 79–100.

Masland, R.H. and O'Malley, D.M. (1988) Co-release of GABA and acetylcholine by an amacrine cell. Neurosci Abst. 14 (1), 162.

Massey, S.C. and Neal, M.J. (1979) The light evoked release of acetylcholine from rabbit retina in vivo and its inhibition by gamma-aminobutyric acid. J. Neurochem. 32, 1327–1329.

Massey, S.C. and Redburn, D.A. (1982) A tonic gamma-aminobutyric acid mediated inhibition of cholinergic amacrine cells in the rabbit retina. J. Neurosci. 2, 1663–1643.

Maturana, H.R. and Frenk, S. (1963) Directional movement and horizontal edge detectors in the pigeon retina. Science. 142, 977–979.

McKenna, O.C. and Wallman, J. (1985) Accessory optic system and pretectum of birds: comparisons with those of other vertebrates. Brain Behav. Evol. 26, 91–116.

McLean, J. and Palmer, L. (1989) Contribution of linear spatiotemporal receptive field structure to velocity selectivity of simple cells in area 17 of cat. Vision Res. 29, 675–679.

Merwine, D.K., Amthor, F.R. and Grzywacz, N.M. (1990) Ganglion cell surround inhibition is divisive, not linear, in rabbit retina. Invest. Ophthalmol. Visual Sci. 31 (5), 115.

Michael, C.R. (1968) Receptive fields of single optic nerve fibers in a mammal with an all cone retina. II. Directionally selective units J. Neurophysiol. 31, 257–267.

Miles, F.A. (1972) Centrifugal control of the avian retina. I. Receptive field properties of retinal ganglion cells. Brain Res. 48, 65–92.

Miller, R.F. (1979) The neuronal basis of ganglion-cell receptive-field organization and the physiology of amacrine cells. In: F.O. Schmitt and F.G. Worden (Eds.), The Neurosciences, Fourth Study Program, MIT, Cambridge, 227–245.

Mustari, M.J., Fuchs, A.F. (1989) Response properties of single units in the lateral terminal nucleus of the accessory optic system in the behaving primate. J. Neurophysiol. 61, 1207–1220.

Newsome, W.T., Wurtz, R.H., Dürsteler, M.R. and Mikami, A. (1985) Deficits in visual motion processing following ibotenic acid lesions of the middle temporal visual area of the macaque monkey. J. Neurosci. 5, 825–840.

Oyster, C.W. (1968) The analysis of image motion by the rabbit retina. J. Physiol. 199, 613–635.

Oyster, C.W., Simpson, J.I., Takahashi, E.S. and Soodak, R.E. (1980) Retinal ganglion cells projecting to the rabbit accessory optic system. J. Comp. Neurol. 190 (1), 49–61.

Poggio, T. and Reichardt, W.E. (1973) Considerations on models of movement detection. Kybernetik. 13, 223–227.

Poggio, T. and Reichardt, W.E. (1976) Visual control of orientation behaviour in the fly: Part II: Towards the underlying neural interactions. Q. Rev. Biophys. 9, 377–438.

Rall, W. (1964) Theoretical significance of dendritic tress for neuronal input-output relations. In: R.F. Reiss (Ed.), Neural Theory and Modelling, Stanford University Press, Stanford, pp. 73–79.

Reid, R.C., Soodak, R.E., Shapley, R.M. (1987) Linear mechanisms of directional selectivity in simple cells of cat striate cortex. Proc. Natl. Acad. Sci. USA 84, 8740–8744.

Rodieck, R.W. (1973) The Vertebrate Retina, Principles of Structure and Function. W.H. Freeman and Company, San Francisco.

Rosenberg, A.F. and Ariel, M. (1990) Visual-response properties of neurons in turtle basal optic nucleus in vitro. J. Neurophysiol. 63 (5), 1033–1045.

Rowe, M.H. and Stone, J. (1976) Properties of ganglion cells in the visual streak of the cat's retina. J. Comp. Neurol. 169, 99–126.

Schiff, D., Cohen, B., Buttner-Ennever, J. and Matsuo, V. (1990) Effects of lesions of the nucleus of the optic tract on optokinetic nystagmus and after-nystagmus in the monkey. Exp. Brain Res. 79 (2), 225–239.

Schiff, D., Cohen, B. and Raphan, T. (1988) Nystagmus induced by stimulation of the nucleus of the optic tract in the monkey. Exp. Brain Res. 70 (1), 1–14.

Schiller, P.H. and Malpeli, J.G. (1977) Properties and tectal projections of monkey retinal ganglion cells. J. Neurophysiol. 40 (2), 428–445.

Schmidt, M., Humphrey, M. and Wassle, H. (1987) Action and localization of acetylcholine in the cat retina. Neurosci. Lett. 59, 235–240.

Seagraves, M.A., Goldberg, M.E., Deng, S.Y., Bruce, C.G., Ungerleider, L.G. and Mishkin, M. (1987) The role of striate cortex in the guidance of eye movements in the monkey. J. Neurosci. 7, 3040–3058.

Smith, R.D., Grzywacz, N.M. and Borg-Graham, L.J. (1991) Picrotoxin's effect on contrast dependence of turtle retinal direction selectivity. Invest. Ophthalmol. Visual Sci. 32, 1263.

Smith, R.D., Grzywacz, N.M. and Borg-Graham, L.J. Effects of antagonists on preferred motion direction of turtle ganglion cells. Manuscript submitted.

Stelzer, A., Kay, A.R. and Wong, R.K. (1988) $GABA_A$-receptor function in hippocampal cells is maintained by phosphorylation factors. Science, 241, 339–341.

Stone, J. and Fabian, M. (1966) Specialized receptive fields of the cat's retina. Science. 152, 1277–1279.

Stone, J. and Hoffman, K.P. (1972) Very slow conducting ganglion cells in the cat's retina: a major new functional type? Brain Res. 43, 610–616.

Tauchi, M. and Masland, R.H. (1984) The shape and arrangement of the cholinergic neurons in the rabbit retina. Proc. R. Soc. Lond. B 223, 101–119.

Thorson, J. (1966) Small-signal analysis of a visual reflex in the locust. II. Frequency dependence. Kybernetik 3, 52–66.

Torre, V. and Poggio, T. (1978) A synaptic mechanism possibly underlying directional selectivity to motion. Proc. R. Soc. Lond. B 202, 409–416.

Vaney, D.I. (1984) "Coronate" amacrine cells in the rabbit retina have the "starburst" dendritic morphology. Proc. R. Soc. Lond. B 220, 501–508.

Vaney, D.I. (1990) The mosaic of amacrine cells in the mammalian retina. In: N. Osborne and J. Chader (Eds.), Progress in Retinal Research (vol. 9), Pergamon Press, Oxford.

Vaney, D.I., Collin, S.P. and Young, H.M. (1989) Dendritic relationships between cholinergic amacrine cells and direction-selective retinal ganglion cells. In: R. Weiler and N.N. Osborne (Eds.), Neurobiology of the Inner Retina, NATO ASI Series, Vol. H31, Springer Verlag, Berlin, pp. 157–168.

Vaney, D.I. and Young, H.M. (1988) GABA-like immunoreactivity in cholinergic amacrine cells of the rabbit retina. Brain Res. 438, 369–373.

Van Santen, J.P.H. and Sperling, G. (1984) A temporal covariance model of motion perception. J. Opt. Soc. Am. A. 1, 451–473.

Watanabe, S.-I. and Murakami, M. (1984) Synaptic mechanism of directional selectivity in ganglion cells of frog retina as revealed by intracellular recordings. Jpn. J. Physiol. 34, 497–511.

Werblin, F.S. (1970) Responses of retinal cells to moving spots: Intracellular recording in Necturus maculosus. J. Neurophysiol. 33, 342–350.

West, R.W. (1976) Light and electron microscopy of the ground squirrel retina: functional considerations. J. Comp. Neurol. 168, 355–378.

West, R.W. and Dowling, J.E. (1972) Synapses onto different morphological types of retinal ganglion cells. Science 178, 510–512.

Wyatt, H.J. and Daw, N.W. (1975) Directionally sensitive ganglion cells in the rabbit retina: Specificity for stimulus direction, size and speed. J. Neurophysiol. 38, 613–626.

Directional Selectivity in the Retina

Norberto M. Grzywacz, Evelyne Sernagor, and Franklin R. Amthor

Introduction

A visual neuron is directionally selective (DS) if back-and-forth motions, symmetric about the middle of its receptive field, elicit different responses. For the axis along which the ratio between the responses to back-and-forth motions is maximal, we call the direction eliciting the largest response the *preferred direction*, and the opposite direction the *null direction*.

There is no evidence that retinal directional selectivity (RDS) contributes to motion perception. However, there is evidence that RDS contributes to oculomotor responses. In vertebrates, RDS is involved in optokinetic nystagmus (for reviews, see Miles and Wallman, 1993). In this article, we discuss the mechanisms and development of RDS.

Mechanism

Theoretical Preliminaries

The theoretical work of Reichardt, Poggio, and collaborators (Poggio and Reichardt, 1976) emphasized two requirements that models of directional selectivity must fulfill. The first is a spatially-asymmetric mechanism. The second is a nonlinear-functional mechanism to yield two different single-number estimates of preferred- and null-direction responses.

Figure 1*A* illustrates the simplest model proposed by Reichardt and colleagues for insects' RDS, in which inputs from two locations converge to an interaction site where these inputs are multiplied (the nonlinearity) and integrated. The inputs are spatially asymmetric, since a slow signal comes from the left and a fast signal from the center. For rightward, but not leftward, motion, the sluggishness of the left pathway is compensated by the fact that the stimulus arrives at it first. Hence, for rightward motion, if the speed is appropriate, both signals reach the multiplication site at roughly the same time, yielding a positive multiplication. In contrast, for leftward motion, the multiplication is near zero.

The multiplication in Figure 1*A* is one of many quadratic nonlinearity models supported by insect data. Poggio and Reichardt investigated the predictions common to all quadratic models of RDS. For that purpose, they used the Volterra formulation. The output under such a formulation for a smooth, time-invariant, nonlinear interaction between the responses to stimuli in spatial locations a (z_a) and b (z_b) is

$$y(t) = h_{0,0} + \sum_{m=1}^{\infty} \sum_{j=0}^{m} h_{j,m-j} *^m z_a^{(j)} z_b^{(m-j)} \qquad (1)$$

where the mth order convolution $*^m$ is

$$h_{j,m-j} *^m z_a^{(j)} z_b^{(m-j)} = \int_{-\infty}^{\infty} \cdots \int_{-\infty}^{\infty} dt_1 \ldots dt_m h_{j,m-j}(t_1, \ldots, t_m) \prod_{i=1}^{j} z_a(t - t_i) \prod_{k=1}^{m-j} z_b(t - t_{j+k}) \qquad (2)$$

and where $h_{j,m-j}$ are the mth order kernels of the interaction. A quadratic, or second-order, nonlinearity is one for which, for $m \geq 3$, $h_{j,m-j} = 0$. Two predictions of models with only quadratic nonlinearities are frequency doubling and superposition of nonlinearities. The former is the appearance in the Fourier spectrum of the response to moving sinusoidal gratings of energy at a frequency twice the fundamental, but not at frequencies higher than that. In superposition of nonlinearities, the nonlinear average response to a grating composed of two sinusoidal gratings of different frequencies, but whose ratio is a rational number, is equal to the sum of the responses to the individual gratings.

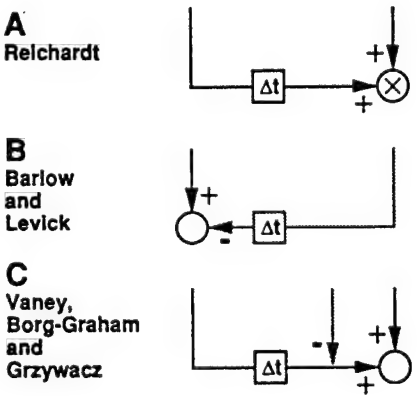

Figure 1. Schemes of models for directional selectivity.

Vertebrate Spatial Asymmetry

The vertebrate retina contains five classes of neurons relevant for RDS (Dowling, 1987). Turtle-retina evidence (Marchiafava, 1979) indicates that the lateral asymmetry mediating RDS does not originate in photoreceptors, horizontal cells, or bipolar cells. Rabbit data (Amthor, Takahashi, and Oyster, 1989) show no correlation between asymmetries in dendritic trees of DS ganglion cells and their preferred-null axes. Consequently, these data suggest that the dendritic trees of amacrine cells mediate the RDS's spatial asymmetry.

Vertebrate Nonlinearities

Barlow and Levick (1965) performed apparent-motion experiments in rabbit retinas and suggested that the nonlinear interaction mediating RDS is inhibitory (Figure 1*B*). In Figure 1*B*, the spatial asymmetry is due to the fact that inputs come only from the right (inhibitory and slow) and center (excitatory and fast). The inhibition is nonlinear, and Barlow and Levick called it *veto inhibition*. The model generates RDS, because when the motion comes from the right, but not the left, the light reaches the inhibitory pathway before the excitatory pathway, compensating for the sluggishness of the former.

Torre and Poggio (1978) proposed a biophysical implementation of this nonlinear veto inhibition. Their rationale was based on RDS's being elicited by motions spanning short distances almost anywhere inside the receptive field (Barlow and Levick, 1965). Torre and Poggio suggested that this subunit-like behavior could be accounted for if each subunit corresponded to a branch of the DS ganglion cell's dendritic tree. To keep the computation constrained to each branch, they suggested that the inhibition mediating RDS works through a synapse that causes local changes of membrane conductance (shunting inhibition) and little hyperpolarization. To understand how

such a synapse works, consider a patch of membrane receiving excitatory (g_e) and shunting inhibitory (g_i) synaptic conductances. Setting without loss of generality the resting and inhibitory reversal potentials to zero, the voltage V obeys

$$C\frac{dV(t)}{dt} + (g_e(t) + g_i(t) + g_{leak})V(t) = g_e(t)E_e + g_{leak}E_{leak} \quad (3)$$

where C is membrane capacitance, g_{leak} is the membrane's leak conductance, and E_e and E_{leak} are reversal potentials of g_e and g_{leak}, respectively. When $g_i \gg g_e, g_{leak}$, then V falls toward the following equilibrium ($dV/dt \to 0$) value:

$$V(t) \to \frac{g_e E_e + g_{leak}E_{leak}}{g_i} \quad (4)$$

which is small, because g_i is large. Therefore, this inhibition is division-like, rather than subtraction-like.

Torre and Poggio also argued that a shunting-inhibition mechanism for vertebrate RDS might be consistent with the insects' quadratic nonlinearity. Their argument was that for sufficiently low contrasts, one can neglect the higher-order nonlinearities (Equation 1), as in a Taylor series approximation.

Problems with Old Models for Retinal Directional Selectivity

Experiments have shown that the inhibitory mechanism mediating RDS in rabbit is division-like (Amthor and Grzywacz, 1993). However, recent experiments did not support the Torre and Poggio model. A quadratic approximation is not valid even for the smallest contrasts (Grzywacz, Amthor, and Mistler, 1990); rabbit DS ganglion cells failed the frequency-doubling and superposition-of-nonlinearities tests. Moreover, a whole-cell patch-clamp experiment by Borg-Graham and Grzywacz (1992) casts doubt that the relevant inhibition acts on the DS ganglion cell.

Recent data also challenged the Barlow and Levick model. Pharmacological evidence indicates that the inhibition mediating RDS is GABAergic via $GABA_A$ receptors (Caldwell, Daw, and Wyatt, 1978). However, when responses of turtles' DS ganglion cells to motion were recorded under picrotoxin (a $GABA_A$ antagonist), preferred and null directions would sometimes reverse as the stimulus's contrast or speed varied (Borg-Graham and Grzywacz, 1992).

Finally, the postulate of an exclusively inhibitory mechanism of RDS is incorrect. Grzywacz and Amthor (1993) expanded earlier experiments by Barlow and Levick (1965) to find that if the spatiotemporal parameters of the stimulus are appropriate, then there is a preferred-direction facilitation that can be as strong as null-direction inhibition.

A New Model

Vaney (1990) and Borg-Graham and Grzywacz (1992) independently proposed new models for RDS (Figure 1*C*). They are similar to the Reichardt model (Figure 1*A*) in that the spatial asymmetry is excitatory (the inhibitory mechanism is spatially symmetric). However, in contrast to that model, the nonlinearity is not quadratic, but inhibitory, as in the Barlow and Levick model, and of the shunting type, as in the Torre and Poggio model. Vaney, and Borg-Graham and Grzywacz, suggested that the DS signal flows from the distal end of each amacrine dendrite to the ganglion cell. Consequently, these dendrites would be autonomous units, bypassing integration at the amacrine soma. In turn, the ganglion cell would sample signals from several dendrites with the same preferred direction (Figure 2).

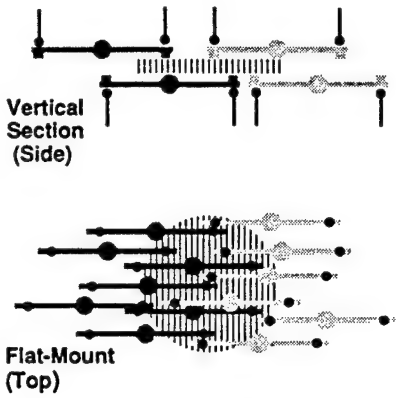

Figure 2. Model for the relationship between amacrine and ganglion dendrites in retinal directional selectivity. The vertically hatched, dark-textured, light-textured, and black elements correspond to one layer of ganglion-cell dendritic field, excitatory amacrine cells making strong synapses, excitatory amacrine cells making weak synapses, and inhibitory synapses, respectively. Preferred direction is to the right.

Computer simulations with this model show that it can generate RDS in individual dendrites of an amacrine cell without leading to RDS in its soma (Borg-Graham and Grzywacz, 1992). Furthermore, simulations show that the model accounts for reversals of preferred and null directions under picrotoxin as a result of saturation of the synapse between the amacrine dendrite and DS ganglion cell. Finally, the model accounts for preferred-direction facilitation as, for example, synaptic facilitation.

Development

Physiology and Anatomy

From studies in turtle (Sernagor and Grzywacz, current research), one can conclude that mature RDS emerges relatively late in retinal development. The adult incidence of DS cells (>20%) emerges after receptive fields reach mature sizes and after the disappearance of spontaneous waves of activity typical of immature retinas (Meister et al., 1991). In addition, RDS matures after orientation selectivity (that is, selectivity to spatial orientation of anisotropic stimuli, such as lines), concentric receptive fields, and surround inhibition. There are some immature DS cells at early stages of turtle embryonic development. However, this embryonic directional selectivity completely disappears at hatching. Directional selectivity is absent in turtle for at least the first 40 days of life, reappearing later on. Embryonic ganglion cells might express directional selectivity because of accidental asymmetric wiring in their polarized, undeveloped dendritic trees. Because mature RDS may emerge mainly at the expense of orientationally selective cells (Sernagor and Grzywacz, current research), it has been suggested that DS cells are modified orientationally selective cells. (RDS also emerges relatively late in rabbit, although its development is faster than that of turtle; Masland, 1977.)

The late emergence of RDS suggests two hypotheses for its development: (1) it requires light exposure, and/or (2) it requires the late emergence of an inhibitory drive onto the network mediating orientation selectivity.

If visual experience is necessary for the development of RDS, then this development probably involves synaptic plasticity. Daw and Wyatt (1974) attempted to test this hypothesis by

raising rabbits from 15 to 60 days after birth such that their only visual experience was motion in one particular direction. These authors did not observe changes in the distribution of preferred directions, and they argued against plasticity in developing retinas. However, a criticism of this interpretation is that, in rabbit, the critical period for establishment of RDS might occur earlier than 15 days postnatal (Masland, 1977).

Models for the Development of Retinal Directional Selectivity

Borg-Graham and Grzywacz (1992) emphasized that the developmental problem is not to create spatial asymmetry, since amacrine dendrites are already asymmetric. Rather, the problem is to coordinate asymmetries of several dendrites (see Figure 2) to explain the subunit-like behavior in ganglion cells. Borg-Graham and Grzywacz suggested that a Hebbian correlational process (see HEBBIAN SYNAPTIC PLASTICITY) could reinforce an initial statistical bias in connections from amacrine cells to proto-DS ganglion cells (Figure 3*A*).

There are two problems with this model: (1) It does not account for the apparent emergence of RDS at the expense of orientationally selective cells. (2) This model predicts homogeneous distribution of preferred directions. The distribution of preferred directions is not necessarily homogeneous; for rabbit on-off cells, the distribution clusters around four directions parallel and perpendicular to the visual streak (Oyster, 1968).

A solution for the first problem would be a two-stage development for RDS (Figure 3*B*). In the first stage, the inhibition necessary for the model in Figures 1*C* and 2 would be absent and a Hebbian mechanism would reinforce statistical biases in orientation rather than direction. (The stimulus for this mechanism would be mainly spontaneous activity.) Dendrites of immature amacrine and ganglion cells could be orientationally selective despite lack of inhibition, because, for instance, a moving edge perpendicular to the dendrite would stimulate it better than a parallel edge, as a result of voltage saturation. In the second stage of the model, emergence of inhibition onto certain amacrine dendrites would turn them into DS cells, and a Hebbian process would coordinate the preferred directions, as in Figure 2.

The mechanism underlying the nonhomogeneous distribution of preferred directions might tap temporal-nasal, superior-inferior asymmetries of ganglion-cell densities, which, like directional selectivity, mature relatively late.

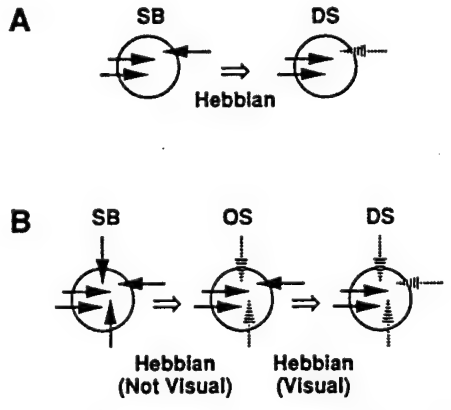

Figure 3. Two models for the development of retinal directional selectivity.

Since this mechanism's development might involve Hebbian processes driven by spontaneous activity and light, RDS may be an excellent paradigm to study dendritic computations and brain self-organization.

Acknowledgments. Support for this work came from a grant from the Office of Naval Research (N00014–91–J–1280), a grant from the National Eye Institute (EY08921), and an award from the Paul L. and Phyllis C. Wattis Foundation to N.M.G.; from a grant from the National Eye Institute (EY05070) to F.R.A.; and from a core grant from the National Eye Institute to Smith-Kettlewell (EY06883).

Road Map: Vision
Background: Axonal Modeling
Related Reading: Directional Selectivity in the Cortex; Retina; Visuomotor Coordination in Flies

References

Amthor, F. R., and Grzywacz, N. M., 1993, Inhibition in On-Off directionally selective ganglion cells in the rabbit retina, *J. Neurophysiol.*, 69:2174–2187.

Amthor, F. R., Takahashi, E. S., and Oyster, C. W., 1989, Morphologies of rabbit retinal ganglion cells with complex receptive fields, *J. Comp. Neurol.*, 280:97–121.

Barlow, H. B., 1953, Summation and inhibition in the frog's retina, *J. Physiol., Lond.*, 119:69–88.

Barlow, H. B., and Levick, W. R., 1965, The mechanism of directionally selective units in rabbit's retina, *J. Physiol.*, 178:477–504.

Borg-Graham, L. J., and Grzywacz, N. M., 1992, A model of the direction selectivity circuit in retina: Transformations by neurons singly and in concert, in *Single Neuron Computation* (T. McKenna, J. Davis, and S. F. Zornetzer, Eds.), Orlando: Academic Press, pp. 347–375. ◆

Caldwell, J. H., Daw, N. W., and Wyatt, H. J., 1978, Effects of picrotoxin and strychnine on rabbit retinal ganglion cells: lateral interactions for cells with more complex receptive fields, *J. Physiol.*, 276:277–298.

Daw, N. W., and Wyatt, H. J., 1974, Raising rabbits in a moving visual environment: An attempt to modify direction sensitivity in the retina, *J. Physiol. (Lond.)*, 240:309–330.

Dowling, J. E., 1987, *The Retina: An Approachable Part of the Brain*, Cambridge, MA: Harvard University Press. ◆

Grzywacz, N. M., and Amthor, F. R., 1993, Facilitation in On-Off directionally selective ganglion cells in the rabbit retina, *J. Neurophysiol.*, 69:2188–2199.

Grzywacz, N. M., Amthor, F. R., and Mistler, L. A., 1990, Applicability of quadratic and threshold models to motion discrimination in the rabbit retina, *Biol. Cybern.*, 64:41–49.

Marchiafava, P. L., 1979, The responses of retinal ganglion cells to stationary and moving visual stimuli, *Vis. Res.*, 19:1203–1211.

Masland, R. H., 1977, Maturation of function in the developing rabbit retina, *J. Comp. Neurol.*, 175:275–286.

Meister, M., Wong, R. O. L., Baylor, D. A., and Shatz, C. J., 1991, Synchronous bursts of action potentials in ganglion cells of the developing mammalian retina, *Science*, 252:939–943.

Miles, F. A., and Wallman, J., Eds., 1993, *Visual Motion and Its Role in the Stabilization of Gaze*, Amsterdam: Elsevier. ◆

Oyster, C. W., 1968, The analysis of image motion by the rabbit retina, *J. Physiol.*, 199:613–635.

Poggio, T., and Reichardt, W. E., 1976, Visual control of orientation behaviour in the fly: Part II: Towards the underlying neural interactions, *Q. Rev. Biophys.*, 9:377–438. ◆

Torre, V., and Poggio, T., 1978, A synaptic mechanism possibly underlying directional selectivity to motion, *Proc. R. Soc. Lond. B*, 202: 409–416.

Vaney, D. I., 1990, The mosaic of amacrine cells in the mammalian retina, in *Progress in Retinal Research*, vol. 9 (N. Osborne and J. Chader, Eds.), Oxford: Pergamon, pp. 49–100. ◆

ELSEVIER

Journal of Neuroscience Methods 56 (1995) 77–88

JOURNAL OF NEUROSCIENCE METHODS

Automating the quantitative analysis of 2-D neural dendritic trees

Mark F. Villa [a], Franklin R. Amthor [b,*]

[a] *Department of Computer and Information Sciences, University of Alabama at Birmingham, Birmingham, AL 35294-1170, USA*
[b] *Department of Psychology and Neurobiology Research Center, University of Alabama at Birmingham, Birmingham, AL 35294-1170, USA*

Received 5 October 1993; revised 9 June 1994; accepted 16 June 1994

Abstract

Neurons in the central and peripheral nervous system vary widely in their dendritic branching patterns. Quantification of the morphological characteristics used to identify different classes of neurons and relate neural structure to function requires that accurate metric and non-metric data be obtained from neural images obtained by camera-lucida drawing or from digitized video images made with transmitted, fluorescence or confocal microscopy. This paper describes a largely automated procedure for determining the dendritic tree structure of largely planar cells (such as retinal ganglion cells or cells in tissue culture monolayers) from an initial pictorial representation or digitized image. From this structure, non-metric data (such as the ordered 'tree' of branches) and metric information (such as total dendritic length and dendritic field area) can be automatically computed. The use of this method is specifically illustrated in the capture of the dendritic tree structure of retinal ganglion cells from the rabbit retina.

Keywords: Dendritic tree; Retinal ganglion cell; Tracing; Thinning

1. Introduction

The dendritic arborizations of neurons can be a significant factor in their function. The location and arrangement of the neuron's dendrites determine what inputs may be received by the neuron and how those excitatory and inhibitory inputs, varying in a temporally complex manner, are integrated. The dendritic morphology of neurons can be visualized by a number of techniques. These include staining methods such as the Golgi method, intracellular filling with fluorescent dyes or horseradish peroxidase, staining with antibodies to intracellular constituents specific to particular neurons, and phase-contrast microscopy of unstained cells (usually in tissue culture monolayers) (Mize, 1985). A hard-copy rendering that is particularly common in neuroscience is camera-lucida hand drawing in which a microscope drawing tube optically superimposes the drawing being executed with the microscope field in which the neuron is viewed. Digitized images of neurons that are relatively flat (such as in tissue culture or some retinal neurons, for example) are increasingly being captured digitally by video cameras or confocal microscope systems.

However the image of the neuron is obtained, the goal of morphometric analysis is to obtain quantitative information from the images that is useful for describing particular cell types and distinguishing among them. In this paper a method is reported that produces from a drawn, photographed or other high signal-to-noise rendering of a neuron, an output file that contains a formalized list of points from which can be determined (1) the ordered branching structure of the tree consisting of connected branches, branch points and endpoints, (2) non-metric information such as the total number of dendrites and dendritic branch angles, and (3) metric dendritic tree parameters (which, by definition, require the inclusion of an accurate scale), such as dendritic length, dendritic field area and the spatial distributions of dendritic branch points and endpoints.

The procedure described in this paper is designed to eliminate as much human intervention as currently practical in the acquisition of the quantitative parameters. This procedure consists of 4 major steps: (1) digitizing the image by electronically scanning a camera-lucida drawing or conversion of an image-digitized

* Corresponding author. Tel.: (205) 934-2694; Fax: (205) 975-6110; INTERNET: amthor@cis.uab.edu.

SSDI 0165-0270(94)00109-X

by video capture into a standard file format, (2) *thinning* the dendritic tree to a single pixel width in its entirety, (3) automatic production of an ordered stick-figure *tracing* of the original cell including resolution of dendritic crossings and image noise, and (4) computation of required metric and non-metric morphometric measurements.

This paper described the application of the method to two types of digitized images, camera-lucida hand-drawn cell pictures, and video images of cells captured with a microscope video camera. However, virtually any method by which a reasonably high signal-to-noise digital file can be created could be a candidate input to the rest of the procedure. After image acquisition, some noise reduction or image enhancement may be done before the image is thinned. Then, the thinning procedure described trims away the outer pixels of the dendritic tree, leaving a connected 'skeleton' of the original image only 1 pixel thick. The tracing algorithm then traces along dendrites, keeping track of continuation points, endpoints and branch points. From this sequence of 4 major steps, we can then automatically derive metric and non-metric attributes such as the total dendritic length and the locations of all branching points and endpoints and also a measurement of the cell's 2-dimensional area.

A number of researchers have previously developed and described computer-assisted programs for analysis of dendritic arborizations (Mize, 1985; Capowski, 1989; Stewart, 1992). Manual input systems, such as those of Amthor and coworkers (Amthor et. al., 1983; Amthor, 1985) have typically made use of a digitizing tablet in which individual points of the cell were accumulated by tracing over the cell by hand with the tablet cursor. Other manual methods have involved the use of a video camera and software to trace branches interactively with a mouse or joystick over a video image of the cell. Some of these systems interact with the microscope stage to scroll portions of the cell into view to simplify tracing; an early system is described by Overdijk et al. (1978). Glaser and Glaser (1990), among others, have described a system capable of handling 3-D images.

Attempts have also been made at more completely automatic tracing (e.g., Coleman, 1977; Capowski, 1989). Results from these studies indicate that systems which incorporate a human 'image processor' are likely to outperform fully automated systems for some time to come, although the application of powerful computer hardware and advanced image processing techniques (Villanueva and Lebars, 1993) may hasten that day. In the system reported here, it is possible to automatically generate the dendritic tree structure from a digitized image of the cell. This reduced requirement for human intervention, along with the flexibility to handle different types of cell images, and the ability to work with 80486 computers commonly available in neuromorphology setups are advantages of our method over some previous ones [1].

2. Methods

2.1. Digitizing the image

The procedure described here currently uses an IBM PC-AT compatible computer (80486-SLC2/66 MHz PC-AT, 16 MB RAM, 350 MB hard disk) running Windows for some pre-processing. We also currently use a Sun SPARCstation 2 (Sun Microsystems, Mountain View, CA) (32 MB RAM, 64 MB virtual memory, 400 + MB disk) for thinning and executing the tracing procedure, but this additional computing power is not necessary for most of the procedures; the Unix-based operating system on the Sun simplifies programming and speeds throughput by providing simple access to large (more than 1 MB) blocks of RAM; PC programs using DOS extenders or the use of more advanced operating systems such as Windows NT would allow replacing the SPARCstation by an 80486 machine.

Camera-lucida drawings are reduced to a 8.5×11 in. standard size (if necessary) and fed into a binary, 300 dpi digitizing scanner, such as The Complete Page Scanner (Boca Research, Milpitas, CA), installed in a PC-AT. Our original camera-lucida drawings are high-contrast figures in which crossing dendrites are conventionally represented with the lower dendrite broken (see for example the lower left corner of Fig. 2A). Gross image editing, such as removing large blocks of noise, can be handled with standard commercial software, such as PC Paintbrush IV + (ZSoft, Marietta, GA) in the MS-DOS environment and Adobe Photoshop (Abode Systems, Mountain View, CA) or Graphics Tools (Deltapoint, Monterey, CA) in Windows. The scanner produces.PCX files, and PC-based software uses either.PCX or.TIFF (a more advanced format than.PCX) files while Sun-based software uses Sun raster format. To convert between file types, one of the above PC programs or the HiJaak (Inset Systems, Brookfield, CT) conversion program, along with conversion programs based on software by Rimmer (1990) and executing on the Sun, may be used.

Images digitized by video 'frame grabber' cards may replace the scanning step in the digitizing procedure. In our system, video images are captured by a Matrox (Matrox, Montreal) MVP-AT. However, video images are of lower resolution and noisier than camera-lucida

[1] Contact F.R.A. for information on availability of the software described by this paper.

drawings and thus may require considerably more 'clean-up' before becoming an appropriate input to the thinning step. We discuss both a camera-lucida and a video application in the Results section.

PostScript print files (Adobe Systems, Mountain View, CA) are generated at the final stage of the tracing process to confirm that the traced tree matches the original image. Because some file operations are performed on a PC and others on a Sun, the use of the Sun Microsystems PC-NFS Local Area Network reduces the burden of file transfers by allowing the SparcStation to act as a file server so that a single copy of a file can be shared by both machines.

2.2. Thinning

In our procedure, the thinning process is the key to automatically acquiring dendritic tree parameters from a bitmap image. Thinning has significant advantages over more commonly used processes such as 'erosion' (Jain, 1989) (see the Results section). Thinning (as well as erosion) algorithms work by repeatedly processing small pieces or 'neighborhoods' (Haralick and Shapiro, 1991) of the binary bitmap. In a rectangular coordinate system, a neighborhood consists of the 8 pixels surrounding a given pixel; thus, in this and other neighborhood schemes, the new value of a neighborhood's center pixel depends only on its own value and the value of the 8 neighboring pixels. The tracing program itself also uses neighborhood operators.

2.3. Tracing

2.3.1. Noise elimination prior to tracing

Tracing requires a bi-level skeleton. Some editing of the thinned image may be necessary prior to tracing, primarily to remove irrelevant branches (such as the axon or false branches created by thinning), or if there are discontinuities or loops in the branches. In our procedure, editing of noise normally needs to be done only on portions of the image connected to the cell because structures distant from the cell are ignored by the tracing algorithm. Gross editing and image cropping are handled by commercial software such as Photoshop or Graphics Tools.

2.3.2. Tracing algorithm

Thinning produces a tree which is traceable — if we start from some point, we know which point is next since, by definition, all pixels not needed to create a skeleton are removed (some minor deviations from this ideal are handled by the tracing program). Once tracing has begun, the procedure keeps track of both traced continuation points and any branch points and endpoints found. This combination of tracing and bookkeeping allow us to trace simple trees to their completion. For typical images, however, there are 4 complicating factors which the procedure must handle: (1) removal of non-dendritic structures left close to the dendritic tree after thinning, (2) branch points are not always easy to detect; (3) the tree may have (intentional or non-intentional) breaks, meaning that what at first glance are endpoints are instead only the proximal end of a break in a dendrite, the other end of which must be found so that tracing may continue on that branch; and (4) the tree may have loops, that is, it may not be obvious (even to a human observer) where a particular branch begins and ends. The means by which each of these problems are dealt with are discussed in the Results section.

2.4. Computation of quantitative parameters

From the thinned and traced tree, it is straightforward to automatically calculate such non-metric parameters as number of nodes and sequences of branch order because all the pixels in the file are labeled as either a node, dendritic continuation, or endpoint. Calculation of metric parameters requires association of scale information with the final file. In our system, this is done by digitizing a scale bar directly on the original image. With this scale information, metric attributes such as total dendritic length, dendritic length by branch order, and so forth, are directly calculated. A digital implementation of the convex hull around of the dendritic area also allows direct estimation of dendritic domain area.

3. Results

3.1. Image acquisition

3.1.1. Image methods

The first step is the acquisition of a suitable digital image of the neuron. This has been produced by a number of methods; here we primarily report the use of camera-lucida drawings and captured video images. Camera-lucida drawings were typically photoreduced to a scannable size prior to scanning. Video images were captured by the Matrox 512×480 frame grabber attached to a MTI Dage SIT camera. In most cases, more than one video image was assembled into a mosaic (using Adobe Photoshop) to capture the entire dendritic tree of the cell. We typically converted the mosaic image directly into a bi-level drawing by a threshold process, sometimes with some preprocessing such as standard high-pass filters. It is also possible to hand-trace the video image. Tracing results in a more noiseless, but usually lower resolution image than thresholding, and is therefore similar to camera-lucida drawing as an input. Both video thresholding and

hand-tracing have been used on video images as the input to subsequent stages.

3.1.2. Initial noise reduction

Small noise structures in the digitized image that are not too close to the cell can be ignored because the tracing procedure ignores objects distant from the main cell skeleton. On the other hand, noise prolongs the running time of some subsequent stages so there are some computational tradeoffs in early noise reduction. A number of inexpensive DOS or Windows-based commercial packages are available for reducing initial noise in a scanned or traced figure, as described in Methods.

3.2. Thinning

3.2.1. Rationale

Trimming the outer pixels of a dendritic tree leaves a connected 'skeleton' of the original image, only 1 pixel thick, that makes it potentially traceable to produce a set of data from which the major elements of the original cell — total dendritic length, total number of dendrites, etc. — can be quantified.

3.2.2. Strategies for thinning the image

Two methods have been commonly used to reduce the number of 'non-skeletal' pixels in a binary image. Erosion applies a mask to each pixel in an image and removes it if it is an edge pixel, as determined by the mask. An image may be repeatedly eroded, ultimately reducing objects to arbitrarily small sizes in both X and Y dimensions and then, finally, deleting the object entirely when it has been eroded to a few pixels. Thus, erosion is non-specific in that it does not retain connectivity and does not cease when a 1-pixel-thick skeleton in a particular region is reached.

Thinning differs from erosion in that thinning requires the use of more than one mask, and it uses a set of mask-dependent procedures to remove pixels which are not essential to maintaining connectivity. We have tried several distinct thinning algorithms. Our current method is based on algorithms by Zhang and Suen (1984) and Guo and Hall (1984) because these algorithms are better matched to our problem than those, for example, oriented towards processing on a parallel machine (Chin et al., 1987), or which thin the branches to widths of more than 1 pixel (O'Gorman, 1990).

We have found Zhang-Sueng thinning to be generally the best overall for this purpose. One iteration of Zhang-Suen thinning is composed of two sub-iterations. In the first sub-iteration, the neighborhood of every pixel is examined for the pixel's potential contribution to skeletal connectivity. Then two pre-defined masks are applied. If the pixel currently under examination is not needed for connectivity, it is removed. After all pixels have been tested, the second sub-iteration repeats in a manner similar to the first, but with the two masks rotated 180°. This 2-stage process is repeated until no more pixels can be removed. Complete details of this thinning operator are given by Zhang and Suen (1984).

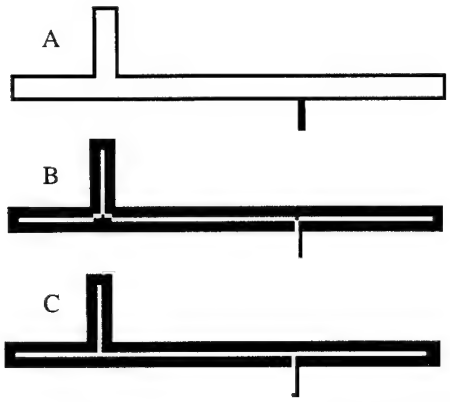

Fig. 1. Results of applying different image operators to the same sample dendrite. Pixels removed by the procedures are in black, and the resultant tree is in white. Enlarged pixels are used here for representational clarity. One iteration of erosion (A) is performed, while thinning (B and C) is allowed to self-terminate. A: erosion smoothly removes 1 pixel from the perimeter but also completely removes a 2-pixel wide branch. B: Guo-Hall thinning removes an acceptable number of pixels but slightly exaggerates the presence of branches. C: Zhang-Suen thinning best retains the shape of the dendrite while slightly shortening one end and the lower branch.

Fig. 1 compares the effects of erosion, Zhang-Suen thinning and Guo-Hall thinning on the same sample dendritic segment. The resultant image after stages of thinning appears as a white sub-portion of the original image, with black indicating those pixels removed by the respective operation. One iteration of erosion (Fig. 1A) has produced a tree which is not completely thinned but in which a branch has already been completely disconnected. The Guo-Hall method (Fig. 1B) generally produces a thinner tree with better length accuracy than the Zhang-Suen method (Fig. 1C), but the Zhang-Suen method executes faster and produces more accurate representation of curves, and fewer spurious branches than the Guo-Hall method. Depending on the application, our program sometimes uses either or both of these algorithms.

We have markedly increased the speed of the thinning algorithms in our application by restricting the final thinning iterations to the area immediately around the soma, since nothing can be gained from repeatedly applying the thinning operations to areas already thinned to 1 pixel. The soma is the last part of the cell to be thinned because it is almost always the thickest portion of the cell. We use a neighbor of the last pixel thinned as the center of the cell body which means that we can automatically generate this data item (soma center) rather than requiring it to be selected by the human operator. Although the soma center may be

selected manually by different methods, the last pixel to be thinned procedure is both reasonably objective and repeatable.

Several cardinal steps of the thinning procedure are shown for a relatively simple neuron in Fig. 2A–C. Fig. 2A shows a portion of the scanned camera-lucida image original of the neuron. The point at which the dendrites have been reduced to virtually 1 pixel wide is shown at B, and the final thinned skeleton, with the soma reduced to a single pixel, at C. Fig. 2D shows the thinned skeleton superimposed on the original scanned image. It takes less than 3.5 min to thin a typical retinal ganglion cell on a SPARCStation 2 workstation (Sun Microsystems, Mountain View, CA).

3.3. Tracing

3.3.1. Overview

Thinning produces a tree skeleton which is traceable. Our tracing algorithm works in a manner similar to a person tracing the image with their finger, keeping track of sections already traced (continuation points), and noting important points such as endpoints and branch points. Once tracing has begun, the procedure keeps track of both traced continuation points and any branch points and endpoints found. As described in Methods, there are 4 types of problems the procedure must handle: (1) removal of non-dendritic structures left close to the dendritic tree after thinning, (2) detecting branch points, (3) dealing with gaps or breaks in dendrites, and (4) dealing with dendritic loops.

3.3.2. Removal of non-dendritic structures left after thinning

After the image has been thinned, certain portions of the image that may interfere with the tracing process must be removed. Normally there is no need to completely 'clean' the image prior to tracing because most noise will be ignored as the tracing process proceeds from the soma outward to the branch tips, com-

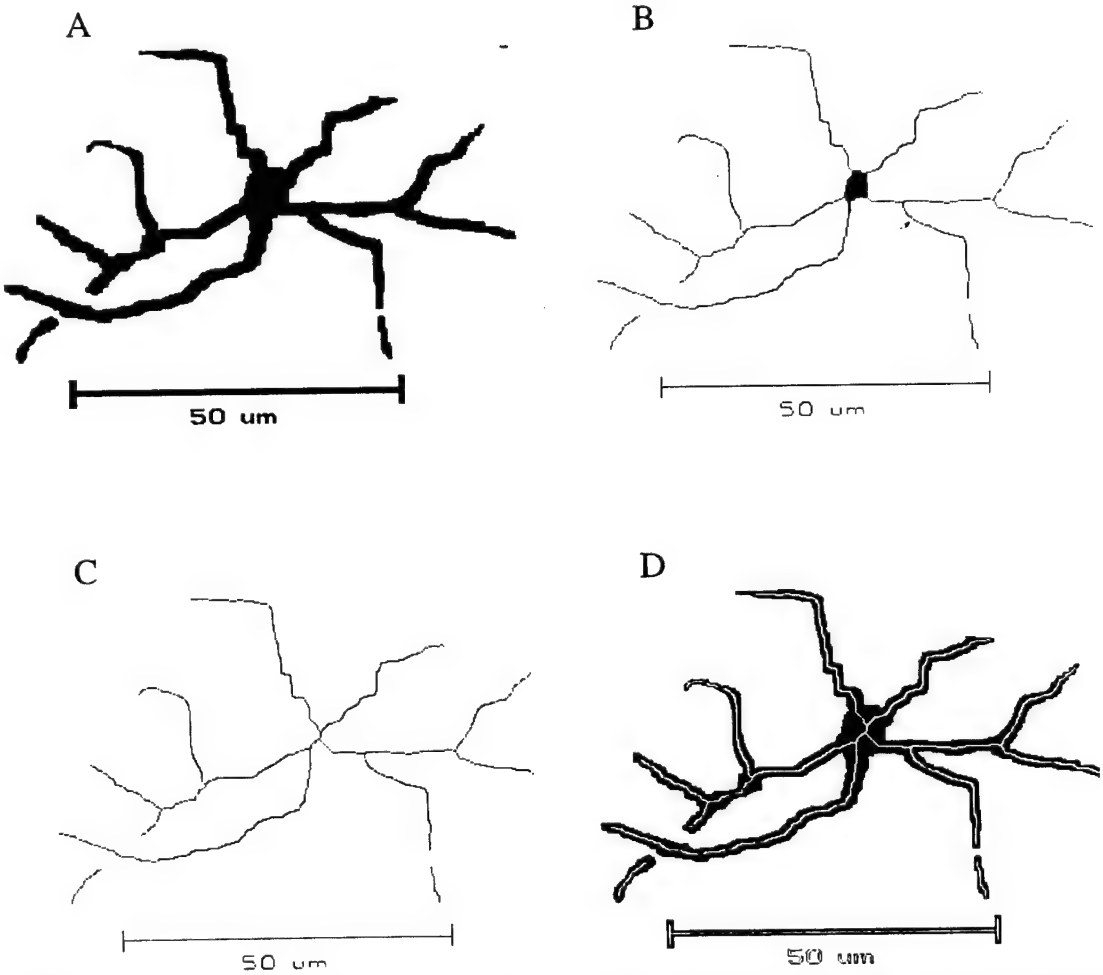

Fig. 2. A: simplified dendritic tree whose bitmap is used as an input to the thinning algorithm. One dendritic crossing is apparent in the lower left. One break in a dendrite, induced by noise somewhere in the capture process, is in the lower right. B: bitmap of the dendritic tree at a point in the recursive thinning algorithm where the dendrites are essentially reduced to a 1 pixel thickness, but the soma remains as a large thick object. C: final thinned bitmap. D: final thinned bitmap superimposed in reverse contrast on the original bitmap for comparison.

Start → Scan → Convert → Prepare → Thin → **Trace** → Stop

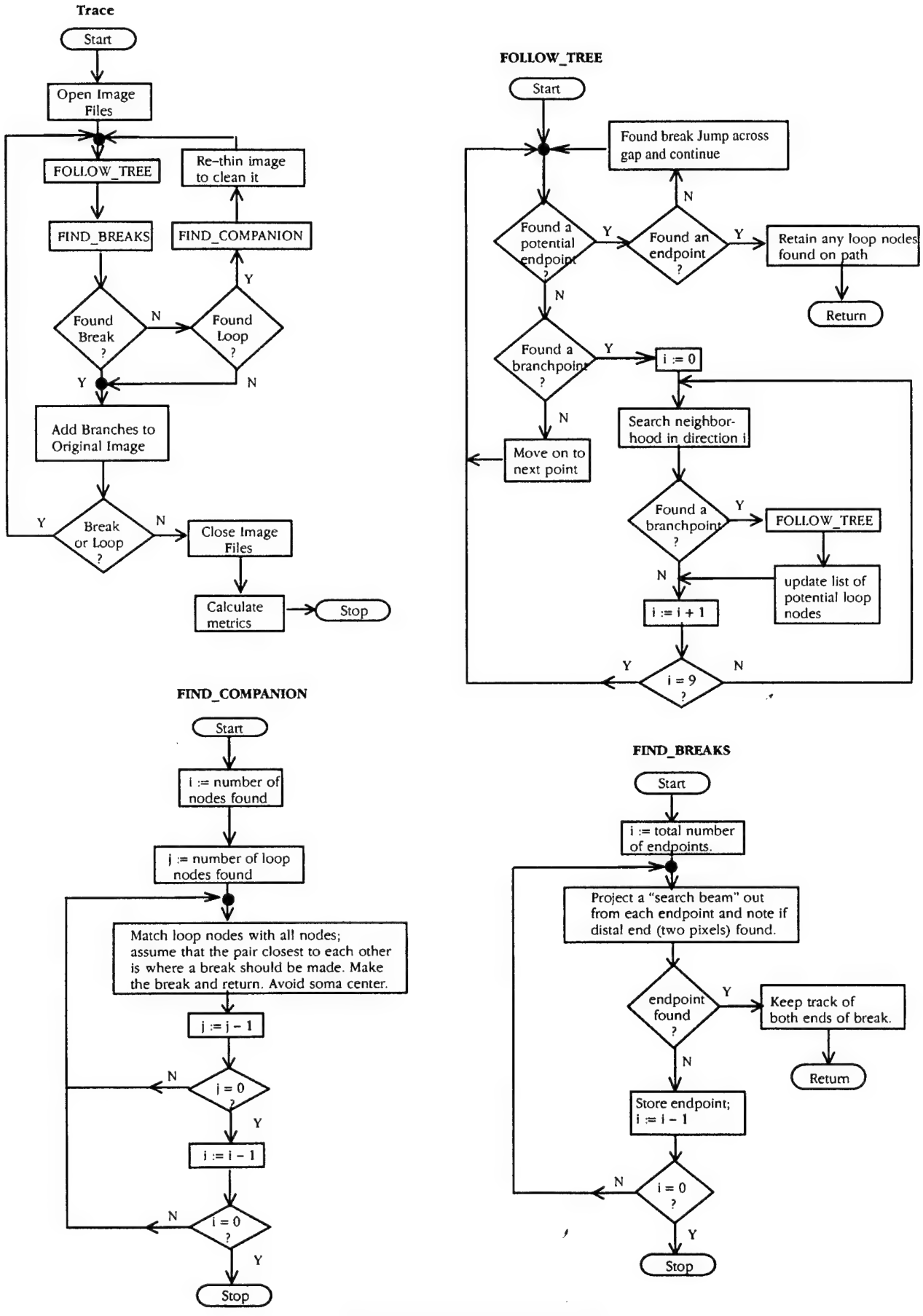

Fig. 3. Flowchart for the tracing program.

pletely ignoring most of the non-tree portion of the image (except when bridging gaps). Any large non-dendritic structure touching or close to the dendritic tree, such as the axon, must be detached or removed, however.

3.3.3. Tracing flowchart

A flowchart for the major routines of tracing appears in Fig. 3. After pre-processing stages are complete, program *Trace* repeatedly traces the tree and handles exceptions to the simple tree: breaks and loops. For an image with no 'Break or Loop"s (see Fig. 3), the main program loop in *Trace* will only execute once. FOLLOW_TREE successively examines the neighborhood around a pixel to categorize the pixel as dendrite (continuation), branch point or endpoint. The greater part of the image contains a series of continuation pixels which can be easily traced ('move on to next point' box). However, aside from simple dendrites, branch points and endpoints, the routine must check to make sure that an aliased line — the jagged line with surplus pixels which results from digitizing a smooth curve — is not mistaken for a branch point. Also, it must recognize different forms of branch points, such as tee's, so that it will know which pixel is the branch point. Loops are optionally broken by FIND_COMPANION, but an attempt is always made by FIND_BREAKS to bridge across gaps (regardless of cause). Note that FOLLOW_TREE calls itself recursively, processing a series of identically structured subitems, in this case, the branches of the tree.

3.3.4. Tracing dendrites

The tracing process is related to boundary tracking (Davies, 1990) (also known as boundary tracing), in which an outline of an object is traced until all pixels in the outline have been found. The major difference here is that we are tracking a tree skeleton — and the process terminates when all endpoints have been found. The tracing procedure searches a small sub-portion of the image to identify branch points and endpoints. This is similar to the Coleman approach (1977), but we search a smaller area on black-and-white, not grayscale, images.

Fig. 4 shows how the tracing procedure works. Fig. 4A is a magnification of 1 pixel and its 'neighborhood' (the pixels it directly touches). The basic operation on the bitmap is to apply a kernel (a neighborhood with 0 or more 'on' pixels) against every pixel in the bitmap, perform some comparison operation with the kernel and the examined pixel's neighborhood, and (possibly) replace the original pixel. Although neighborhoods may be of different sizes (Russ, 1992), we choose 3×3 because it is the size used by the thinning algorithms, it is computationally advantageous, and it simplifies the process of identifying branch points.

3.3.5. Detecting branch points

Fig. 4B–E show how a simple branch is traced and a branch point detected. Each figure (4B–E) represents one iteration of the search process. Tracing begins (Fig. 4B) at the ON pixel at position 1 ('up') in the neighborhood of some branch point (possibly the center of the soma), since it is the only ON pixel in the neighborhood. Fig. 4C contains this pixel (gray circle), the new pixel (white circle), and the next pixel (black circle). The next pixel is also the only ON pixel, so it is traced, as shown in Fig. 4D. There are now 2 traced (gray) pixels. Fig. 4D also contains 2 black pixels, indicating either a branch point or merely a 90° change of direction. To make this determination, the program searches in the nearby neighborhoods around for 'interesting' pixels. Fig. 4E shows the result of this search, a detected branch point. At this point, the tracing routine calls itself recursively, continues with the direction 0 ON pixel as a branch point, and traces it out until all branches terminate in endpoints/dendritic breaks, and returns to carry out the same process for the direction-3 branch in Fig. 4E. With the exception of handling breaks and loops, the program continues with this process until the entire tree is traced.

A branch point is identified as a neighborhood containing 2 or more ON pixels with at least one intervening space. Neighborhoods with ON (black) pix-

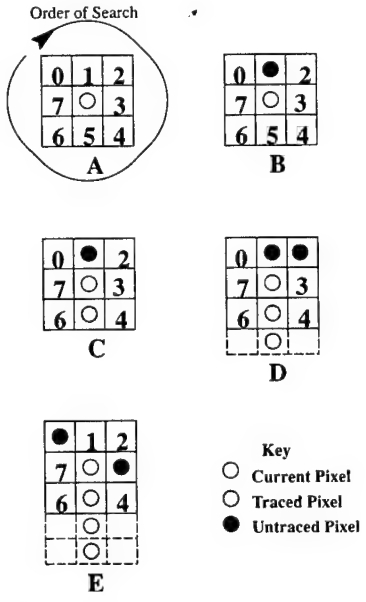

Fig. 4. A: neighborhood of a pixel. The numbers correspond to the order in which pixels are followed: if pixel 0 is on, it is the next point to be followed, if it is not on, pixel 1 is checked, and so on. B: pixel is detected position 1. C: this pixel is traced and another position 1 pixel is found. D: 2 new pixels are found. The local area must be searched to determine whether this is a branch point. E: 2 pixels are found, indicating that the current pixel is a branch point. The procedure traces starting from the position 0 pixel and, when complete for that branch, will return and trace starting from the position 3 pixel.

els only at positions 0 and 3, for example (Fig. 4E), are all potential branch points. This simple scheme must be augmented, however, since the tracing process may approach any branch point from any angle. The program solves this problem by looking at neighborhoods around the current point to find additional ON pixels. If a valid branch point is found, it becomes the new starting point for tracing. As long as the thinning algorithm completely thinned the tree successfully, the tracing program will continue, interrupted only to handle breaks or loops.

3.3.6. Bridging gaps

Breaks or gaps in the dendritic tree result either from failures in the digitalization process or from overlapping dendrites (dendrites crossing in different planes) that are drawn with a break to indicate the overlap. In either case, the bridging process begins after all endpoints have been collected for one cell. Each initially found endpoint is potentially not an endpoint at all, but merely one end of a break. To determine if this is the case, a 'search beam' (about 75 pixels wide and 65 pixels long) is projected out from each endpoint, and any pixels found within the beam (that so far have not been included in the traced skeleton) are examined to see if they may be the distal end of a break (Fig. 5). Separate 'traced' and 'not-yet-traced' bitmaps are updated, and the search beam searches only the remaining 'not-yet-traced' bitmap. Our tracing method ignores single pixels (considered to be noise) and pieces of dendrite which point in the same direction as the traced piece of a dendrite (a U-turn in this short space is unlikely, whereas, if one pixel is removed from a straight line, the two segments 'point' in *opposite* directions.) Otherwise, the first pixel found in the search beam is considered to be the distal end of the break, and a line is generated which will bridge the gap. This line is simply the shortest-distance line, as no other reliable information for reconstructing the break is available. The size of the search beam strictly limits the search area for the connection process, and has no effect on the type of operations performed within it. The size, while developed by trial-and-error, works with a wide variety of cell morphologies.

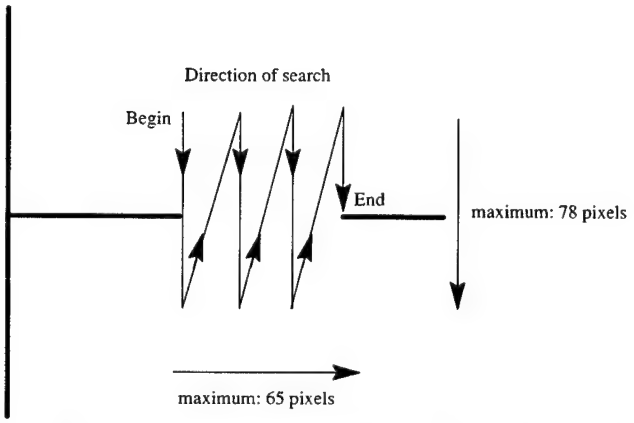

Fig. 5. Bridging a break in the dendritic tree. When tracing out from the soma, potential endpoints are recognized when a 1-pixel-wide branch has no new pixel to follow. A search path is then projected from this endpoint to determine if there are any similarly terminated pieces of dendrite nearby. Dendrites already traced, single pixels, and branches which point in the same direction (and are unlikely to be a continuation of the current branch) are ignored. If an acceptable piece is found, the second piece is accepted as simply a continuation of the first and the two are joined. Experience has shown that good results are obtained when the search path is no longer than about 75 pixels wide and 65 pixels long.

3.3.7. Detecting and breaking loops

Loops occur in neuron images — either naturally or as a side effect of the imaging process. Where they exist, where the individual dendrites begin and end must be resolved. In our system, the operator may edit the image to remove a loop when it is detected, or allow the program to do it automatically. Loop breaking is carried out in a way to minimize the possibility that the tracing algorithm completely loses track of some sub-portion of the tree. Fig. 6 displays a sample cell which has been thinned, and traced, which contains a loop that was broken automatically by our tracing procedure. Fig. 6A contains the original image, and Fig. 6B–H show the output of the thinning and tracing procedures. In Fig. 6B the cell is thinned, and the soma center noted. In Fig. 6C, the first level of branches is found (sometimes an irregularly shaped soma does not always thin down to exactly one point, which can produce one or more short dendrites; a filtering mechanism could collapse these short branches into one, if necessary).

Fig. 6D,E shows the next levels traced. Tracing stops in Fig. 6E because a loop is found. In Fig. 6F, three potential points at which the loop could be broken are shown in magnified form (for clarity, the magnified lines are shown as straight and smooth, rather than jagged and pixelized, as in the actual image). Branch points are chosen, instead of one or more continuation points because it is highly unlikely that a perfect loop will be formed by two ends precisely meeting at the endpoints with no crossover. The three magnified portions represent search areas around the branch points which are inspected for 'companions', which are other branches most likely to be continuations of one branch crossing over another. Although we have coded for ideal crossover points, which are perpendicular (shaped like a '+' sign), crossings similar to that seen in the top-right circle are found much more frequently, since dendrites themselves are not so regularly shaped and do not usually reduce to simple, regular forms. In this case, the first companion found

after searching around all three crossover points is shown in the top-right circle.

To break the loop, we remove exactly 1 pixel from each of its two tee-like branches, as shown in Fig. 6G. The completely traced cell, shown in Fig. 6H, contains exactly two level-1 branches and two level-2 branches, one of which contains this created break which is noted by the tracing program. The image is not filled in again at this point because this gap is easily detected and jumped when found. For the final display, the original connection is denoted by a line drawn between the two breaks. Although shown on a small scale here, these procedures work for much more complicated cells, as shown in Fig. 7.

Most loops can be broken automatically, and hand-editing is needed only when the image is noisy or the operator's choice of break location differs from that chosen by the program. Automatic loop breaking requires, even in the worst case, much less hand-processing than the manual approach. The worst case occurs when there is a dropout of pixels in the image in a thick process such that a 'bubble' is generated by the thinning program at or near a branch point. When this occurs, the loop breaking and later tracing processes will cause one branch to be followed and another to be removed entirely. If there is actually a large dendritic loop of any consequential size, the automatic loop-breaking process will cause a whole branch to be removed. This missing branch may be easily detected by a comparison between the original cell image and the thinned skeleton (Fig. 2D). For most cases where the digitized image is relatively noiseless, all loops are

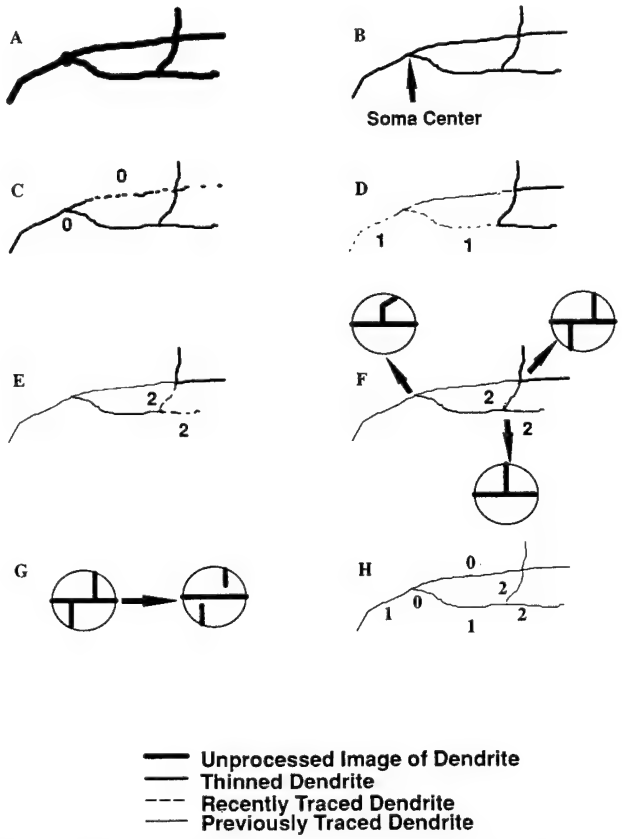

Fig. 6. Automatic loop-breaking. A: sample image. B: same image thinned, with soma center denoted. C: image with first-level branches traced. D: image with second-level branches traced. E: same image with third-level branches traced. A loop is also detected when tracing attempts to re-trace a point. F: loop contains 3 crossover points which are candidates for breaking. The top-right circle contains 2-branch points near each other, indicating that this crossover is the best candidate for breaking. G: break made at the crossover. One pixel is removed from each branch. H: traced cell. The gap caused by loop-breaking is spanned only during the output process, i.e., the gap is left open during any future tracing iteration.

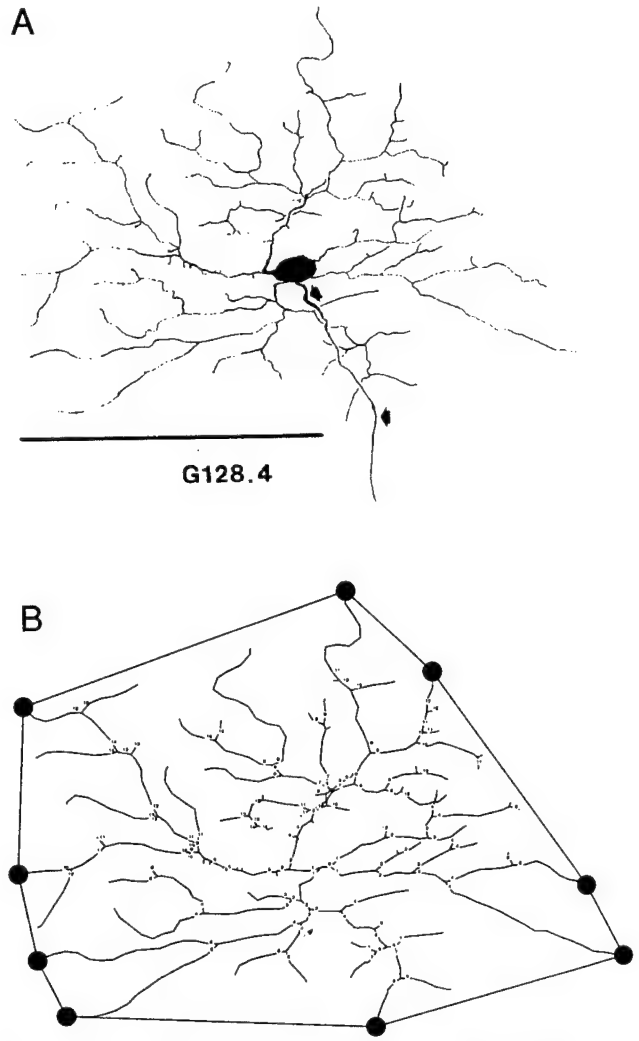

Fig. 7. Rabbit retinal ganglion cell G128-4. A: original image. B: PostScript output produced by applying the tracing procedure to (A). The filled circles in (B) are the convex hull points, which determine the smallest convex polygon (a 'rubber band'-like perimeter) enclosing the cell. Due to limitations in printing, (B) shows less resolution than the method is capable of showing.

broken automatically and all branches are traced to the end, and an accurate result set is produced with no human intervention.

3.3.8. Scale bar

In a viewing program, the user can 'click' on the ends of the scale bar with the mouse and the tracing program will automatically generate factors to convert between image coordinates (in pixels) and cell coordinates (in μm). In a relatively high signal-to-noise figure this (and axon removal, if necessary) is often the only mandatory hand-editing procedure.

3.3.9. Application to camera-lucida drawings of rabbit retinal ganglion cells

This method has been used to generate results for a number of retinal ganglion cells, and an example case is shown in Fig. 7. A rabbit cell is shown in Fig. 7A and the results of the entire process with all gaps bridged and branches labeled (the axon was trimmed off prior to tracing so it will not appear in the final drawing) are shown in Fig. 7B. The only manual intervention required for this cell was the designation of the scale bar and removal of the axon from the original Fig. 7A. In addition, the points on the convex hull are indicated with filled circles. The convex hull (Cormen, 1992), which is analogous to snapping a rubber band around the outermost endpoints of the image, serves as one estimate of the area of the dendritic field.

It takes less than 10 MB of RAM and approximately 15–45 min to process typical images which breaks down as follows: about 3 min to scan, 5–15 min to prepare, and 10 min for the first thinning/tracing pass (subsequent passes usually take less time, as most thinning and noise reduction is already done). It is easy to batch much of the work since processing passes are automatic and audio-output is used to cue the operator on completion of each pass.

3.3.10. Tracing video images

We have also generated morphological data from video images. Fig. 8A shows a gray-scale video image of a fluorescently stained cell, and Fig. 8B shows the output of the tracing program. Several filtering methods were applied in Photoshop to clean up the noise in the video image, such as a median filter, prior to application of thresholding operator to produce the bi-level image which was input to the thinning procedure.

3.4. Computation of quantitative parameters

A number of parameters are generated directly by the program. These include total and average dendritic lengths, dendritic densities, and distances and distributions of dendritic endpoints and branch points (see Amthor, 1985, for a treatment of some quantitative attributes used to classify ganglion cells). Dendritic field area is calculated by the convex hull method. Convex hull points may be thought of as those points that a rubber band stretched around the dendritic tree would touch and are almost always a subset of the

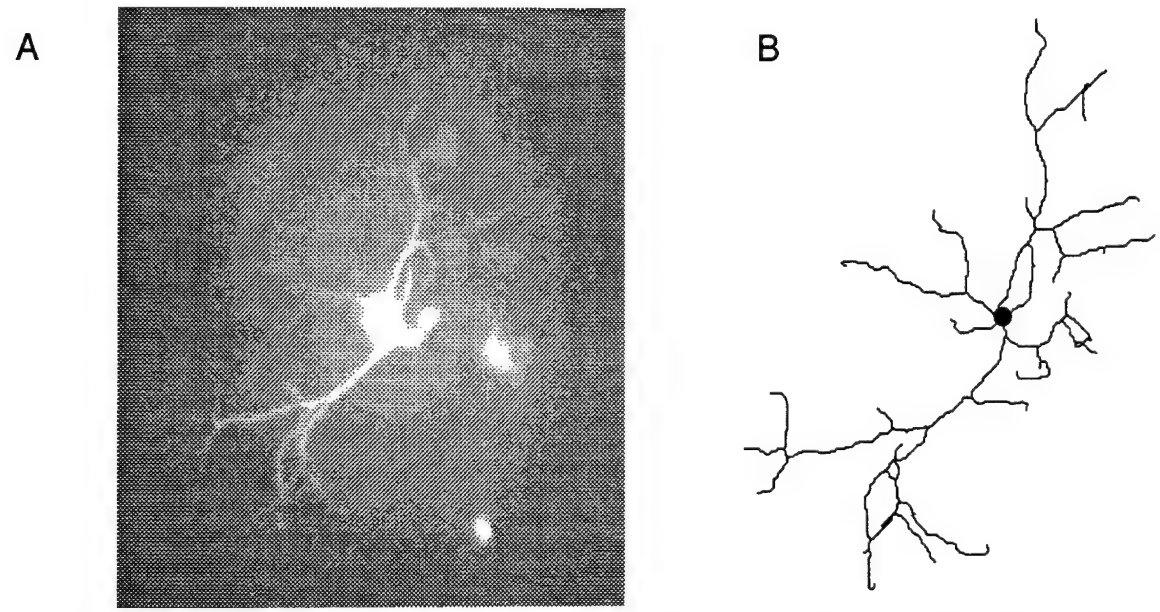

Fig. 8. A: video image of cell with hand-traced dendritic tree. B: tracing is separated by thresholding the image; only the traced color remains. C: generated tree and showing convex hull. Note that an artifact line of the video capture process does not appear in the output tracing because the pixels attaching it to the cell were removed after thinning (i.e., the whole line does not need to be deleted).

Cormen, T.H., Leiserson, C.E. and Rivest, R.L. (1987) Introduction to Algorithms, MIT Press, Cambridge, MA, 1028 pp.

Davies, E.R. (1990) Machine Vision: Theory, Algorithms, Practicalities, Academic Press, London, pp. 547.

Guo, Z. and Hall, R.W. (1984) Parallel thinning with two-subiteration algorithms, Comm. ACM, 32: 359–373.

Glaser, J.R. and Glaser, E.M. (1990) Neuron imaging with Neurolucida — a PC-based system for image combining microscopy. Comput. Med. Imaging Graphics, 14: 307–317.

Haralick, R.M. and Shapiro, L.G. (1991) Glossary of Computer Vision Terms, Pattern Recognition, 24: 69–93.

Jain, A.K. (1989) Fundamentals of Digital Image Processing, Prentice Hall, Englewood Cliffs, 569 pp.

Lindsay, R.D. (1977) Computer Analysis of Neuronal Structures. Plenum Press, New York.

Mize R.R. (Ed.) (1985) The Microcomputer in Cell and Neurobiology Research, Elsevier, New York, 481 pp.

O'Gorman, L. (1990) k×k Thinning, Comput. Vision Graphics Image Process., 51: 195–215.

Overdijk J., Uylings, H.B., Kuypers, K. and Kamstra, A.W. (1978) An economical, semi-automatic system for measuring tree structures in three dimensions, with special emphasis on Golgi-impregnated neurons. J. Microsc., 114: 271–284.

Rimmer, S. (1990) Bit-Mapped Graphics, Windcrest Books, Blue Ridge Summit, 492 pp.

Russ, J.C. (1992) The Image Processing Handbook. CRC Press, Boca Raton, FL, 445 pp.

Stewart, M.G. (1992) Quantitative Methods in Neuroanatomy, John Wiley, New York.

Villanueva, L. and Lebars, D. (1993) Computer assisted reconstruction of axonal arborizations anterogradely labeled with the *Phaseolus-vulgaris*-leukoagglutinin technique. J. Neurosci. Methods, 50: 217–224.

Zhang, T.Y. and Suen, C.Y. (1984) A fast parallel algorithm for thinning digital patterns, Commun. ACM. 27: 236–239.

dendritic terminals. To select hull points, the terminal with the minimum Y position (which guarantees that it will be a hull point) is chosen as the first hull point and all other endpoints are sorted by angle relative to that first point from the soma center. Proceeding in a counterclockwise direction, points that create a dent in the surface of the hull are discarded. Hull point area is calculated by summing the area of the triangles formed between hull points and the soma center.

4. Discussion

We have shown that, in cases where the original digitization is relatively noiseless and free of loops (such as Fig. 8), neural dendritic trees can be automatically thinned to a skeleton and traced with little human intervention. Even when human intervention is required to resolve some ambiguities, less time and skill of a technician are required using these methods than, for example, in complete hand-tracing camera-lucida drawings on a digitizing tablet. The accuracy of the automatic method can meet or exceed that of the manual method because the automated procedure for such features, as determining the soma center, is reproducible and because the accuracy of point location, such as dendritic endpoints, is equal to the original resolution of the digitized file.

The key to the automated method is the production, from the raw image file, of an accurate skeleton of the cell image. This, in turn, depends on the quality of the original image and on the use of the proper thinning technique. Original images having low resolution or high noise, such a video images, pose several kinds of difficulties. Compared to high contrast, 300 dpi bi-level scans of camera-lucida drawings, the lower resolution of 512×480 pixel video images results in some fine dendritic processes being lost at the very beginning of the procedure.

Video images also are notorious for their poor and inconsistent contrast range which has the effect of thwarting the ability of a simple operator, like a threshold, from differentiating cell from non-cell. For example, one commonly encountered problem with video microscope images is the fact that incident light intensity varies considerably across the images due to inhomogeneity in the illumination itself and absorption by out of focus structures above and below the plane of focus. Typically, for example, non-cell areas near the outer edge of the image frequently are absolutely darker than very darkly stained portions of the cell in the center of the image. Subtraction of an out-of-focus frame from the cell-in-focus frame helps this problem to some extent but also introduces other problems like blurring or removing central parts of the cell soma.

There are several changes which would improve the overall performance of the automated procedure. The bridging of gaps could be made faster and more accurate if meaningful, perhaps data-dependent, values were used for the beam width and length. Several improvements in loop breaking would be worthwhile, such as better handling of 'bubbles' at branch points and making use of image information to detect when a branch has been left off the traced tree.

Our method, as developed so far, also deals only with 2-D images, or images that have been rendered 2-D by methods such as camera-lucida drawing which deals with cell processes existing in more than one plane of focus by having the human illustrator follow processes to their terminals regardless of changes in depth in the section. We have made no attempt to deal directly with 3-D images in our system so far. However, it is conceivable that the thinning and tracing procedures could be applied to high signal-to-noise 3-D 'voxel' files (such as obtained with confocal microscopes) by extension of their operators from 2-D to 3-D neighborhoods.

Acknowledgements

This work was supported by grants to F.R.A. from the Office of Naval Research (N00014-91-J-1280) and the National Eye Institute (EY05070), and by a core grant from the National Eye Institute to the Vision Science Research Center of the University of Alabama at Birmingham (EY03039). M.F.V. would like to extend special thanks to Kevin D. Reilly for academic advising and counsel. We would like to thank Lorraine DeAngelis for technical support, Jill Gemmill for technical discussions, Darrel Tjepkes for Fig. 8, and the Department of Computer and Information Sciences for equipment support.

References

Amthor, F.R., Oyster, C.W. and Takahashi, E.S. (1983) Quantitative morphology of rabbit retinal ganglion cells. Proc. Roy. Soc. B., 217: 341–355.

Amthor, F.R. (1985) Quantitative analysis and three dimensional color reconstruction of retinal ganglion cells. In: R.R. Mize (Ed.), The Microcomputer in Cell and Neurobiology Research, Elsevier, New York, pp. 135–153.

Capowski, J.J. (1989) Computer Techniques in Neuroanatomy. Plenum, New York.

Chin, R.T., Wan, H.-K., Stover, D.L. and Iverson, R.D. (1987) A one-pass thinning algorithm and its parallel implementation, Comput. Vision Graphics Image Process., 40: 30–40.

Coleman, P.D., Garvey, C.F., Young, P.H. and Simon, W. (1977) Semiautomatic tracking of neuronal processes. In: R.D. Lindsay (ed.), Computer Analysis of Neuronal Structures, Plenum, New York, pp. 91–109.

2

Computational and Neural Constraints for the Measurement of Local Visual Motion

Norberto M. Grzywacz[1], Julie M. Harris[1] and Franklin R. Amthor[2]

[1]The Smith-Kettlewell Eye Research Institute, San Francisco and [2]University of Alabama at Birmingham,

1 PHILOSOPHY

A good starting point for the study of a particular brain function is to ask what benefits this function may bestow upon the animal. Such a question will not only motivate the inquiry, but might also place computational constraints on it. In the case of visual perception, for instance, the question might help to focus our attention on image measurements that are relevant to the animal. However, the ideal measurements to perform from a computational perspective might not coincide with the ideal measurements to perform from the brain's perspective. The brain uses computational elements, for example, neurons, synapses, and ionic channels, that might not be well suited to implement these 'ideal computations', but might instead be more suitable for other computations that have sufficient survival value to the animal. Hence, an effective inquiry into a brain function must be constrained both from computational and neural perspectives. This chapter will take this approach to explore the measurement of local visual motion in the brain. We will start the chapter (section 2) by asking the 'why' and 'what' questions, that is, we will start with the computational perspective. We ask *why* the visual system would benefit from having motion information and *what* information is available to the brain. Then, sections 3 and 4 will deal with the two main answers to the 'what' question, namely, speed and direction of visual motion. Finally, section 5 will deal with the 'how' question, by discussing the biophysical details of how direction of visual motion is measured in the retinas of turtles and rabbits.

VISUAL DETECTION OF MOTION
ISBN 0-12-651660-X

2 COMPUTATIONAL PERSPECTIVE

This section will begin by considering the computations performed by the visual system that benefit from measurements of visual motion. Then, we will discuss the fundamental variables of visual motion. The question of whether the visual system must measure all these variables with equal emphasis will be addressed in section 2.3. Finally, section 2.4 will deal with how local these measurements must be.

2.1 Why measure visual motion?

Visual-motion cues play a role in various functions of biological visual systems (Nakayama, 1985, gives a comprehensive review). For instance, when an animal is moving (egomotion), motion cues could help it avoid obstacles along the way (Gibson, 1950). In the same context, motion measurements play a role in helping the animal to find its direction of heading, that is, helping it navigate (Warren & Hannon, 1988; Hildreth, 1992). Besides aiding egomotion, visual motion measurements may also be used to determine whether an object coming towards the animal will hit it (see Chapter 12 by Cumming). This is particularly useful to escape from one's predators. In turn, if an animal is a predator or is trying to approach a mate, then motion measurements can be useful in the interception process (Lee, 1976; Reichardt & Poggio, 1976). (Of course, interception is also used in functions of more socio-biological relevance such as hitting a baseball – or perhaps we should say: in a batsman's defense of the wicket.)

All of the examples above involve analyzing a scene that is being modulated by essentially translatory motion of individual objects. However, other examples illustrate the usefulness of measurements of motion that involve rotations, multiple objects, or simply trying to bring the main portions of the image into focus. For instance, the motion of an object can be used to determine its three-dimensional structure (see Chapter 13 by Braunstein). This process could be useful in determining the shape of a head when it is shaking or when viewing a car turning at an intersection. When there are multiple objects moving in the scene, differences in measured visual motion in different portions of the scene may help the animal to parse the scene for further analysis (Nakayama & Loomis, 1974). This image parsing or segregation is useful when an animal needs to penetrate another animal's camouflage (Helmholtz, 1910/1962; Regan & Beverley, 1984). One way in which measurements of visual motion are useful for bringing the essential portions of the scene into focus is by telling the eyes where to move and how fast to move (saccades and smooth pursuit; see Chapter 15 by Krauzlis) to bring a feature of interest into the fovea (for reviews see Sparks and Mays, 1990, and the book edited by Miles and Wallman, 1993). Another way is by deblurring (Burr *et al.*, 1986), that is, by compensating for the same type of blur that occurs when one does not set the photographic camera's shutter to a sufficiently fast speed.

2.2 Fundamental variables of visual motion

In physics, the most fundamental variables of motion are velocity (the derivative of position over time) and acceleration (the derivative of velocity over time).

Consequently, it would seem valuable for an animal's visual system to determine these variables accurately. Unfortunately, the only data available to animals about motion in the external world come from the projections onto the eyes' retinas, which by being essentially two-dimensional, cannot encode directly the three-dimensionality of the world (Wheatstone, 1838; Marr, 1982).

Therefore, in visual perception, a more fundamental variable of motion might be the 'optic flow' (see Chapter 11 by M. Harris). This flow is a spatial distribution of velocity vectors that is close to the distribution obtained by projecting the three-dimensional motion vectors of a moving scene onto the retina. The usefulness of this vector field quantity has been discussed by both psychologists (for example, Gibson, 1950; Regan, 1986) and computer scientists (Koenderink & van Doorn, 1976; Longuet-Higgins & Prazdny, 1980). To mention one example of the use of optic flow, when one moves forward in a straight line, the optic flow is that of an expansion (or contraction if translating away from the scene), whose focus signals the direction of heading (see Regan *et al.*, 1986). A proposed definition of optic flow is in terms of the 'image constraint equation' $dE/dt = 0$ where E is the image's brightness (Fennema & Thompson, 1979; Horn & Schunck, 1981). This equation, which assumes that brightness varies slowly over time, defines an optic flow $\vec{v}$ from brightness as

$$\nabla E \cdot \vec{v} + \frac{\partial E}{\partial t} = 0. \tag{1}$$

(Because this is one equation and there are two variables, the horizontal and vertical components of $\vec{v}$, another constraint must be included so that it is possible to solve for $\vec{v}$. Typically, a smoothing assumption is made such that large discontinuities are not allowed (Horn & Schunck, 1981).

However, a handicap of considering optic flow as a fundamental variable of visual motion, is that definitions different from that expressed in equation 1 are possible (Grzywacz & Poggio, 1990; Verri *et al.*, 1989). The definition is not unique, since image motion can be influenced by parameters unrelated to motion, such as the reflectance properties of the viewed objects (For example, a specularity on an object – mirror-like reflection of a nearby light source – often moves in a different direction to the object itself; Grzywacz and Poggio, 1990). The non-uniqueness of local motion measurement is emphasized by the so-called 'correspondence problem' (Julesz, 1971; Ullman, 1979b). This problem is to find correspondences between image features at one instant in time and (hopefully the same) features at the next instant in time.

Nevertheless, despite its non-uniqueness, optic flow has been useful in emphasizing the importance of measuring image velocity vectors, and in particular their direction and speed components. (Optic flow equations also demonstrate the mathematical similarities between certain types of visual motion such as translatory egomotion and translatory external motion.) In addition, some definitions of optic flow require measuring image acceleration vectors (Verri *et al.*, 1989) and thus one must consider this variable too. The image velocity and acceleration variables must be measured locally as required by their derivative definition. In section 2.4 locality below, we will consider the implications of this requirement of locality.

2.3 Are all variables of visual motion equally important?

There are several reasons why visual systems may not need to measure visual motion too precisely. One is that the portion of the visual system devoted to the measurement of motion does not work in isolation. Visual motion is just one piece in the puzzle of the reconstruction of the external world (Marr, 1982). Furthermore, since visual systems have limited resources, it might not be to their advantage to try to compute all the possibly relevant variables. It might be better to compute certain variables with precision while ignoring other variables altogether, than to try to compute everything poorly (Ratliff, 1965).

One example of how the motion system is aided by another visual module is in the computation of structure from motion (Wallach & O'Connell, 1953; Ullman, 1979a, 1984; see Chapter 13 by Braunstein). On its own, this computation essentially requires that the viewed object rotates about an axis contained by the fronto-parallel plane to obtain the object's three-dimensional structure from visual motion. Even if this very specific motion occurs, the structure-from-motion system may often be unable to tell the direction of rotation because of an ambiguity in the velocity field when perspective cues are weak (Howard, 1961). The addition of stereopsis in the recovery of three-dimensional shape disambiguates the direction of rotation (Nawrot & Blake, 1991) and may allow a full recovery of the object's shape and distance (Richards, 1985; Tittle & Braunstein, 1991). Another example of how the motion system is helped by stereopsis may occur in egomotion. Although neither motion (Longuet-Higgins, 1984) nor stereo (Foley, 1980; Johnston, 1991) information can give, on their own, the absolute distance of an obstacle, the combination of egomotion and stereo can, in principle, yield this distance (Harris & Grzywacz, personal communication).

As mentioned above, due to the limited resources of the visual system, it might not be to its advantage to measure all the variables of visual motion with equal accuracy. One variable that the visual system 'should seriously consider ignoring' is image acceleration. To begin with, acceleration is the derivative of velocity over time or the second derivative of position over time. Hence, because any method or algorithm to measure derivatives practically are unstable in the sense that small changes in the initial data do not produce correspondingly small changes in the final results (Burden & Faires, 1989), and because the second derivative is a derivative of a derivative, the measurement of acceleration as a second-order derivative should be highly susceptible to noise. This problem becomes even more serious when one notices that psychophysically determined measurements of local speed are themselves very noisy (Vaina *et al.*, 1990; Bravo & Watamaniuk, 1991; Watamaniuk & Duchon, 1992). To add to these problems, in none of the computations mentioned in section 2.1 was acceleration needed. For instance, to measure contracting or expanding optic flows and thus determine direction of heading, one only needs image velocities (e.g. Rieger & Lawton, 1985; Hildreth, 1992). Similarly, the putative computation of divergence, curl and shear from optic flows could be performed from global estimates based on local velocity measurements (Werkhoven & Koenderink, 1991; Sekuler, 1992) and not necessarily from their derivatives as has been suggested (Koenderink & van Doorn, 1976; Longuet-Higgins & Prazdny, 1980). (To be fair, a possible exception to the irrelevance of acceleration might occur when a baseball outfielder has to catch a fly ball.) Therefore, if acceleration is difficult to compute and is not used for relevant

computations by visual systems, then why should it be measured? Psychophysical data strongly suggest that it is not (e.g. Gottsdanker, 1956; Schmerler, 1976).

We also argue that visual systems might be better off concentrating on measuring the direction of motion rather than speed. Firstly, it is difficult to measure the latter, since it is the magnitude of the derivative of position over time and thus requires precise spatio-temporal information. In contrast, to measure direction, one only requires two relatively imprecise position measurements (see section 4). Moreover, one can perform many important visual motion computations with directional measurements alone. For instance, it is often theoretically possible to determine the direction of one's heading during egomotion without using speed information. When 'ego-translating' one can find the optic flow's focus of expansion, and thus heading, with only the directional measurements (Figure 1A; Koenderink, 1986; Regan, 1986). Another example of visual-motion computations without speed occurs in structure-from-motion. Human patients who have lost their ability to measure speed due to a brain stroke can still recover structure from motion (Vaina *et al.*, 1990). This ability might be due to an independent recovery of the axis of rotation (Hoffman & Bennett, 1985, 1986). Another function that can be computed with directional information alone is image segregation. A sharp change of direction of motion at boundaries is

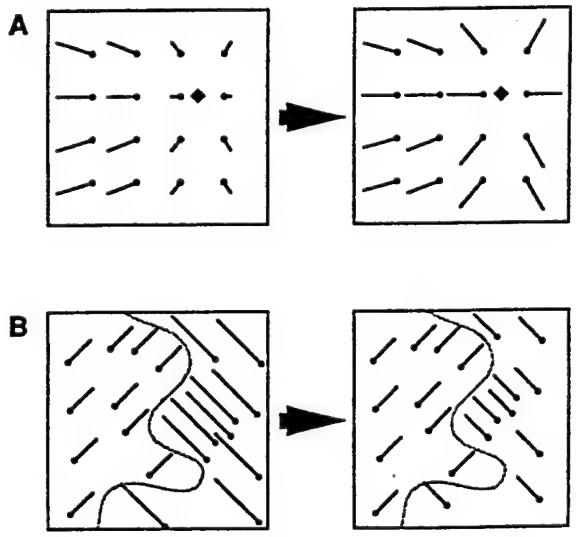

Figure 2.1 Examples of visual information from directional measurements. The left panels illustrate optic flows elicited by an ego-translation towards the black diamond (A) and two objects sliding past each other (B). The local velocity vectors in the flow begin at the small black circles, and the vectors' direction and speed are represented by the orientation and length of the associated lines respectively. The right panels are obtained from the left panels by setting the speeds to a constant value. In A, to determine the direction of heading, one must measure the location of the focus of expansion, which can be performed with directional measurements alone (right panel). In B, to find the discontinuity edge (curvy textured line), it is sufficient to detect discontinuities in the directional field.

theoretically and experimentally sufficient for the perceptual localization of the boundary (Figure 1B – Nakayama & Loomis, 1974; Baker & Braddick, 1982). Finally, directional signals could, in principle, be sufficient to mediate smooth-pursuit eye movements (Komatsu & Wurtz, 1988). These signals could encode the direction of retinal slips and thus tell the eye what direction to accelerate in to minimize slip. Following these arguments, it may not be surprising that direction is the first motion-related variable neurally encoded in visual pathways (Barlow *et al.*, 1964; Hubel & Wiesel, 1962) and that its overall measurement is quite precise (to within 1° discriminability – see Chapter 4 by McKee and Watamaniuk).

Unlike acceleration, speed signals should probably not be ignored by the visual system, since they can be useful. A recent model (Hildreth, 1992) uses both direction and speed signals to account for the 1–2° precision in the estimation of heading direction (Warren & Hannon, 1988). Furthermore, models of structure from motion based on full optic-flow information (Ullman, 1979a, 1984) suggest that this computation would benefit from speed information. Psychophysical findings indicate that one can segrerate images based only on gradients of speed signals (Hildreth, 1983; Sekuler, 1990). Both smooth pursuit and saccades could be more precise if speed signals were used in their computations (Komatsu & Wurtz, 1988; Sparks & Mays, 1990) and the visual system must somehow use speed signals to achieve effective deblurring (Burr *et al.*, 1986; Watamaniuk, 1992). Consequently, to take advantage of this useful information, visual systems compute speed locally (McKee *et al.*, 1986; Vaina *et al.*, 1990; Bravo & Watamaniuk, 1991). However, this computation is less precise than that of the direction of motion.

2.4 How local is local?

The preceding section suggested that visual systems should devote energy to the measurement of local direction and speed of motion. We now address the implications of the 'locality' requirement. Spatial locality first emerges in the context of the computation of motion, because velocity is the derivative of position over time. By definition, this derivative requires the use of positions that are infinitesimally close. However, in practice, any physical system would have to measure this derivative by using positions that are separated by a finite amount. At a minimum, these positions must be separated by the spatial resolution of the system. But sometimes, it may make sense to measure the derivatives with positions that are separated by a distance that is significantly larger than the system's resolution. This is because the relative precision of the measurement will increase as the distance increases. For instance, if one measures 1 mm with a ruler that has 1 mm resolution, then the error may be 100%, but if one measures 30 cm with the same ruler, then the error is about 0.3%. In other words, for the derivative of position over time to be known accurately, information from a large area must be used and so the location at which the derivative is measured becomes uncertain. Conversely, if only very local information is used the location is known precisely but there will be uncertainty in the value of the calculated derivative.

Hence, there is a tradeoff between locality and precision of visual motion measurement that is reminiscent of the Heisenberg uncertainty principle in quantum mechanics, where the multiplication of errors in the measurement of position and

momentum has a lower bound. This principle for measurement of visual motion will be addressed more formally in section 3.

Given this uncertainty principle in the computation of visual motion, the question arises of how much locality to give up. Visual systems cannot give up locality too much, because if they did so, they would lose their ability to locate discontinuities based on gradients of motion signals (see Figure 1B) since a more 'global' measurement would smooth (or average) out any motion discontinuities. Loss of locality would also impair the ability to detect foci of expansion (Figure 1A) and thus impair computation of direction of heading in egomotion. Perhaps most important of all, except at singularities and discontinuities, local measurements allow the visual system to decompose arbitrarily complex motions into a collection of local translations. This allows for a relatively simple interpretation of global motions by later stages of the visual pathway (e.g. Hildreth, 1992; Yuille & Grzywacz, 1988).

One way to avoid losing locality and at the same time retain precision is by using multiple scales of measurement. By this method, the visual system would make fine-scale relatively imprecise measurements of visual motion in parallel with large-scale relatively precise measurements. This could be achieved by using multiple mechanisms each tuned to a different spatial scale. The visual system does this by using motion-selective receptive fields of various sizes (Dow, 1974). However, exactly how the visual system 'chooses' what scales of processing to use under different circumstances is an open question.

2.5 Summary of computational perspective

Consideration of the types of computation that local visual-motion measurements may contribute to, and the ease of measurement of each fundamental visual-motion variable, suggested focusing our inquiry into direction and speed separately. Direction may be a more fundamental variable than speed and thus we will pay more attention to the measurement of the former. In both cases, we will consider multi-scale measurements to address the tradeoff between locality requirements and precision of measurement.

3 FORAY INTO THE MEASUREMENT OF LOCAL SPEED

In the preceding section, we argued that speed is a less fundamental visual-motion variable than direction. The argument was based on direction being neurally encoded in the visual pathway before speed, on the ease of computing direction as compared to speed, and on the large number of useful computations that one can perform based on direction measurements alone. Sections 4 and 5 will discuss the measurement of direction at length. Although direction is a more fundamental variable than speed, we decided to consider local speed and discuss models for its measurement first. We did this because, while this section will focus only on computational issues, the sections on the measurement of direction will underscore the necessity to use a multilevel approach combining the computational, behavioral and neural perspectives.

Humans can measure speed quite precisely if provided with a relatively long trajectory of motion (McKee & Welch, 1985; and see Chapter XX by McKee and

Watamaniuk). Under these conditions, the errors made in discriminating speed can be as low as 5%. This high precision seems to be achieved by integrating relatively imprecise local-speed signals over time, since local signals are available (McKee *et al.*, 1986; Vaina *et al.*, 1990; Bravo & Watamaniuk, 1991). The relative errors in the measurement of local speed have been estimated to be between 30 to 100% (Vaina *et al.*, 1990; Bravo & Watamaniuk, 1991).

Perhaps the simplest method for measuring local visual speed is by its derivative definition: find the positions of an image feature in two discrete instances in time and then compute the ratio between the positional distance and the temporal delay. This is essentially the approach proposed by Ullman in his Minimal Mapping theory (Ullman, 1979b). He proposed that the main problem facing the visual system to measure motion is to solve the correspondence problem (section 2.2). He suggested that the features correspond so as to minimize the total distance traveled. After correspondence is established, then distance and delay, and thus the velocity of a feature, can be calculated. Serious challenges to Ullman's emphasis of the correspondence problem, and thus his method to measure visual speed, have been raised by motion psychophysicists (Adelson & Bergen, 1985). They pointed out that his theory was not immediately consistent with known neural processes underlying motion perception. In addition, they argued that the correspondence problem is essentially nonexistent when one deals with real neural receptive fields, even if the stimulus motion is discontinuous (apparent motion). Finally, another difficulty with Ullman's Minimal Mapping theory is that it does not lend itself to a multiple scale analysis.

Models for the measurement of local speed based on known properties of neurons that are selective for the direction of motion do not begin with the intuitive definition of velocity based on derivatives, but are more suitable for multi-scale analysis (Adelson & Bergen, 1985; Watson & Ahumada, 1985; Heeger, 1987; Grzywacz & Yuille, 1990, 1991). These models begin by looking at the responses of a population of directionally selective (DS) neurons of different receptive-field sizes. These are neurons that can discriminate the direction of motion through the strength of their response to stimuli moving in different directions (the mechanisms underlying direction selectivity will be addressed in detail in sections 4 and 5). It is known that striate cortex neurons with larger and larger receptive-field sizes are tuned to lower and lower spatial frequencies when stimulated with sinusoidal gratings (Hochstein & Shapley, 1976; Maffei & Fiorentini, 1977; Andrews & Pollen, 1979). Moreover, different neurons tend to be tuned to different temporal frequencies of the gratings. The DS-cell-based models for local speed measurement consider a three-dimensional space whose two abcissas are the optimal horizontal and vertical spatial frequencies that drive a given DS cell, and whose ordinate is the optimal temporal frequency that drives the cell. (We denote the optimal temporal frequency by Ω_t, optimal spatial frequency by Ω_r, and DS cell's preferred direction by $\vec{u}$. Therefore, the optimal horizontal and vertical spatial frequencies are the projections of $\Omega_r\vec{u}$ onto the horizontal and vertical frequency axes respectively.) A point in this space corresponds to a DS cell. What is interesting about this space is that when a visual translation of velocity $\vec{v}$ covers the receptive fields of these cells, the optimal responses tend to fall in the plane

$$\Omega_r\vec{u}\ \ \vec{v} + \Omega_t = 0. \qquad (2)$$

Consequently, to measure local speed in DS-cell-based models, all one needs to do is to detect the slant of this plane relative to the temporal frequency axis (Figure 2; local direction can be obtained from the tilt of the plane relative to the spatial frequency axis). Several schemes to detect this plane have been proposed in the literature (Watson & Ahumada, 1985; Heeger, 1987; Grzywacz & Yuille, 1990, 1991).

To understand the origin of this plane, consider the spatio-temporal Fourier transform of a general translating image $I = F(\vec{r} - \vec{v}t)$, where F is the spatial profile of the image, $\vec{r}$ is spatial position, and t is time. The transform is

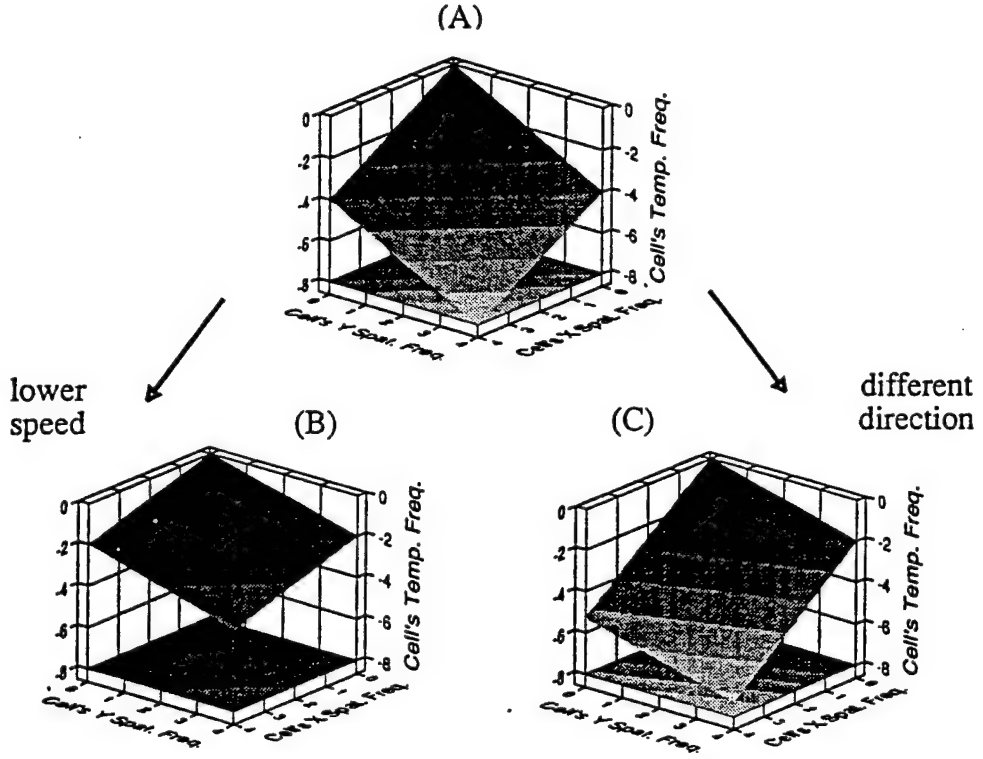

Figure 2.2 Measurement of velocity in the space of neuron parameters. Each triplet of abcissas and ordinate in this plot corresponds to a neuron in a population of directionally selective neurons. The values of the abcissas and ordinate are the neuron's optimal spatial frequency in the horizontal and vertical directions, and the optimal temporal frequency. If the neurons are stimulated with a translation, then the shaded slanted plane is where the maximal responses tend to lie. The slant of the plane from the floor (also shaded) is equal to the speed of motion. The tilt of the plane relative to the spatial-frequency axes is equal to the direction of motion. The greater slant of (A) as compared to (B) indicates that in (A) the translation is faster than in (B). While the translations in (A) and (B) have identical directions of motion (45° between vertical and horizontal), the motion in (C) has much more motion in the horizontal than vertical direction (making an angle of about 20° with the horizontal axis).

$$\tilde{I}(\vec{\omega}_r, \omega_t) = 2\pi\tilde{F}(\vec{\omega}_r)\delta(\vec{\omega}_r \cdot \vec{v} + \omega_t), \tag{3}$$

where the tilde represents a Fourier transform, $\vec{\omega}_r$ and ω_t are the spatial- and temporal-frequency variables of the transform, and δ is the Dirac delta function (where $\delta(x)$ is an infinitely sharp impulse at $x = 0$, with unit integral). Equation fourier is a multiplication of a term that depends only on $\vec{\omega}_r$ and a term that is (infinitely) sharply tuned on a plane that is very similar to the plane expressed in equation 2. (The relationship between this plane and the Fourier transform of a general translation was first pointed out by Fahle and Poggio, 1981, and then exploited by Watson and Ahumada in a model of motion detection, 1985).

The difference between the planes expressed in equations 2 and 3 is that while the variables in equation 3 belong to the stimulus's Fourier transform, the variables in equation 2 are properties of the cells themselves. Hence, in one sense, to implement a DS-cell-based model of local speed measurement, the cells must perform a sort of spatio-temporal Fourier transform of the image. A true Fourier transform integrates the image (after multiplying it with sines and cosines) over an infinite spatio-temporal range. Because cells have finite receptive fields and temporal windows, they cannot, strictly speaking, perform a true Fourier transform of the image. They must somehow perform a finite approximation of a Fourier transform.

If one think of cells as implementing a filter, as is often done, then it turns out that there is a tradeoff between the size of their receptive fields and how sharply tuned the cell can be to spatial frequency (Hochstein & Shapley, 1976; Maffei & Fiorentini, 1977; Andrews & Pollen, 1979). In other words, there is a tradeoff between how well a cell can localize a stimulus and how precise its Fourier transform of the image is. This tradeoff is the root of the uncertainty principle for localization and velocity measurements described in section 2.4. If a cell can localize a stimulus well (if it has a small receptive field), then the cell will add a lot of thickness to the optimal plane in equation 2. This thickness will result in uncertainty about the velocity estimate, since finding velocity is essentially the detection of that plane.

Is there a receptive-field or filter profile for which this tradeoff problem is minimal? It is possible to show that under a certain minimization metric, the optimal profile is the Gabor function (Gabor, 1946; Daugman, 1985). A spatio-temporal representation of this function (Grzywacz & Yuille, 1990, 1991) is

$$G(\vec{r}, t) = \frac{1}{(2\pi)^{3/2}(\sigma_r)^2(\sigma_t)} \exp\left(-\frac{|\vec{r}|^2}{2\sigma_r^2}\right)\exp(-i\Omega_r\vec{u}\cdot\vec{r}) \exp\left(-\frac{t^2}{2\sigma_t^2}\right)\exp(-i\Omega_t t), \tag{4}$$

where $\sigma_r > 0$ and $\sigma_t > 0$ are scalar parameters.

Grzywacz and Yuille (1990) argued that besides being optimal from the uncertainty perspective, the Gabor function is also optimal for motion measurements, since it is the only function that will not create maxima outside the plane described by equation 2. Also, the spatial portion of this function approximates reasonably well the spatial profiles of receptive fields in striate cortex (Jones & Palmer, 1987). Its temporal portion does not do such a good job, since it is non-causal, that is, it is non-zero at negative times. However, Grzywacz and Yuille (1990, 1991) argued that the non-

causality problem is not serious if the brain's computation of velocity is slightly delayed (< 100 ms) relative to the image's motion. Alternatively, a non-Gabor filter might be used, removing the non-causality but allowing strong responses off the plane sometimes.

4 MEASUREMENT OF LOCAL DIRECTION OF MOTION

The most basic mechanism used by the visual system to measure direction of motion is directional selectivity. A visual neuron is said to be directionally selective (DS) if back and forth motions symmetric about the middle of its receptive field elicit different responses (non-symmetric motions may cause artifactual direction selectivity – see Barlow *et al.*, 1964). For the axis along which the ratio between the responses to back and forth motions is maximal, we call the direction eliciting the largest response the preferred direction and the opposite direction the null or non-preferred direction. Such DS neurons are abundant in the retinas of insects and small-brained vertebrates (Maturana *et al.*, 1960; Barlow & Levick, 1965; Hausen, 1981), and in the visual cortex of large-brained vertebrates (Tolhurst & Movshon, 1975; Holub & Morton-Gibson, 1981).

It is unlikely that individual DS neurons compute the direction of motion on their own. The amplitudes of their responses confound the direction of motion with other visual parameters such as contrast. To disambiguate the responses, a comparison over a population of neurons is probably performed. For example, consider a pair of neurons with opposite preferred directions. Even when the contrast varies, the response of the neuron whose preferred direction is in the direction of visual motion will be larger than the response of the neuron with opposite preferred direction. Therefore, the brain can conclude that the direction of motion is not that of the latter neuron. A computation over more than two neurons (such as that proposed in the plane calculation described by equation 2) can trim the candidate directions significantly, thus constituting a precise estimate of local direction.

In the rest of this section we will not dwell further on how the output of several DS cells may be combined to measure direction. Rather, we will focus on how the brain achieves directional selectivity. The discussion will begin with theoretical preliminaries derived from studies on insects. Then, sections 4.2 and 4.3 will deal with the two main requirements raised by the theoretical preliminaries for directional selectivity, namely, spatial asymmetries and nonlinearities.

4.1 Theoretical preliminaries

The theoretical work of Reichardt, Poggio, and collaborators (Reichardt, 1961; Poggio & Reichardt, 1976) emphasized two requirements that any model of directional selectivity must fulfill: The first is a spatially-asymmetric mechanism. The second is a nonlinear mechanism to yield two different single-number responses for preferred- and null-direction responses. (Single-number responses refer to quantities like total number of spikes, as opposed to time course of the spikes. Poggio and Reichardt emphasized the necessity of computing a single number from each response to allow a

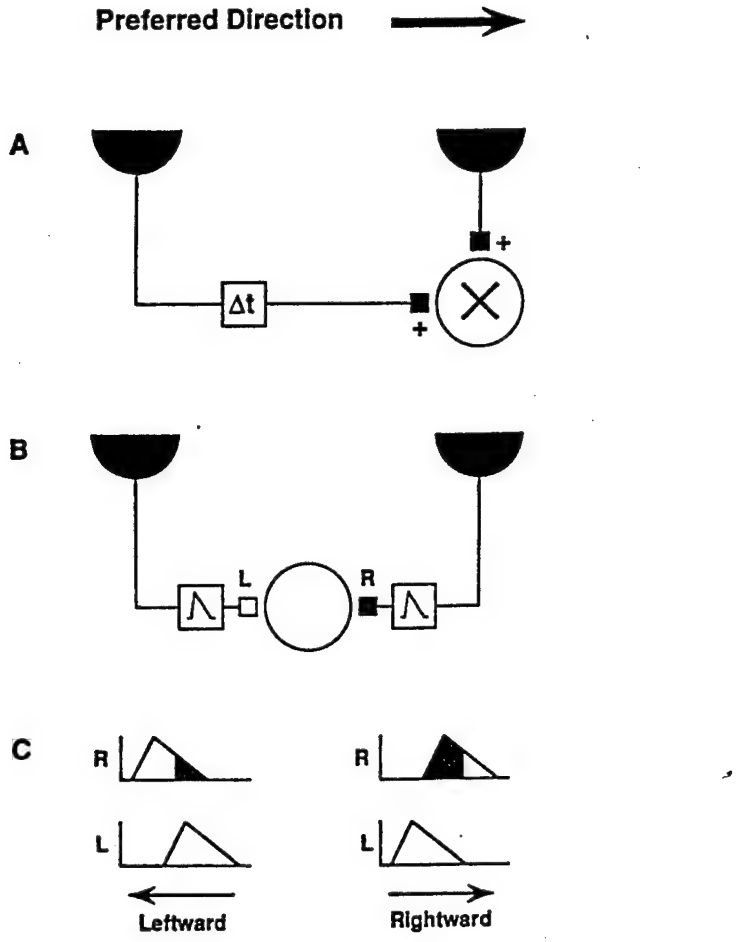

Figure 2.3 The Reichardt model for directional selectivity and a variant. A. The Reichardt model has a slow input from the left (Δt box) and a fast input from the center. The inputs are excitatory (textured squares) and the nonlinear interaction is multiplicative. For rightward, but not leftward motion, the sluggishness of the left pathway is compensated by the light reaching it before reaching the center pathway. Hence, only for rightward motion, the signals arrive at the multiplication site roughly simultaneously. The black semi-circles indicate that each input integrates information over a finite area of the image. This integration helps against aliasing by filtering out high spatial frequencies. B. This variant of the Reichardt model illustrates that a difference in the inputs' time courses (indicated by the traces inside the boxes) is not necessary for directional selectivity. It is sufficient that the inputs have a different role (indicated by the black (R) and white (L) squares) in the nonlinear interaction. C. We illustrate one example of how different roles in the nonlinear interaction could lead to direction selectivity. For a rightward motion (right of the figure), the L input precedes the R input (and vice versa for leftward motion – shown on the left of the figure). Suppose that the L input gates the R input (L input allows R input signal to be transmitted further) when the L input is sufficiently high. Then, the responses would be proportional to the textured area of the R input curves and therefore different for leftward and rightward motion.

decision on the direction of motion. They proved that if there are no nonlinearities, then the computed numbers are identical for all directions of motion. Large portions of the system computing direction selectivity could be linear (Watson & Ahumada, 1985), but at some stage, a nonlinearity is required, for instance the detection of amplitude or a decision rule.)

Figure 3A illustrates the simplest model proposed by Reichardt and colleagues (Reichardt, 1961) for insects' directional selectivity, in which inputs from two spatial locations converge onto an interaction site where these inputs are multiplied (the nonlinearity) and integrated. The inputs are spatially asymmetric, since there is only a slow signal coming from the left and a fast signal coming from the center. For rightward, but not leftward motion, the sluggishness of the left pathway is compensated for by the stimulus arriving at it first. Consequently, for rightward motion, if the speed is appropriate, both signals reach the multiplication site at roughly the same time, yielding a positive multiplication. In contrast, for leftward motion, the multiplication will yield a value close to zero.

The multiplication in Figure 3A is one of many quadratic-nonlinearity models supported by insect data. Poggio and Reichardt (1973) investigated the predictions common to all quadratic models of direction selectivity. For that purpose, they used the Volterra-series formulation. The output under such a formulation for a smooth, time-invariant, nonlinear interaction between the responses to stimuli in spatial locations a (z_a) and b (z_b) is

$$y(t) = h_{0,0} + \sum_{m=1}^{\infty} \sum_{j=0}^{m} h_{j,m-j} *^m z_a^{(j)} z_b^{(m-j)} \qquad (5)$$

where $*^m$ is the mth order convolution and where $h_{j,m-j}$ are the mth order kernels of the interaction. An mth order kernal describes the nonlinear interaction between the responses to stimuli at m different instants in time. A quadratic nonlinearity is one for which if $m \geq 3$, $h_{j,m-j} = 0$. This means that a quadratic nonlinearity describes multiplicative interactions between responses to stimuli at *pairs* of times. Multiplication and squaring are particular examples of general quadratic interactions.

Two predictions of models with only quadratic nonlinearities are frequency doubling and superposition of nonlinearities. The former is the appearance in the Fourier spectrum of the response to moving sinusoidal gratings of energy at a frequency of twice the fundamental, but not at frequencies higher than that. Superposition of nonlinearities is the property in which the nonlinear average response to a grating composed of two sinusoidal gratings of different frequencies, but whose ratio is a rational number, is equal to the sum of the responses to the individual gratings. These two properties of quadratic nonlinearities can serve as a tool to test whether a system computes direction selectivity with this type of nonlinearity (they will be used in section 4.3.1 for this purpose).

4.2 Spatial asymmetries

As mentioned in the preceding section, spatial asymmetries are one of the fundamental requirements for models of directional selectivity. Put in other words, this requirement

simply says that if a cell responds better to a motion coming from the left than to a motion coming from the right, then something must be different between left and right.

The simplest version of the Reichardt model illustrated in Figure 3A uses arguably the simplest form of spatial asymmetry possible. Inputs from only two spatial locations arrive at the site of interaction. (An input from a single location could not produce an asymmetry, of course.) To make the inputs different, thus creating an asymmetry, Reichardt and colleagues attributed different temporal properties to each input. However, in principle, there are other ways to differentiate the inputs and thus create an asymmetry (Figure 3B). For instance, if one input cannot cause a response on its own, but its activity enables (gates) a response proportional to the other input, then if the inputs have a fast rise time and slow decay, directional selectivity could be achieved (Figure 3C). Alternatively, one input could be inhibitory and the other excitatory, and their interaction nonlinear. Hence, although spatial asymmetries are necessary for directional selectivity, temporal differences between the inputs are not. This is an important point, since all models for directional selectivity presented in the literature have used temporal differences between inputs.

The spatial scale relevant for motion computations in a Reichardt model is given by the distance between the model's two inputs. Therefore, to achieve a multi-scale measurement of local direction based on this model, a visual system must compute the direction of motion several times in parallel (possibly using several different neurons), each time with the inputs separated by a different amount. An example of such a computation has been described in the literature (Reichardt *et al.*, 1988). Another relevant spatial scale illustrated in Figure 3A comes from the possible spatial low-pass filtering performed by each of the two inputs. The importance of this filtering was emphasized by van Santen and Sperling (1985) to get rid of spatial aliasing not observed in human perception of motion. To understand aliasing, note that in the absence of filtering, moving sinewave gratings of higher and higher spatial frequencies would stimulate the inputs with arbitrary phase difference, thus making the model report incorrect directions of motion (Figure 4). If, however, low-pass filtering removes signals induced by frequencies higher than one over the distance between the inputs, then the possible phase differences are small and the correct direction can be reported. Another issue emphasized by van Santen and Sperling, and also, by Reichardt and colleagues is motion opponency, that is, the comparison of cells of opposite preferred directions for the computation of absolute local direction (see also the introduction to section 4).

Another important class of models, called Motion-Energy models (Adelson & Bergen, 1985), uses a distributed spatial asymmetry (as opposed to the two-input spatial asymmetry in the Reichardt model). This distributed spatial asymmetry arises from different locations in the receptive field having slightly different time courses of response (Figure 5A). Imagine that the region of the receptive field first reached by a stimulus moving in the preferred direction has a slow response. The next region reached by the stimulus has a slightly faster response. In fact, the later a region is reached, the faster its response. Consequently, if the stimulus speed is appropriate, the time-courses of all the responses will overlap to yield a total response of large amplitude. For a motion in the opposite direction, the responses from the different regions will not overlap and thus the amplitude of the total response will be small. A model for such

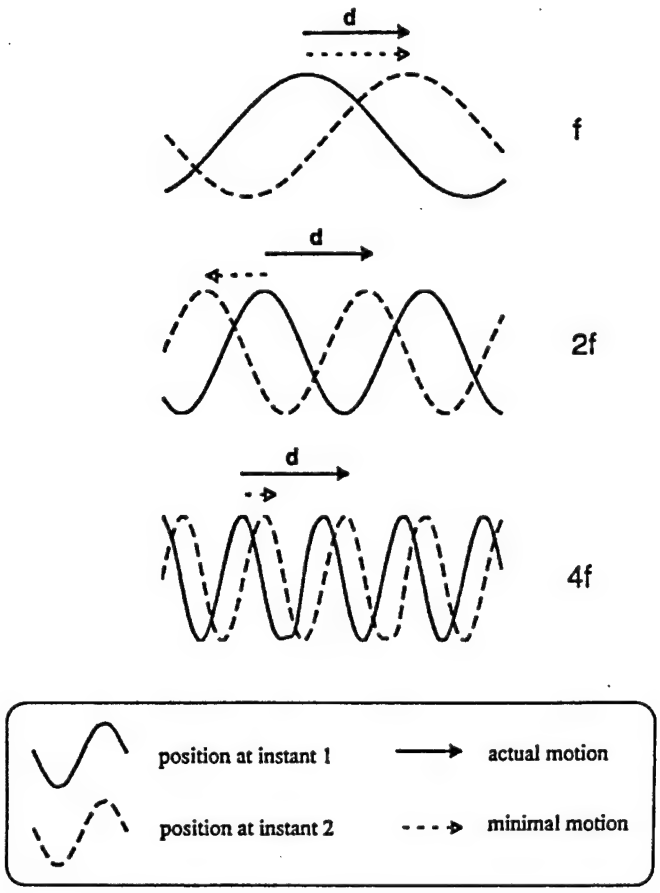

Figure 2.4 Aliasing of high spatial-frequency components. Imagine an image jumping to the right a distance d (indicated by the solid arrows). Let us concentrate on three of the image's Fourier components at frequencies f, 2f, and 4f. The solid curves show the position of these components before the jump and the dashed curves show the position after the jump. The open arrow shows the smallest displacement that would bring the Fourier components to the position of the dashed line. Hence, if the visual system bases its computations on this minimal motion, then only when the spatial frequency is sufficiently low will the actual and the computed motions coincide.

space-and-time co-dependence uses a receptive-field profile based on Gabor functions (Grzywacz & Yuille, 1990, 1991) such as that described in equation 4.

According to Motion-Energy models, directional selectivity is interpreted as orientation in space–time. This can be seen by plotting the time-course of responses of different positions of the receptive field on space–time axes as schematically illustrated in Figure 5B.

Figure 5A illustrates the most important spatial scale in Motion-Energy models. It is the largest distance in the distributed spatial asymmetry. In terms of equation 4, this scale corresponds roughly to σ_r, the size of the receptive field. However, another

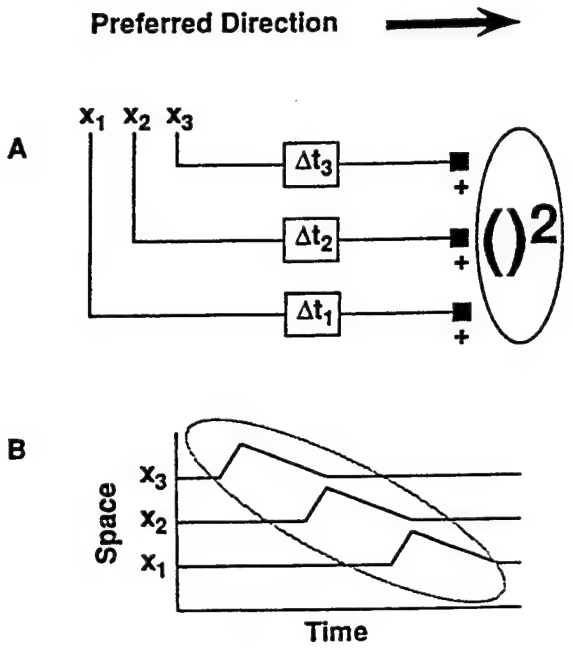

Figure 2.5 The Motion-Energy model for directional selectivity. A. This model has several slow inputs from the left (at x_1, x_2 and x_3) and no inputs from the right and center. It is required that the time-course for the inputs are such that $\Delta t_1 > \Delta t_2 > \Delta t_3$. The nonlinear interaction between inputs is a squaring operation after they are summed. For rightward, but not leftward motion, the decreasing sluggishness of the Δt_1, Δt_2, and Δt_3 pathways allows the responses from these pathways to overlap such that the total response has high amplitude. B. The Motion-Energy model (Figure 1B) can be viewed as a receptive-field profile tilted in space and time (dotted ellipse), that is, different spatial positions (for example x_1, x_2, x_3) will elicit responses with different time courses.

spatial scale that is often discussed in conjunction with Motion-Energy models is one over the optimal spatial frequency that stimulates a DS cell. In terms of equation 4, this scale corresponds roughly to $1/\Omega_r$. It turns out that these two scales are essentially proportional in real DS cells (Hochstein & Shapley, 1976; Maffei & Fiorentini, 1977; Andrews & Pollen, 1979) and thus can be interchanged. Consequently, to achieve a multiscale measurement of local direction based on Motion-Energy models, visual systems must compute the direction of motion several times in parallel, each time with a different range of spatial asymmetries or similarly, with different optimal spatial frequencies.

The above discussion of the Reichardt and Motion-Energy models does not include many of the details emphasized by the authors of the models. For instance, Adelson and Bergen (1985) postulated that pairs of space–time oriented receptive fields with different zones of excitation and inhibition (quadrature pairs) would be necessary to make the responses independent of the phase of the Fourier components of the stimuli.

Our goal in this chapter was not to discuss specific details but simply to enquire into the origins of direction selectivity. We refer the reader to Chapter 5 by Mather for more details on models of early motion detectors.

4.3 Nonlinearities

As mentioned in section 4.1, the presence of a nonlinearity is one of the fundamental requirements for models of directional selectivity. Poggio and Reichardt (1973) proved mathematically that if the system is linear, then even though the time courses of the responses to motions in different directions might be different, the system cannot decide in what direction the motion is going. This section will be divided into two subsections, the first dealing with quadratic nonlinearities and the second with non-quadratic nonlinearities.

4.3.1 Quadratic nonlinearities

The simplest type of nonlinearity is a quadratic one. This type of nonlinearity implies that the behavior of the DS system depends only on the multiplications of pairs of input values. In other words, the quadratic interaction between inputs at three or more instants in time can be understood by decomposing it into pairwise interactions. The simplicity of quadratic nonlinearities has its origin in it being the lowest order nonlinear term in a Taylor-series approximation (or, more generally, in the Volterra series – equation 5).

The Reichardt model uses as its quadratic nonlinearity the multiplication. The engineering motivation for using multiplication is to make the analogy between this model and the idea of statistical correlation complete. Hence, the Reichardt model can be thought of as computing the degree of correlation between the image in two different spatial positions in different instants in time. In contrast, the Motion-Energy model does not attempt to make a full analogy with statistical correlation. Instead of multiplication, many versions of the Motion-Energy model use a squaring operation, also a quadratic nonlinearity. Squaring polls the extent to which the signals passing through the various lateral asymmetric paths (Figure 5A) agree with one another. Multiplication and squaring emphasize different aspects of the signals. While multiplication is intended to make an analogy with the cross-correlation of two inputs (whether the input signals have the same shape), squaring is intended to emphasize the temporal overlap of signals from various inputs (whether input signals arrive together).

There are some important similarities between the behaviors of the Reichardt and the Motion-Energy models, which arise because of their common use of quadratic nonlinearities. One similarity is that these models only respond correctly to the so-called Fourier motions. These motions are such that the Fourier components of the image move coherently. (Humans can also respond to motions in which this condition is not met, prompting the postulate of additional nonlinearities – Chubb & Sperling, 1988). Besides responding correctly only to Fourier motions, another similarity between the Reichardt model (in the extended version studied by van Santen and Sperling, 1985) and the Motion-Energy model is that on average, they yield identical

responses to motion (Adelson & Bergen, 1985; van Santen & Sperling, 1985). (However, the details of the time courses of the various components of these models are different. Emerson *et al.* (1992) used these differences to argue from physiological data that the brain implements the Motion-Energy model.) The theoretical foundation for why the Extended Reichardt and Motion-Energy models share similar properties was laid down by Poggio and Reichardt (1976). They proved that a quadratic system with n inputs is equivalent to the sum of $n(n-1)/2$ two-input quadratic systems, which are all possible combinations of the n channels, two by two. Therefore, since the Motion-Energy model is a quadratic combination of multiple spatial inputs (Figure 5), it can be represented as multiple quadratic interactions of each pair of these inputs. Similarly, the Extended Reichardt model has multiple spatial inputs in the sense that each signal arriving at the quadratic interaction site is pooled from several spatial locations by the model's early spatial filtering (Figure 3). Consequently, the response of the Extended Reichardt model can also be analyzed as pairwise quadratic interactions of multiple spatial inputs.

From the computational perspective, there is a lot to be said in favor of using quadratic nonlinearities in models of directional selectivity. Besides being the simplest type of nonlinearity, quadratic interactions are optimal in terms of the 'resolution limit'. The resolving power of a DS system is determined by the spatial separation between the inputs to the system, here denoted by $\Delta\phi$. In agreement with the Shannon Sampling theorem, a periodic array of equidistant inputs can resolve uniquely the direction of movement of a periodic grating only if $\lambda \geq 2\Delta\phi$, where λ is the spatial wavelength of the grating. The resolution limit $\lambda = 2\Delta\phi$ is obtained by quadratic interactions between neighboring inputs (Poggio & Reichardt, 1976). Nonlinearities of higher order can (but will not necessarily) deteriorate the resolution limit set by the sampling theorem.

The experimental data are not conclusive about whether visual systems use quadratic nonlinearities for directional selectivity. van Santen and Sperling (1985), and Adelson and Bergen (1985) described human perceptual evidence in favor of the Reichardt and Motion-Energy models. However, all the discussed evidence hinged on the type of spatial asymmetry used by the models and their spatial scale, rather than on their nonlinearities. For instance, one widely documented piece of evidence is from the Missing-Fundamental paradigm (Adelson & Bergen, 1985; Georgeson & Shackleton, 1989). Here, a squarewave grating first jumps to the right a distance equal to $\frac{1}{4}$ of its cycle (90°) and observers see it move to the right. Next, the grating's Fourier fundamental is removed before the remaining grating makes the same jump. Now subjects see a motion to the left. This result is explained by saying that by removing the fundamental from the squarewave grating, the lowest Fourier component left has three times the spatial frequency of the fundamental. Hence, this component jumps $\frac{3}{4}$ of its cycle to the right (270°) or equivalently, $\frac{1}{4}$ of its cycle to the left (90°). Because both the Reichardt and Motion-Energy models can use motion detecting units of appropriate spatial scale to detect the Fourier component of highest amplitude (the third harmonic in this case), these models can account for the outcome of the Missing-Fundamental paradigm. However, in both cases, the explanation does not depend on the type of nonlinearity, but rather on the spatial scale of the asymmetry and on the stimulus.

Can psychophysical data argue in favor of the nonlinearity of human directional

selectivity being quadratic? The task seems hard, since even if the relevant interactions are quadratic, other postulated nonlinearities such as half-wave rectification (Albrecht & De Valois, 1981) or inhibitory normalization (Heeger, 1993) might make the visual system's response appear non-quadratic. Conversely, even if the relevant interactions are higher order than quadratic, noise in the system would tend to get rid of the higher order nonlinearities, making the system appear more quadratic than it is. Nevertheless, Adelson and Bergen (1985), who analyzed the Motion-Energy model's psychophysical predictions with a quadratic nonlinearity for the sake of simplicity, argued that interaction at the output of the model (Figure 5) should probably not be quadratic. Their argument was that a quadratic nonlinearity would make the dynamic range of DS cells small. For example, a threefold increase in input would cause an almost tenfold increase in output, quickly forcing the cell's response out of its dynamic range.

Behavioral and physiological data in flies, and physiological data in cat striate cortex suggest that quadratic nonlinearities are used in these systems' DS cells. For example, in the fly, the optomotor reflex (turning in the direction of a visual motion) is independent of the relative phase of the Fourier components of the moving stimulus (phase invariance), as predicted by quadratic models (reviewed by Poggio & Reichardt, 1976). The evidence for quadratic nonlinearity in cat cortex comes from measurement of Wiener kernels (which resemble the Volterra kernels described above) by Emerson *et al.* (1992). In their data, kernels of order higher than second were found to be negligible.

In contrast to results in the fly and in cat cortex, experiments with the rabbit retina showed that the nonlinearity mediating directional selectivity is probably not quadratic (Grzywacz *et al.*, 1990). In particular, the retina's DS cells failed the frequency-doubling and superposition-of-nonlinearity tests described in section 4.1. The authors of the rabbit retina study cautioned that their results do not imply that there is a difference in the type of nonlinearity used in the directional selectivity of rabbits, flies, and cats, since the tests of quadratic nonlinearity applied to the latter two species might not have been sufficiently strong. For instance, a previous theoretical study showed that non-quadratic nonlinearities do not violate phase invariance grossly (Grzywacz & Koch, 1987), which thus might have appeared to hold in the fly experiments, even if it did not. Furthermore, the amplitude of kernels falls fast with the kernels' order (as do the coefficients of high order terms in a Taylor expansion), and thus the kernels with order higher than second might be difficult to detect.

4.3.2 Non-quadratic nonlinearities

From the preceding discussion, one may conclude that quadratic nonlinearities do not apply to DS cells in the rabbit retina, and might not even apply to DS cells in fly and in cat cortex. Why might visual systems not always use a nonlinearity that is the simplest and the optimal from a sampling-resolution perspective? One possible answer (mentioned above) is that quadratic nonlinearities are not favorable in view of a neuron's limited dynamic range (Adelson & Bergen, 1985). Another answer is that it is hard to implement quadratic nonlinearities with the biophysical processes available to neurons. The simplest way to implement this nonlinearity would be to restrict the inputs to the DS cells to small values, thus making the contribution of high order

nonlinearities negligible (as in a Taylor-series approximation, when high order terms are neglected). However, Grzywacz and Koch (1987) analyzed the main biophysical mechanisms thought to be involved in directional selectivity, using criteria like frequency doubling and superposition of nonlinearities, and concluded that a small-signal approximation to a quadratic nonlinearity is not practical. They showed that the signal would have to be so small that it would be buried in the noise. We want to stress, however, that the problem of using quadratic nonlinearities is not a fundamental one, but arises from implementational difficulties.

If not quadratic, then what sorts of nonlinearities may be involved in directional selectivity? For the rabbit retina, the seminal work of Barlow and Levick (1965) suggested the involvement of a spatially-asymmetric nonlinear inhibitory process, which they called veto inhibition. Figure 6 illustrates their model in which the spatial asymmetry is due to inputs only coming from the right (inhibitory and slow) and center (excitatory and fast). The model generates directional selectivity, because when the motion comes from the right, but not the left, the sluggishness of the inhibitory pathway makes the signals from inhibitory and excitatory pathways arrive at about the same time. Hence, the excitatory signal is vetoed by the inhibitory signal. Recent experiments have shown that the underlying inhibitory nonlinearity is not all-or-none (as would be implied by the term 'veto'), but rather, it divides the excitatory response by a factor that is monotonically related to the stimulus contrast (Amthor & Grzywacz, 1991, 1993). Therefore, the nonlinearity involved in the rabbit retina directional selectivity is a division-like inhibition (Figure 6).

Striate-cortex investigators are still debating whether a nonlinear inhibitory mechanism also underlies cortical directional selectivity. Reid *et al.* (1991) indicated that, for non-preferred directions, an inhibitory mechanism might suppress responses.

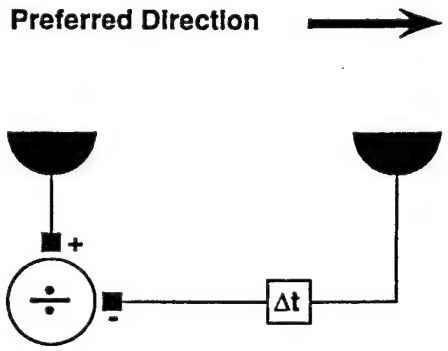

Figure 2.6 The Barlow and Levick model for retinal directional selectivity. This model has a slow input from the right and a fast input from the center. The center input is excitatory and the slow input causes a nonlinear inhibition (black box). For leftward, but not rightward motion, the sluggishness of the right pathway is compensated by the light reaching it before reaching the center pathway. Therefore, the signals arrive at the interaction site roughly simultaneously, and the inhibition vetoes the excitation. Recent data indicated that the inhibition is division-like (÷), rather than subtraction-like or all-or-none veto.

They suggested that this mechanism might be nonlinear inhibition similar to that which Barlow and Levick proposed for retinal directional selectivity. Reid *et al.*'s interpretation for cortical inhibition shares its asymmetry with the mechanism suggested by Douglas and Martin (1992) in their model of cortical directional selectivity. However, the nonlinearity underlying Douglas and Martin's 'functional microcircuit' for cortex is positive feedback mediated by intracortical excitation, which is prevented from being 'ignited' by relatively weak, and essentially linear inhibition. In contrast, Heeger (1993) reinterpreted Reid *et al.*'s data by suggesting that the non-preferred-direction suppression might be due to a cortical inhibitory network devoted to normalizing neural responses.

If the mechanism mediating cortical directional selectivity is a division-like inhibition as in the retina, then this mechanism might be an implementation of a computational model of directional selectivity called the Gradient model (Marr & Ullman, 1981; Harris, 1986). This model computes image velocity, and thus direction of motion as the ratio between temporal and spatial gradients, as suggested by equation 1. Because the model requires a division, a division-like inhibition could implement it (Poggio, 1983; Harris, 1986). (Marr and Ullman, (1981) showed that one can also implement the Gradient model with an 'And' operation instead of a division-like nonlinearity.)

Finally, another nonlinearity that has been frequently mentioned in the literature in the context of directional selectivity is threshold (Grzywacz & Koch, 1987). It could replace the multiplication or the squaring in Reichardt and Motion-Energy models respectively. In this case, during preferred, but not null-direction motions, the signals arriving at the interaction site would temporally coincide and their sum would cross threshold. The nice feature of this model is that above threshold, the responses could behave linearly as reported in early studies of cortical directional selectivity (Albrecht & De Valois, 1981; Reid *et al.*, 1987). However, an exclusive threshold mechanism for directional selectivity would have the disadvantage of preventing responses at low stimulus contrasts. At these contrasts, regardless of whether the motion is in the preferred or null direction, the signals would be too small to cross threshold.

5 BIOPHYSICS OF RETINAL DIRECTIONAL SELECTIVITY

In section 4.3.1, we provided two reasons for why, despite being the simplest nonlinearity and optimal from a sampling-resolution perspective, a quadratic mechanism might not be used by biological visual systems computing directional selectivity. The first reason was that a quadratic nonlinearity will often cause the output to be beyond the dynamic range of neurons. The second reason was that it is difficult to implement a quadratic nonlinearity with the biophysical elements available to neurons. These reasons emphasize that the mechanisms used in a particular computation, in this case directional selectivity, are not just constrained by the computation itself but also by neural limitations. Consequently, we feel that to understand what is involved in the computation of local motion, it is important to consider an example of a computation of local motion that is being worked out in as much biophysical detail as possible. The example we chose is that of retinal directional selectivity. We begin with a section describing the experimental background. This section will emphasize

the importance of a nonlinear, GABAergic, inhibitory mechanism. The next section presents the first detailed biophysical model proposed in the literature, the shunting-inhibition model. Section 5.3 argues that there are serious experimental challenges to this model, and to the Barlow and Levick model. This argument is followed by a section proposing an alternative biophysical model for retinal directional selectivity.

5.1 Experimental preliminaries

In their classical investigation of the On–Off DS ganglion cells of the rabbit retina, Barlow and Levick (1965) showed the importance, for directional selectivity, of inhibition within the excitatory receptive field center. In their two-slit apparent-motion experiments, they demonstrated that turning on and off two spatially separated slits at some appropriate delay, in a manner similar to that which yields apparent motion illusions in humans, elicited direction-associated, asymmetric responses from the On–Off DS ganglion cells. When the two-slit apparent motion corresponded to the null direction, the number of spikes elicited by the second slit was much smaller than that elicited by the second slit when it was presented alone. This reduction occurred even though the response to the first slit itself was excitatory. The inhibitory effect of the first slit on the second was not due to saturation, could be observed virtually everywhere within the excitatory receptive field center, and was effective for interslit distances that were much less than the width of the excitatory center of the receptive field. Barlow and Levick concluded from these and similar data that direction-of-motion response asymmetry was computed by numerous, small 'subunits', approximately 0.5° wide, replicated across the excitatory receptive field center. The mechanism for the motion asymmetry was postulated to be a delayed inhibitory effect propagated asymmetrically only in the null direction (see Figure 6).

Experiments by Wyatt and Daw (1975) and more recently, by Amthor and Grzywacz (1993) quantifed the properties of the inhibitory mechanism mediating directional selectivity in rabbit. The impulse response of the inhibition lasts between 0.5 and 1 second. In response to a long step, rather than a flash of light, the inhibition is sustained. Although the null-direction inhibition is strongest for short interslit distances (on the order of those postulated for Barlow and Levick's subunits), it is still quite effective for interslit distances larger than half the size of the excitatory receptive field center. In On–Off DS ganglion cells, directional selectivity appears to be computed independently for light (On) and dark (Off) regions of moving objects or textures.

Amthor and Grzywacz (1993) also investigated whether the inhibitory interaction with excitation was linear, by determining the contrast dependency of the interaction. If the interaction between null-direction inhibition and excitation were linear, such as a subtraction (which would have to be followed later by some nonlinearity essential for the directional selectivity), increasing the contrast of the first (inhibiting) slit in a two-slit experiment, should cause a downward shift (subtraction) in the response versus contrast function of the second slit. On the other hand, nonlinear interactions could cause changes in the shape of the response versus contrast function. For example, a shunting-inhibition mechanism (Torre & Poggio, 1978) would tend to divide the response versus contrast function by a constant factor. The data showed that

the contrast dependency of the null-direction inhibition is division-like, rather than subtraction-like.

Pharmacological studies in rabbit and turtle retina indicated that the inhibitory neurotransmitter gamma-aminobutyric acid (GABA) (via $GABA_A$ receptors) mediates null-direction inhibition in DS ganglion cells (Caldwell *et al.*, 1978; Ariel & Adolph, 1985). In the presence of picrotoxin, a GABA antagonist, the null-direction responses of the DS ganglion cells increased to levels similar to the levels elicited by preferred-direction motion. Similar experiments using antagonists to glycine (such as strychnine) showed that glycine had little specific effect on directional selectivity in either the On–Off or On DS ganglion cells of the retina.

An important question about the mechanism of null-direction inhibition is its site of action: does the null-direction inhibition act on the ganglion cell itself or at some presynaptic site? A ganglion-cell mechanism might be evidenced by inhibitory conductances and perhaps hyperpolarizations during null-direction motions in intracellular recordings. Miller (1979) and Werblin (1970) reported such hyper-polarizations in On–Off DS ganglion cells of rabbit and mudpuppy respectively. However, other recordings in these and other species have not exhibited such hyperpolarizations. Amthor *et al.* (1989) observed small depolarizations during null-direction motion in On–Off DS ganglion cells of the rabbit. Similar depolarizations for null-direction motion have also been observed in experiments with turtle (Marchiafava, 1979) and frog (Watanabe & Murakami, 1984).

These studies indicate the possible existence of a direct inhibitory input onto the DS ganglion cell. However, they do not settle the question of whether the inhibitory input mediates directional selectivity or has a different role. In section 5.3 we will discuss recent patch-clamp data indicating that the latter is correct in turtle. Before that, we will describe detailed biophysical models of the inhibitory mechanism of retinal directional selectivity, which motivated the patch-clamp studies.

5.2 Shunting inhibition mechanism for directional selectivity

Torre and Poggio (1978) proposed a biophysical implementation of the nonlinear inhibition advanced by Barlow and Levick. Their rationale was based on retinal directional selectivity being elicited by motions spanning short distances almost anywhere inside the receptive field (see preceding section). Torre and Poggio suggested that this subunit-like behavior could be accounted for by each subunit corresponding to a branch of the DS ganglion cell's dendritic tree. To keep the computation constrained to each branch, they suggested that the inhibition mediating retinal directional selectivity works through a synapse that causes local changes of membrane conductance (shunting inhibition) and little hyperpolarization. To do so, the synapse would have its reversal potential near the cell's resting potential. To understand how such a synapse works, consider a patch of membrane receiving excitatory (g_e) and shunting inhibitory (g_i) synaptic conductances. Setting the resting and inhibitory reversal potentials to zero (without loss of generality), the voltage V obeys:

$$C\frac{dV(t)}{dt} + (g_e(t) + g_i(t) + g_{leak})V(t) = g_e(t)E_e + g_{leak}E_{leak} \qquad (6)$$

where C is membrane capacitance, g_{leak} is the membrane's leak conductance, and E_e and E_{leak} are reversal potentials of g_e and g_{leak} respectively. When g_i is large, that is, $g_i \gg g_e, g_{leak}$, then V falls rapidly towards the following equilibrium ($dV/dt \to 0$) value:

$$V(t) \to \frac{g_e E_e + g_{leak} E_{leak}}{g_i} \tag{7}$$

which is nearly zero, because g_i is large. Therefore, this inhibition is division-like, rather than subtraction-like.

Torre and Poggio also pointed out that a shunting-inhibition mechanism for vertebrate retinal directional selectivity might be consistent with the quadratic nonlinearity observed in insects. Their argument was that for sufficiently low contrasts, one can neglect the higher order nonlinearities (equation 5), as in Taylor-series approximation.

5.3 Problems with previous models for retinal directional selectivity

The involvement of shunting inhibition in vertebrate retinal directional selectivity has been supported experimentally by the inhibitory mechanism mediating retinal directional selectivity in rabbit being division-like (see section 5.1). Moreover, as pointed out in section 5.1, there is evidence for a direct shunting inhibitory input onto the DS ganglion cell, as postulated by the Torre and Poggio model.

However, recent experiments did not support other aspects of the Torre and Poggio model. A quadratic approximation is not valid even for the smallest contrasts (Grzywacz *et al.*, 1990). This was demonstrated by the failure of rabbit DS ganglion cells in the frequency-doubling and superposition-of-nonlinearities tests. (Previously, Grzywacz and Koch (1987) argued theoretically that the quadratic approximation for shunting inhibition would probably not be valid under physiological conditions.) Furthermore, a whole-cell patch-clamp experiment by Borg-Graham and Grzywacz (1992) casts doubt on whether the relevant inhibition acts on the DS ganglion cell of turtle. In whole-cell patch-clamp recordings, in which there was no ATP or Mg^{2+} in the electrode, direct inhibition of the ganglion cell was blocked. Under these conditions, ganglion cells maintained directionality despite lack of inhibition. Borg-Graham & Grzywacz concluded that the site of the nonlinear inhibitory mechanism is in an amacrine cell's dendrite, since its origin appears not to be in bipolar (Werblin, 1970; Marchiafava, 1979) or ganglion cells (Borg-Graham and Grzywacz, 1992), and one does not observe it in amacrine-cell somas (Werblin, 1970; Marchiafava, 1979). (The direct inhibition onto the DS ganglion cells in turtle probably mediates other functions than directional selectivity, such as gain control.)

Recent data also challenge the Barlow and Levick model. As pointed out in section 5.1, pharmacological evidence indicates that the inhibition mediating retinal directional selectivity is GABAergic via $GABA_A$ receptors. Smith *et al.* (1991, 1994) extended the analysis of the effect of picrotoxin on turtle retinal directional selectivity. They studied this effect as a function of contrast and speed of a continuously moving slit, and for apparent motions. Their data showed that picrotoxin does not eliminate directional selectivity in every single cell. In 28% of the DS ganglion cells,

the preferred and null directions were actually reversed under picrotoxin. In 28% of the cells, directional selectivity was maintained despite saturating concentrations of picrotoxin. From these results, Smith *et al.* suggested that GABA does not mediate directional selectivity by being at the output of a synapse whose receptive field is asymmetric (as the Barlow and Levick model would suggest). Otherwise, GABA antagonists should eliminate directional selectivity and most certainly, should not reverse it.

Finally, the postulate of an exclusive inhibitory mechanism of retinal directional selectivity is not correct. Grzywacz and Amthor (1993) expanded earlier experiments of Barlow and Levick (1965) to find that if the spatio-temporal parameters of the stimulus are appropriate, then there is a strong preferred-direction facilitation. They also obtained evidence (based on apparent-motion protocols) that the facilitatory effect is not entirely due to non-specific mechanisms such as ganglion-cell spiking threshold. In addition, facilitation is not just dis-inhibition. When facilitatory and inhibitory effects were disentangled with appropriate control of stimulus parameters such as the use of steps, rather than flashes of light, Grzywacz and Amthor showed that the maximal strength of inhibition was only slightly larger (by a factor of about 1.30) than the maximal strength of facilitation across a large range of contrasts (10 to 70%). Maximal strength of inhibition (faciliation) is defined as the maximal reduction (increase) in the number of spikes illicited by the second frame of the apparent motion. Because facilitation and inhibition have comparable maxima under some conditions, one cannot neglect the contributions of facilitation to the properties of retinal directional selectivity.

5.4 A new model for retinal directional selectivity

Vaney (1990), and Borg-Graham and Grzywacz (1992) independently proposed new models for retinal directional selectivity that overcome the difficulties discussed in the previous section. Figure 7 illustrates some of the common points of the Vaney, and Borg-Graham and Grzywacz models. They are similar to the Reichardt model (Figure 3A) in that the spatial asymmetry is excitatory, that is, the inhibitory mechanism is spatially *symmetric*. However, different than that model, the nonlinearity is not quadratic, but rather inhibitory, as in the Barlow and Levick model, and of the shunting type, as in the Torre and Poggio model. Based on their patch-clamp results, Borg-Graham and Grzywacz suggested that the inhibition acts on an amacrine cell's dendrite. Based on anatomical findings, Vaney emphasized that this amacrine dendrite might belong to the cholinergic starburst amacrine cell. Because this cell exists in two subpopulations, one responding to light onset and another responding to light offset (Famigletti, 1983, 1991), directional selectivity would be computed separately for light (On) and dark (Off) regions of moving objects or textures, this is consistent with available data (see section 5.1).

Computer simulations with this model show that it can generate retinal directional selectivity in the dendrites of an amacrine cell without leading to retinal directional selectivity in its soma (Borg-Graham & Grzywacz, 1992). In addition, simulations show that the model can account for reversals of preferred and null directions under picrotoxin as a result of saturation of the synapse between the amacrine dendrite and

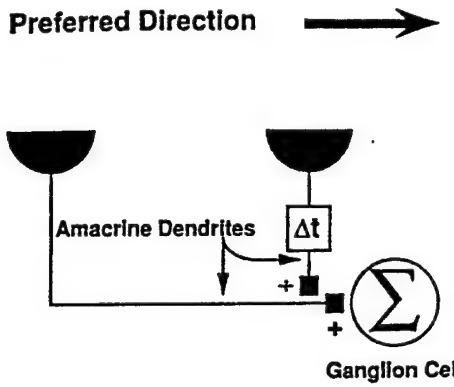

Figure 2.7 An amacrine-cell model for retinal directional selectivity. This model is similar to the Reichardt model in that the asymmetry is excitatory. But this model's nonlinearity is inhibitory, as in the Barlow and Levick model. Because it resulted from detailed retinal studies, one can identify in this model the underlying cellular processes. The ganglion cell sums ($\sum$) the inputs from several asymmetric excitatory amacrine dendrites, which in turn, are inhibited by shunting inhibitory (amacrine) processes.

DS ganglion cell. Finally, the model can account for preferred-direction facilitation as, for example, synaptic facilitation. Such a facilitatory mechanism is consistent with an extension of facilitation outside the ganglion cell's dendritic tree (Grzywacz & Amthor, 1993) without an extension of its excitatory receptive field (Amthor *et al.*, 1984; Amthor *et al.*, 1989; Yang & Masland, 1992).

6 CONCLUSIONS

We have argued that because of computational constraints, visual systems do not try to compute detailed and precise optic flows. Rather, they focus on the measurement of direction of local motion and estimate local speed roughly from the spatial and temporal properties of directionally selective neurons. To measure direction, directionally selective neurons must use a spatially asymmetric process and a nonlinearity. Although from a computational perspective, the latter should ideally be quadratic, neural mechanisms are not suitable for it, for practical reasons. Inspection of retinal directional selectivity, an example of a system for which much anatomical, physiological, and pharmacological data are available, reveals that local direction measurement might be based on a division-like inhibitory process. In the retina, amacrine-cell dendrites might be the substrate of spatial asymmetry.

The general lesson is that to understand a visual computation, or more generally, a brain computation, it is at least useful, if not necessary, to use a multi-level approach combining the computational, behavioral, and neural perspectives.

ACKNOWLEDGMENTS

Support for this work came from a grant from the Office of Naval Research (N00014-91-J-1280), from grants from the National Eye Institute (EY08921) and Air Force Office of Sponsored Research (F49620-92-J0156), and an award from the Paul L. and Phyllis C. Wattis Foundation to N.M.G., from a grant from the National Eye Institute (EY05070) to F.R.A., from a Human Frontiers Science Program Organisation Long-term Fellowship to J.M.H., and from a core grant from the National Eye Institute to Smith-Kettlewell (EY06883). We thank Suzanne McKee for helpful comments on the manuscript.

REFERENCES

Adelson, E. H. & Bergen, J. R. (1985). Spatio-temporal energy models for the perception of motion. *J. Opt. Soc. Am. A*, **2**, 284–299.

Albrecht, D. G. & De Valois, R. L. (1981). Striate cortex responses to periodic patterns with and without the fundamental harmonics. *J. Physiol.*, **319**, 497–514.

Amthor, F. R. & Grzywacz, N. M. (1991). The nonlinearity of the inhibition underlying retinal directional selectivity. *Vis. Neurosci.*, **6**, 197–206.

Amthor, F. R. & Grzywacz, N. M. (1993). Inhibition in On-Off directionally selective ganglion cells in the rabbit retina. *J. Neurophysiol.*, **69**, 2174–2187.

Amthor, F. R., Oyster, C. W. & Takahashi, E. S. (1984). Morphology of ON–OFF direction selective ganglion cells in the rabbit retina. *Brain Res.*, **298**, 187–190.

Amthor, F. R., Takahashi, E. S. & Oyster, C. W., (1989). Morphologies of rabbit retinal ganglion cells with complex receptive fields. *J. Comp. Neurol.*, **280**, 97–121.

Andrews, B. W. & Pollen, D. A. (1979). Relationship between spatial frequency selectivity and receptive field profile of simple cells. *J. Physiol.*, **287**, 163–176.

Ariel, M. & Adolph, A. R. (1985). Neurotransmitter inputs of directionally sensitive turtle retinal ganglion cells. *J. Neurophysiol.*, **54**, 1123–1143.

Baker, C. L. & Braddick, O. J. (1982). Does segregation of differently moving areas depend on relative or absolute displacement? *Vision Res.*, **22**, 851–856.

Barlow, H. B. & Levick, W. R. (1965). The mechanism of directionally selective units in rabbit's retina. *J. Physiol.*, **178**, 477–504.

Barlow, H. B., Hill, R. M. & Levick, W. R. (1964). Retinal ganglion cells responding selectively to direction and speed of motion in the rabbit. *J. Physiol.*, **173**, 377–407.

Borg-Graham, L. J. & Grzywacz, N. M. (1992). A model of the direction selectivity circuit in retina: Transformations by neurons singly and in concert. In T. McKenna, J. Davis & S. F. Zornetzer (Eds.) *Single Neuron Computation*, pp. 347–375. Academic Press, Orlando, Florida, USA.

Bravo, M. J. & Watamaniuk, S. N. J. (1991). Speed segregation and transparency in random dot displays. *Invest. Ophthalmic. Vis. Sci.*, **33**, 1050.

Burr, D. C., Ross, J. & Morrone, M. C. (1986). Seeing objects in motion. *Proc. R. Soc. Lond. B*, **227**, 249–265.

Caldwell, J. H., Daw N. W. & Wyatt H. J. (1978). Effects of picrotoxin and strychnine on rabbit retinal ganglion cells: lateral interactions for cells with more complex receptive fields. *J. Physiol.*, **276**, 277–298.

Chubb, C. & Sperling, G. (1988). Drift-balanced random stimuli: a general basis for studying non-Fourier motion perception. *J. Opt. Soc. Am. A*, **5**, 1986–2006.

Daugman, J. G. (1985). Uncertainty relation for resolution in space, spatial frequency, and orientation optimized by two dimensional visual cortical filters. *J. Opt. Soc. Am. A*, **2**, 1160–1169.

Douglas, R. J. & Martin, K. A. C. (1992). Exploring cortical microcircuits: a combined anatomical, physiological, and computational approach. In T. McKenna, J. Davis & S. F. Zornetzer (Eds.) *Single Neuron Computation*, pp. 381–412. Academic Press, Orlando, Florida, USA.

Dow, B. M. (1974). Functional classes of cells and their laminar distribution in monkey visual cortex. *J. Neurophysiol.*, **37**, 927–946.

Emerson, R. C., Bergen, J. R. & Adelson, E. H. (1992). Directionally selective complex cells and the computation of motion energy in cat visual cortex. *Vision Res.*, **32**, 203–218.

Fahle, M. & Poggio, T. (1981). Visual hyperacuity: Spatio-temporal interpolation in human vision. *Proc. R. Soc. Lond. B.*, **213**, 451–477.

Famiglietti E. V. (1983). On and Off pathways through amacrine cells in mammalian retina: the synaptic connections of 'starburst' amacrine cells. *Vision Res.*, **23**, 1265–1279.

Famiglietti, E. V. (1991). Synaptic organization of starburst amacrine cells in rabbit retina: Analysis of serial thin sections by electron microscopy and graphic reconstruction. *J. Comp. Neurol.*, **309**, 40–70.

Fennema, C. I. & Thompson, W. B. (1979). Velocity determination in scenes containing several moving objects. *Comput. Graph. Image Proc.*, **9**, 301–315.

Foley, J. M. (1980. Binocular distance perception. *Psychol. Rev.*, **87**, 411–434.

Gabor, D. (1946). Theory of communication. *J. Inst. Electr. Eng.*, **93**, 429–457.

Georgeson, M. A. & Shackleton, T. M. (1989). Monocular motion sensing, binocular motion perception. *Vision Res.*, **29**, 1511–1523.

Gibson, J. J. (1950). *The Perception of the Visual World.* Houghton-Mifflin, Boston, Mass.

Gottsdanker, R. M. (1956). The ability of human operators to detect acceleration of target motion. *Psychol. Bull.*, **53**, 477–487.

Grzywacz, N. M. & Amthor, F. R. (1993). Facilitation in On-Off directionally selective ganglion cells in the rabbit retina. *J. Neurophysiol.*, **69**, 2188–2199.

Grzywacz, N. M. & Koch, C. (1987). Functional properties of models for direction selectivity in the retina. *Synapse*, **1**, 417–434.

Grzywacz, N. M. & Poggio, T. (1990). Computation of motion by real neurons. In S. F. Zornetzer, J. L. Davis and C. Lau. (Eds.) *An Introduction to Neural and Electronic Networks*, pp. 379–403. Academic Press, San Diego, USA.

Grzywacz, N. M. & Yuille, A. L. (1990). A model for the estimate of local image velocity by cells in the visual cortex. *Proc. R. Soc. Land. B*, **239**, 129–161.

Grzywacz, N. M. & Yuille, A. L. (1991). Theories for the visual perception of local velocity and coherent motion. In M. S. Landy & J. A. Movshon (Eds.) *Computational Models of Visual Processing*, pp. 231–252. MIT Press, Cambridge, MA.

Grzywacz, N. M., Amthor, F. R. & Mistler, L. A. (1990). Applicability of quadratic and threshold models to motion discrimination in the rabbit retina. *Biol. Cybernet.*, **64**, 41–49.

Harris, M. G. (1986). The perception of moving stimuli: a model of spatiotemporal coding in human vision. *Vision Res.*, **26**, 1281–1287.

Hausen, K. (1981). Monocular and binocular computation of motion in the Lobula Plate of the fly. ÛŠ2ÛTVerh. Dtsch. Zool. Ges., **74**, 49–70.

Helmholtz, H. V. (1910/1962). *Physiological Optics.* (Vol. III), Dover, New York.

Heeger, D. J. (1987). A model for the extraction of image flow. *J. Opt. Soc. Am. A*, **4**, 1455–1471.

Heeger, D. J. (1993). Modeling simple cell direction selectivity with normalized, half-squared, linear operators. Submitted for publication.

Hildreth, E. C. (1992). Recovering Heading for Visually Guided Navigation. *Vision Res.*, **32**, 1177–1192.

Hildreth, E. C. (1983). *The Measurement of Visual Motion.* MIT Press, Cambridge, MA.

Hochstein, S. & Shapley, R. M. (1976). Quantitative analysis of retinal ganglion cell classifications. *J. Physiol.*, **262**, 264.

Hoffman, D. D. & Bennett, B. M. (1985). The computation of structure from fixed-axis motion: nonrigid structures. *Biol. Cybernet.*, **51**, 293–300.

Hoffman, D. D. & Bennett, B. M. (1986). The computation of structure from fixed-axis motion: rigid structures. *Biol. Cybernet.*, **54**, 71–83.

Holub, R. A. & Morton-Gibson, M. (1981). Response of visual cortical neurons of the cat to moving sinusoidal gratings: Response-contrast functions and spatiotemporal integration. *J. Neurophysiol.*, **46**, 1244–1259.

Horn, B. K. P. & Schunck, B. G. (1981). Determining optical flow. *Artificial Intelligence*, **17**, 185–203.

Howard, I. P. (1961). An investigation of the satiation process in the reversible perspective of revolving skeletal shapes. *Q. J. Exp. Psychol.*, **9**, 19–33.

Hubel, D. H. & Wiesel, T. N. (1962). Receptive fields, binocular interaction and functional architecture in the cat's visual cortex. *J. Physiol.*, **1160**, 106–154.

Johnston, E. B. (1991). Systematic distortions of shape from stereopsis. *Vision Res.*, 1351–1360.

Jones, J. P. & Palmer, L. A. (1987). An evaluation of the two-dimensional Gabor filter model of simple receptive fields in cat striate cortex. *J. Neurophysiol.*, **58**, 1233–1258.

Koenderink, J. J. (1986). Optic flow. *Vision Res.*, **26**, 161–170.

Koenderink, J. J. & van Doorn, A. J. (1976). Local structure of movement parallax of the plane. *J. Opt. Soc. Am.*, **66**, 717–723.

Komatsu, H. & Wurtz, R. H. (1988). Relation and cortical areas MT and MST to pursuit eye movements. III. Interaction with full-field visual stimulation. *J. Neurophysiol.*, **60**, 621–644.

Lee, D. N. (1976). A theory of visual control of braking based on information about time-to-collision. *Perception*, **5**, 437–457.

Longuet-Higgins, H. C. (1984). The visual ambiguity of a moving plane. *Proc. R. Soc. Lond. B.*, **223**, 165–175.

Longuet-Higgins, H. C. & Prazdny, K. (1980). The interpretation of moving retinal images. *Proc. R. Soc. Lond. B.*, **208**, 385–397.

Maffei, L. & Fiorentini, A. (1977). Spatial frequency rows in the striate visual cortex. *Vision Res.*, **17**, 257–264.

Marchiafava, P. L. (1979). The responses of retinal ganglion cells to stationary and moving visual stimuli. *Vision Res.*, **19**, 1203–1211.

Marr, D. (1982). *Vision: A Computerised Investigation into the Human Representation and Processing of Visual Information.* Freeman, San Francisco.

Marr, D. C. & Ullman, C. (1981). Directional selectivity and its use in early visual processing. *Proc. R. Soc. Lond. B*, **211**, 1881–1887.

Maturana, H. R., Lettvin, J. Y., McCulloch, W. S. & Pitts, W. H. (1960). Anatomy and physiology of vision in the frog (*Rana Pipiens*). *J. Gen. Physiol.*, **43** (Suppl. 2), 129–171.

McKee, S. P. & Welch, L. (1985). Sequential recruitment in the discrimination of velocity. *J. Opt. Soc. Am. A*, **2**, 243–251.

McKee, S. P., Silverman, G. H. & Nakayama, K. (1986). Precise velocity discrimination despite random variations in temporal frequency and contrast. *Vision Res.*, **26**, 609–619.

Miles, F. A. & Wallman, J., (Eds.) (1993). *Visual Motion and Its Role in the Stabilization of Gaze.* Elsevier, Amsterdam.

Miller, R. F. (1979). The neuronal basis of ganglion-cell receptive-field organization and the physiology of amacrine cells. In F. O. Schmitt & F. G. Worden, (Eds.) *The Neurosciences, Fourth Study Program*, pp. 227–245. MIT Press, Cambridge, Massachusetts.

Nakayama, K. (1985). Biological image motion processing: a review. *Vision Res.*, **25**, 625–660.

Nakayama, K. & Loomis, J. M. (1974). Optical velocity patterns, velocity-sensitive neurons, and space perception: a hypothesis. *Perception*, **3**, 63–80.

Nawrot, M. & Blake, R. (1991). The interplay between stereopsis and structure from motion. *Percept. Psychophys.*, **49**, 230–244.

Poggio, T. (1983). Visual Algorithms. In Braddick, O. J. & Sleigh, A. C. (Eds.) *Physical and Biological Processing of Images*, pp. 128–153, Springer-Verlag, Berlin.

Poggio, T. & Reichardt, W. E. (1973). Considerations on models of movement detection. *Kybernetik*, **13**, 223–227.

Poggio, T. & Reichardt, W. E. (1976). Visual control of orientation behaviour in the fly: Part II: Towards the underlying neural interactions. *Q. Rev. Biophys.*, **9**, 377–438.

Ratliff, F. (1965). *Mach Bands: Quantitative Studies on Neural Networks in the Retina.* Holden-Day, San Francisco.

Regan, D. (1986). Visual processing of four kinds of relative motion. *Vision Res.*, **26**, 127–145.

Regan, D. & Beverley, K. I. (1984). Figure-ground segregation by motion contrast and by luminance contrast. *J. Opt. Soc. Am. A*, **1**, 433–442.

Regan, D. M., Kaufman, L. & Lincoln, J. (1986). Motion in depth and visual acceleration. In K. R. Boff, L. Kaufman & J. P. Thomas (Eds.) *Handbook of Perception and Human Performance. Volume I. Sensory Processes and Perception.* Wiley, New York.

Reid, R. C., Soodak, R. E. & Shapley, R. M. (1987). Linear mechanisms of directional selectivity in simple cells of cat striate cortex. *Proc. Natl. Acad. Sci. USA*, **84**, 8740–8744.

Reid, R. C., Soodak, R. E. & Shapley, R. M. (1991). Directional selectivity and

spatiotemporal structure of receptive fields of simple cells in cat striate cortex. *J. Neurophysiol.*, **66**, 505–529.

Reichardt, W. (1961). Autocorrelation, a principle for the evaluation of sensory information by the nervous system. In Rosenblith, (Ed.) *Sensory Communication.* Wiley, New York.

Reichardt, W. & Poggio, T. (1976). Visual control of orientation behaviour in the fly. Part I. A quantitative analysis. *Q. Rev. Biophys.*, **9**, 311–375.

Reichardt, W., Egelhaaf, M. & Schlögl, R. W. (1988). Movement detectors provide sufficient information for local computation of 2-D velocity field. *Die Naturwissenschaften*, **75**, 313–315.

Rieger, J. H. & Lawton, D. T. (1985). Processing differential image motion. *J. Opt. Soc. Am. A*, **2**, 354–360

Richards, W. (1985). Structure from stereo and motion. *J. Opt. Soc. Am. A*, **2**, 343–349.

Smith, R. D., Grzywacz, N. M. & Borg-Graham, L. (1991). Picrotoxin's effect on contrast dependence of turtle retinal directional selectivity. *Invest. Ophthalmol. Vis. Sci.*, **32**, 1263.

Smith, R. D., Grzywacz, N. M. & Borg-Graham, L. (1994). Effects of $GABA_A$ antagonists on preferred motion direction of turtle ganglion cells. Submitted for publication.

Schmerler, J. (1976). The visual perception of accelerated motion. *Perception*, **5**, 167–185.

Sekuler, A. B. (1990). Motion segregation from speed differences: evidence for nonlinear processing. *Vision Res.*, **30**, 785–795.

Sekuler, A. B. (1992). Simple-pooling of undirectional motion predicts speed discrimination for looming stimuli. *Vision Res.*, **32**, 2277–2288.

Sparks, D. L. & Mays, L. E. (1990). Signal transformation required for the generation of saccadic eye movements. *Ann. Rev. Neurosci.*, **13**, 309–336.

Tittle, J. S. & Braunstein, M. L. (1991). Shape perception from binocular disparity and structure-from-motion. In *Sensor Fusion III: 3-D Perception and Recognition, Proceedings of the SPIE*, **1383**, 225–234.

Tolhurst, D. J. & Movshon, J. A. (1975). Spatial and temporal contrast sensitivity of striate cortical neurons. *Nature*, **257**, 674–675.

Torre, V. & Poggio, T. (1978). A synaptic mechanism possibly underlying directional selectivity to motion. *Proc. R. Soc. Lond. B.*, **202**, 409–416.

Ullman, S. (1979a). The interpretation of structure from motion. *Proc. R. Soc. Lond. B*, **203**, 405–426.

Ullman, S. (1979b). *Interpretation of Visual Motion.* MIT Press, Cambridge, Mass.

Ullman, S. (1984). Maximizing rigidly: the incremental recovery of 3-D structure from rigid and nonrigid motion. *Perception*, **13**, 255–274.

Vaina, L. M., Grzywacz, N. M. & LeMay, M. (1990). Structure from motion with impaired local-speed and global motion-field computations. *Neural Comp.*, **2**, 416–432.

Vaina, L. M., Grzywacz, N. M. & LeMay, M. (1993). Perception of motion discontinuities in patients with selective motion deficits. Submitted for publication.

Vaney, D. I. (1990). The mosaic of amacrine cells in the mammalian retina. In N. Osborne & J. Chader (Eds.) *Progress in Retinal Research* (vol 9), pp. 49–100. Pergamon Press, Oxford.

van Santen, J. P. H. & Sperling, G. (1985). Elaborated Reichardt detectors. *J. Opt. Soc. Am. A*, **2**, 300–320.

Verri, A., Girosi, F. & Torre, V. (1989). Mathematical properties of the two-dimensional motion field: From singular points to motion parameters. *J. Opt. Soc. Am. A*, **6**, 698–712.

Wallach, H. & O'Connell, D. N. (1953). The kinetic depth effect. *J. Exp. Psychol.*, **45**, 205–217.

Warren, W. H. & Hannon, D. J. (1988). Direction of self-motion is perceived from optical flow. *Nature*, **336**, 162–163.

Watamaniuk, S. N. J. (1992). Visible persistence is reduced by fixed-trajectory motion but not by random motion. *Perception*, **21**, 791–802.

Watamaniuk, S. N. J. & Duchon, A. (1992). The human visual system averages speed information. *Vision Res.*, **32**, 931–941.

Watanabe, S.-I. & Murakami, M. (1984). Synaptic mechanism of directional selectivity in ganglion cells of frog retina as revealed by intracellular recordings. *Jpn. J. Physiol.*, **34**, 497–511.

Watson, A. B. & Ahumada, A. J. (1985). Model of human visual motion sensing. *J. Opt. Soc. Am. A*, **2**, 322–342.

Werblin, F. S. (1970). Responses of retinal cells to moving spots: Intracellular recording in *Necturus maculosus*. *J. Neurophysical.*, **33**, 342–350.

Werkhoven, P. & Koenderink, J. J. (1991). Visual processing of rotary motion. *Percept. Psychophys.*, **499**, 73–82.

Wheatstone, C. (1838). Contributions to the physiology of vision. Part the first. On some remarkable, and hitherto unobserved, phenomena of binocular vision. *Phil. Trans. R. Soc.*, **128**, 371–392.

Wyatt, H. J. & Daw, N. W. (1975). Directionally sensitive ganglion cells in the rabbit retina: Specificity for stimulus direction, size and speed. *J. Neurophysiol.*, **38**, 613–626.

Yang, G. & Masland, R. H. (1992). Direct visualization of the dendritic and receptive fields of directionally selective retinal ganglion cells. *Science*, **258**, 1949–1952.

Yuille, A. L. & N. M. Grzywacz (1988). A computational theory for the perception of coherent visual motion. *Nature*, **333**, 71–74.